THE STABILITY OF ARTICULATED TIPPING TRAILER UNITS

by Simon G Pickering, BEng

Thesis submitted to the University of Nottingham
for the degree of Doctor of Philosophy
January 1994

CONTENTS

ABSTRACT

When an articulated tipper unit is being loaded or is tipping, it is unlikely to be standing on perfectly level ground. Also, the centre of gravity of the load is unlikely to be in the centre of the body. Hence the loads carried by the suspension and tyres on one side of the tipper will be greater than those on the other side. This uneven loading will cause the tyres and suspension on one side of the tipper unit to deform more than those on the other side. It will also cause the chassis to deform; the twisting about its longitudinal axis being the most significant mode of deformation. As a result of these deformations caused by the uneven loading, the position of the centre of gravity will be shifted even further towards the more heavily loaded side. This will cause even more uneven loading and further deformations.

Under stable conditions a situation will exist at which the position of the centre of gravity, the deformations and the forces transmitted through the system are compatible. Instability, resulting in roll-over would occur if the overall centre of gravity of the load, body, chassis etc. were to fall outside the area bounded by the contact of the wheel with the ground, before a stable condition was reached.

Many factors influence the roll stability. To increase stability, an understanding of the influence of components of the lorry on the stability is required. In order to achieve this, a theoretical model of an articulated tipper was developed which will allow roll-over predictions to be made for a given lorry in likely attitudes. In this model dimensions and stiffness of the lorry components can be altered to assess their influence on roll stability.

The previous theoretical roll-over models were based on lumped mass systems, representing various parts of the lorry inter-connected by compliant elements. Certain flexibilities such as the tyres, suspension units, etc. could be obtained from the respective components manufacturers but the tractor and trailer chassis flexibilities are unknown. To overcome this problem the flexibilities were obtained from full scale static tilt tests. This is a very expensive undertaking, providing a limited means in which to assess those elements of trailer design which are important in improving stability, without further recourse to more tilt tests. It was decided that the finite element method should be used to model the tractor and trailer, in order to determine the important deformations. Once the finite element model is created it is relatively straight forward to make changes to the structure. Hence an assessment of component contribution to roll stability can be undertaken relatively inexpensively.

Whilst a vehicle operator should always endeavour to discharge the payload with the vehicle standing on level ground, practical situations arise where this is not possible. This may be due to the absence of level ground or poor judgement by the operator, which may result in the vehicle being tipped on a lateral ground slope. As a result of this, the maximum ground slope angle considered for the theoretical model is limited to eight degrees, as this position is at least twice the severity of ground slope on which a vehicle should normally be tipped.

For each trailer design, the magnitude of the load, position of the load, ram length and ground slope can be varied in any combination. Four payloads and up to nine payload positions are considered, varying the ground slope from 0 to 8 degrees and varying the ram length from 2 to 8 meters. Also, three further chassis configurations, based on the reference chassis were modelled to investigate the contribution of important component flexibilities on roll stability.

ACKNOWLEDGEMENTS

The author wishes to thank all those colleagues who have assisted him with this work. Particular thanks are due to Professor Henry Fessler and Professor Tom Hyde who provided tremendous enthusiasm, encouragement and guidance. Thanks also to York Trailers Ltd and the SERC who provided financial support for this work.

The author also wishes to thank Mr Bob Davies (York Trailers Ltd) for guidance on technical issues, and to Judith Bray for her care and patience in typing this script; and Helen Geraghty and my parents for providing much needed support during the writing of this thesis.

NOTATION

Forces

A_L, A_R	left and right airbag forces, see Fig. 3.5
A_{R1} and A_{R2}	forces at the top and bottom of the right hand airbag of the 1st suspension, see Fig. 3.5
A_{R3} and A_{R4}	forces at the top and bottom of the right hand airbag of the 2nd suspension, see Fig. 3.5
A_{R5} and A_{R6}	forces at the top and bottom of the right hand airbag of the 3rd suspension, see Fig. 3.5
$\underset{\sim}{A}_R$ (A_{R1}, A_{R2}, A_{R3}, A_{R4}, A_{R5}, A_{R6})	column of forces applied to the right hand airbags
$\underset{\sim}{B}$ (B_y, B_z)	body force vector
$\underset{\sim}{F}$, $\underset{\sim}{F}^{'}$, $\underset{\sim}{F}^{''}$,	column matrices of all important chassis forces
$\underset{\sim}{G}$ (G_{L1}, G_{L2}, G_{L3}, G_{R1}, G_{R2}, G_{R3})	column matrix containing the left and right vertical tyre forces
$\underset{\sim}{H}_L$ (H_{Lx}, H_{Ly}, H_{Lz})	left hinge force vector
$\underset{\sim}{H}_R$ (H_{Rx}, H_{Ry})	right hinge force vector
L	force applied to cantilever
$\underset{\sim}{P}$ (P_x, P_y, P_z)	payload force vector
$\underset{\sim}{R}$ (R_x, R_y, R_z)	ram force vector
$\underset{\sim}{T}$ (T_L, T_R)	column matrix containing the left and right tie bar forces
$\underset{\sim}{W}$ (W_x, W_y, W_z)	wind force vector
$\underset{\sim}{W}_T$ (W_{Ty}, W_{Tz})	tractor self-weight vector
$\underset{\sim}{W}_c$ (W_{cy}, W_{cz})	chassis self-weight vector

Position Vectors (relative to origin of X, Y, Z coordinate system)

$\underset{\sim}{b}$ (b_x, b_y, b_z)	position of the centre of gravity of body
$\underset{\sim}{p}$ (p_x, p_y, p_z)	position of the centre of gravity of payload
$\underset{\sim}{h}_l$ (h_{lx}, h_{ly}, h_{lz})	position of the left hinge
$\underset{\sim}{h}_r$ (h_{rx}, h_{ry}, h_{rz})	position of the right hinge
$\underset{\sim}{r}_b$ (r_{bx}, r_{by}, r_{bz})	position of the bottom of ram
$\underset{\sim}{r}_t$ (r_{tx}, r_{ty}, r_{tz})	position of the top of ram
$\underset{\sim}{w}$ (w_x, w_y, w_z)	position of the centroid of wind pressure
$\underset{\sim}{r}_{tb}$	position of the top of the ram relative to the bottom of the ram

Displacements

$\underset{\sim}{u}$, $\underset{\sim}{u}^*$	column matrix of all important chassis displacements
$\underset{\sim}{u}_{hl}$ (u_{hl}, v_{hl}, w_{hl})	left hinge displacement vector
$\underset{\sim}{u}_{hr}$ (u_{hr}, v_{hr}, w_{hr})	right hinge displacement vector
$\underset{\sim}{u}_{rb}$ (u_{rb}, v_{rb}, w_{rb})	bottom of ram displacement vector
v_{a1} and v_{a2}	y components of displacement of the upper and lower, right hand airbag ends of 1st suspension, see Fig. 3.5
v_{a3} and v_{a4}	y components of displacement of the upper and lower, right hand ends of the 2nd suspension, see Fig. 3.5
v_{a5} and v_{a6}	y components of displacement of the upper and lower, right hand ends of the 3rd suspension, see Fig. 3.5
$\underset{\sim}{v}_a$ $(v_{a1}, v_{a2}, v_{a3}, v_{a4}, v_{a5}, v_{a6})$	column matrix of the y components of displacements of the right hand airbags
$\Delta^{(i)}$	vertical displacement of cantilever beam tip
$\phi^{(i)}$	rotation of cantilever beam tip
θ	hinge bar rotation about X axis, see Fig. 3.1
θ_p	slope of the ground, see Fig. 3.1
ψ	hinge bar rotation about Y axis, see Fig. 3.1

Others

a, b	dimensions of the rigid frame attached to the tip of the cantilever, see Fig. 3.2
E	Young's modulus
I	second moment of area
$[I^{(a)}]$, $[I^{(b)}]$, $[I^{(c)}]$	influence matrices relating the important chassis displacements to the important chassis forces for different airbag conditions
$[I^{(a)}{}_T]$, $[I^{(b)}{}_T]$, $[I^{(c)}{}_T]$	influence matrices relating the tie bar forces to the important chassis forces for different airbag conditions
$[I^{(a)}{}_G]$, $[I^{(b)}{}_G]$, $[I^{(c)}{}_G]$ $[I^{(d)}{}_G]$	influences matrices relating the ground/tyre reaction forces to the important chassis forces (or displacement) for different airbag conditions
$[I^{(b)}]$	influence matrix relating the right hand airbag displacements to the important chassis forces
[K]	stiffness matrix relating the important chassis forces to the important chassis displacements
l	length of cantilever, see Fig. 3.2
l_o	length of gas contained in the airbag cylinders at the limiting pressure
n	exponent in the equation for polytropic compression of a gas
Q	constant in Equation 3.17
X, Y, Z	co-ordinate system with its origin at the centre of the hinge bar
β	inclination of the body relative to the x axis
γ	angle between the vectors $\underset{\sim}{r}_t$ and $\underset{\sim}{r}_b$
δ	angle between the vectors $\underset{\sim}{r}_t$ and $\underset{\sim}{p}$
^	vector product
.	scalar product
+	vector addition
-	vector subtraction

CHAPTER ONE
INTRODUCTION

1.1 Size of the problem

Articulated tipping units are used in many different industries for transporting many different types of payloads. In 1984 Keen et al [1] estimated that the number of vehicles having tipping facilities (articulated and rigid) was 120,000 with articulated tippers accounting for 15%. Following the amendments to the Construction and Use Regulations, which came into effect on 1st May 1983, the maximum gross vehicle weight of articulated tipper units was increased from 32 to 38 tonnes. Due to the increase in payload capacity, articulated tipping trailers have become more popular.

Information from official sources on the extent of tipper lorry rollovers during discharge of loads is limited to those where fatalities and or serious injuries result, as notification of non injury type incidents are not mandatory. A survey of hauliers by Keen et al [1], with a combined fleet of 600 tipper, found that the number of static rollovers accounted for 0.75% of the total fleet. Scaling up suggested an annual occurrence of 900 static rollovers for the UK.!

Many factors influence the roll stability of articulated tippers, while they are discharging their payloads. To increase stability, an understanding of the influence of components of the lorry on stability is required. This work describes a theoretical model of an articulated tipper which will allow rollover prediction to be made for a given lorry in likely attitudes. In this model dimensions and stiffnesses of the lorry components, payload magnitude and position body attitude and transverse ground slope can be altered to assess their influence on roll stability.

1.2 Trailer construction

There are two main categories into which tipper lorries can be grouped, rigid and articulated tipper units. The rigid tipper has a maximum gross vehicle weight of 30 tonnes, with the payload body and cab supported on one chassis, mounted on two steering wheels and four driving wheels. The articulated tipper has a maximum gross vehicle weight of 38 tonnes, with the payload body supported by the trailer chassis, mounted on six wheels and the driver's cab supported by the tractor chassis mounted on two steering wheels and two driving wheels. The tractor and trailer unit are detachable and are connected by a coupling known as the "fifth wheel".

This work is only concerned with 38 tonne articulated tipper units. A typical tractor and trailer unit is shown in Fig. 1.1.

1.2.1 Trailer design

The design of articulated tippers has been concerned more with the static strength of the vehicle, than its stability characteristics in either dynamic or tipping situations. The object of this work is to study the static tipping of articulated tipper units and develop a mathematical model which predicts the stability characteristics for a given lorry configuration. The mathematical model incorporates all of the important tractor and trailer flexibilities which can be changed to enable an assessment of their contribution to stability. This will allow designs to be produced based on stability criteria as well as strength criteria.

1.2.2 Trailer structures

Lorry chassis structures may be comprised of all open section channel or two longitudinal I beams inter-connected by cross members to form a ladder type structure. Open section channel chassis are used for rigid vehicles to form a ladder type structure. Two longitudinal I beams inter-connected by cross members forming a ladder type structure are used for articulated tipper units.

Mild steel is widely used in the construction of the ladder type structures for articulated tippers. The cross members are constructed from closed sections (rectangular, circular etc.) as the section is efficient in resisting bending and torsional forces. The longitudinal members are constructed from I beams as the section is efficient in resisting bending forces due to vertical loads.

The payload is transported in the "body" which is usually constructed from an aluminium alloy. The body is supported at three points, during tipping, by two hinges at the rear of the chassis and by the lifting ram at the front of the chassis. The chassis has to predominantly resist twisting about the longitudinal axis and bending about the transverse axis during tipping.

The forces generated by the payload the self weight of the vehicle are transmitted through the suspension system, which are more commonly air suspension, and tyres to ground reactions.

Chapter 3 describes the method of modelling the air suspension in the theoretical model.

1.3 Theoretical model

No published material has been found relating to the stability of articulated tipping trailer units. Previous work has been undertaken on the dynamic stability of non tipping trailer negotiating corners. Theoretical models developed to predict vehicle stability in such conditions relies upon full scale experimental tests to provide flexibility data. This is not only an expensive undertaking, but makes further design investigations difficult to undertake without further experimental testing.

This work is only concerned with the static stability of articulated tipping trailer units.

The theoretical model developed to predict vehicle stability incorporates the following flexibilities.

(i) Tractor and trailer chassis structure

(ii) Tractor and trailer axles

(iii) Tractor leaf spring suspensions

(iv) Trailer air suspension and height control mechanism

(v) Tractor and trailer tyres

The important flexibilities (i), (ii) and (iii) are determined using the finite element method. General flexibility matrices are developed using the finite element results, to enable stability characteristics to be determined, for a given lorry configuration, for any payload magnitude and position and body attitude.

Chapter 4 describes the finite element model.

The flexibilities (iv) and (v) are determined experimentally as described in Appendices A and B and are included in the F.E. model.

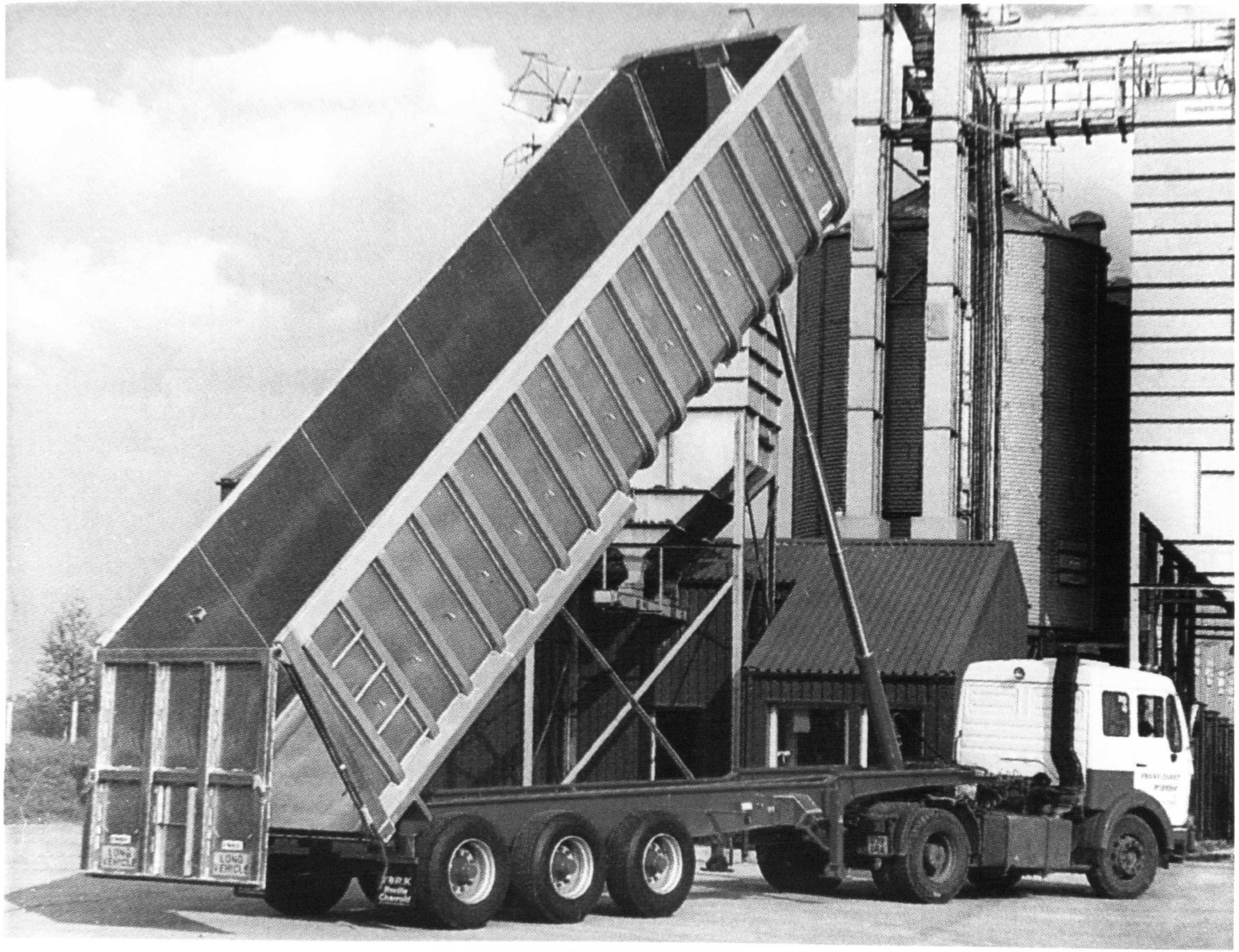

Fig. 1.1 A typical articulated tipping trailer unit

CHAPTER 2

GENERAL BACKGROUND

2.1 General description of tipping trailer units and operation

A schematic of a typical tipping trailer unit is shown in Fig. 2.1, it consists of a tractor unit connected to a trailer unit by a fifth wheel coupling. The tractor unit provides the motive force to pull the trailer and in most cases; provides the hydraulic pressure to raise the trailer's body by means of a telescopic ram. A tractor unit has a flexible chassis with a pair of single steering wheels and a pair of dual driving wheels connected to the chassis by leaf springs, as shown in Fig. 2.2.

A trailer unit is comprised of a flexible chassis, suspension and tyres supporting a body used for transporting the payload, as shown in Fig. 2.3. The longitudinal members (usually I sections) with circular, rectangular, hexagonal or similar hollow cross-members. The cross-members are welded to the longitudinal members with the joints often stiffened by local reinforcing, as indicated in Fig. 2.4. Steels or aluminium alloys are used in the manufacture of the chassis.

There are two main types of suspension used on articulated tippers, ie. leaf springs and air suspension. Because the modern trend is towards the use of air-bag suspension systems, only this type of suspension is described. Typically there are three air-bags on each side of the trailer, connected to three pairs of wheels, as indicated in Fig. 2.5. Each air-bag is connected to a wheel by a "trailing arm", which rotates about the pivot mounting and each wheel is attached to an axle tube, which in turn is attached to a pivot arm on the left and right side of the trailer, shown in Fig. 2.5. The distance between the middle axle and chassis frame, known as the 'ride height' is automatically maintained by the airbags; each set of three airbags, on the left and right hand sides of the chassis, are pressurised independently. Because there is a maximum pressure limit, during tipping, the ride height may not be maintained due to excessive loading on one side of the trailer.

The tyres now predominantly used in modern tipping trailer units are so called "super singles", which, as the name suggests, are one large tyre instead of two smaller tyres used side by side. Flexibility data exists so that these tyres can be modelled mathematically using three mutually perpendicular springs.

The telescopic ram used to raise and lower the body usually have four or five stages. These rams can be used to tip the body to between 40 and 50 degrees, relative to the horizontal. Since this type of ram has a relatively low resistance to transverse deformation, it can be regarded as a strut, with ball joints at the ram to body and ram to chassis connecting points, for modelling purposes.

The fifth wheel and king pin unit which connects the tractor unit to the trailer allows relative rotation between the tractor and trailer about the vertical and transverse axis. However, only limited relative rotation of the tractor and trailer can occur about the longitudinal axis. The relative longitudinal rotation, which is not intended for design purposes, is due to the inevitable relative vertical displacement which must exist for practical purposes. This limited, relative vertical movement has a non-linear effect on the roll stability However, since this "play" can only contribute to the behaviour when roll-over is in progress it has not been taken into account in the modelling presented in this thesis.

The body, in which the payload is transported, is usually made from an aluminium alloy to minimise the weight of the trailer. It is attached to the chassis by two hinges at the rear and by the ram at the front. For the purpose of calculation, in this thesis it is assumed that the body is rigid and that during tipping operation, the body is only connected to the chassis via the hinges and the ram.

Standing on a firm, level site is the ideal situation in which to tip the body, in order to discharge the payload. However, tipping takes place under a wide range of conditions on sites such as building sites, landfill sites etc. and the vehicle operator may not always be able to find a firm and level place to tip. Hence, in practice some vehicles are tipped on uneven, inclined and soft ground and in these adverse conditions, the possibility of roll over exists. Although, with experience, an operator may be able to judge, by eye, whether a site is reasonably level. The operator cannot be sure that there isn't soft ground under one side of the trailer and that the payload will not discharge in a non-uniform manner, moving the payload centre of gravity from the longitudinal centre line of the body; a combination of these events may lead to vehicle roll over.

If the payload sticks in the body of a trailer at maximum tip angle, with the body fully tipped an operator may drive the vehicle, and then apply the brakes sharply, in an attempt to free the stuck payload. It has been suggested by Keen et al [1] that if a vehicle is driven over irregular terrain, under these conditions, a pendulum motion can occur and that this could lead to roll over; this problem is not specifically addressed in this thesis.

2.2 Loading modes

When stationary, the external forces experienced by a tipping trailer unit are due to the gravitational load, wind loads and tyre reaction forces.

When standing on horizontal ground the gravitational forces only act normal to the ground and therefore there are no resultant transverse or longitudinal forces. However, when standing on a slope, components of the gravitational force many be experienced in the transverse and longitudinal directions.

The unsprung masses of a tipping trailer unit are defined as those masses which are not directly supported by the vehicles suspension. These masses on the trailer consist of the wheels, hubs and axles. For modelling purposes, the unsprung mass of each axle may be divided into two lumped masses located at the centre of each tyre. No detailed data, relating to the mass distribution, was obtainable for the tractor. Only the gross vehicle weight was obtained, and therefore the mass was taken to be entirely sprung for modelling purposes.

The trailer sprung masses, which are those supported by the trailer suspension, are the chassis mass and all of the accessories which are located on, or attached to, the chassis. The PAFEC finite element package [2] was used to obtain some of the information used in the model developed to assess the stability of a tipping trailer unit, part of the sprung mass is determined using the density and the volume of the material used for constructing the chassis. The remaining sprung masses were modelled by locating a lumped mass at the centre of gravity determined using the finite element package. The tractors sprung mass is comprised of the chassis, cab and engine, together with all the associated accessories.

The tractor's gross weight and the position of its centre of gravity were obtained from the information provided by the manufacturer. As no information was available relating to the distribution of the tractor mass, it was modelled using a single lumped mass, positioned at the centre of gravity of the tractor unit.

The present work is concerned with the stability of a vehicle tipping in a static position. Although there is no published information relating to this problem, work has been undertaken relating the stability of vehicles travelling round corners Sweatman et al [3], Kemp et al [4], Miller et al [5] and Isermann [6]. Where a vehicle travels around a corner of radius r, speed v and mass m, a transverse force, acting in the radial direction, of magnitude mv^2/r is induced. If this force should become large enough, the vehicle can roll over. This previous work has been concerned with predicting roll over under cornering conditions, by comparing results obtained from static tilt tests, where the concerning force mv^2/r was replaced by a component of the gravitational force, ie. mgcos θ, where θ is the transverse tilt angle and g is the acceleration due to gravity.

In the present investigation the body and payload are assumed to be rigid. A single force, representing the body self weight is taken to act along its centre line, whereas a single force, representing the payload, may be taken to act at a suitable position, which can be defined by the user of the theoretical model. During the analysis, the position of the payload relative to the body remains unchanged, although the position of the body can change as the body/chassis contact points move due to deformation of the chassis, tyres, suspension etc.

Wind loading can produce significant forces, especially when the vehicle is at the maximum tip angle. A transverse wind force has been included in the theoretical model. However, the method for obtaining the magnitude and line of action of wind forces was outside the scope of the present work. Previous work by Hollis [7] undertaken on determining wind forces on crane structures, up to 20 m high, showed that the measured values could be as much as 100 to 150% greater than those predicted, shows that this problem is relevant to the tipping trailer situation.

Conventional leaf springs suspension exert forces on the chassis which are proportional to the suspension deformation. However, with air suspension the airbag exerts a combined force which is related to the sprung mass (including payload and body weight). Under normal conditions, the pressures on the left hand and right hand sets of airbags are increased or decreased independently to maintain a fixed "ride height" for the centre axle. However, once a maximum allowed pressure is reached on one side, a valve closes and the set of three airbags compress under constant mass of gas conditions; the behaviour is taken to be adiabatic compression of the gas for modelling purposes, the airbag forces are treated as externally applied loads.

2.3 Design features

Although no research work, related to the stability of tipping trailer units, operating under tipping conditions, has been published, a number of experimental [3, 4, 5, 6, 8, 9, 10] and theoretical [3, 4, 5, 6, 10, 11, 12, 13] investigations on stability under cornering conditions have been published.

A survey undertaken by Miller and Barter [5] found that operators were surprised at the lack of warning they had obtained before roll over occurred. This was put down to a lack of "feel" in the drivers cab for the trailer roll behaviour. Kemp, Chinn and Brock [4] indicated that design changes could improve roll stability performance. Although the greatest reduction in roll over accidents might be achieved by operators accepting that roll over is caused by travelling at too high a speed for a particular radius of turn, it is clear that designers have a significant role to play in minimising the possibility of roll over instability.

Some of the major details over which the design has control include:

(i) the tyre and suspension type and operating conditions.

(ii) dimensions and materials, which may be varied in order to increase the chassis stiffness, particularly the torsional stiffness about the longitudinal axis.

(iii) the body materials and construction, which can be altered to minimise weight and increase rigidity.

The tyre and suspension stiffness were found by Laird [10] to significantly effect roll stability. It was found that the tractor drive suspension and trailer suspension could significantly affect roll stability, while the tractor front suspension only has a moderate influence.

Encouraged by legislative procedures, air suspension systems have become more popular than conventional leaf springs. However, the design of air suspension systems is still relatively new and further significant improvements are likely to occur. Current suspension systems predominantly use a combination of traditional leaf springs and air suspension bags, as indicated in Fig. 2.5. Current air bag designs, only accommodate loading along their longitudinal axis. Therefore leaf springs have been used to resist the large multi-directional forces resulting from side scrub between tyres and road, bumping into curbs or verges etc. It has been estimated by Dickson-Simpson [14] that these forces can be more than three times the nominal axle load. The air suspension system, modelled in this thesis, see Fig. 2.5, consists of elliptic leaf springs, each hinged to the chassis at one end, and supported at the other end by an air bag. Each axle tube is then rigidly clamped to the middle of the left and right leaf springs. Simultaneous displacements of the left and right tyres are primarily accommodated by the air suspension bags. However, when uneven loading on the tyres occurs (when cornering or tipping on uneven ground, etc.) the leaf springs and axle tube, which in effect form an anti-roll bar system, accommodate the uneven displacements.

Due to the trend towards the use of air suspension systems on commercial vehicles, height control valves have been developed to automatically govern the vehicles design ride height. This is accomplished by adjusting the pressure in the air bags in response to changes in vehicle loading which force the valve lever to move up or down as the chassis to axle spacing changes. A consistent design height is one advantage of air suspension over mechanical suspension. To maintain the design height while using a minimum amount of air, a time delay is incorporated into the design. The time delay feature prevents the valve from allowing air flow to or from the airbags during momentary changes in the chassis to axle spacing. In addition to the time delay, the valve may be biased to the centre position, so that it is slow to open but quick to close, thus eliminating the tendency for the valve to oscillate, when repeated small variations in load occur.

A typical control valve operation, described by Hillebrand [15], is shown in Fig. 2.6. The valve is designed with a minimal "dead band" shown in Fig. 2.6a. This is the neutral zone where the lever arm attached to the axle can move without allowing air to enter or leave the air bag. The "dead band" is kept to a minimum to maintain an accurate spacing between the axle and chassis and minimise air usage.

The valve is attached to the vehicle frame and the lever arm is connected to the middle axle only through a linkage. On tipping trailer units there are two height control valves for left and right air bags . When tipping it is assumed that the left and right airbags operate independently. As the valve is opened the air flow into the airbag is shown in Fig. 2.6b. As the valve closes the air flow into the air as is shown in Fig. 2.6c. This combination of delayed opening and rapid closing provides a biasing tendency towards the centre closed position.

An increase in the torsional rigidity of a typical trailer chassis about this longitudinal axis, was shown by Holmes [8] to improve its stability and handling. Also, by eliminating fifth wheel play, it was shown by Sweatman and Mai [12] that the transverse acceleration could be increased by 4% before first wheel lift occurred.

The most important design parameters, effecting roll stability is obviously the height of the centre of gravity of the trailer. Sweatman and Mai [12] showed that for a typical trailer design, an increase in the height of the centre of gravity of 26% (1.95 m to 2.35 m) caused the first wheel lift acceleration to reduce by 26%. Also, they showed that increasing the trailer axle track width by 10% resulted in an increase in first wheel lift acceleration of 10%.

In experiments conducted by MIRA, [16], a fifth wheel, which was constructed with a load cell, to measure vertical, longitudinal and transverse loads was used to determine fifth wheel dynamic loads during driving conditions. These loads were required in order to perform realistic long term fatigue tests under laboratory conditions. The typical and maximum forces measured are given in Table 2.1.

Since 1978, some trailer designs have been constructed using extruded sections welded to aluminium plates, to form a strong light weight box, Brock [17]. There are two basic types of box design which are now commonly used. The first design is constructed from extruded "U" shaped channels welded to a large rail forming the top rail of the body. Aluminum plate forms the skin of the body to contain the payload. The other design is constructed from extruded aluminium channels which form the side and floor supports, as shown in Fig. 2.7. These are welded to a large rail which forms the floor corners of the body. Aluminium plate is again used for the skin of the body. Finite element analyses [17] indicated that, for the latter design, the bottom pillar joints, shown in Fig. 2.7, were the most highly stressed joints.

The stiffness of the bottom rail and the way in which it is connected to the floor sections is intrinsic to construction strength. Fabrication procedures and the adoption of MIG welding procedures have enabled improved quality and enhance fatigue life performance.

2.4 Roll over models

A thorough literature survey and discussions with manufacturers of tipping trailer units has shown that all previous work on articulated roll stability has been directed towards non-tipping trailers, negotiating corners. The theoretical models, developed to predict the cornering roll stability, have all been based on unsprung and sprung masses, connected by compliant elements under the influence of gravitational and transverse forces. In 1970 a theoretical model was developed by Isermann [6] which included the flexibilities of the tyres, the suspension and tractor unit chassis with a rigid trailer chassis. This was later refined by Kemp et al [4] and Sweatman et al [5] to incorporate a torsional stiffness associated with the trailer. One of the major draw backs with these models is that a theoretical estimation of the various flexibilities is required or, alternatively, a vehicle has to be experimentally tested under static rolling conditions so that measurements of various displacements can be obtained in order to give an indication of the trailers torsional stiffness etc. In 1984 Sweatman [12] developed a further model which reduced the number of variables to be measured experimentally to three, namely the percentage of wheel load transferred laterally in the trailer and the drive and steering axle groups of the tractor unit during a tilt test. Again the model is based on a set of constant masses interconnected by massless compliant elements.

The above models have been used to assess a number of design parameters in order to determine their effect on vehicle roll stability. Structural changes to an actual chassis would require expensive tilt tests to be undertaken, to enable accurate assessment of their effect on roll stability. Therefore, in order to make an initial assessment of possible design changes, these models have been found to be useful.

2.5 General discussions and conclusions

No information, which relates directly to the roll stability of articulated tipping trailer units in operation, has been published in the open literature. Although some of the results of work related to cornering roll stability is applicable in a general sense, to static tipping roll stability, little or no information exists for the types of forces generated by a tipped vehicle and on the effect of vehicle design parameters on roll stability during this mode of operation.

Published theoretical models, relating to roll stability are all based on rigid masses interconnected by compliant elements. Application of these methods requires full scale experimental tilt testing, in order to determine important compliancies. In the present work, the finite element method is introduced to eliminate the need for static tilt tests. Also air bag suspension systems are modelled so that the forces generated by the tipped body, on the chassis, can be properly determined, in order to accurately model the roll stability of an articulated tipper unit. All of the important design parameters can be changed in order to assess the influence of them on the roll stability, without the need for static tilt tests. Also, although the required finite element analyses are simple small deformation, linear elastic analyses, the computer program written to perform the stability calculations is iterative and can cope with the large movements of the payload.

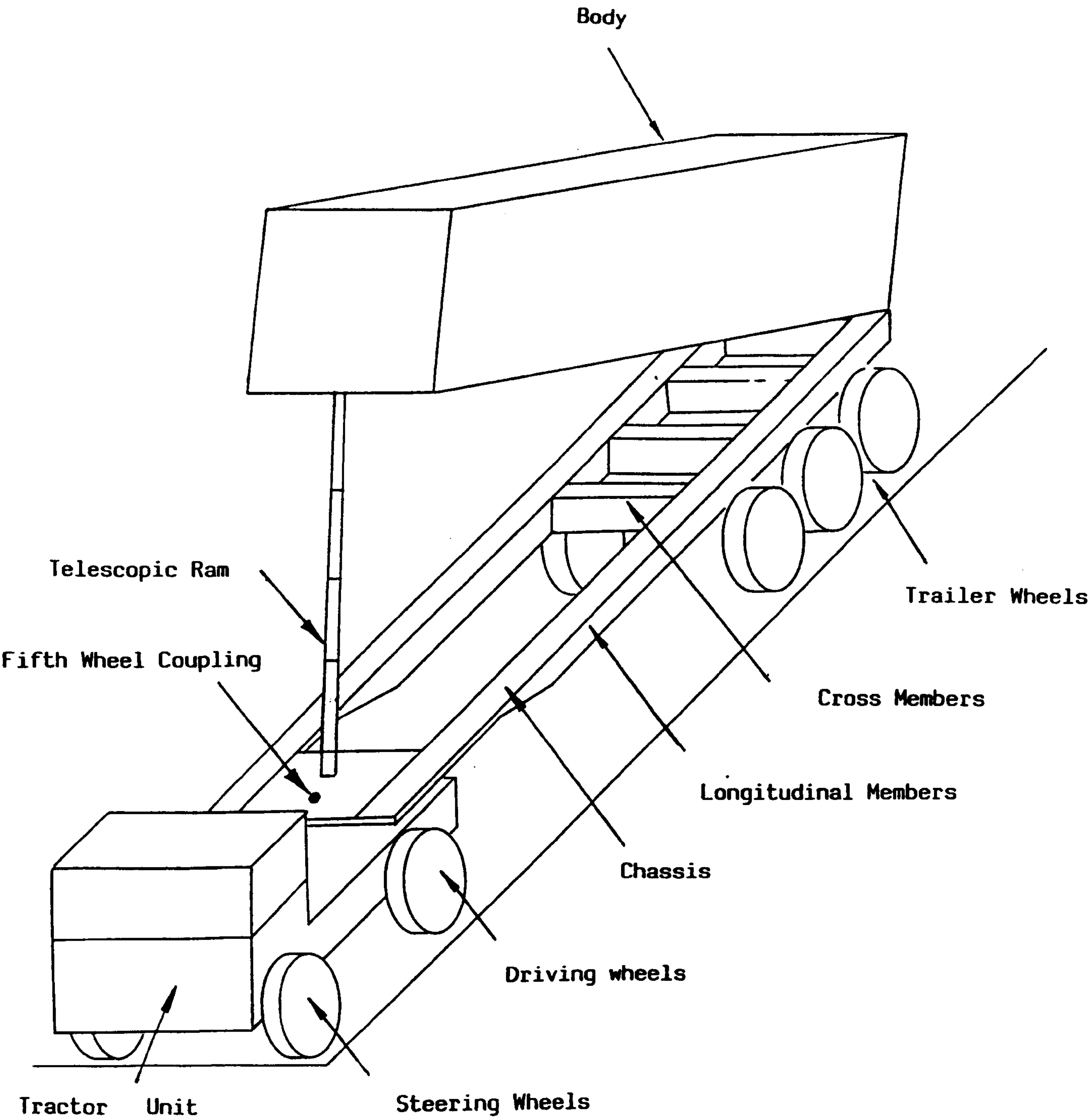

Fig. 2.1 A schematic diagram of a tipping trailer unit

Plated Weights Kg	Design	U.K. Legal
GVW	19500	17000**
Front Axle	6700	6700*
Rear Axle	13000	10500
GCW/GTW	44000	38000

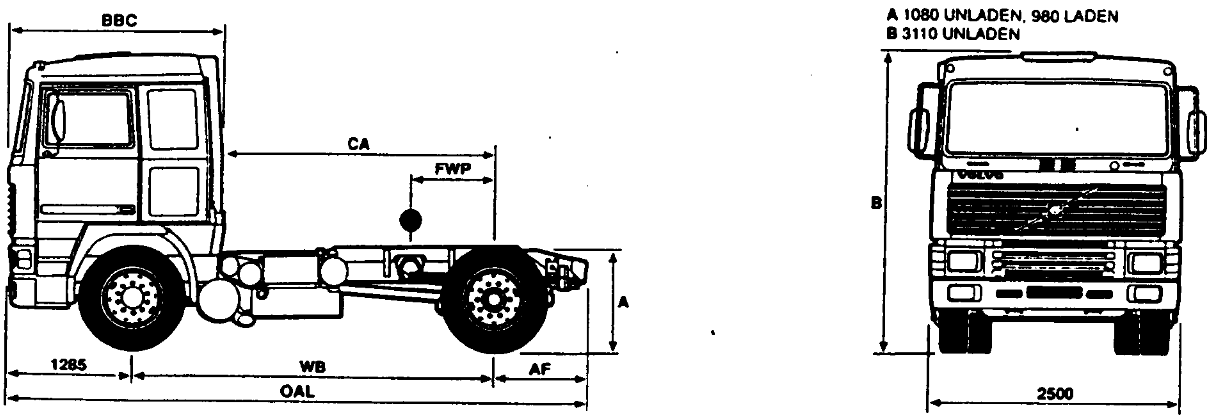

Chassis Dimensions mm

WB	Wheelbase	3400	3700
OAL	Overall Length	5619	5919
AF	Rear overhang	934	934
BBC#	Bumper to back of air intake	2220	2220
CA@	Back of air intake to axle centre	2465	2765
Turning Circle Diameter(Kerb to Kerb)		12100	13000
FWP Fifth Wheel Position for 16.5m OAL		350	650

F.W.P. For accurate fith wheel positioning, in terms of axle weights and dimensions, consult SSS program
Note 1) Height measurements calculated on 295/80R 22.5 tyres.
2) Do not use this drawing for 5th. wheel mounting, refer to F superstructures manual and coachbuilder drawing.
Day cab -320. @ Day cab +320

Chassis Kerb Weights Kg (Tolerance ±2%)

Front Axle	4560	4570
Rear Axle	1930	1940
Total Kerb Weight	6490	6510

Note:Weights for vehicles to standard specification i.e. sleeper cab, R1400 gearbox, twin plate clutch, 550 litre fuel tank(full), 295/80R22.5 tyres, water and tools, but excluding spare wheel and carrier.

Fig. 2.2 A Typical tractor unit

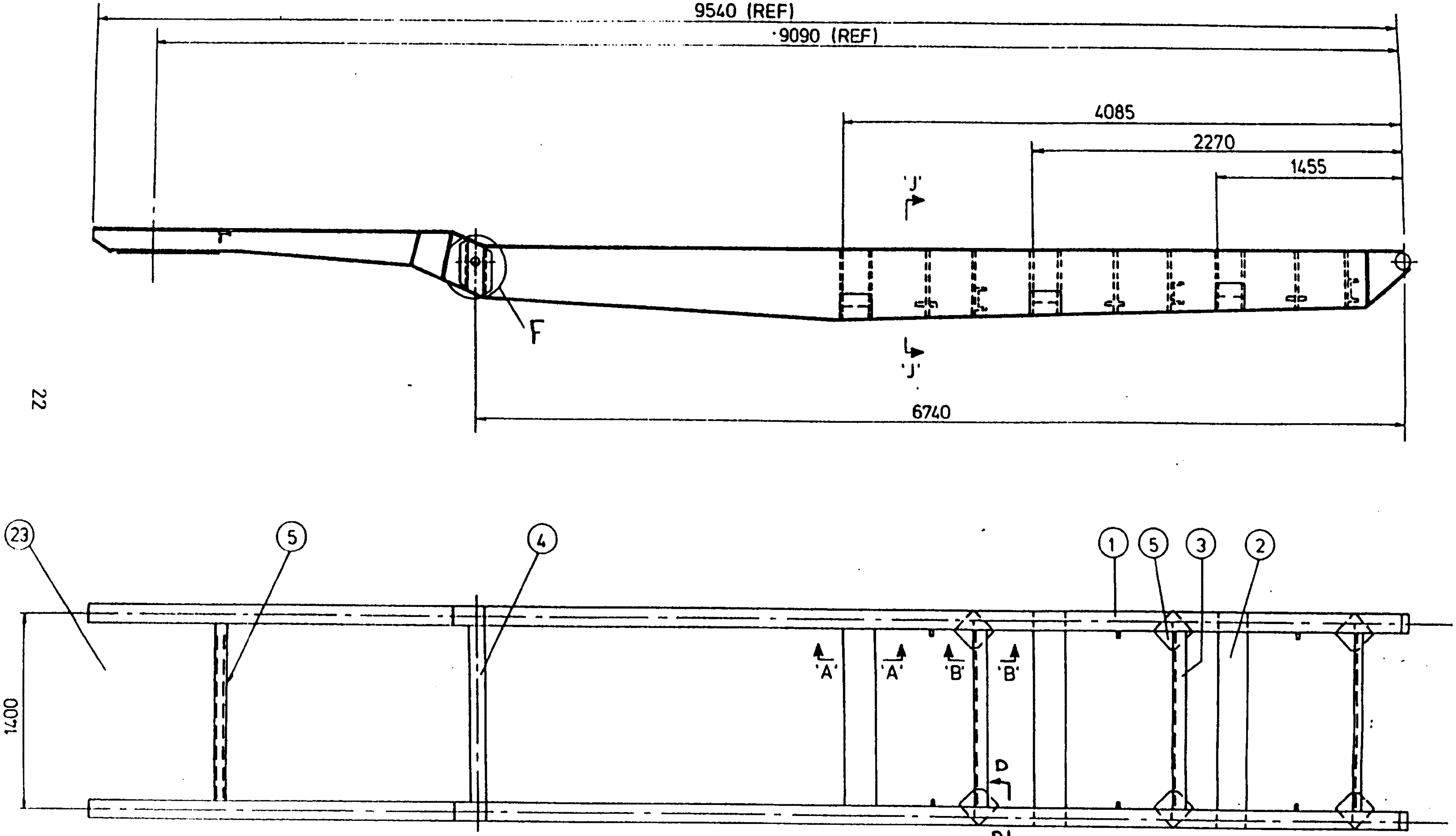

Fig. 2.3a A Typical trailer chassis

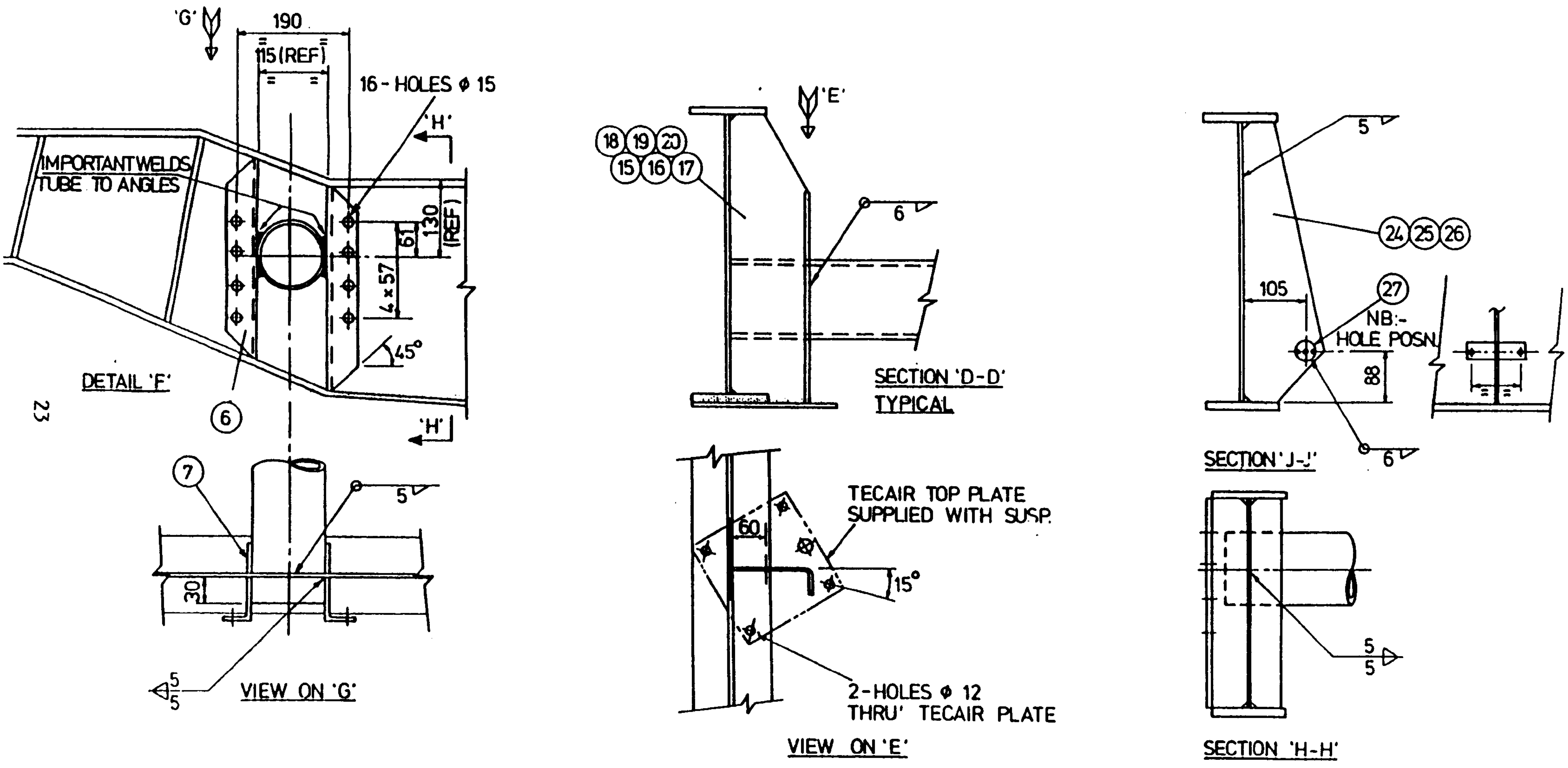

Fig. 2.3b Typical trailer chassis details

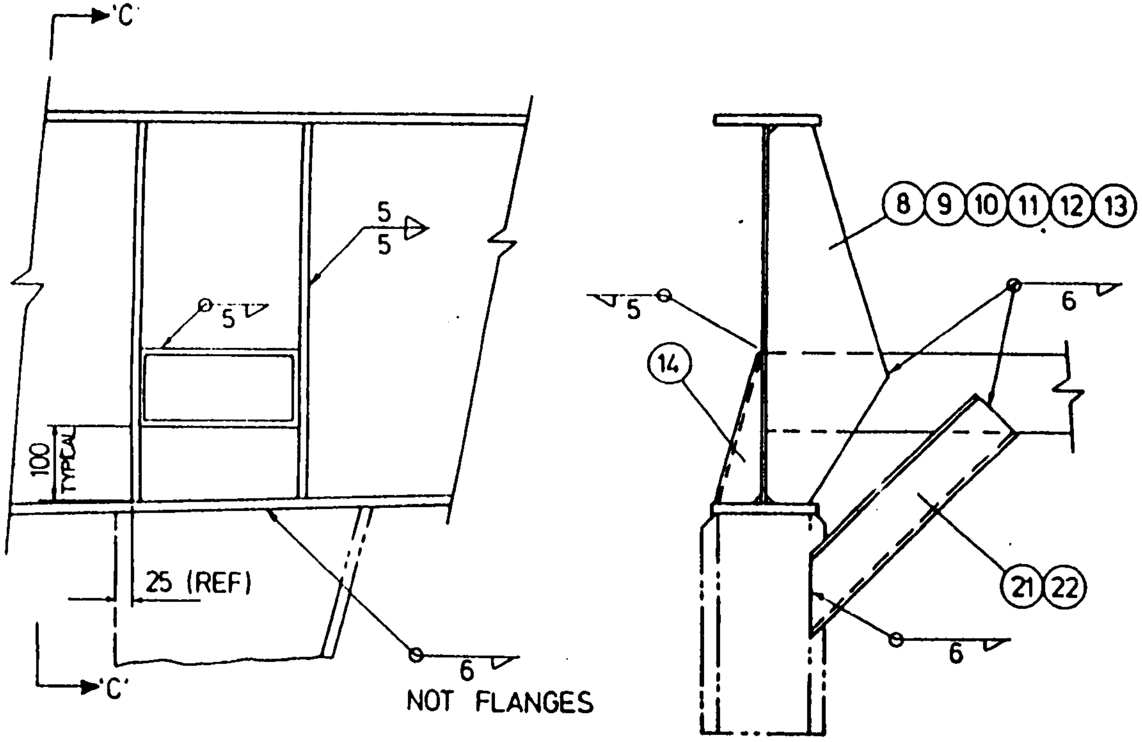

SECTION 'A-A'
TYPICAL

SECTION 'C-C'
TYPICAL

Fig. 2.3c Typical trailer chassis details

ITEM	PART NUMBER	QTY	DESCRIPTION
30			
29			
28			
27		6	PIN
26		2	AXLE RESTRAINT RIB
25		2	" " "
24		2	" " "
23	RD 891113	1	PUP ASS.
22	896775	2	HANGER BRACE LH
21	896776	2	HANGER BRACE RH
20		1	STIFFENER LH
19		1	" LH
18		1	" LH
17		1	STIFFENER RH
16		1	" RH
15		1	" RH
14		6	GUSSET - FOLDED
13		2	STIFFENER
12		2	"
11		2	"
10		2	"
9		2	"
8		2	"
7		4	STIFFENER
6		4	RSA 50×75×6×360 LG
5		1	CROSSMEMBER BS4360-GR50B
4		1	TUBE ϕ 114.3×5 WT×1460 LG
3		3	CROSSMEMBER
2		3	CROSSMEMBER RHS 200×100×5× 1395LG
1	RD 891112	2	MAINRAIL

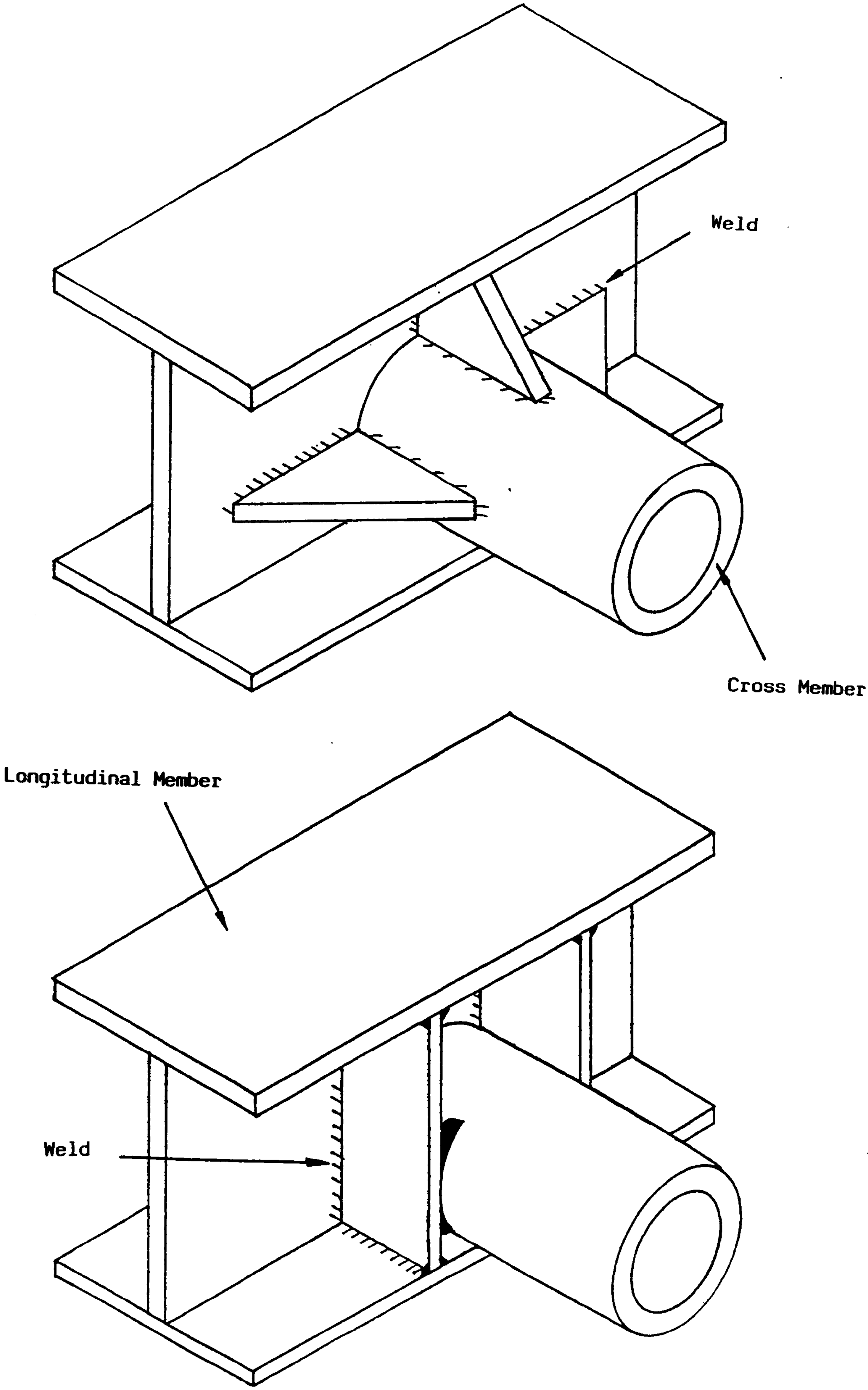

Fig. 2.4 Connection of chassis cross-members to longitudinal members

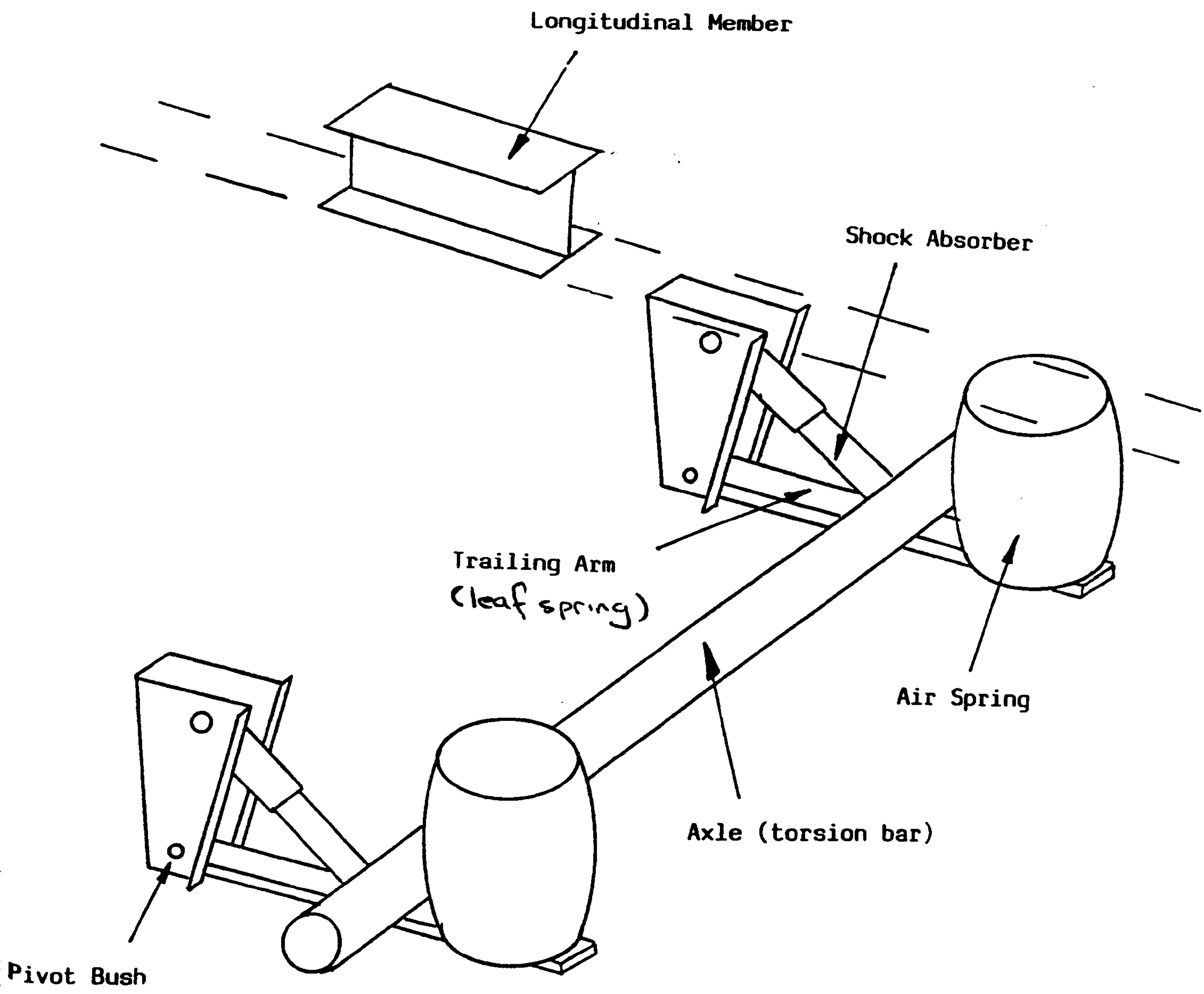

Fig. 2.5 Airbag suspension system

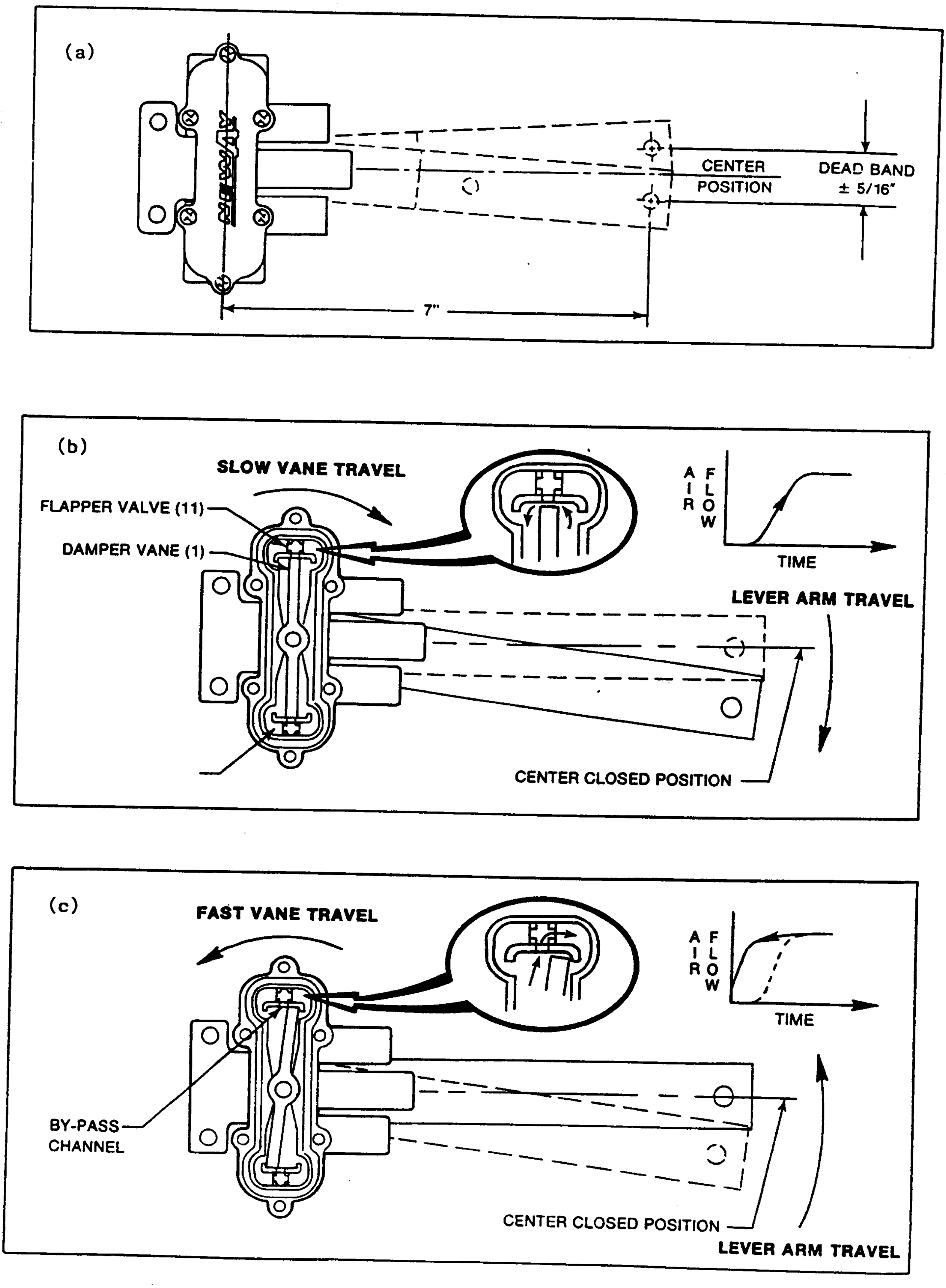

Fig 2.6 Typical suspension height control valve operating modes

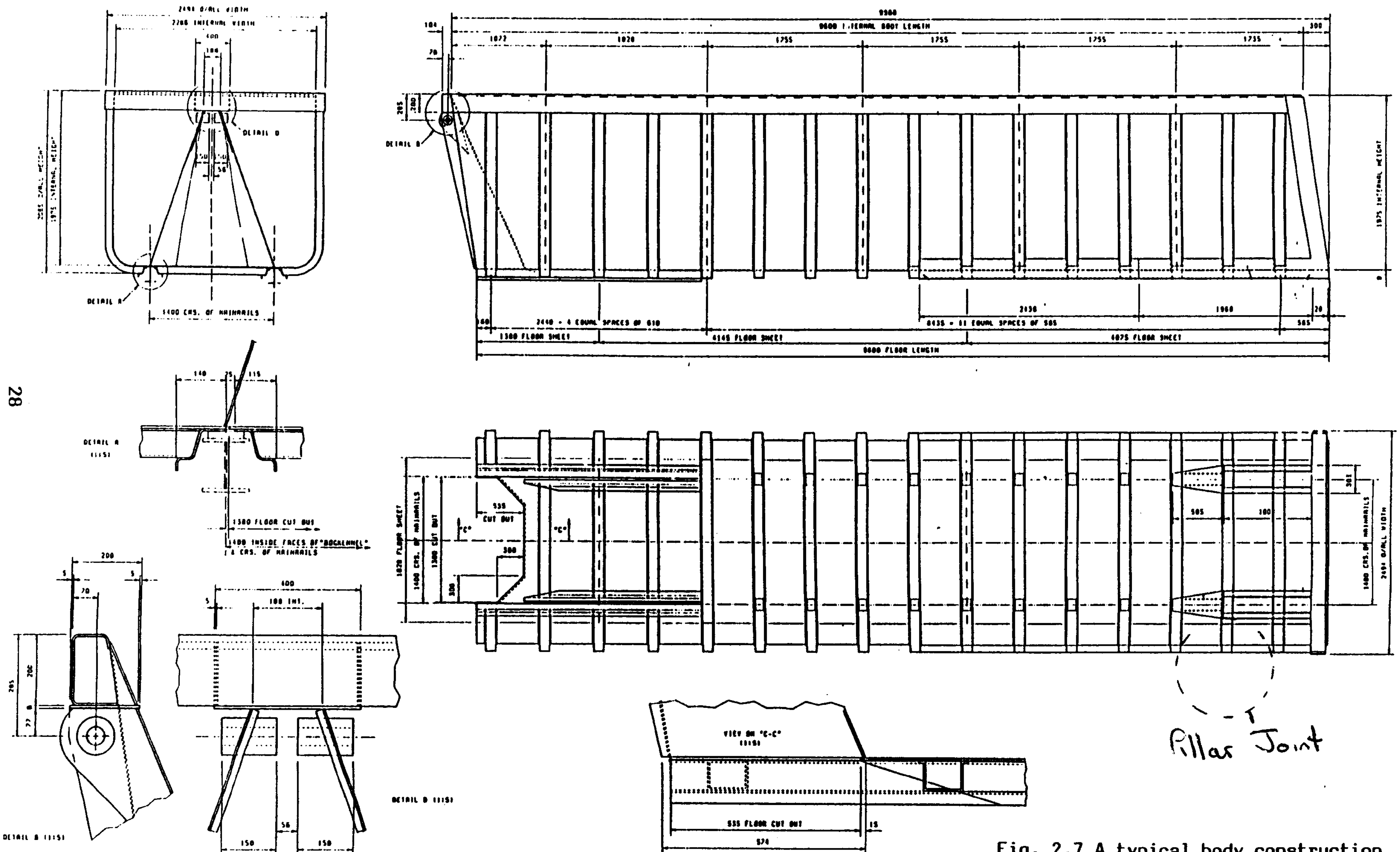

Fig. 2.7 A typical body construction

Table 2.1 - Dynamic fifth loads occuring once per km for a 32 tonne fully laden articulated lorry

LOADING MODE	DYNAMIC LOADS	
	Average	Maximum
LONGITUDINAL LOADING (+ve load, trailer pushing tractor)	+20kN to -40 kN	+120 kN
VERTICAL LOADING (+ve load downards)	±7 kN	±24 kN
LATERAL LOADING (+ve loading applied from Kerbside)	±20 kN	+33 kN

CHAPTER 3

BASIS OF THE THEORETICAL MODEL

3.1 Introduction

When an articulated tipper unit is being loaded or is tipping, it is unlikely to be standing on perfectly level ground. Also, the centre of gravity of the load is unlikely to be in the centre of the body. Hence the loads carried by the suspension and tyres on one side of the tipper will be greater than those on the other side. This uneven loading will cause the tyres and suspension on one side of the tipper unit to deform more than those on the other side. It will also cause the chassis to deform; the twisting about its longitudinal axis is the most significant mode of deformation. As a result of these deformations, caused by the uneven loading, the position of the centre of gravity moves even further towards the more heavily loaded side. This causes even more uneven loading and further deformations.

Under stable conditions, a situation will exist at which the position of the centre of gravity, the deformations and the forces transmitted through the system are compatible. Instability, resulting in roll-over would occur if the overall centre of gravity of the load, body, chassis etc. were to fall outside the area bounded by the contact of the wheels with the ground.

Although the stresses within the chassis, suspension, tyres etc. may be well within the linear elastic limits for the materials used, the position of the centre of gravity of the load can be significantly altered by the elastic deformations. The movement of the centre of gravity is largest when tipping is in progress. In order to analyse this type of non-linear, elastic system, an iterative procedure must be adopted. The basic procedure is illustrated in Section 3.4.1 using a simple example.

In some articulated tipper units, a further non-linearity arises from the use of height-controlled, pneumatically pressurised, airbag suspension units. In such systems, the distance between the axle of the centre pair of wheels and the chassis, is maintained constant on both, by increasing or decreasing the pressure in the airbags on each side independently. Under normal driving conditions this reduces the significant effect that the suspension deformations have on the overall movement of the centre of gravity. However, other deformations, such as the tyre compression, chassis twisting etc. still cause significant movements of the centre of gravity.

Two further non-linear situations can result from this type of airbag suspension. Firstly, if the pressure to one side should become zero (gauge), no further control is exerted, ie. the airbag is effectively removed from that side. Secondly, above a maximum allowable pressure, a cut-off valve operates and the compression of the fixed volume of air trapped in the system at this stage controls the deformation of the suspension. Under these conditions, an effectively polytropic compression of the gas occurs.

Other non-linear effects, such as clearance in the hinges connecting the body to the chassis and separation of the fifth wheel plate and the king pin have not been included. However, unless wear is very great and/or the tipper unit is in an unstable condition, these effects are likely to be small compared to those described above.

The theoretical model developed for predicting the behaviour of a tipping trailer unit, under tipping conditions, requires only one set of finite element analyses to calculate the flexibility matrix for a particular chassis and tractor. A computer program was developed based on the theoretical model. It requires the use of the chassis finite element results, tyre stiffnesses, air-bag characteristics, etc. It can be used to assess the stability of the particular tipping trailer unit, for any combination of ground slope, payload and tipping angle.

3.2 Co-ordinate system

The theoretical model requires a system to define the initial undeformed and subsequent deformed positions of the tipping trailer unit. A trailer datum, coordinate axis, ground slope and ram length are required.

(i) The trailer datum and coordinate axis are used to describe the position of the elements in the finite element model in an undeformed and deformed position. The coordinate system is also used to describe the position of the ram to body contact when tipped and the body and payload centre of gravity in an undeformed or deformed position. The datum position is at the centre of the chassis/body hinges. The +X direction is defined from the datum along a line parallel to the ground in the forward direction. The +Z direction is defined from the datum along a line passing through the right body chassis hinge in a undeformed state when viewed from the rear of the trailer. The +Y direction is upwards (perpendicular to the XZ plane), they form a right handed system of axes, as shown in Fig. 3.1.

(ii) The ground slope is used to describe the trailer unit's position (XZ plane) relative to the horizontal, and is a rotation about the X axis only. The ground slope, θ_p, is shown in Fig. 3.1. Only a positive ground slope (clockwise rotation about the X axis) is considered.

(iii) The ram length is used to describe the tipped position of the body, and varies between 2 and 8 meters.

3.3 Assumptions

The main assumptions made in this work are as follows:

3.3.1 The body

The body discussed in Section 2.1 is assumed to be rigid and to be connected to the chassis by a hinge bar at the back and a ram at the front. The connection at the hinge bar is assumed to have no clearance in it. It is further assumed that there is negligible friction in this hinge and that the force acting along the hinge bar, due to its contact with the chassis, ie. in the transverse direction of the tipper unit, occurs at the left hinge. The connection between the ram and the body is assumed to be a pin-joint with negligible friction.

3.3.2 The chassis (Trailer & Tractor)

The mainrails and cross-members of the trailer and tractor chassis described in Section 2.1 are assumed to stretch, compress, bend and twist according to beam theory. That is, local deformations at the connections between cross-members and mainrails, and at load application points are assumed to be negligible. The components welded to the underside of the chassis, containing the pivot bush (hinge), which connects the trailing arm to the chassis, is also represented by a cantilever beam.

The trailer chassis is connected to the body by a hinge bar at the back and a ram at the front. It is assumed that there is negligible friction in the hinge and that the transverse force acting on the chassis, at the hinge bar, occurs on the upper side of the chassis. The connection between the ram and the chassis is assumed to be a pin-joint with negligible friction.

The fifth wheel and king pin unit, described in Section 2.1, connects the chassis to the fifth wheel plate on the tractor unit. It is assumed to allow relative rotation of the fifth wheel plate and the chassis plate, about an axis perpendicular to these plates, through the king pin, and about a transverse axis in the Z direction through the king pin only. Other displacements of the tractor and chassis, at the point of contact between the king pin and the fifth wheel plate, are assumed to be the same for the tractor and chassis. That is, it is assumed that there is no clearance in the connection between the king pin and fifth wheel and that there is no separation between the fifth wheel plate and chassis plate. It is also assumed that friction effects in the region of contact between the tractor and chassis is negligible.

The trailing arms on the suspension, which connect the axle to the chassis, described in Section 2.1, are assumed to be connected by hinges. That is, free (frictionless) relative rotation of the chassis and trailing arms is allowed about an axis through the point of contact which runs transverse relative to the chassis. Other deflections of the chassis and trailing arms at the points of contact between them, are assumed to be the same, ie. it is assumed that there is no clearance in the hinges.

Each airbag is assumed to apply a force to the chassis at the point on the chassis which is on the centre-line of the airbag. It is further assumed that the force acts along the axis of the airbag, ie. the resistance to motion, of one end of the airbag relative to the other, perpendicular to its axis, is assumed to be negligible.

3.3.3 The suspension

The suspension systems, described in Section 2.1, are comprised of trailing arms and torsion beams and are assumed to stretch, compress, bend and twist according to beam theory. That is, local deformations at the connections between these components and the mainrails and at load application points are assumed to be negligible. Also, it is assumed that the trailing arm seats rigidly attach the trailing arms to the torsion beams. The shock absorbers, which are intended to damp out vibrations when the trailer is in motion have little effect when the trailer is stationary. The shock absorbers are therefore assumed to be inactive in the present analysis.

Each airbag is assumed to apply a force to a trailing arm at the point on the trailing arm which is on the axis of the airbag. It is further assumed that the force acts along the axis of the airbag, ie. the resistance to transverse motion of one end of an airbag relative to the other, perpendicular to its axis, is assumed to be negligible.

The forces exerted by the airbags, when operating under pressure control, are assumed to be proportional to the pressure. This has been verified experimentally; details are given in Appendix A. Once the maximum pressure is achieved in the airbags on one side, and the cut-off valve operates, the force, F, in the three bags on that side and the sum of the lengths of the three airbags, Σl, are assumed to be governed by a polytrophic gas law, ie. $F(\Sigma l)^n$ = a constant. This has been verified experimentally and the value of n has been determined; details are given in Appendix A.

Each of the trailer wheel/tyre units, which is connected to the end of a torsion bar, is assumed to be represented by three springs. Each of these three springs has a stiffness which represents the relationship between the force and displacements of the axis of the wheel, in the radial, rolling and transverse directions, assuming no slip between the tyre and the ground.

The vertical spring stiffness was obtained experimentally; details are given in Appendix B. The fore/aft and transverse spring stiffnesses were also determined experimentally, however the manufacturers data was used, as the experimental procedure over estimated them, as explained in Appendix B.

Each of the tractor wheel/tyre units is assumed to be represented by three mutually perpendicular springs. The stiffnesses were obtained from manufacturers information.

3.3.4 Ground conditions

All contact areas between wheels and the ground (tractor and trailer) are assumed to lie on a plane with all lower wheels at the same elevation and all upper wheels at the same elevation. The ground is assumed to be rigid, ie. the axles only move due to compression of the tyres, no compression of soft or loose ground is included because this would be difficult to define.

3.4 Theoretical basis

3.4.1 Simple illustration of principle

For the tipping trailer unit, the body containing the payload is assumed to be rigid and the rest of the system, comprising the tractor unit, the trailer chassis, suspension and tyres, is assumed to undergo linear elastic deformations. A tipping trailer unit is similar to a number of other engineering systems in the sense that small, linear elastic deformations of some parts of the system can cause large displacements of the positions of the loads (eg. the centre of gravity of the payload, the top of the ram and the line of action of the wind load).

The simple cantilever beam, of length l, made of a material with a Young's modulus of E and with a cross-section having a second moment of area about the horizontal axis of I, loaded by a constant, relatively small load, L, carried on a rigid frame, as shown in Fig. 3.2a, illustrates the type of problem for which this is the case. In the undeformed position, the end of the beam is subjected to a force L and a moment of magnitude La, as shown in Fig. 3.2b. However, these cause displacement $\Delta^{(1)}$ and rotation $\phi^{(1)}$ of the tip of the cantilever, where

$$\Delta^{(1)} = \frac{Ll^3}{3EI} + \frac{Lal^2}{2EI} \quad \text{(3.1a)}$$

and

$$\phi^{(1)} = \frac{Ll^2}{2EI} + \frac{Lal}{EI} \quad \text{(3.1b)}$$

resulting in a movement of the rigid frame, and hence a change in the load position, as shown in Fig. 3.2c. In this deformed position, the load on the beam is still L, but the moment becomes $L(a+b\theta)$, assuming that θ is small enough for $\sin\phi \simeq \phi$ and $\cos\phi \simeq 1$.

Hence, using the updated load and moment, the displacement and rotation of the tip of the beam, $\Delta^{(2)}$ and $\phi^{(2)}$, can be obtained, ie.,

$$\Delta^{(2)} = \frac{Ll^3}{3EI} + \frac{L(a+b\phi^{(1)})l^2}{2EI} \quad \text{(3.2a)}$$

and

$$\phi^{(2)} = \frac{Ll^2}{2EI} + \frac{L(a+b\phi^{(1)})l}{EI} \quad \text{(3.2b).}$$

Although, in this example a further iteration is not necessary.

If the process is repeated i times, the displacement, $\Delta^{(i)}$, and rotation, $\phi^{(i)}$, of the tip of the cantilever are given by

$$\Delta^{(i)} = \frac{Ll^3}{3EI} + \frac{L(a+b\phi^{(i-1)})l^2}{2EI} \tag{3.3a}$$

and

$$\phi^{(i)} = \frac{Ll^2}{2EI} + \frac{L(a+b\phi^{(i-1)})l}{EI} \tag{3.3b}$$

By continuing the iterative procedure until the differences between $\Delta^{(i)}$ and $\Delta^{(i-1)}$ and between $\phi^{(i)}$ and $\phi^{(i-1)}$ are negligible, the actual solution is obtained. At this stage, the load and moment transmitted to the beam, through the displaced rigid frame, are compatible with the displacement and rotation of the tip of the beam calculated using these forces and moments.

3.4.2 Principle applied to tipping trailer

The whole of the following description and calculation applies to one initial position of the body, ie. one fixed ram length. It has to be repeated for other ram lengths to analyse the complete tipping operation of a particular truck, unloading in a particular position. The body (assumed to be rigid) of the tipping trailer corresponds to the rigid frame in Fig. 3.2a. It is loaded by the payload $\underset{\sim}{P}$, and wind load $\underset{\sim}{W}$. As shown in Fig. 3.3, the equilibrium of the body is maintained by forces $\underset{\sim}{H}_L$ at the left hand hinge, $\underset{\sim}{H}_R$ at the right hand hinge and $\underset{\sim}{R}$ at the bottom of the ram (which is considered as part of the body). Just like the tip of the cantilever in Fig. 3.2a, the positions of these reactions change under load, because $\underset{\sim}{H}_L$, $\underset{\sim}{H}_R$ and $\underset{\sim}{R}$ are supported by the flexible chassis. Instead of Equ. 3.2, a stiffness matrix for the flexible parts of the vehicle (chassis, tyres and suspension etc.) has to be used to obtain the displacements of the connecting 'points' between the body and chassis (see Fig. 3.4). A similar iterative procedure to that used in the simple cantilever example allows the true displacements to be determined.

There are two other important differences between the simple illustration and the tipping trailer. The distributed weight of the chassis, wheels and suspension of the trailer, $\underset{\sim}{W}_C$, and the weight of the tractor, $\underset{\sim}{W}_T$, are significant loads on the chassis, which have to be included in the calculation of the displacements. Also, the airbags exert forces which have to be determined.

The three airbags on each side are connected so that they exert six identical forces, A_L, on the left and six other identical forces, A_R, on the right, as shown in Fig. 3.5. However, there are four possible operating conditions which exist for the airbag suspension system. Under normal conditions, the airbag pressure is continuously changed to maintain 'height control' (called 'H'), ie., the distance between each side of the central wheel axle and the chassis is maintained at a constant value. If the pressure in one of the sets of airbags reaches a maximum value, a cut-off valve operates and polytropic compression of the fixed mass of gas (called 'C') controls the airbag force and hence the deformations of the suspension on this side, while the other side can still be height controlled. Also, if the gauge pressure becomes zero for one of the sets of airbags , no further control is exerted on that set of airbags (called 'F'). Hence the airbags will be effectively removed form one side while the other side may be either height controlled, or controlled by the polytropic compression of a fixed mass of gas. In summary, for rolling to the right, the four possible airbag conditions are:

(a) the left and right side airbag pressures are both adjusted to give height control on both sides (ie., LH/RH),

(b) the left airbag pressure is adjusted to give height control on this side while the right side is controlled by the polytropic compression of a fixed mass of gas (ie., LH/RC),

(c) the left airbag is inoperative (gauge pressure of zero) while the right airbag pressure is adjusted to give height control on this side (ie., LF/RH) and

(d) the left airbag is removed while the right side is controlled by the polytropic compression of a fixed mass of gas (ie., LF/RC).

3.4.3 Basis of the tipping trailer analysis

The forces on the rigid body, and hence on the elastic parts of the system, (in a deformed position) are given in the free body diagrams shown in Fig. 3.3. The origin of the orthogonal, cartesian, co-ordinate system (X, Y, Z) is in the middle of the axis of the hinges which allow the body to be tipped. $\underset{\sim}{H}_L$ and $\underset{\sim}{H}_R$ are the reactions at the centres of the left and right hinge, $\underset{\sim}{B}$ is weight of the body, $\underset{\sim}{P}$ the magnitude of the payload and $\underset{\sim}{W}$ is the resultant of the wind forces acting on the body. $\underset{\sim}{R}$ is the force in the ram which lifts the front end of the body during tipping. In the analysis these forces are split into their cartesian components.

The components of rotation about the X and Y directions of the hinge-bar, which connects the body to the trailer chassis, are defined by θ and ψ, as indicated in Fig. 3.1 and Fig. 3.4.

The points on the chassis at which the deformations control the displaced position of the body and payload are the connection points with the hinge bar (the left, L, and right, R, rear positions on the chassis, see Fig. 3.3) and the connection point with the bottom of the ram. Although analytical solutions, such as those applicable to the deflection and rotation of the cantilever (ie. Equation 3.1), cannot be obtained to relate the deformations of the important points on the chassis to the loads applied to the chassis, the finite element method can be used to obtain the required relationships for each of the four possible suspension conditions.

Unlike the force, L, in the simple illustration in Fig. 3.2, the forces $\underset{\sim}{H}_L$, $\underset{\sim}{H}_R$ and $\underset{\sim}{R}$ vary during the iteration. For each of the four suspension conditions (a, b, c, d in Section 3.4.2) the finite element program was run for one load at a time, making this load unity. The required displacements, due to each unit load, were stored and later multiplied by the i th values of the loads to calculate the (i+1) th values of deformation.

The 14 unit loads were:

a) the cartesian components of the body contact forces, H_{Lx}, H_{Ly}, H_{Lz}, H_{Rx}, H_{Ry}, R_x, R_y, and R_z. (NB. $H_{Rz} = 0$ because there must be axial clearance between the body and chassis at the hinge bar);

b) the distributed weight of the tractor, W_{Ty} and W_{Tz};

c) the distributed weight of the chassis, suspension and wheels, W_{Cy} and W_{Cz};

d) the airbag forces, A_L and A_R, each acting in six positions, as shown in Fig. 3.5.

The reactions to each of these loads were taken where the ten wheels touch the ground (see Fig. 3.3).

The 15 important cartesian components of displacement were:

a) at the connections to the body, u_{hl}, v_{hl}, w_{hl}, u_{hr}, v_{hr}, w_{hr}, u_{rb}, v_{rb} and w_{rb}; (suffices refer to hinges at left and right and the ram bottom end);

b) at the upper ends of the airbags v_{a1}, v_{a3} and v_{a5};

c) at the lower ends of the airbags, v_{a2}, v_{a4}, v_{a6};

Suffices 1 and 2 refer to the 1st airbag, 3 and 4 to the 2nd airbag and 5 and 6 to the 3rd airbag, see Fig. 3.5.

3.4.3a <u>Suspension on both sides operating under height control (LH/RH)</u>

In the finite element analysis, in order to model the situation when both sides are height controlled, tie bar elements were placed between E and B and between C and D (see Fig. 3.5) to keep the distances EB and CD constant. In the truck, the tie bars do not exist, there are only height sensing devices, which do not transmit any forces between EB or CD. Therefore the forces exerted by the airbags must be adjusted during each iteration to make the tie bar forces zero. Hence, an influence matrix,

$[I^a]$, relating the important displacements to the forces can be obtained, such that

$$\underset{\sim}{u} = [I^{(a)}]\ \underset{\sim}{F} \qquad (3.4a)$$

where $[I^a]$ is the flexibility matrix obtained from the finite element work,

$$\underset{\sim}{u}^t = \left[u_{rb}, v_{rb}, w_{rb}, u_{hl}, v_{hl}, w_{hl}, u_{hr}, v_{hr}, w_{hr}, v_{a1}, v_{a2}, v_{a3}, v_{a4}, v_{a5}, v_{a6}\right] \qquad (3.4b)$$

and

$$\underset{\sim}{F}^t = \left[R_x, R_y, R_z, H_{Lx}, H_{Ly}, H_{Lz}, H_{Rx}, H_{Ry}, W_{Ty}, W_{Tz}, W_{cy}, W_{cz}, A_L, A_R\right] \qquad (3.4c).$$

[N.B. The superscript, t, used in equations 4b and 4c, and in subsequent equations, refers to the transpose of the matrix].

Equations 3.4 are the equivalent, for the tractor and trailer system, of Equations 3.1 for the simple cantilever problem used to illustrate the approach.

As well as determining the important displacements, the components of the forces in the tie bars can be obtained from the finite element results for each unit load applied to the finite element mesh; hence, it is possible to determine an influence matrix, $[I_T^{(a)}]$, which relates the tie bar forces, $\underset{\sim}{T}$, to the force vector, $\underset{\sim}{F}$, ie.

$$\underset{\sim}{T} = [I_T^{(a)}]\ \underset{\sim}{F} \qquad (3.5a)$$

where

$$\underset{\sim}{T}^t = \left[T_L, T_R\right] \qquad (3.5b)$$

The relationships between A_L and A_R and the other forces can be obtained from equation 3.5a by imposing the condition $\underset{\sim}{T} = \underset{\sim}{0}$.

From the finite element analyses, the relationship between the tyre forces transmitted to ground, $\underset{\sim}{G}$, and the other forces, $\underset{\sim}{F}$, can be obtained, ie.

$$\underset{\sim}{G} = \left[I_G^{(a)}\right] \underset{\sim}{F} \qquad \textbf{(3.6)}$$

The initial components of the force vector, $\underset{\sim}{F}$, at the connection points between the body and chassis, related to the undeformed position of the system can be obtained by considering the equilibrium of the body and payload in the undeformed position. In the undeformed position, θ and ψ, indicated in Fig. 3.4, are both zero. The force and moment equilibrium equations for the body and payload, in vector form, are as follows:

$$\underset{\sim}{H_L} + \underset{\sim}{H_R} + \underset{\sim}{R} + \underset{\sim}{B} + \underset{\sim}{P} + \underset{\sim}{W} = \underset{\sim}{0} \qquad \textbf{(3.7a)}$$

and

$$\underset{\sim}{H_L} \wedge \underset{\sim}{h_l} + \underset{\sim}{H_R} \wedge \underset{\sim}{h_r} + \underset{\sim}{R} \wedge \underset{\sim}{r_t} + \underset{\sim}{B} \wedge \underset{\sim}{b} + \underset{\sim}{P} \wedge \underset{\sim}{p} + \underset{\sim}{W} \wedge \underset{\sim}{w} = \underset{\sim}{0} \qquad \textbf{(3.7b)}$$

When expanded, equations 3.7 produce six linear equations with eight unknown forces, shown in Fig. 3.6, ie., R_x, R_y, R_z, H_{Lx}, H_{Ly}, H_{Lz}, H_{Rx} and H_{Ry}. By assuming that the ram is pin-jointed at both ends, the ram load components (R_x, R_y and R_z) can be related to the resultant ram force $\underset{\sim}{R}$, which must act along the axis of the ram. In the initial undeformed position, the co-ordinates of the top and bottom of the ram are known from the dimensions of the vehicle. Therefore, the vector, $\underset{\sim}{r}_{tb}$, which defines the position of the top of the ram relative to the bottom of the ram, which in turn defines the line of action of the ram force, $\underset{\sim}{R}$, can be obtained, ie.,

$$\underset{\sim}{r}_{tb} = \underset{\sim}{r}_t - \underset{\sim}{r}_b \quad (3.8)$$

Hence equations 3.4 can be solved to obtain the components of the chassis forces, $\underset{\sim}{F}$, at the connection points between the chassis and body, related to the undeformed position of the body and payload. Using these forces together with the tractor and chassis self weight forces, equations 3.5a can be used, with $\underset{\sim}{T} = \underset{\sim}{0}$, to obtain the suspension forces, A_L and A_R. Hence, the complete force vector, $\underset{\sim}{F}^{(1)}$, related to the undeformed position can be determined. Substituting $\underset{\sim}{F}^{(1)}$ into equations 3.4 and 3.6 allows a first estimates for the important chassis displacements, $\underset{\sim}{u}^{(1)}$, and the left, rear tyre force, $G_{L3}^{(1)}$, to be determined.

Having determined $\underset{\sim}{u}^{(1)}$ values, the updated loads, $\underset{\sim}{F}^{(2)}$, can be obtained using the equilibrium equations 3.7 with the updated position vectors $\underset{\sim}{h}^{(1)}_l$, $\underset{\sim}{h}^{(1)}_r$, $\underset{\sim}{r}^{(1)}_t$, $\underset{\sim}{b}^{(1)}$, $\underset{\sim}{p}^{(1)}$ and $\underset{\sim}{w}^{(1)}$. The facts that the body is assumed to be rigid, the ram length is constant during the iteration process and the small changes in distance between the centre of the hinge bar and the bottom of the ram during the deformation process are insignificant (further explanation is given later) allows the updated, position vectors to be related to the initial position vectors.

The vector defining the position of the top of the ram, $\underset{\sim}{r}_t$ (or $\underset{\sim}{r}_t^{(1)}$), is at right angles to the vector defining the position of the left hinge, $\underset{\sim}{h}_l$ (or $\underset{\sim}{h}_l^{(1)}$); displacement of the body does not affect this, because the body is assumed to be rigid. Therefore, the scalar product of the vectors $\underset{\sim}{r}_t$ (or $\underset{\sim}{r}_t^{(1)}$) and $\underset{\sim}{h}_l$ (or $\underset{\sim}{h}_l^{(1)}$) is zero, ie.,

$$\underset{\sim}{r}_t^{(1)} \cdot \underset{\sim}{h}_l^{(1)} = 0 \tag{3.9}$$

Also, if the distance between the centre line of the hinge bar and the bottom of the ram, r_b, is constant (finite element analysis showed the changes in this distance to be negligible) and the ram length remains constant, then in the displaced position, the angle between the vectors $\underset{\sim}{r}_t$ (or $\underset{\sim}{r}^{(1)}_t$) and $\underset{\sim}{r}_b$ (or $\underset{\sim}{r}^{(1)}_b$), defined as γ, would remain constant. Hence,

$$\underset{\sim}{r}_t^{(1)} \cdot \underset{\sim}{r}_b^{(1)} = r_t \, r_b \cos \gamma \tag{3.10}$$

and

$$\begin{aligned} &\left(r_{tx}^{(1)} - r_{bx}^{(1)}\right)^2 + \left(r_{ty}^{(1)} - r_{by}^{(1)}\right)^2 + \left(r_{tz}^{(1)} - r_{bz}^{(1)}\right)^2 \\ &= \left(r_{tx} - r_{bx}\right)^2 + \left(r_{ty} - r_{by}\right)^2 + \left(r_{tz} - t_{bz}\right)^2 \end{aligned} \tag{3.11}$$

From equations 3.9, 3.10 and 3.11, $\underset{\sim}{r}_t^{(1)}$ ($\underset{\sim}{r}_{tx}^{(1)}, \underset{\sim}{r}_{ty}^{(1)}, \underset{\sim}{r}_{tz}^{(1)}$) can be determined. Having obtained $\underset{\sim}{r}_t^{(1)}$ the other unknown position vectors, ie. $\underset{\sim}{p}^{(1)}$, $\underset{\sim}{b}^{(1)}$ and $\underset{\sim}{w}^{(1)}$ are all obtained in a similar manner. For example, the triangle defined by the centre of the hinge bar, the top of the ram and the centre of gravity of the payload remains fixed in shape, because the body/payload is assumed to be rigid. If the angle between the vectors $\underset{\sim}{r}_t$ and $\underset{\sim}{p}$ is taken to be δ (say), this angle can be obtained on the basis of the undeformed position of the chassis, ie.,

$$\underset{\sim}{r}_t \cdot \underset{\sim}{p} = r_t \, p \cos \delta \tag{3.12}.$$

In the displaced position, δ remains constant, therefore

$$\underset{\sim}{r}_t^{(1)} \cdot \underset{\sim}{p}^{(1)} = r_t \, p \cos \delta = r_t \cdot \underset{\sim}{p} \tag{3.13}$$

Also,and

$$\underset{\sim}{p}^{(1)} \cdot \underset{\sim}{h}_l^{(1)} = \underset{\sim}{p} \cdot h_l \tag{3.14}$$

$$\left(p_x^{(1)}\right)^2 + \left(p_y^{(1)}\right)^2 + \left(p_z^{(1)}\right)^2 = p^2 \tag{3.15}$$

The solution of equations 13, 14 and 15 allow $\underset{\sim}{p}^{(1)}$ (p_x, p_y, p_z) to be determined. By replacing $\underset{\sim}{p}^{(1)}$ by $\underset{\sim}{b}^{(1)}$ or $\underset{\sim}{w}^{(1)}$, then $\underset{\sim}{b}^{(1)}$ and $\underset{\sim}{w}^{(1)}$ can also be obtained.

With the updated position vectors, ie., $\underset{\sim}{h}_l^{(1)}$, $\underset{\sim}{h}_r^{(1)}$, $\underset{\sim}{r}_t^{(1)}$, $\underset{\sim}{b}^{(1)}$, $\underset{\sim}{p}^{(1)}$ and $\underset{\sim}{w}^{(1)}$, equations 3.7 can be solved to obtain the updated components of the forces between the body and chassis. These forces, together with the tractor and chassis self-weight forces can be used in equation 3.5, with $\underset{\sim}{T} = \underset{\sim}{0}$, to obtain updated suspension forces. Hence, an updated total force vector, $\underset{\sim}{F}^{(2)}$, can be obtained. An improved set of displacements, $\underset{\sim}{u}^{(2)}$, and rear, left-hand tyre force, $G_{L3}^{(2)}$, can be obtained using equations 3.4 and 3.6, respectively. These updated displacements can then be used to obtain the updated position of the top of the ram $\underset{\sim}{r}_t^{(2)}$, as indicated by equations 3.9, 3.10 and 3.11. Then, the updated positions of the other important points can also be obtained and used to obtain a further update of the chassis load vector. This process is repeated until either the changes in displacement are negligible or an unstable solution, indicating a rollover condition, is obtained. The onset of instability is taken to be when the rear, left-hand tyre reaction force G_{L3} becomes zero.

A similar approach can be used to assess stability with the other three suspension conditions. The way in which these analyses differ from the one described above are outlined below.

3.4.3b Left suspension height controlled and right suspension governed by polytropic compression of a fixed mass of gas (LH/RC)

In this case, a tie bar is placed between C and D (see Fig. 3.5), as in the previous case. However, the tie bar is removed from the right hand side because the distance between E and B can decrease, governed by the polytropic compression of a fixed mass of gas in the three, connected, right hand airbags. Since the force in the right hand suspension, A_R, is related to the deformation of the system, an iterative procedure is required in this case. Again, unit forces $R_x = 1$ ... $H_{Ry} = 1$, ... $W_{cz} = 1$, $A_L = 1$ and $A_R = 1$, are applied in turn to the finite element mesh. For these units forces the left hand tie bar force, T_L, and the important chassis displacements, at points where the body and ram are attached, ie., $\underset{\sim}{u}$ are determined. As before, $\underset{\sim}{u}$ can be related to $\underset{\sim}{F}$, ie.,

$$\underset{\sim}{u} = \left[I^{(b)}\right] \underset{\sim}{F} \qquad \textbf{(3.16a)},$$

where a subset of matrix equation 16a, related to the right hand side air-bag displacement, is

$$\underset{\sim}{v_a} = \left[I_a^{(b)}\right] \underset{\sim}{F} \qquad \textbf{(3.16b)}$$

Also, as before, the tie-bar force, T_L, can also be related to $\underset{\sim}{F}$, ie.

$$T_L = \left[I_T^{(b)}\right] \underset{\sim}{F} \qquad (3.16c).$$

and the tyre forces, $\underset{\sim}{G}$, can be related to the $\underset{\sim}{F}$, ie.

$$\underset{\sim}{G} = \left[I_G^{(b)}\right] \cdot \underset{\sim}{F} \qquad (3.16d).$$

In addition to the above, the polytropic compression of the fixed mass of gas dictates that

$$A_R \left(3l_o + \sum_{i=1}^{6} v_{ai}\right)^n = constant \ (= Q) \qquad (3.17)$$

where l_o is the length of gas contained in the constant cross-sectional area cylinders, at the limiting pressure, ie., when the pressure supply is cut off, and $\Sigma\, v_{ai}$ is the sum of the changes of length of the three right hand airbags. The constant is obtained by substituting the instantaneous values of A_R and v_{ai} when A_R (which is proportional to the pressure) reaches the limiting value. The values of n and Q (for a given mass of gas) have been determined by performing experiments on airbags.

In order to obtain the solution to equations 3.16 and 3.17, an iterative procedure is adopted. A first estimate, $A_R^{(1)}$ of the force in the right hand airbags is substituted into equation 3.16c with $T_L = 0$, to obtain a first estimate, $A_L^{(1)}$, of the force in the left hand airbags. These first estimates for the airbag forces are then substituted into equation 3.16b to obtain a first estimate, $\underset{\sim}{v}_a^{(1)}$, for the displacements of the ends of the right hand airbags. The $\underset{\sim}{v}_a^{(1)}$ values are then substituted into equation 3.17 to obtain an updated estimate, $A_R^{(2)}$, for the force in the right hand airbags. This iterative procedure is continued until negligible change in the forces and displacements occur between one iteration and the next. At this stage, the $\underset{\sim}{F}$ matrix is substituted into equation 3.16a to obtain the updated displacements, $\underset{\sim}{u}^{(2)}$, which are used to obtain the new displaced position of the body and payload. As for the case described in Section 3.4a, the procedure is repeated, iteratively, until the changes in displacement and forces, including the right-hand airbag values are negligible.

3.4.2c Left suspension airbags inoperative and right suspension height controlled (LF/RH)

When the gauge pressure falls to zero in the left hand suspension, the airbags become inoperative and the forces A_L no longer act. For this condition, it is therefore only necessary to place a tie bar between E and B (Fig. 3.5) and to leave the left suspension free. By obtaining the displacements, $\underset{\sim}{u}$, and right-handed tie bar force, T_R, from the finite element results for each unit load case $R_x = 1, \ldots W_{cz} = 1$ and $A_R = 1$, the influence matrices $[I^{(c)}]$, $[I_T^{(c)}]$ and $[I_G^{(c)}]$ can be determined, such that

$$\underset{\sim}{u} = \left[I^{(c)}\right] \underset{\sim}{F} \qquad \textbf{(3.18a),}$$

$$T_R = \left[I_T^{(c)}\right] \underset{\sim}{F} \qquad \textbf{(3.18b).}$$

and

$$\underset{\sim}{G} = \left[I_G^{(c)}\right] \underset{\sim}{F}' \qquad \textbf{(3.18c)}$$

Note, in this case, the force vector, $\underset{\sim}{F}'$, does not contain left-hand airbag force, ie. $A_L = 0$, and the influence matrices $[I^{(c)}]$ and $[I_T^{(c)}]$ are smaller than the corresponding $[I^{(a)}]$, $[I^{(b)}]$, $[I_T^{(a)}]$ or $[I_T^{(b)}]$ matrices.

In operation, with height control between E and B, $T_R = 0$ would be applicable. Therefore, for a given set of forces, at the connections between the body and chassis, and using tractor and chassis components of self-weight, the right hand airbag force, A_R, can be obtained by setting $T_R = 0$ in equation 3.18b. This value of A_R is then substituted into equation 3.18a, along with the other forces to obtain the displacement, $\underset{\sim}{u}$, which define the updated displaced position of the body and payload. An iterative procedure is again adopted until the changes in displacements and forces are negligible.

3.4.2d Left suspension airbags inoperative and right suspension governed by polytropic compression of a fixed mass of gas (LF/RC)

In this case, $A_L = 0$ and the left hand tie bar is removed, because the left hand suspension system is inoperative, ie., no tie bar is present between C and D, as well as $A_L = 0$. Because the maximum pressure, and hence the maximum allowed value of A_R, has been reached, no tie bar is included between E and B either (see Fig. 3.5). Therefore, the method of applying unit loads in order to determine the influence matrices cannot be applied in this situation, because the finite element mesh would act as a mechanism.

By applying unit displacements to each of the important positions on the chassis in turn (ie., $u_{rb} = 1$, or $v_{rb} = 1$ or $w_{rb} = 1$ or $u_{hl} = 1$ or $v_{hl} = 1$ or $w_{hl} = 1$ or $u_{hr} = 1$ or $v_{hr} = 1$) and to the six right-hand airbag connection points in turn (ie., $v_{a1} = 1$ or $v_{a2} = 1$ ... or $v_{a6} = 1$), while restraining each of the other points, the reaction forces at the restrained positions can be obtained. These reaction forces form components in a stiffness matrix, such that,

$$[K]\,\underset{\sim}{u} = \begin{Bmatrix} \underset{\sim}{F}'' \\ \underset{\sim}{A_R} \end{Bmatrix} \qquad \textbf{(3.19a)}$$

where $\underset{\sim}{F}''$ is the same as $\underset{\sim}{F}$, but with the terms A_L and A_R omitted and

$$\underset{\sim}{A_R^t} = \left(A_{R1}, A_{R2}, A_{R3}, A_{R4}, A_{R5}, A_{R6}\right) \qquad \textbf{(3.19b)}$$

which are the forces corresponding to the right-hand airbag displacement, $\underset{\sim}{v}_a$. In reality, all of the A_{Ri} values (i = 1 to 6) must be the same, because the airbags are interconnected.

Matrix equation 3.19a can be rewritten as

$$\begin{bmatrix} [K_{11}] & [K_{12}] \\ [K_{21}] & [K_{22}] \end{bmatrix} \begin{Bmatrix} \underset{\sim}{u}'' \\ \underset{\sim}{v_a} \end{Bmatrix} = \begin{Bmatrix} \underset{\sim}{F}'' \\ \underset{\sim}{A_R} \end{Bmatrix} \qquad \textbf{(3.20).}$$

By eliminating $\underset{\sim}{u}''$, which is the same as $\underset{\sim}{u}$ but with the $\underset{\sim}{v}_a$ terms omitted, from matrix equation 3.20 and rearranging, an expression for $\underset{\sim}{v}_a$ can be obtained, ie.,

$$\underset{\sim}{v_a} = \left[[K_{22}] - [K_{21}]\,[K_{11}]^{-1}\,[K_{12}]\right]^{-1} \left\{\underset{\sim}{A_R} - [K_{21}]\,[K_{11}]^{-1}\,\underset{\sim}{F}''\right\} \qquad \textbf{(3.21).}$$

In addition to the above, the right hand side airbag forces, A_R, are related to the airbag displacement, $\underset{\sim}{v}_a$, via the gas equation which governs the polytropic compression of the fixed mass of gas, ie., equation 3.17 is applicable.

The solution, in this case, also requires an iterative approach. A first estimate, $\underset{\sim}{A}_R^{(1)}$, of the forces in the right hand airbags (each component in $\underset{\sim}{A}_R$ is taken to be the same) is substituted into equation 3.21 to obtain the first estimate for the right hand side airbag displacements, $\underset{\sim}{v}_a^{(1)}$. These airbag displacements can then be used in equation 3.17 to obtain an updated airbag force, $\underset{\sim}{A}_R^{(2)}$. This iteration, between equations 3.21 and 3.17, is continued until negligible changes in the airbag forces and displacements occur between one iteration and the next. Having obtained the airbag forces and displacement, equation 3.20 can be rearranged to allow the other chassis displacements, $\underset{\sim}{u}^*$, to be determined, ie.,

$$\underset{\sim}{u}^* = [K_{11}]^{-1} \left\{ \underset{\sim}{F}^* - [K_{12}] \, \underset{\sim}{v}_a \right\} \qquad \textbf{(3.22a)}$$

These updated chassis displacements, $\underset{\sim}{u}^*$, can now be used to obtain the updated, displaced position of the body and payload. Also, the forces at the contact points between the tyres and the ground can be related to $\underset{\sim}{u}$, ie.,

$$\underset{\sim}{G} = \left[I_G^{(d)} \right] \underset{\sim}{u} \qquad \textbf{(3.22b)}$$

An iterative procedure is again adopted until the changes in displacement and forces are negligible.

3.5. Outline of the overall solution procedure

The theoretical model, which enables the positions of the important points on the body, body/chassis contact point reactions, suspension forces, chassis displacements and tyre forces to be determined, requires a method to govern the sequence of operations. The theoretical model involves the solution of complicated equations, repetitive iterations and the multiplication of many matrices. This type of problem lends itself to solution by digital computer. Hence a program was written for an Akhter 286 PC using Turbo Basic; with this language, modifications are relatively easy and separate sub-routines can be written.

For each ground slope, ram length, wind loading and payload, the iterative calculation procedure used to establish the airbag operating conditions, deformed position, tyre force, etc., is outlined in the flow diagram shown in Fig. 3.7. A separate loop is applicable for each of the four possible airbag conditions. Within each of the four loops, there are some common features. The important position vectors (ie. $\underset{\sim}{h}_l$, $\underset{\sim}{h}_r$, $\underset{\sim}{r}_t$, $\underset{\sim}{b}$, $\underset{\sim}{p}$ and $\underset{\sim}{w}$) are determined using equations 3.9 to 3.15 and the direction of the ram is obtained using equation 3.8. With these position and direction vectors, equations 3.7a and 3.7b are solved to determine the forces on the body (ie. $\underset{\sim}{R}$, $\underset{\sim}{H}_L$ and $\underset{\sim}{H}_R$). Hence, the equal and opposite forces applied to the chassis by the hinge bar, connecting the chassis to the body, and the bottom of the ram are obtained. Using the appropriate airbag conditions, the airbag forces can be determined and hence the total force vector, $\underset{\sim}{F}$, applied to the chassis can be obtained. This force vector, $\underset{\sim}{F}$, is then used with the influence matrices (for the appropriate airbag conditions) to obtain the updated displacements. The procedure is continued until the changes in the predicted displacements are negligible. The tyre forces are then calculated.

The program's initial execution of each iteration is governed by the undeformed position of the tractor and trailer and body. For the first iteration, the transverse ground slope is taken to be zero and the body is considered in the untipped position. For this ram length, after each iteration of the ground slope is increased in 0.1° interval until a ground slope of 10° is reached or until instability occurs, ie. the rear left wheel force becomes zero. The ground slope is then zeroed and the ram length is increased by 0.5 m. Further iterations are again undertaken increasing the ground slope up to 10° or until instability occurs. The program's execution is terminated when the ram length reaches 8 m and instability occurs for the given ground slope.

Appendix C, "Computer Program and Flow Chart", describes the program subroutines and how they operate in a flow diagram and the program coding.

Appendix D, "Program User Guide" gives the necessary information to enable the user to run the program, use the results and change positional, loading and flexibility/stiffness matrices variables.

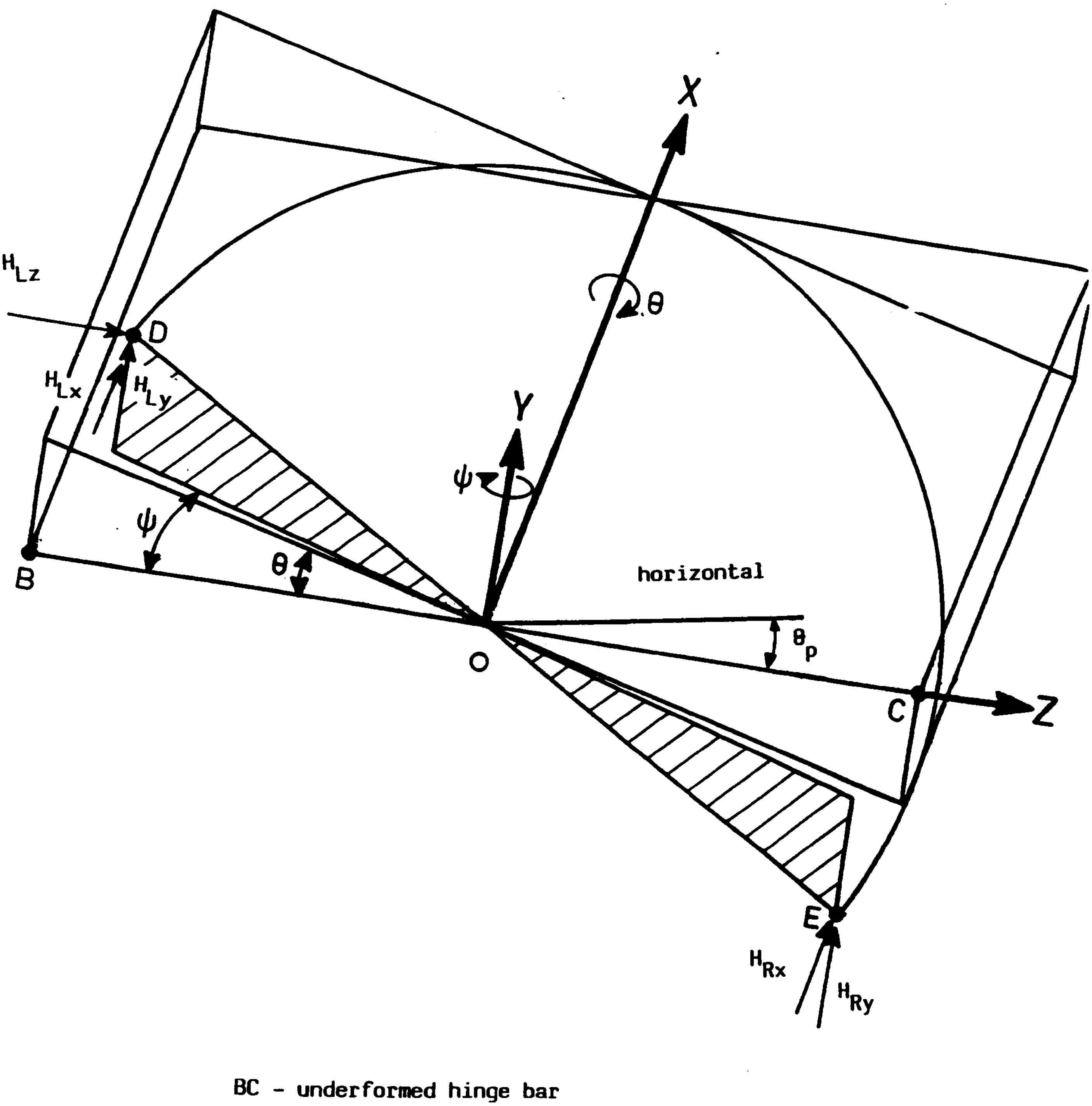

BC - underformed hinge bar

DE - deformed hinge bar

Fig. 3.1 Coordinate system and angular movement of hinge bar

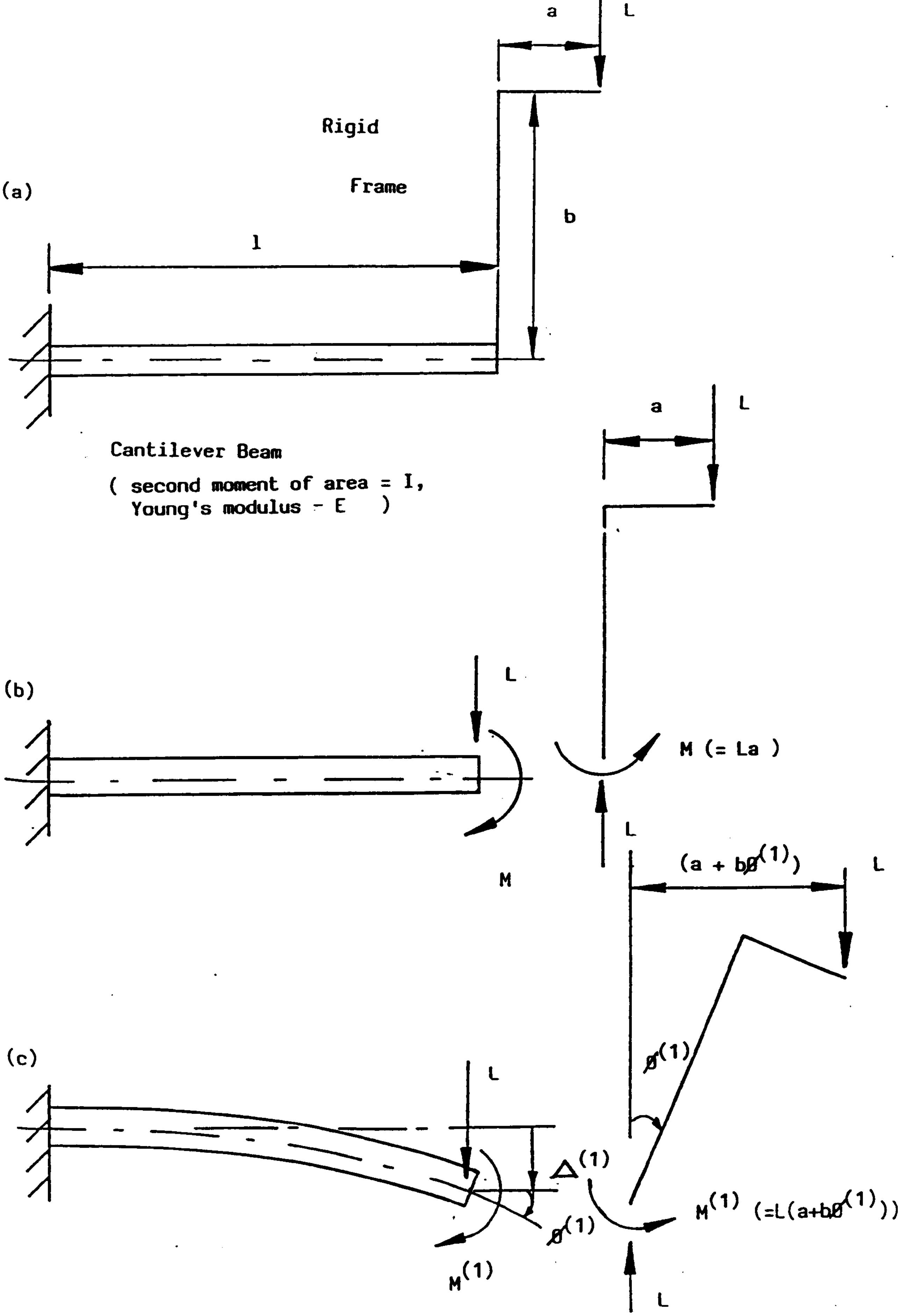

Fig. 3.2 Simple, cantilever example, to illustrate the interaction between small, elastic deformation and load position

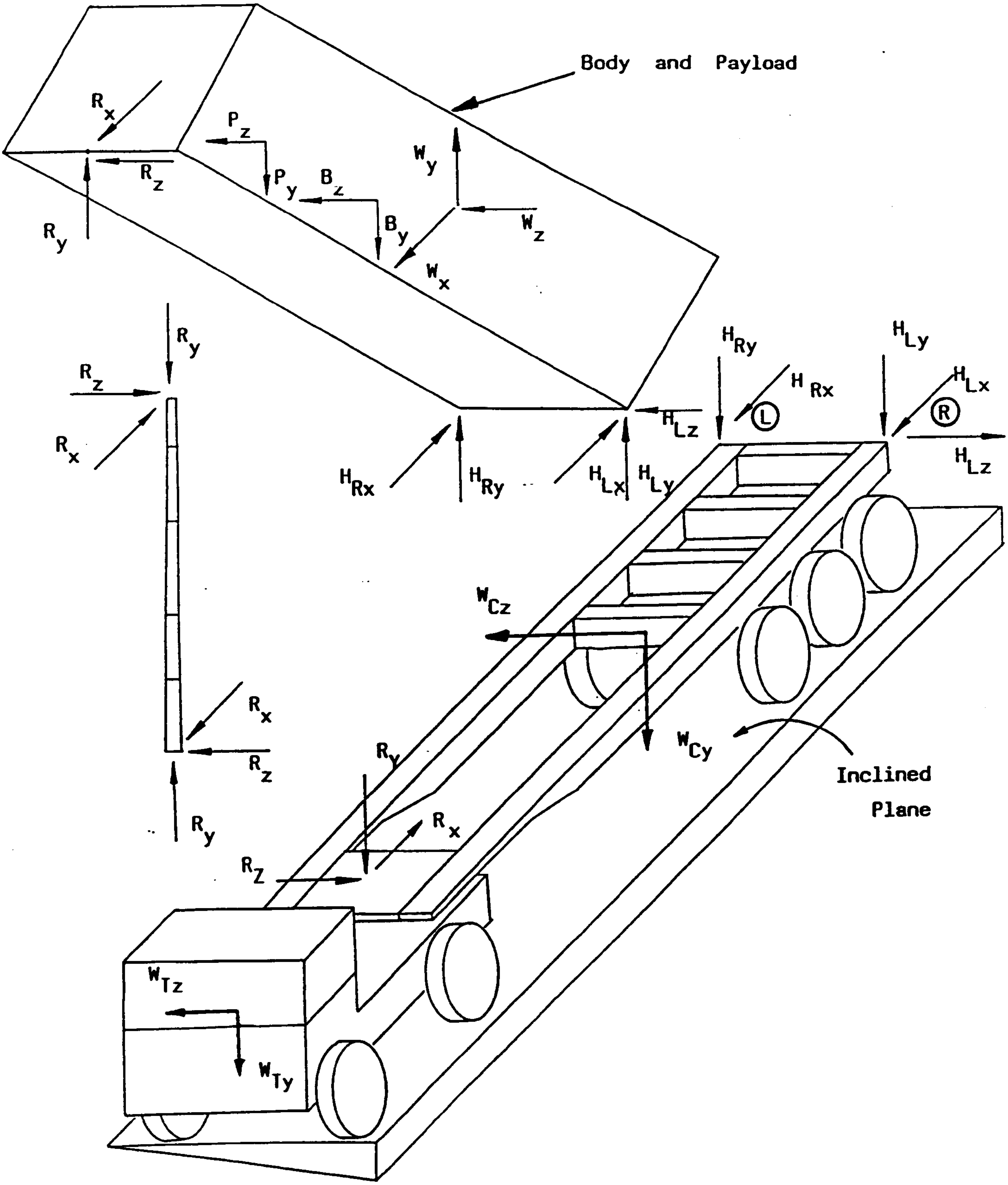

Fig. 3.3 Free body diagrams of

(i) the body and payload in a displaced position,

(ii) the ram in a displaced position, and

(ii) the tractor unit, trailer chassis, suspension and tyres combination in an undeformed position.

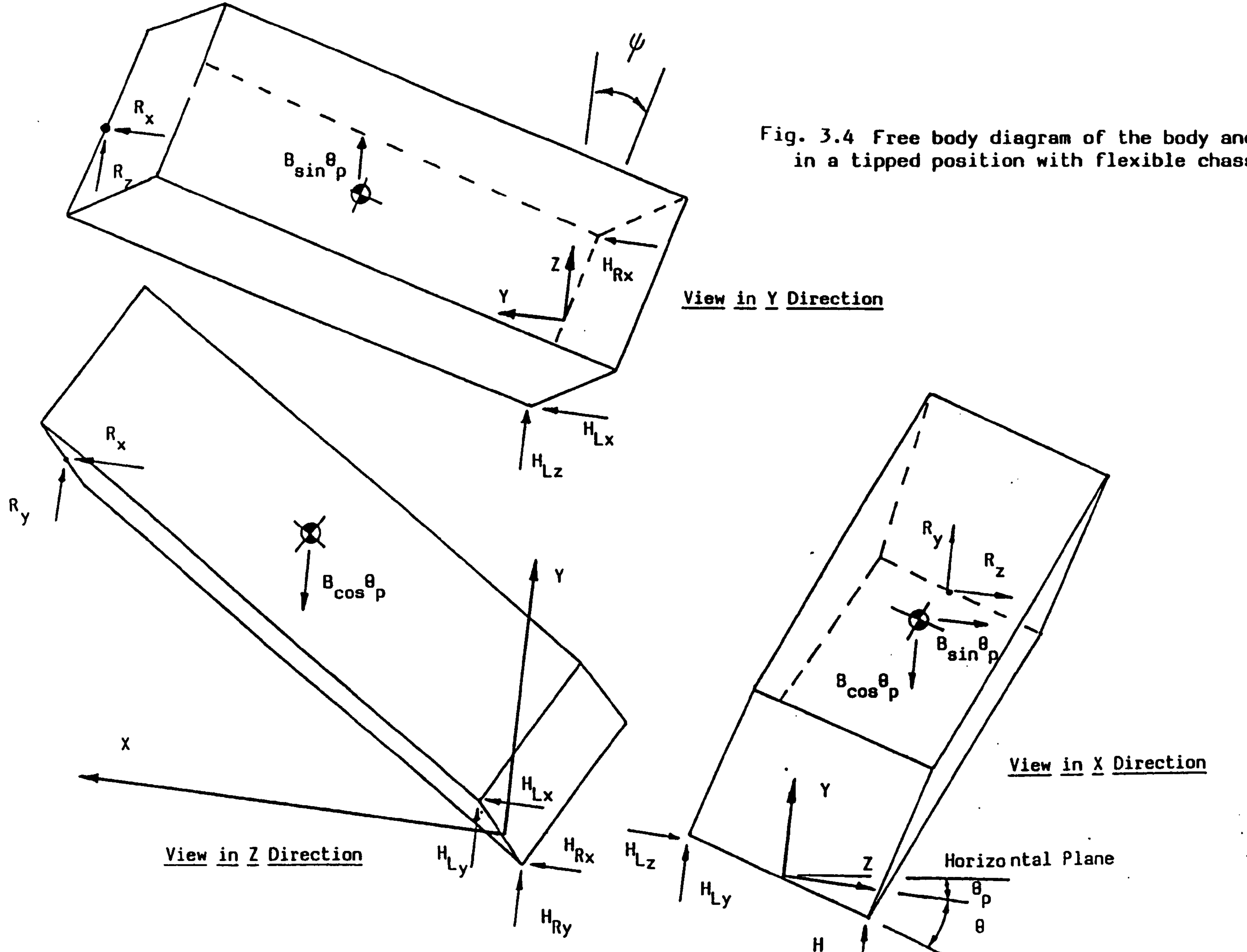

Fig. 3.4 Free body diagram of the body and payload in a tipped position with flexible chassis

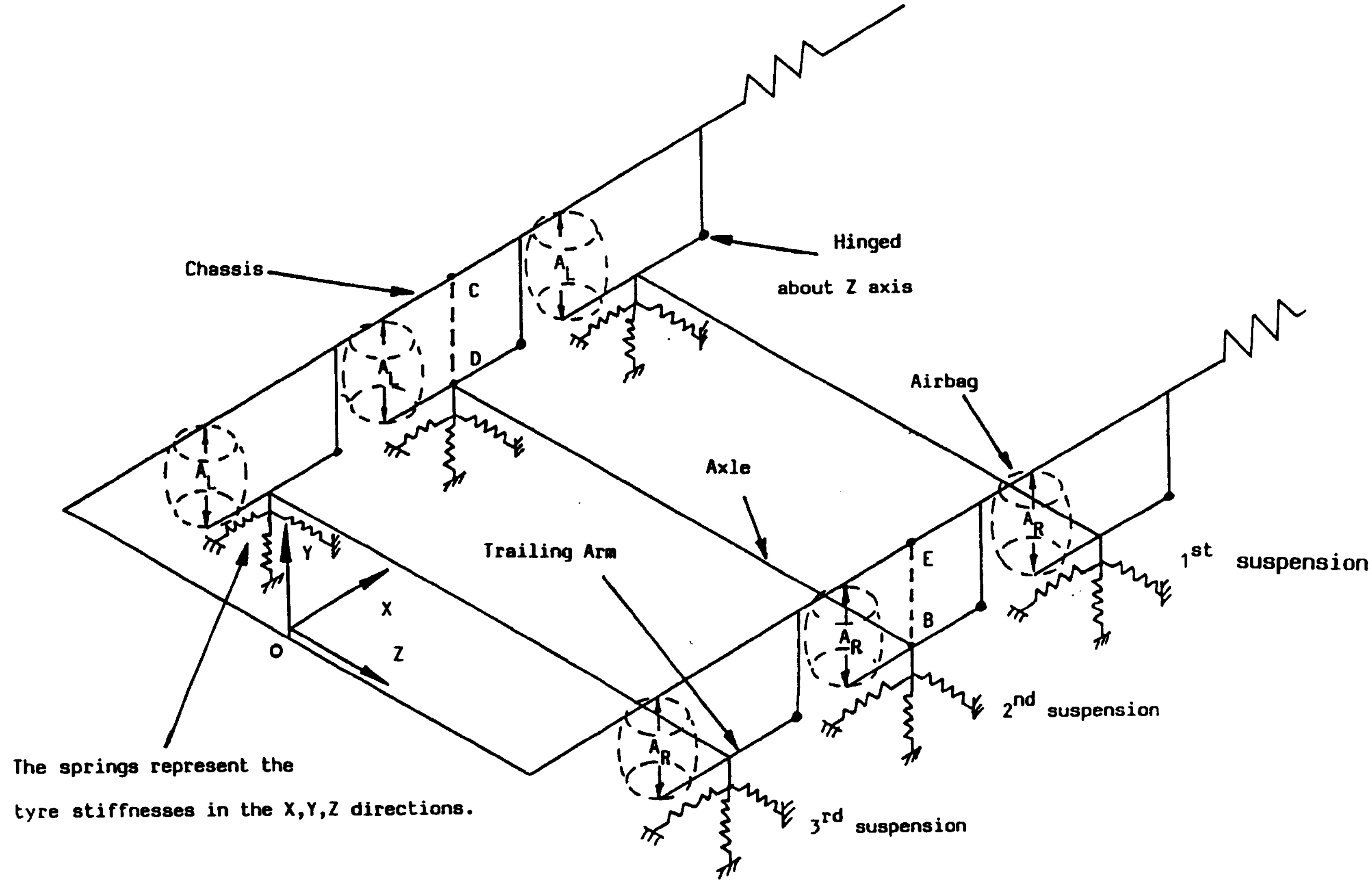

Fig. 3.5 Schematic diagram representing the rear part of the chassis, the suspension and tyres The forces A_L and A_R represent the forces applied by the left and right airbags. EB and CD are the height control positions.

Fig. 3.6 Force and moment equilibrium equations expanded into matrix form

$$
\begin{bmatrix}
1 & 1 & 0 & 0 & 0 & nx \\
-h_{1z} & -h_{rz} & 0 & 0 & h_{1x} & -nx(r_{tz}) + nz(r_{tz}) \\
0 & 0 & -h_{1z} & -h_{rz} & h_{1y} & -ny(r_{tz}) + nz(r_{ty}) \\
0 & 0 & 1 & 1 & 0 & ny \\
0 & 0 & 0 & 0 & 1 & nz \\
-h_{1y} & -h_{ry} & h_{1x} & h_{rx} & 0 & -nx(r_{ty}) + ny(r_{tx})
\end{bmatrix}
\times
\begin{bmatrix}
H_{Lx} \\ H_{Rx} \\ H_{Ly} \\ H_{Ry} \\ H_{Lz} \\ R
\end{bmatrix}
=
\begin{bmatrix}
-W_x \\
-W_z(w_x) + W_x(w_z) - B_x(b_z) - P_z(p_x) \\
-B_z(b_y) - B_y(b_z) - P_z(p_y) - P_y(p_z) - W_z(w_y) + W_y(w_z) \\
B_y + P_y - W_y \\
-B_z - P_z - W_z \\
B_y(b_x) + P_y(p_x) - W_y(w_x) - W_y(w_y)
\end{bmatrix}
$$

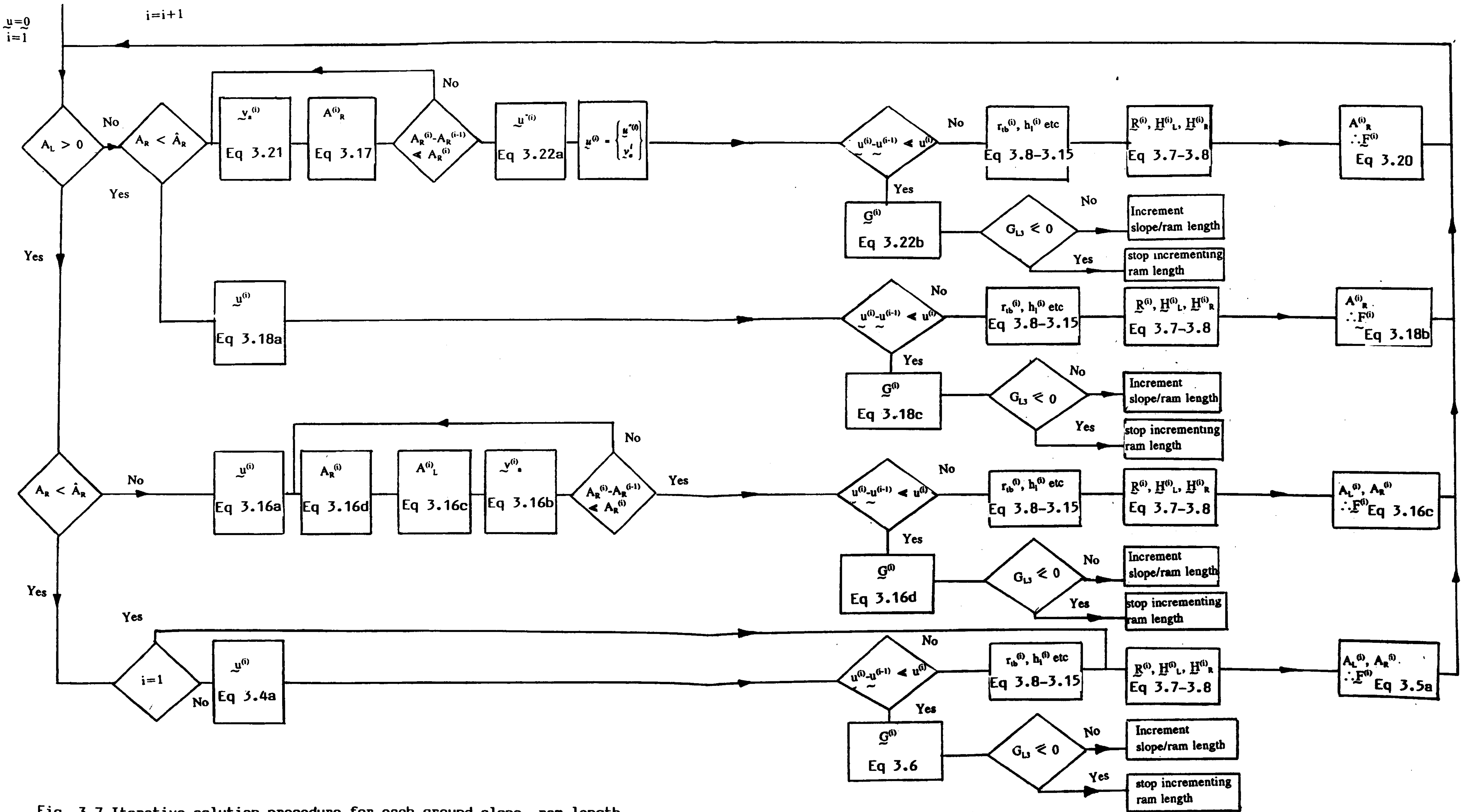

Fig. 3.7 Iterative solution procedure for each ground slope, ram length and payload.

CHAPTER FOUR

FINITE ELEMENT ANALYSES

4.1 Introduction

The previous theoretical roll-over models were based on lumped mass systems, representing various parts of the lorry inter-connected by compliant elements. Certain flexibilities such as the tyres, suspension units etc. could be obtained from the respective component manufacturers but the tractor and trailer chassis flexibilities are unknown. To overcome this problem the flexibilities of these components were obtained from full scale tests. This is a very expensive undertaking, providing a limited means in which to assess those elements of trailer design which are important in improving stability, without further recourse to more tilt tests.

It was decided that the finite element method should be used to model the tractor and trailer, in order to determine the important deformations. Once the finite element model is created it is relatively straight forward to make changes to the structure. Hence an assessment of component contribution to roll stability can be undertaken relatively inexpensively.

4.1.1 Flexible elements

Finite element analysis allows a structure to be simulated by dividing it into a number of elements which model its flexibility. This enables a relationship to be established between the structures applied loads and its displacement.

The tractor's components which are considered to be flexible are the chassis, suspension and tyres. The driver's cab is not considered as it is connected to the chassis by very flexible springs.

The trailer's components which are considered to be flexible are the chassis, suspension, tyres and axial tubes. The trailer's body is considered to be rigid as its flexibility is thought to have a second order effect on roll over stability. The fifth wheel model enables rotation between the tractor and trailer about the vertical (Y axis) and transverse (Z axis) axes only.

The finite element line diagram shown in Figs. 4.1 and 4.2 represent the Tractor and Trailer structure respectively, with node numbers denoted by a prefix "N" and the remaining numbers referring to element numbers. The element numbers can be used in conjunction with Table 4.1 to obtain the element property number. This can then be used in conjunction with Table 4.2 to obtain the element's mechanical properties (ie. second moment of area, stiffness, cross sectional area etc.) depending on the type of element.

4.1.2 Suspension operating modes

The suspension operating modes discussed in Section 3.4.2 affect the loading and boundary/loading conditions for the finite element model. For the three suspension operating modes (a, b, c) where at least one side is height controlled, the displacement and forces are derived from unit load flexibility and influence matrices.

As the air suspensions are represented by only forces, the finite element model of the suspension forms a mechanism. To overcome the problem of loading a mechanism, tie bars are inserted in the finite element model to maintain the required ride height. A tie bar is only inserted in the left or right suspension if it is height controlled.

For the remaining suspension operating mode (d) where neither side is height controlled, a tie bar cannot be inserted in the finite element model to overcome the problem of loading a mechanism. It is therefore not possible for the displacement and forces of such a structure to be obtained from unit load, flexibility matrices. Instead a unit displacement stiffness matrix was generated to determine the chassis displacements and suspension forces. A module within the PAFEC finite element package allows prescribed displacements to be imposed on the structure. The nodes of interest, where forces or displacements are required, are restrained in the appropriate directions.

4.2 Finite element meshes

The finite element mesh is constructed from six different elements and modules. These are used to model component flexibility, fifth wheel and suspension hinges and tyre/ground contacts.

4.2.1 Elements and modules

(i) Simple Beam Element: A straight simple beam element with a node at each end of the shear centre. The element is connected to the remainder of the structure by these nodes or by offset nodes. The element formulation includes bending in two directions, axial force and twisting. The main application of this element is for frame structures and stiffened plates.

(ii) Eight Noded Facet Shell Element: A flat thin shell element which can carry bending and membrane loads. The main applications are for shell problems in which either or both in-plane and out-of-plane effects are important.

(iii) Spring Element: A spring element which connects any pair of nodes with translatory stiffness in the x, y, z directions and with rotational stiffness about the X, Y, Z axes. The element is used whenever a discrete flexibility or stiffness needs to be introduced.

(iv) Mass Element: The mass element is used to model concentrated masses with a stiffness greater than those of the surrounding structure.

(v) Repeated Freedoms: The repeated freedom module is used to join two nodes which are to have one or more identical freedoms. The module can be used to provide relative movement between coincident nodes in order to model a hinge or slide connection.

(vi) Restraints: The restraints module is used to restrain the freedom of a node. The node can have all or just one of its six freedoms restrained.

(vii) Gravity: The gravity module is used to simulate the self weight of a structure by applying an acceleration of 9.81 m/s^2, or whatever the user defines.

4.2.2 Tractor chassis

The tractor unit described in Section 2.1, models the flexibilities of the chassis, suspension, tyres and fifth wheel. The finite element line diagram of the tractor unit, shown in Fig. 4.1 represents these details. The element numbers are given and the corresponding property values (depending on which type of element is being considered) can be obtained from Table 4.1 and 4.2.

The tractor chassis is divided into a series of beam elements to represent the ladder structure, with dimensions being obtained from detail drawings and the measurement of an actual vehicle. The chassis beams are channel sections welded together forming a ladder type structure, with the intersection of cross members and longitudinal members being treated as rigid joints. Beam elements 175 to 200 describe the chassis.

The leaf spring suspensions are modelled by translation springs, with their stiffnesses being obtained from manufacturers information. The front and rear suspension springs are connected between the chassis beams and the axle beam and are described by elements 213, 214 and 215, 216 respectively. In order to model the leaf springs the ends of each spring are made to have the same U_x and U_z displacement, with the U_y displacement being independent of each other, hence achieving a flexible connection in the y direction only.

The tractor has front and rear axles connected to the chassis by leaf springs and roll bars with single steering wheels attached to the front axle and dual driving wheels attached to the rear axle. The front and rear roll bars are described by elements 227 to 238, the front and rear axles are described by elements 219 to 226 and the tyres are described by elements 210 to 121. The tyre model is described in Section 4.2.5.

The tractor's mass is modelled by applying unit loads to the centre of gravity in the Y and Z directions. From gross vehicle axle weights the position of the centre of gravity could be determined in the fore/aft direction but the vertical position was obtained from an estimation made by the manufacturer.

4.2.3 Fifth wheel connection

The fifth wheel coupling described in Section 2.1 is modelled using the repeated freedoms module between nodes on the tractor unit and trailer unit. This allows rotation between the tractor and trailer unit about the Y and Z axes. The play between components which allows limited rotation about the X axis between the tractor and trailer is not modelled. Three nodes (292, 293, 294) shown in Fig. 4.2

on the tractor and three corresponding nodes (43, 40, 47) shown in Fig. 4.2 on the trailer were constrained to have certain displacements the same. The nodes 292, 43 and 294, 47 were constrained to have the same U_y displacements, while the nodes 293, 40 were constrained to have the same U_x and U_z displacements.

4.2.4 Trailer chassis

The trailer unit described in Section 2.1 models the flexibilities of the chassis suspension, tyres and king pin. The finite element line diagram shown in Fig. 4.2 represents these details. The element numbers are given and the corresponding property values (depending on which type of element is being considered) can be obtained from Table 4.1 and 4.2.

The chassis is divided into a series of beam elements with appropriate second moments of area and plate elements to represent the ladder structure, with dimensions being obtained from detail drawings. As the chassis beams vary in cross-section along their length, the average value of the second moment of area at the ends of each beam are used. The intersection of cross members and longitudinal members have been treated as rigid joints. The fifth wheel plate is represented by plate elements interconnected with beam elements. Plate elements 1 to 20 and beam elements 21 to 127 describe the chassis, see Fig. 4.2.

4.2.5 Trailer suspension

Each suspension unit consists of two airbags. The middle suspension system is described by nodes 180-211, 199-220, an axle tube described by beam elements 179, 252, 253, 173 two suspension supports described by beam elements 133, 148, two trailing arms described by beam elements 134, 135, 149, 150 and two tyres described by spring elements 137, 163, 152, 166 as shown in Fig. 4.2. The trailing arms on either side pivot about nodes 226 and 229 as the airbag height changes. In order to model the pivot the suspension support beam 133 and trailing arm beam 134 and 135 connection is made to have the same U_x, U_y, U_z displacements rotation. The z rotation is made independent of each other, hence achieving a pivot connection. This arrangement is repeated for the opposite side.

The tyres on the tractor and trailer are modelled using a vertical spring and two horizontal springs connected to the vertical spring at a distance of a tyre radius below the tyre centre. The base of the vertical spring is restrained in the vertical direction, with the fore/aft and lateral freedoms being restrained by the two horizontal springs. The other ends of these springs are completely restrained as shown in Fig. 4.3. The tyres on the trailer are described by the elements 132, 137, 142, 147, 152 and 157 as shown in Fig. 4.2. The tyres on the tractor are described by 201, 203, 205, 207, 209, and 211 as shown in Fig. 4.1.

4.3 Design investigations

Individual lorry components can be altered in the finite element model allowing an assessment of their contribution to roll stability to be made. Following discussions with the trailer manufacturer, three areas of chassis design were changed individually to assess their effect on roll stability.

(i) A 3 mm plate was attached between the left and right longitudinal chassis I beams, being located along their neutral axes.. The plate is attached from the hinge bar, nodes 186 and 205, to the third torsion box cross member, nodes 174 and 193 as shown in Fig. 4.1. It is thought that this would stiffen the rear of the chassis when subjected to fore/aft loading.

(ii) The three large torsion box cross members were doubled in size, from 100 x 200 x 5 mm to 200 x 200 x 5 mm. These elements are attached between nodes 182 to 201, 178 to 197 and 174 and 193 as shown in Fig. 4.2. It is thought that this would increase the torsional stiffness of the chassis as a whole.

(iii) The six trailing arm leaf springs were reduced in size to double their bending flexibility. The leaf springs are connected between nodes 214 to 212, 211 to 209, 208 to 206, 223 to 221, 220 to 218 and 217 to 215, as shown in Fig. 4.3.

4.4 Loading of F.E. meshes

The loads applied to the vehicle, described in Section 2.2, are used to obtain the displacements from the finite element analyses. The iterative procedure adopted in Chapter 3 to analyse this type of non-linear, elastic system, necessitates the need for a general procedure for determining the displacement. There are two solutions required to determine the F.E. displacement, depending upon the suspension operating conditions.

For the three suspension operating conditions a, b or c, described in Section 3.4.2, in which at least one suspension side is height controlled, unit loads (one newton) are individually applied to the F.E. model, at nodes where forces are applied on the real structure. The forces are always applied to the F.E. model in the positive X, Y, Z directions (except for the suspension forces), representing the body/chassis contact forces at nodes 186, 205, 314, the tractor self weight at node 313, the chassis self weight using the gravity module, the left suspension forces at nodes 176, 208, 180, 211, 184, 214 and the right suspension forces at nodes 195, 217, 199, 220, 203, 233. The body/chassis contact forces are modelled by applying individual unit forces to the right hinge in the X, Y, Z direction, to the right hinge in the X, Y directions and to the ram/chassis contact point in the X, Y, Z direction. The tractor unit self weight in the vertical and lateral directions is modelled by applying individual unit forces in the Y, Z direction. The unsprung and sprung mass of the actual trailer and the finite element model are different as only the masses of the flexible components are taken into account. Therefore, the trailers actual sprung and unsprung mass is modelled by locating an additional mass at the trailers centre of gravity and at the ends of each axle and applying an individual unit acceleration in the Y and Z direction using the gravity module of the finite element package. The suspension forces are modelled by applying three pairs of forces to each side, with each pairs of forces representing the expansion forces of each airbag. The six forces on one side are applied simultaneously and in the direction of the actual forces. The forces are applied simultaneously as the suspension forces on each side are all equal.

For the remaining suspension operating conditions, (d) in which neither side is height controlled, unit displacements (one mm) are individually applied to the F.E. model at nodes where forces are applied to the structure. The displacements are always applied to the F.E. model in the positive X, Y, Z directions, (except for the suspension displacements), to the body/chassis contact points at nodes 186, 205, 314, the tractor self weight at node 313, the chassis sprung weight at node 315, the chassis unsprung weight at nodes 316, 317, 318 and the right suspension forces at nodes 195, 217, 199, 220, 203, 223.

The body/chassis contact point forces are modelled by applying individual unit displacements to the left hinge in the X, Y, Z directions to the right hinge in the X, Y direction and to the ram/chassis contact point in the X, Y, Z directions. The tractor self weight is modelled by applying individual unit displacements to the centre of gravity in the Y, Z directions. The chassis unsprung weight is modelled by applying individual unit displacements to the middle of each axle in the Y, Z directions. The right suspension forces are modelled by applying individual unit displacements in the Y direction representing the expansion forces of each airbag. Although the displacements are applied individually it is still assumed that the right suspension forces are all equal.

To obtain the tyre forces in the Y direction the restraint in the Y direction at the tyre/ground contact node is released and unit displacements are individually applied in the y direction to the nodes 231 to 233.

4.5 Flexibility, influence and stiffness matrices

For the three suspension operating conditions, (a, b, c described in Section 3.4.2) in which at least one suspension side is height controlled, the unit load finite element results enable flexibility and influence matrices to be generated. From these matrices, chassis displacements, suspension displacements, suspension forces and tyre forces can be determined for any given loading condition. For each flexibility or influence matrix described there are three types which are directly related to the suspension operating condition. The matrices will be discussed in general with the specific matrices given at the ends of this section for the original chassis design.

For the remaining suspension operating condition, (described in Section 3.4.2), in which neither suspension is height controlled, unit displacement finite element results enable a stiffness matrix to be generated. From this single matrix chassis displacement, suspension displacement, suspension forces and tyre forces can be determined for any given loading condition. The matrix will be discussed in general with the specific matrix given at the end of this section for the original chassis design.

4.5.1 Chassis displacement flexibility matrix

To determine the chassis displacements at the body/chassis contact points for any given loading condition, a unit load flexibility matrix was generated using the results from the finite element model. At the nodes of interest, the displacement at these points, resulting from the individually applied unit loads to the finite element model, form the coefficients of the unit load flexibility matrix. These results are used to form the unit load flexibility matrix which gives a relationship between the body/chassis contact forces, the tractor self weight, the chassis self weight, the suspension forces and the chassis displacements at the body/chassis contact point. The unit load flexibility matrices relating to the suspension operating conditions a, b, and c are given in Tables 4.3, 4.4 and 4.5 respectively.

4.5.2 Suspension displacement flexibility matrix

To calculate the compression of the left airbags, the displacement of the two ends of each airbag are required. To determine these displacements for any given loading condition a unit load flexibility matrix was generated using the results from the finite element model in the same manner as the unit load chassis, displacement flexibility matrix. These results are used to form the unit load flexibility matrix, which gives a relationship between the body/chassis contact forces, the tractor self weight, the chassis self weight, the suspension forces and the suspension displacements at the ends of each airbag. The suspension displacements form the coefficients of the unit load suspension displacement flexibility matrix. The unit load flexibility matrices relating to the suspension operating conditions a, b, c are given in Tables 4.6, 4.7 and 4.8 respectively.

4.5.3 Suspension force influence matrix

To determine the left and right suspension forces for any given loading condition, a unit load influence matrix was generated using the results from the finite element model. The tie bar forces resulting from the individually applied unit loads to the finite element model form the coefficients of the unit load influence matrix. From these results the unit load influence matrix can be generated which gives a relationship between the body/chassis contact forces, unit tractor self weight, the chassis self weight and the suspension forces. The unit load influence matrices relating to the suspension operating conditions a, b and c are given in Tables 4.9, 4.10 and 4.11 respectively.

4.5.4 Tyre force influence matrix

To determine the vertical tyre forces in the trailer wheels for any given loading condition, a unit load influence matrix was generated using the results from the finite element model. The forces in the tyre springs resulting from the individually applied unit loads to the finite element model form the coefficients of the unit load influence matrix. These results are used to form the unit load influence matrix which gives a relationship between the body/chassis contact forces the tractor self weight, the chassis self weight, the suspension forces and the vertical tyre forces. The unit load influence matrices relating to the suspension operating conditions a, b and c are given in Tables 4.12, 4.13 and 4.14 respectively.

4.5.5 Stiffness matrix

For the remaining suspension operating condition, d, described in Section 3.4.2, in which neither suspension is height controlled, unit displacements are applied to the finite element model instead of unit forces, with the nodes of interest being restrained in the desired directions. The reaction forces resulting from the individually applied unit displacements to the finite element model form the coefficient of the unit displacement stiffness matrix. The finite element results enable a unit displacement stiffness matrix, shown in Table 4.15, to be generated from which the chassis displacements, the suspension displacements, the suspension forces and the tyre forces can be determined for any given loading condition. The method of calculating the unknown displacement and forces is fully described in Section 3.4.3.

4.6 Discussion

Two different methods have been devised for determining chassis displacements, suspension displacements, suspension forces and tyre forces using the finite element method. Depending upon the suspension operating condition, unit forces are used to generate the flexibility and influence matrices where at least one suspension is height controlled, with unit displacements being used to generate the stiffness matrix where neither suspension is height controlled.

The validity of each method for determining displacements and forces is confirmed by cross checking the forces and displacements obtained at the point at which the analysis changes the suspension operating condition. The four different methods can all be cross checked in a similar manner to confirm their validity, as the analysis changes from one suspension operating condition to another.

The continuity of the graphs shown in Figs. 5.1 to 5.4, show that good agreement has been obtained between the forces and displacements determined by either suspension operating condition at the point of cross over.

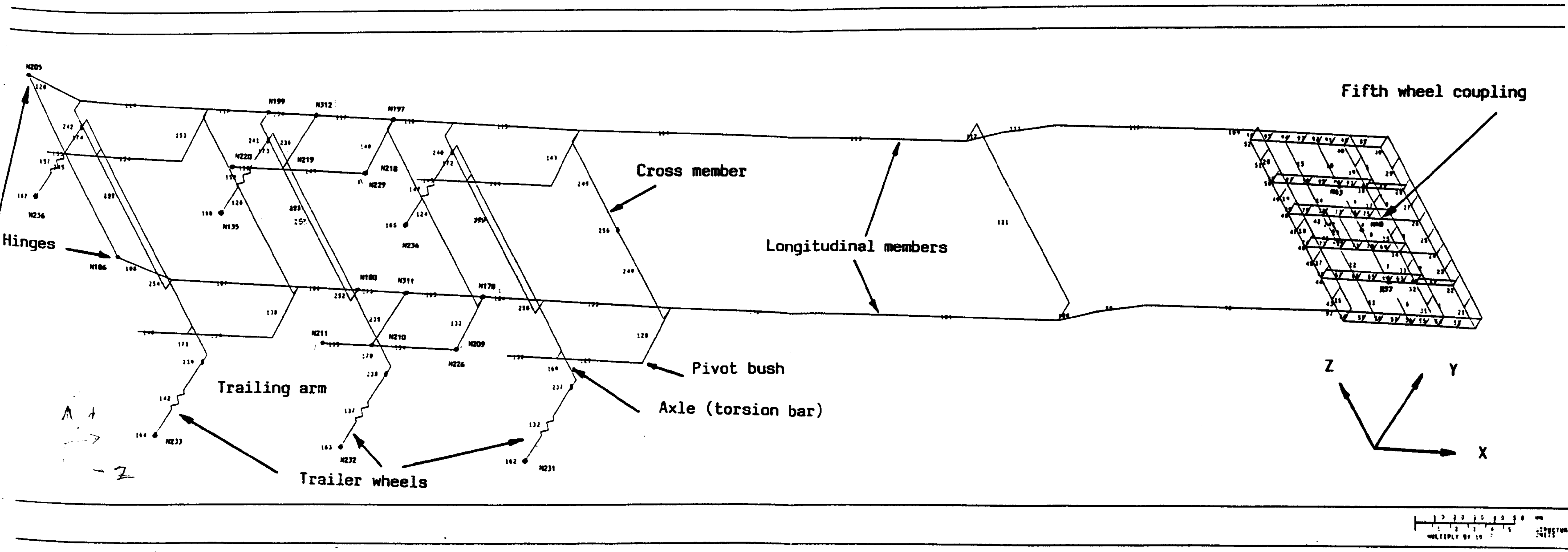

Fig. 4.1 Trailer finite element line diagram

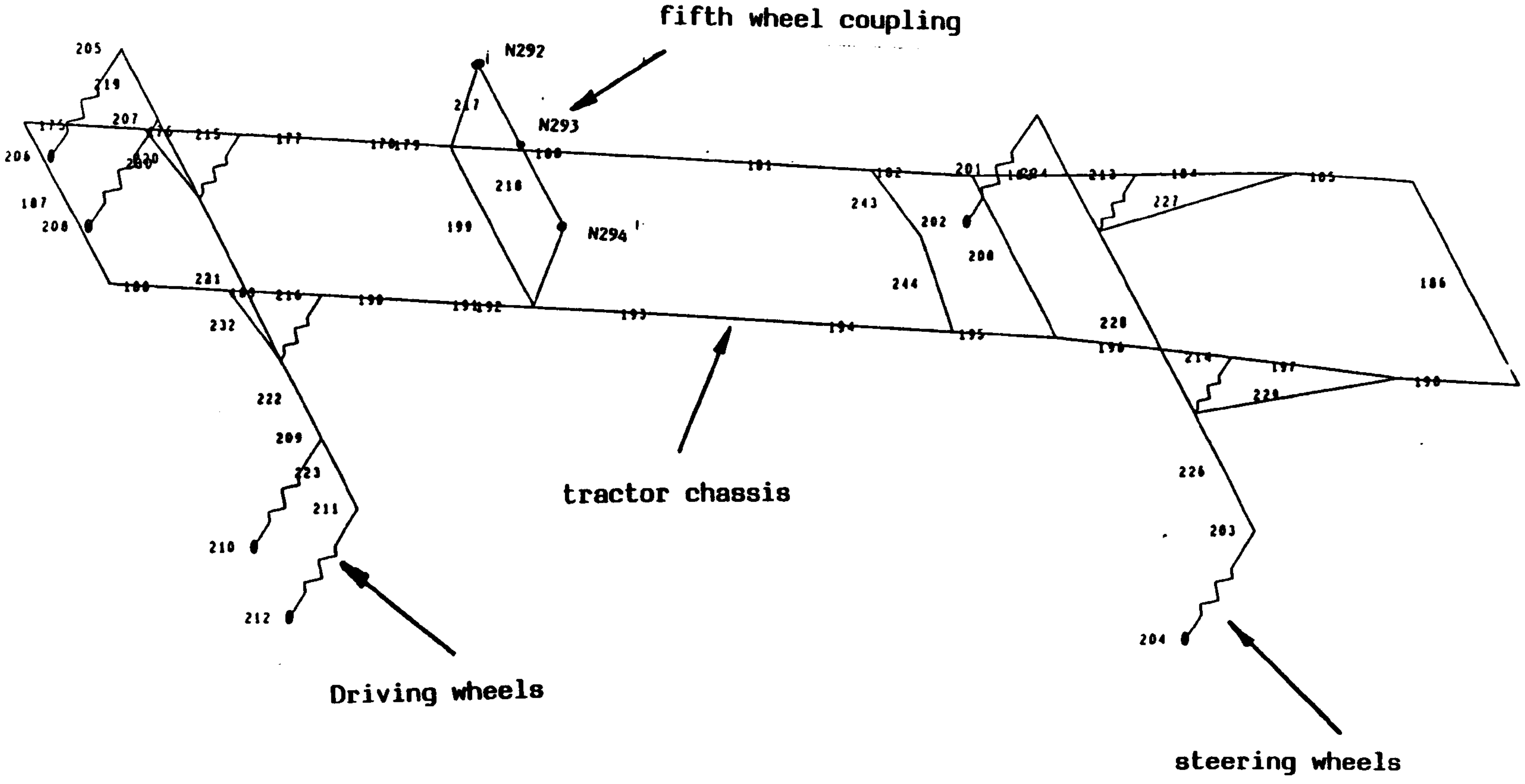

Fig. 4.2 Tractor finite element line diagram

PAFEC

VIEW FROM X = 1000
Y = 1000
Z = 1000

ELEMENT GROUPS= 3

DRAWING NO. 1
SCALE =0.6250 E 4
DRAWING TYPE= 3

MM.
STRUCTURAL UNITS
MULTIPLY BY 10

Table 4.1a - Element Property Numbers

Element Numbers	Property Numbers	Element Numbers	Property Numbers
1-20	28	112	13
21-30	7	113	14
31-40	2	114	15
41-42	3	115	16
43-52	6	116	17
53-60	1	117	18
61-62	3	118	19
63-68	4	119	20
69-80	5	120	21
81-82	3	121	10
83-88	4	123	9
89-97	1	124	8
98	11	125	9
99	12	126	8
100	13	127	9
101	14	128	22
102	15	129	24
103	16	130	31
104	17	132	26
105	18	133	22
106	19	134	24
107	20	135	31
108	21	137	26
109	1	138	22
110	11	139	24
111	12	140	31

Table 4.1b - Element Property Numbers

Element Numbers	Property Numbers	Element Numbers	Property Numbers
142	26	210	34
143	22	211	35
144	24	212	34
145	31	213, 214	33
147	26	215, 216	32
148	22	217, 218	36
149	24	219 - 226	37
150	31	227 - 232	38
152	26	233, 234	18
153	22	235, 236	40
154	24	237 - 242	41
155	31	243, 244	18
157	26	245	42
162 - 167	29	246	17
169 - 174	23	247	17
175 - 200	36	248, 249	8
210	35	250 - 255	23
202	34	256	43
203	35		
204	34		
205	35		
206	34		
207	35		
208	34		
209	35		

Table 4.2a - Property Number Values

Beam Property Number	I_{yy} (mm)^4 x 10^6	I_{zz} (mm)^4 x 10^6	K (mm)^4 x 10^3	Area (mm)^2
1	3.663	13.667	92.5	3250
2	1.464	9.193	93.333	2800
3	2.46	0.393	60.0	1800
4	0.571	5.343	77.666	6570
5	0.189	6.351	755.208	3625
6	0.813	2.686	10.208	1225
7	0.388	7.801	43.52	2040
8	15.224	5.124	11834	2900
9	0.362	1.298	8125	1000
10	2.569	2.569	5138	1717
11	3.664	25.025	0.0942	3458
12	3.665	69.249	0.0988	4008
13	3.665	105.286	0.1019	4375
14	3.664	125.099	0.0952	4162
15	3.664	170.164	0.0965	4406
16	3.664	186.195	0.09695	4488
17	3.664	174.025	0.0966	4430
18	3.664	162.496	0.0964	4372
19	3.664	151.253	0.0961	4314
20	3.664	140.986	0.0957	4258
21	3.664	140.986	0.0957	4258
22	8.919	17.756	0.0241	2875
23	80.55	80.55	16109	49700
24	2.084	0.777	1926	3908
31	1.042	0.389	963	1954
36	1.585	27.551	30.744	2598
37	100000	10000	100	1000
38	0.134	0.134	267.803	1297.2
39	0.397	0.397	794.716	2234.6
40	0	0	0	900
42	1.113	1.113	2226.26	1995

Table 4.2b - Property Number Values

Spring Property Number	**Spring Stiffness**	**Spring Stiffness**	**Spring Stiffness**
	K_x (N/mm)	K_y (N/mm)	K_z (N/mm)
26	-	1070	-
29	749	-	412
32	-	872	-
33	-	403	-
34	755	-	350
35	-	981	-
Mass Property	**Mass (kg)**		
41	17.666		
43	1220		
Plate Property Number	**Plate Thickness (mm)**		
28	8		

Table 4.3 - Displacement flexibility matrix, original chassis, case 1

Unit forces / Unit force displacements	H_{Lx}	H_{Rx}	H_{Ly}	H_{Ry}	H_{Lz}	R_x	R_y	R_z	W_{Ty}	W_{Tz}	W_{xy}	W_{cz}	A_R	A_L
N186-X	0.1562	0.0919	0.0839	0.0505	-0.1082	0.1163	-0.0135	0.0408	-0.0122	0.0286	0.028	-0.0043	0.0926	0.0693
N186-Y	0.0839	0.0505	1.3528	0.7072	0.1345	0.0442	-0.799	0.0088	-0.0777	0.0015	0.2506	0.0145	2.2495	1.7450
N186-Z	-0.1082	0.1082	0.1345	-0.1345	1.2801	0	0	-0.083 6	0	-0.0630	0	0.3613	0.1051	-0.1050
N250-X	0.0919	0.1562	0.0505	0.0839	0.1802	0.1163	-0.0135	- 0.0408	-0.0122	-0.0286	0	0.0043	0.0693	0.0296
N250-Y	0.0505	0.0839	0.7072	1.3528	-0.1345	0.0442	-0.799	- 0.0088	-0.0777	-0.0012	0.2056	-0.0145	1.7450	2.2495
N250-Z	-0.1082	0.1082	0.1345	-0.1345	1.2785	0	0	-0.836	0 .	-0.0630	0	0.3613	1.051	-0.1050
N314-X	0.1163	0.1163	0.0442	0.0442	0	0.1185	-0.0126	0.0150	-0.0112	0	0.0043	0	0.0667	0.0667
N314-Y	-0.0135	0.0135	0.0800	-0.0800	0	-0.0126	0.2826	0.004	0.2639	0	0.0579	0	0.0316	0.0316
N314-Z	0.0408	-0.0408	0.0088	-0.0088	-0.0836	0	0	0.3203	0	0.4085	0	0.1219	0.069	-0.0070

Table 4.4 - Displacement flexibiliyt matrix, original chassis, case 2

Unit forces / Unit force displacements	H_{Lx}	H_{Rx}	H_{Ly}	H_{Ry}	H_{Lz}	R_x	R_y	R_z	W_{Ty}	W_{Tz}	W_{xy}	W_{cz}	A_R
N186-X	0.1567	0.0922	0.1011	0.0511	-0.1046	0.1166	-0.0133	0.0411	-0.0122	0.0287	0.056	-0.0040	0.0954
N186-Y	0.1011	0.0615	1.965	0.8703	0.2617	0.0572	-0.0736	0.0167	-0.0763	0.0043	0.3481	0.0263	1.6727
N186-Z	-0.1047	0.1105	0.2617	-0.1006	1.3065	0.0027	0.0013	-0.0820	0.0003	-0.0624	0.0203	0.3638	0.0877
N250-X	0.0922	0.1564	0.0615	0.0868	0.1105	0.1165	-0.0134	-0.0406	-0.0122	-0.0285	0.0046	0.0045	0.1092
N250-Y	0.0551	0.0868	0.8703	1.3963	-0.1006	0.0477	-0.0782	-0.0067	-0.0773	-0.0003	0.2766	-0.0113	2.4966
N250-Z	-0.1047	0.1105	0.2617	-0.1006	1.3049	0.0027	0.0013	-0.0820	0.0003	-0.0624	0.0203	0.3638	0.0877
N314-X	0.1167	0.1165	0.0572	0.0477	0.0027	0.1187	-0.0124	0.0002	-0.0112	0.0007	0.0064	0.0003	0.0863
N314-Y	-0.0133	-0.0134	-0.0736	-0.0783	0.0013	-0.0124	0.2827	0.0001	-0.2640	0	0.0589	0.0001	0.0413
N314-Z	0.0411	-0.0407	0.0167	-0.0067	-0.0820	0.002	0.0001	0.6212	0	0.4086	0.0013	0.1220	0.050

Table 4.5 - Displacement flexibility matrix, original chassis, case 4

Unit forces / Unit force displacements	H_{Lx}	H_{Rx}	H_{Ly}	H_{Ry}	H_{Lz}	R_x	R_y	R_z	W_{Ty}	W_{Tz}	W_{xy}	W_{cz}	A_R	A_L
N186-X	0.1564	0.0922	0.0868	0.0615	-0.1105	0.1165	-0.0134	0.0407	-0.0122	0.0285	0.0045	-0.0045	0.1092	0.1035
N186-Y	0.0868	0.0551	1.3963	0.8703	0.1007	0.0477	-0.0782	0.0067	-0.0773	0.0003	0.2766	0.0113	2.4966	2.2539
N186-Z	-0.1105	0.1047	0.1007	0.2617	1.3065	-0.0027	-0.0013	-0.0820	-0.0003	-0.0624	-0.0203	0.3638	-0.0876	-0.5017
N250-X	0.0922	0.1567	0.0551	0.1012	0.1046	0.1166	-0.0133	-0.0410	-0.0122	-0.0286	0.0055	0.0040	0.0954	0.1464
N250-Y	0.0615	0.1012	0.8703	1.9650	-0.2616	0.0572	-0.0736	-0.0167	-0.0763	-0.0043	0.2481	-0.0263	2,6727	4.1598
N250-Z	-0.1105	0.1047	0.1007	-0.2617	1.3049	-0.0027	-0.0013	-0.0820	-0.003	-0.0624	-0.0202	0.3638	-0.0876	-0.5018
N314-X	0.1165	0.1167	0.0477	0.0572	-0.0027	0.1187	-0.0124	-0.0002	-0.0001	-0.0001	0.0064	-0.0002	0.0863	0.1071
N314-Y	-0.0133	-0.0133	-0.0783	-0.0736	-0.0013	-0.0214	0.2827	-0.0001	-0.2640	0	0.0589	-0.0001	0.0413	0.0515
N314-Z	0.0407	-0.0411	0.0067	-0.0167	-0.0820	-0.0002	-0.0001	0.06212	0	0.4086	-0.0013	0.1220	-0.0050	-0.0315

Table 4.6 - Suspension displacement flexibility matrix, original chassis, case 1

Unit forces / Unit force displacements	H_{Lx}	H_{Rx}	H_{Ly}	H_{Ry}	H_{Lz}	R_x	R_y	R_z	W_{Ty}	W_{Tz}	W_{xy}	W_{cz}	A_R	A_L
N195-Y	0.0148	-0.0023	0.3534	0.5399	-0.1094	0.0012	0.0511	-0.0065	0.00386	-0.0075	0.2202	-0.0176	1.1810	1.3474
N217-Y	0.0103	-0.0041	-0.2113	-0.5139	-0.0614	-0.0010	-0.0528	-0.0042	-0.0430	-0.0064	0.0013	-0.0127	-1.7704	-2.1217
N199-Y	0.0287	0.0279	0.4941	0.8413	-0.01186	0.0238	-0.0047	-0.0072	-0.0109	-0.0043	0.2329	-0.0165	1.4093	1.6999
N220-Y	0.0304	0.0248	0.5108	0.8104	-0.1158	0.00236	-0.0047	-0.0069	-0.0109	-0.0049	0.2322	-0.0168	1.3457	1.4240
N203-Y	0.0447	0.0679	0.6508	1.2129	-0.1301	0.0388	-0.0606	-0.0084	-0.0603	-0.0019	0.2549	-0.0150	1.6568	2.1038
N223-Y	-0.0219	-0.0199	-0.5461	-0.3118	-0.0760	-0.0165	0.0119	-0.0040	0.0145	-0.0018	-0.0148	-0.01117	-2.1747	-2.3856

Table 4.7 - Suspension displacement flexibility matrix, original chassis, case 2

Unit forces / Unit force displacements	H_{Lx}	H_{Rx}	H_{Ly}	H_{Ry}	H_{Lz}	R_x	R_y	R_z	W_{Ty}	W_{Tz}	W_{xy}	W_{cz}	A_R
N195-Y	0.01878	0.0002	0.4946	0.5575	-0.0801	0.0131	0.0526	-0.0047	0.0389	-0.0068	0.2426	-0.0149	1.5613
N217-Y	0.0054	-0.0072	-0.3871	-0.2008	-0.0979	-0.0047	-0.0546	-0.0064	-0.0438	-0.0073	-0.0266	-0.0161	-2.3880
N199-Y	0.0328	0.0305	0.6413	0.8805	-0.0881	0.0269	-0.0031	-0.0053	-0.0106	-0.0035	0.2563	-0.0137	1.9229
N220-Y	0.0301	0.0246	0.5002	0.8076	-0.1180	0.0234	-0.0048	-0.0071	-0.0110	-0.0030	0.2306	-0.0170	1.4081
N203-Y	0.0492	0.0708	0.8093	1.2552	-0.0971	0.0422	-0.0587	-0.0063	-0.0599	-0.0011	0.2712	-0.0120	2.3441
N223-Y	-0.0302	-0.0252	-0.8407	-0.3903	-0.1372	-0.0227	-0.0088	-0.0078	0.0139	-0.0033	-0.0617	-0.0174	-2.8321

Table 4.8 - Suspension displacement flexibility matrix, original chassis, case 4

Unit forces / Unit force displacements	H_{Lx}	H_{Rx}	H_{Ly}	H_{Ry}	H_{Lz}	R_x	R_y	R_z	W_{Ty}	W_{Tz}	W_{xy}	W_{cz}	A_R	A_L-
N195-Y	0.0215	0.0082	0.04532	0.9145	-0.1873	0.0180	0.0550	-0.0114	0.0394	-0.0094	0.2800	-0.0249	1.7487	2.5165
N217-Y	0.0849	-0.0062	-0.02330	-0.2314	-0.0453	-0.0027	-0.0536	-0.0032	-0.0432	-0.0060	-0.0110	-0.0112	-1.8879	-2.3635
N199-Y	0.0372	0.0413	0.6218	1.3204	-0.2182	0.0340	0.0003	-0.0103	-0.0099	-0.0068	0.3092	-0.0258	2.1354	3.1951
N220-Y	0.0248	0.0160	0.4270	0.4961	-0.0505	0.0170	-0.0080	-0.0029	-0.0117	-0.0034	0.1822	-0.0108	0.8695	0.4434
N203-Y	0.0551	0.0842	0.8047	1.7908	-0.2501	0.0511	-0.0543	-0.0158	-0.5090	-0.0049	0.3380	-0.0262	1.5236	3.9072
N223-Y	-0.0234	-0.0233	-0.5692	-0.3987	-0.0579	-0.0183	0.0110	-0.0029	0.0143	-0.0014	-0.0287	-0.0100	-2.3064	-2.6568

Table 4.9 - Suspension force influence matrix, original chassis, case 1

Unit forces / Unit force displacements	H_{Lx}	H_{Rx}	H_{Ly}	H_{Ry}	H_{Lz}	R_x	R_y	R_z	W_{Ty}	W_{Tz}	W_{xy}	W_{cz}	A_R	A_L-
N311-Y	-0.0286	-0.0182	-1.0618	-0.2709	-0.2113	-0.0215	-0.0106	-0.0131	-0.0022	-0.0052	-0.1619	-0.196	-3.1736	-1.5410
N312-Y	-0.0182	-0.0286	-0.2708	-1.1068	0.2112	-0.0215	-0.0106	0.0131	-0.0022	0.0052	-0.01619	0.0196	-1.5413	-3.1733

Table 4.10 - Suspension force influence matrix, original chassis, case 2

Unit forces / Unit force displacements	H_{Lx}	H_{Rx}	H_{Ly}	H_{Ry}	H_{Lz}	R_x	R_y	R_z	W_{Ty}	W_{Tz}	W_{xy}	W_{cz}	A_R
N312-Y	-0.0457	-0.0468	-1.2827	-1.2864	0.0010	-0.0429	-0.0211	0.001	-0.0044	0	-0.3232	0	4.7075

Table 4.11 - Suspension force influence matrix, original chassi, case 4

Unit forces / Unit force displacements	H_{Lx}	H_{Rx}	H_{Ly}	H_{Ry}	H_{Lz}	R_x	R_y	R_z	W_{Ty}	W_{Tz}	W_{xy}	W_{cz}	A_R	A_L
N311-Y	-0.0467	-0.0467	-1.2866	-1.2832	-0.0011	-0.0429	-0.0212	-0.001	-0.004	0	-0.3231	-0.0001	-4.7075	-4.6992

Table 4.12 - Tyre force influence matrix, original chassis, case 1

Unit forces / Unit force displacements	H_{Lx}	H_{Rx}	H_{Ly}	H_{Ry}	H_{Lz}	R_x	R_y	R_z	W_{Ty}	W_{Tz}	W_{xy}	W_{cz}	A_R	A_L
N231-Y	0.0105	-0.0102	-0.0413	0.0412	-0.088	0.0001	0	-0.0059	0.0018	-0.0091	-0.0826	-0.0181	0.911	0.669
N232-Y	-0.0192	-0.0274	-0.854	-0.434	-0.0163	-0.0214	-0.0106	-0.0098	-0.0022	-0.0071	-0.2446	-0.0238	-1.74	-1.39
N233-Y	-0.0014	0.0017	-0.168	0.168	-0.109	0.001	0	-0.0058	0	-0.0027	-0.0826	-0.0167	0.810	0.770
N234-Y	-0.0102	0.0105	0.0412	-0.0413	0.088	0.0001	0	0.0059	0	0.0091	-0.0826	0.0181	0.669	0.911
N235-Y	-0.0274	-0.0192	-0.434	-0.854	0.163	-0.0214	-0.0106	0.0098	-0.0022	0.0071	-0.2446	0.0238	-1.39	-1.74
N236-Y	0.0017	-0.0014	0.168	-0.168	0.109	0.0001	0	0.0058	0	0.0027	-0.0826	00167	0.770	0.810

Table 4.13 - Tyre force influence matrix, original chassis, case 2

Unit forces / Unit force displacements	H_{Lx}	H_{Rx}	H_{Ly}	H_{Ry}	H_{Lz}	R_x	R_y	R_z	W_{Ty}	W_{Tz}	W_{xy}	W_{cz}	A_R
N231-Y	0.085	-0.0115	-0.112	0.0224	-0.103	-0.0014	-0.0007	-0.0068	-0.0001	-0.0095	-0.0938	-0.0194	-0.5620
N232-Y	-0.0134	-0.0237	-0.647	-0.379	-0.120	-0.017	-0.0084	-0.0071	-0.017	-0.0060	-0.2116	-0.0198	-1.080
N233-Y	-0.0056	-0.0010	-0.318	-0.129	-0.140	-0.003	-0.0015	-0.0678	-0.0003	-0.0034	-0.1062	-0.0195	0.544
N234-Y	-0.0082	-0.0118	0.112	-0.0225	0.103	0.0016	0.0008	0.0068	0.0002	0.0095	-0.0713	0.0194	1.02
N235-Y-	-0.0331	-0.0228	-0.636	-0.908	-0.121	-0.0256	-0.0127	0.0072	-0.0026	0.0061	-0.2768	0.0199	-2.05
N236-Y	0.0059	0.0013	0.318	-0.129	0.140	0.0033	0.0016	0.0077	0.0003	0.0034	-0.059	0.0195	1.04

Table 4.14 - Tyre force influence matrix, original chassis, case 4

Unit forces / Unit force displacements	H_{Lx}	H_{Rx}	H_{Ly}	H_{Ry}	H_{Lz}	R_x	R_y	R_z	W_{Ty}	W_{Tz}	W_{xy}	W_{cz}	A_R	A_L
N231-Y	0.0117	-0.0082	-0.0225	0.112	-0.103	0.0016	0.0008	-0.0068	0.0002	-0.0095	-0.7125	-0.01944	1.0	0.890
N232-Y	-0.0228	-0.0331	-0.908	-0.636	-0.121	-0.0256	-0.0127	-0.0072	-0.0026	-0.0061	-0.2768	-0.199	-2.05	-2.02
N233-Y	0.0013	0.0059	-0.129	0.318	-0.140	0.0044	0.0016	-0.0078	0.0003	-0.0034	-0.0588	-0.0195	1.04	1.24
N234-Y	-0.0115	0.0085	0.0224	-0.112	0.103	-0.0014	-0.0007	-0.0068	-0.0001	0.0095	-0.938	0.0194	0.562	0.690
N235-Y-	-0.0237	-0.0134	-0.379	-0.637	0.120	-0.0170	-0.0008	0.0071	-0.0018	0.0060	-0.2116	0.0198	-1.08	-1.10
N236-Y	-0.0010	-0.0056	0.129	-0.318	0.140	-0.0030	-0.0015	-0.0078	-0.0003	0.0034	-0.1062	0.0195	0.544	0.344

Unit displacement forces / Unit displacements	H_{Lx}	H_{Ly}	H_{Lz}	H_{Rx}	H_{Ry}	R_x	R_y	R_z	W_{sy}	W_{sz}	W_{m1y}	W_{m1z}	W_{m2y}	W_{m2z}	W_{m3y}	W_{m3z}	W_{Ty}	W_{Tz}	A_{R1}	A_{R2}	A_{R3}	A_{R4}	A_{R5}	A_{R6}
N186-X	49187	-2497	2785	10570	-2948	-57919	-1715	-839	4599	-6917	960	2205	1156	1161	929	1743	232	-52	-5088	-617	4363	-739	2245	-594
N186-Y	-2497	1654	-721	63	-213	2575	519	37	-865	454	-151	-280	-721	-10	-1489	493	-41	18	739	97	-778	461	-113	952
N186-Z	2785	-721	2745	-2550	836	-228	-6	7	-329	-339	-66	48	-71	-469	-39	-1992	2	-0.1	327	43	414	45	-459	25
N205-X	10569	63	-2550	5330	-16054	-61830	-1891	914	-768	8539	-113	-3120	81	-1602	155	-2317	275	59	3176	74	1436	-52	13563	-98
N205-Y	-2948	-213	836	-16051	258220	18491	951	-273	1271	-3219	-83	1506	-71	617	-32	494	-116	-38	-28689	52	139440	45	-37804	20
N314-X	-57919	2575	-288	-61829	18491	124720	3673	-78	-3472	-1554	-787	869	-1194	423	-1058	565	-508	-6	2147	506	-5941	764	-15556	667
N314-Y	-17[illegible]5	516	-6	-1891	943	3674	9520	-9	-1736	-198	-234	172	-54	56	3	-20	-5626	-5	-1674	152	2309	37	-1367	-2
N314-Z	-841	38	7	918	-279	-71	1	2535	-74	-514	-15	49	-19	66	-16	36	0.	-1005	67	10	10	12	256	10
N315-Y	4598	-865	-329	-768	1271	-3471	-1073	-72	11796	-3193	-2624	2286	-1892	958	-990	367	195	-39	-11540	1670	4994	1210	-2218	634
N315-Z	-6917	454	-339	8539	-3219	-1555	-167	-513	-3193	13055	-632	-8455	-529	-2947	-320	-771	29	-33	6644	406	-3773	339	3670	205
N316-Y	960	-151	-66	-113	-83	-787	-236	-15	-2624	-632	8260	440	-376	174	-194	69	30	-13	1655	-3935	-1007	240	328	124
N316-Z	2205	-280	48	-3121	1506	869	143	48	2286	-8455	442	9424	363	-146	184	-83	-22	28	-5414	-285	3672	-232	-2246	-117
N317-Y	1155	-721	-71	82	-71	-1194	-53	-19	-1891	-529	-376	362	8378	88	-261	134	14	-4	1115	242	741	-4009	252	167
N317-Z	1161	-10	-469	-1603	617	422	54	66	957	-2497	174	-146	92	5698	106	-1645	-9	5	-2066	-112	1240	-60	-919	-68
N318-Y	929	-1489	-39	155	-32	-1057	3	-16	-990	-320	-194	184	-261	106	8545	48	6	-1	565	125	-413	167	126	-4119
N318-Z	1743	492	-1992	-2318	494	565	-20	36	367	-771	69	-83	134	-1645	51	5312	-1	1	397	-44	-1472	-85	-353	-33
N313-Y	232	-41	2	275	-116	-508	-5626	1	194	28	30	-22	14	-9	6	-1.2	5910	0.2	172	-19	-186	-9	149	-4
N313-Z	-52	19	-0.1	59	-38	-6	-3	-1005	-39	-33	-13	28	-4	5	-1	1	-0.2	1547	128	8	-124	3	63	1
N195-Y	-5088	739	327	3175	-28689	2145	-1690	66	-11540	6644	1656	-5412	1114	-2062	565	397	171	128	53949	-1051	-80065	-712	65800	-362
N217-Y	-617	97	43	74	52	506	152	9	1670	406	-3934	-283	242	-112	125	-44	-19	8	-1051	2515	641	-155	-208	-80
N199-Y	4363	-778	414	1437	139440	-5940	2332	11	4994	-3773	-1008	3670	-741	1239	-412	-1470	-184	-123	-80065	641	183970	474	-25804	264
N220-Y	-738	461	45	-52	45	764	34	12	1210	339	240	-232	-4010	-56	167	-85	-9	3	-712	-155	474	2565	-161	-107
N203-Y	2245	-113	-459	13560	-37804	-15556	-1403	250	-2218	3670	328	-2246	252	-919	126	-353	148	64	65800	-208	-25804	-161	556980	-81
N223-Y	-594	952	25	-98	20	677	-2	10	634	205	124	-117	167	-68	-4118	-31	-4	1	-362	-80	264	-107	-81	2634
N231-Y	93	-13	-6	-0.05	-62	-90	-4	-1	-155	-50	-1740	32	-33	13	-17	6	1	-2	761	440	-410	21	153	11
N232-Y	77	-52	-4	11	19	-85	-6	-2	-143	-29	-27	14	-1722	-10	-19	12	1	-0.2	372	17	114	428	-40	12
N233-Y	63	-109	1	16	-82	-78	1	-1	-71	-22	-14	14	-19	12	-1710	-11	0.4	-0.1	7	9	311	12	203	421
N234-Y	-77	10	5	-2	63	77	-0.2	1	141	40	-303	-25	27	-10	14	-5	-0.5	2	-756	-479	405	-17	-152	-9
N235-Y	-65	44	4	-10	-20	72	5	1	123	23	23	-20	317	11	16	-11	-1	0.2	-361	-15	-122	-471	43	-10
N236-Y	-54	93	-1	-14	81	67	-0.8	1	61	19	12	-12	17	-10	-327	12	0.3	0.1	3	-8	-315	-11	-201	-464

Table 4.15 - Unit displacement stiffness matrix, original chassis, case d

CHAPTER FIVE

DESIGN INVESTIGATIONS

5.1 Introduction

Whilst a vehicle operator should always endeavour to discharge the payload with the vehicle standing on level ground, practical situations arise where this is not possible. This may be due to the absence of level ground or poor judgement by the operator, which may result in the vehicle being tipped on a lateral ground slope. As a result of this, the maximum ground slope angle considered for the theoretical model is limited to ten degrees, as this position is at least twice the severity of ground slope on which a vehicle should normally be tipped.

For each trailer design the magnitude of the load, position of the load, ram length and ground slope can be varied in any combination. Four payload and up to nine payload positions are considered, varying the ground slope from 0 to 8 degrees and varying the ram length from 2 to 8 meters. Also, three further chassis configurations, described in Section 4.3, based on the reference chassis were modelled to investigate the contribution of important component flexibilities to stability.

From the theoretical results, three types of graphs are obtained giving details of the stability of the vehicle. The first set of graphs give details of how the rear left trailer tyre force varies with ground slope and ram length for a given payload magnitude and position. The ground slope varies between 0 to 10 degrees in steps of 1 degree for each graph. The graphs for the four chassis configurations are shown on one page for each payload magnitude and position, to enable a direct comparison of their stability characteristics and are shown in Fig. 5.1 to Fig. 5.4. The graph also shows what condition the suspension is operating in. The data points are only marked if the suspension is operating using condition, b, c or d as discussed in section 3.4.2. The data points are labelled only where the suspension operating condition changes (eg. a to b or b to c etc). The data points following a labelled data point are the same (ie. no change in the suspension operating condition).

The second set of graphs give details of how the rear left trailer tyre force varies with payload magnitude and horizontal and vertical payload position for a 4 degree ground slope and a 4 meter ram length and are shown in Fig. 5.5 to Fig. 5.10.

The third set of graphs give details of a stability envelope for each chassis configuration for a given payload magnitude and position. The graphs give details of what ram length and ground slope give rise to a zero rear left trailer tyre force for a given payload magnitude and position and are shown in Fig. 5.11 to Fig. 5.13.

5.2 Reference chassis

The reference chassis is the tipper chassis in production at the moment, and is described fully in Section 2.1. The stability criterion is quantified by the rear left trailer tyre force for a given payload magnitude and position. For the present analysis the vehicle is considered to be in a stable position as long as the rear left tyre force is greater than zero.

For stability comparisons between different chassis configurations, where the tyre force is greater than zero, the larger the tyre force the more stable the vehicle is for the given situation. Where the tyre force has reached zero the larger the ram length the more stable the vehicle is for the given situation.

Nine payload positions are considered for the present analyses to demonstrate how the initial payload position within the body effects the vehicles stability. As the body is assumed to be rigid the payload remains the same position relative to the body throughout the analysis. The positions are described with the vehicle standing on horizontal ground with the body untipped. The positions lie in the X-Y plane (ie. z=0) and are spaced symmetrically about the centroid of the body. The payload of centre of gravity positions and their co-ordinates are shown in Fig. 5.14.

5.2.1 General tipping behaviour

The suspension's operating mode, discussed in Section 3.4.2, is dependent upon the payload magnitude and position within the body, ground slope and ram length for a given chassis. From the stability graphs in Fig. 5.1 to 5.4 which show how the rear left tyre force varies with ram length and ground slope for a given payload magnitude and position, described in the previous section, it can also be seen how the suspension operating condition changes.

For smallest payload of 2500 kg the suspension operates using predominantly mode a with mode b being used in the more extreme body attitudes greater than $\theta_p = 5^\circ$ and

RL = 6m when considering payload position nine, as shown in Fig. 5.1i. The position of the payload in the fore/aft direction increases the occurrence of suspension mode b. However for each of the fore/aft positions considered, the vertical position does not significantly change the suspension mode.

As the payload increases to 10000 kg the suspension still operates using mode a with mode b being used more frequently in body attitudes greater than the θ_p = 3° and RL = 5m when considering payload position nine, as shown in Fig. 5.2i. The position of the payload in the fore/aft direction increases the occurrence of suspension b, mode b with the vertical position beginning to influence the occurrence of mode b.

For the 17500 kg payload the suspension operates under all four operating modes. Where the payload is positioned at the rear of the body the suspension operates using mode a with mode c being used in body attitudes greater than θ_p = 2° and RL = 7 m, when considering payload position seven as shown in Fig. 5.3g. With the payload positioned mid-way along the body the suspension operates under mode a with modes b, c, d occurring in body attitudes greater than θ_p = 2° and RL = 7m, when considering payload position eight as shown in Fig. 5.3h. When the payload is positioned in the most forward position the suspension operates under mode a and b with modes c and d only occurring in extreme body attitudes. Suspension mode b and d occurs in body attitudes greater than θ_p = 2° and RL = 6m when considering payload position nine as shown in Fig. 5.3i.

With the maximum payload of 25000 kg the suspension operates under modes a and c, with the latter being most prevalent. It should be noted that the most forward payload positions three, six and nine are not considered for this payload as they are impractical positions for this payload. The suspension operates using mode a with mode c being used in body attitudes greater than θ_p = 1° and Rl = 4m, when considering payload position seven, as shown in Fig. 5.4e. For each of the fore/aft positions, considered, the vertical position does not significantly influence the suspension mode.

The payload magnitudes and the position of the payload centre of gravity's effect on the rear left tyre force can be conveniently demonstrated from the second set of stability graphs, by comparing the rear left tyre force for all nine payload positions with the vehicle standing on a ground slope of 4° at a 4m ram length. From Figs. 5.5 to Fig. 5.10 it can be seen that the tyre force is not proportional to load, for loads above 10000 kg. The graphs in Fig. 5.5 to Fig. 5.7 show how the rear left tyre force varies with the fore/aft position and payload magnitude of three vertical payload heights. For loads of above 10000 kg this tyre force is not proportional to the change in the fore/aft payload position and is made worse with increasing the vertical height. The graphs in Fig. 5.8 to Fig. 5.10 show how the tyre force varies with vertical height and payload magnitude for three fore/aft payload positions. For loads above 17500 kg the tyre force is not proportional to the change in vertical height and is made worse with increasing the fore/aft position.

5.2.2 Rollover condition

When the trailer's rear left tyre force approaches or becomes zero it is in an unstable position and rollover is imminent. From the first set of stability graphs in Fig. 5.1 to Fig. 5.4 the stability characteristics of a trailer can be determined for a range of payload magnitudes and positions. To obtain a more general view of the rollover characteristics the ram length and ground slope data at which the graphs cross the X-axis (ie. zero tyre force) can be plotted against each other to produce the graphs in Fig. 5.11 to Fig. 5.13. From these results a stability envelope is created for a payload magnitude and position, which show that the vehicle is in a stable position below the graph line and in an unstable position above the graph line. As some payload position and magnitude combinations do not cause the vehicle to become unstable ie. rollover, not all payload positions are shown. Each payload magnitude and its unstable payload positions are shown on one graph. It should be noted that the 2500 kg payload does not have a stability envelope graph due to the tyre force remaining positive for all of the payload positions considered.

5.3 The effect of design changes on stability

To quantify the increase or decrease in stability resulting from design changes, the rear left tyre force, for a given body attitude, ground slope, payload and chassis configuration, is compared to the reference chassis.

5.3.1 The effect of introducing a sheardeck on stability

The sheardeck, described in Section 4.3 made a reasonable improvement to the stability characteristics.

For the 2500 kg payload the chassis change hardly effected the stability characteristic. Considering payload position 9, shown in Fig. 5.1i, $\theta_p = 8°$ and RL = 8m, the rear left tyre force is increased from 3047 N to 3509 N, a 15% increase.

For the 10000 kg payload the chassis change has a more noticeable effect on the stability characteristics considering payload position 9, shown in Fig. 5.2i, $\theta_p = 4°$ and RL = 8m, the rear left tyre force is increased from 2795 N to 4005 N, a 43% increase.

For the 17500 kg payload the chassis change makes a noticeable effect on the stability characteristics. Considering payload position 9, shown in Fig. 5.3i, $\theta_p = 2°$ and RL = 8m, the rear left tyre force is increased from 6188 N to 8531 N, a 38% increase.

For the 25000 kg payload the chassis change has a noticeable effect on the stability characteristics. Considering payload position 5, shown in Fig. 5.4d, $\theta_p = 1°$ and RL = 8m, the rear left tyre force increases from 21511 N to 24714 N, a 15% increase.

5.4 The effect of increasing the torsional stiffness of the cross members

The torsion chassis, described in Section 4.3, made a significant improvement to the stability characteristics. The improvement to stability is quantified in the same manner as described in Section 5.3.

For the 2500 kg payload the chassis change has made a reasonable effect upon the stability characteristics. Considering payload position 9, shown in Fig. 5.1i, $\theta_p = 8°$ and RL = 8, the rear left tyre force is increased from 3047 N to 4203 N, a 38% increase.

For the 10000 kg payload the chassis change has a large effect on the stability characteristics. Considering payload position 9, shown in Fig. 5.2i, $\theta_p = 4°$ and RL = 8m, the rear left tyre force is increased from 2795 N to 6714 N, a 140% increase.

For the 17500 kg payload the chassis change has a large effect on the stability characteristic. Considering payload position 9, shown in Fig. 5.3i, $\theta_p = 2°$ and RL = 8m, the rear left tyre force is increased from 6188 N to 14703 N, a 138% increase.

For the 25000 kg payload the chassis change has a noticeable effect on the stability characteristic. Considering payload position 5, shown in Fig. 5.4d, the $\theta_p = 1°$ and RL = 8m, the rear left tyre force increases from 21511 N to 32017 N a 49% increase.

5.5 The effect of reducing the trailing arm stiffness

The trailing arm chassis, described in Section 4.3, made little improvement to the stability characteristics. The improvement to stability is quantified in the same manner as described in Section 5.3.

For the 2500 kg payload the chassis change hardly effected the stability characteristics. Considering payload position 9, shown in Fig. 5.1i, $\theta_p = 8°$ and RL = 8m, the rear left tyre force is increased from 3047 N to 3436 N, a 13% increase.

For the 10000 kg payload the chassis change had a slightly adverse effect on the stability characteristic. Considering payload position 9, shown in Fig. 5.2i, $\theta_p = 4°$ and RL = 8m, the rear left tyre force is reduced from 2795 N to 2500 N, an 11% decrease.

For the 17500 kg payload the chassis change had a slightly adverse effect on the stability characteristic. Considering payload position 8, shown in Fig. 5.3i, $\theta_p = 2°$ and RL = 8m, the rear left tyre force is reduced from 11122 to 10549 N, a 5% decrease.

For the 25000 kg payload the chassis change had a noticeable adverse effect on the stability characteristic. Considering payload position 5, shown in Fig. 5.4d, $\theta_p = 1°$ and RL = 8m the rear left tyre force decreases from 21511 N to 11479 N, a 47% decrease.

5.6 Discussion

From the design investigations it can be seen, for a given chassis configuration, how the rear left tyre force varies with payload magnitude and position, ram length and ground slope. From the results it was determined that the rear left tyre force does not vary linearly with these variables and that the non-linear model developed is necessary to determine the stability of a tipping trailer.

The results enable a stability envelope to be generated which gives detail of what ground slope and ram length give rise to a stable/unstable vehicle for a given payload magnitude and position. Future work may be able to utilise these results to develop a system which would not allow the vehicle operator to tip in unstable conditions.

The design investigation demonstrates how the stability characteristics can be assessed for a given chassis configuration and how subsequent chassis modifications can be assessed in improving vehicle stability. The typical stability envelope for all four chassis configurations, is shown in Fig. 5.15 for a 25000 kg payload, in payload position 8. From the results the chassis modifications showed that the torsional stiffness of the cross-members make an important contribution to the vehicle's stability. The introduction of a sheardeck to the chassis made a small but significant increase in the vehicle stability, with the trailing stiffness being found to make little contribution to the vehicle's stability, and in some case an adverse effect resulted.

The program could also be used to investigate the effect of other design parameters on stability

(i) tyre and suspension flexibilities

(ii) suspension operating conditions

(iii) different chassis design (dimensions and materials)

(iv) the importance of matching a tractor and trailer flexibilities (eg. a stiff tractor suspension combined with a stiff trailer suspension etc.)

(v) wind loading

With some modifications to the program the effect of other design parameters on stability could also be investigated

(vi) a flowing payload during tipping

(vii) trailer body flexibility (currently assumed rigid).

Unit load or unit displacement stress matrices can be generated from the finite element analyses undertaken, these results would indicate which parts of the chassis are under or over stressed, during tipping highlighting those areas that would benefit from design changes.

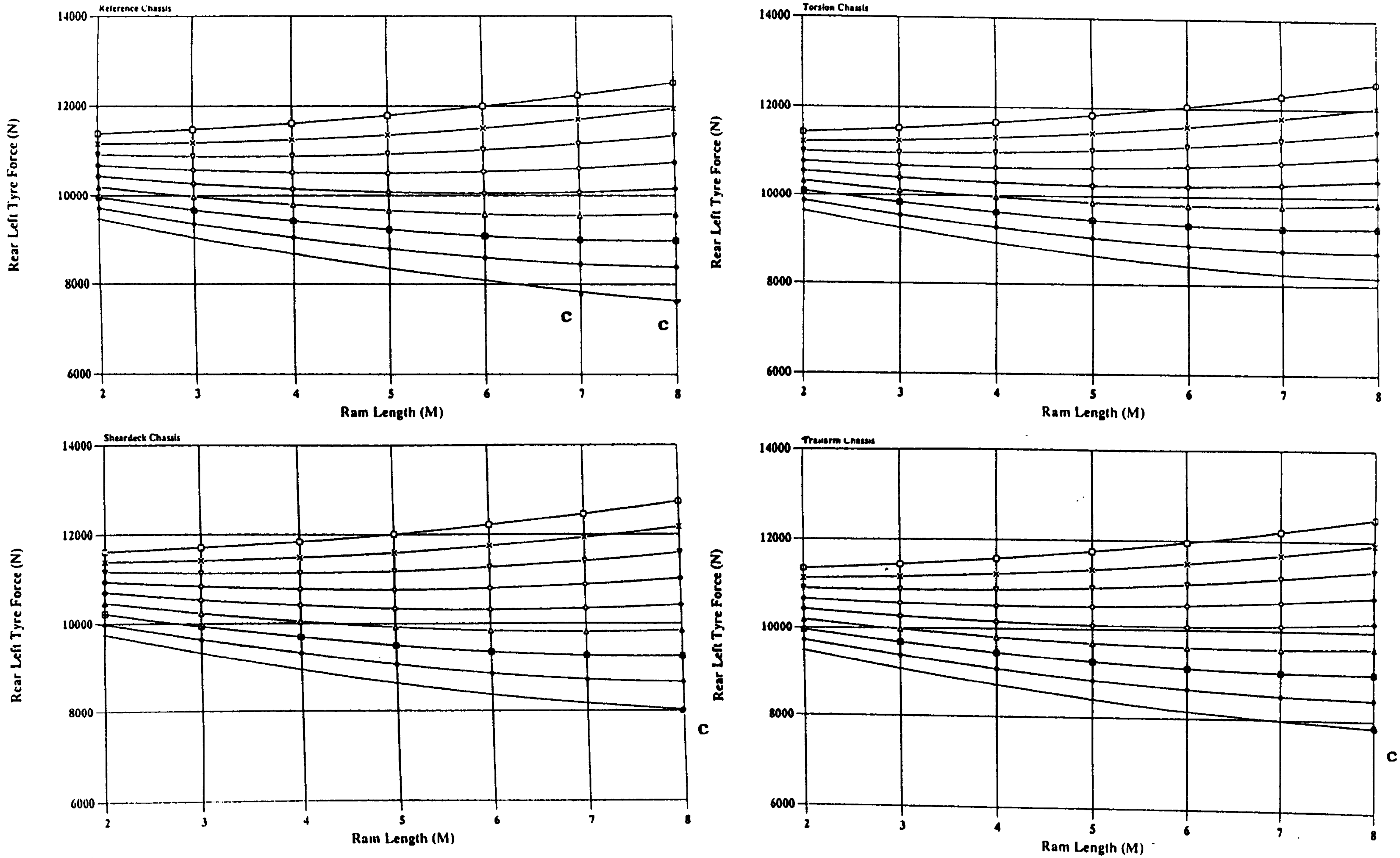

□ = level ground
▽ = 2° ground slope
◇ = 4° ground slope
⊞ = 6° ground slope
— = 8° ground slope

Fig. 5.1a Rear left tyre force versus Ram length and ground slope combinations for a 2500 Kg payload in body position 1 .

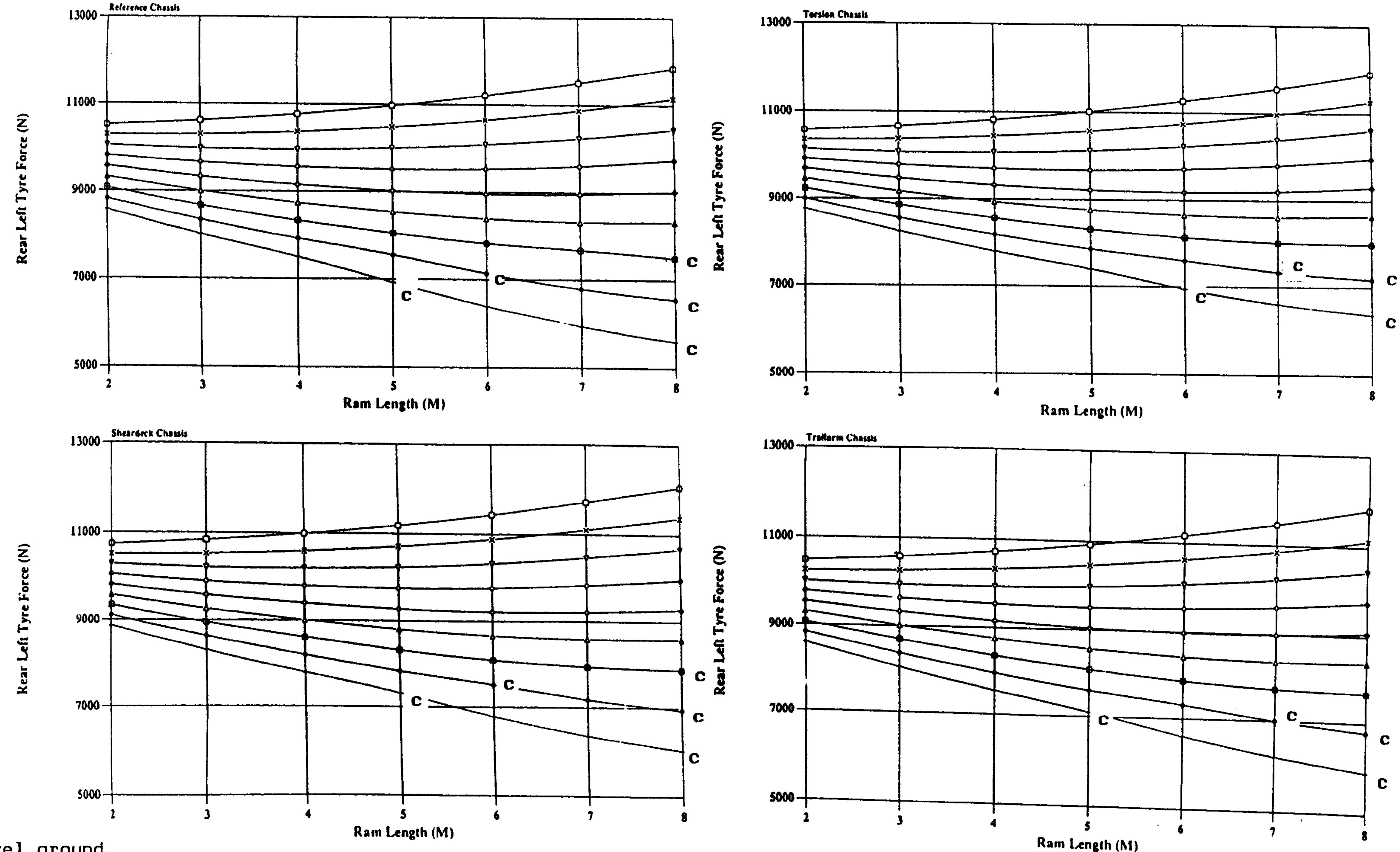

□= level ground
▽= 2° ground slope
◇= 4° ground slope
⊞= 6° ground slope
⌣= 8° ground slope

Fig. 5.1b Rear left tyre force versus Ram length and ground slope combinations for a 2500 Kg payload in body position 2 .

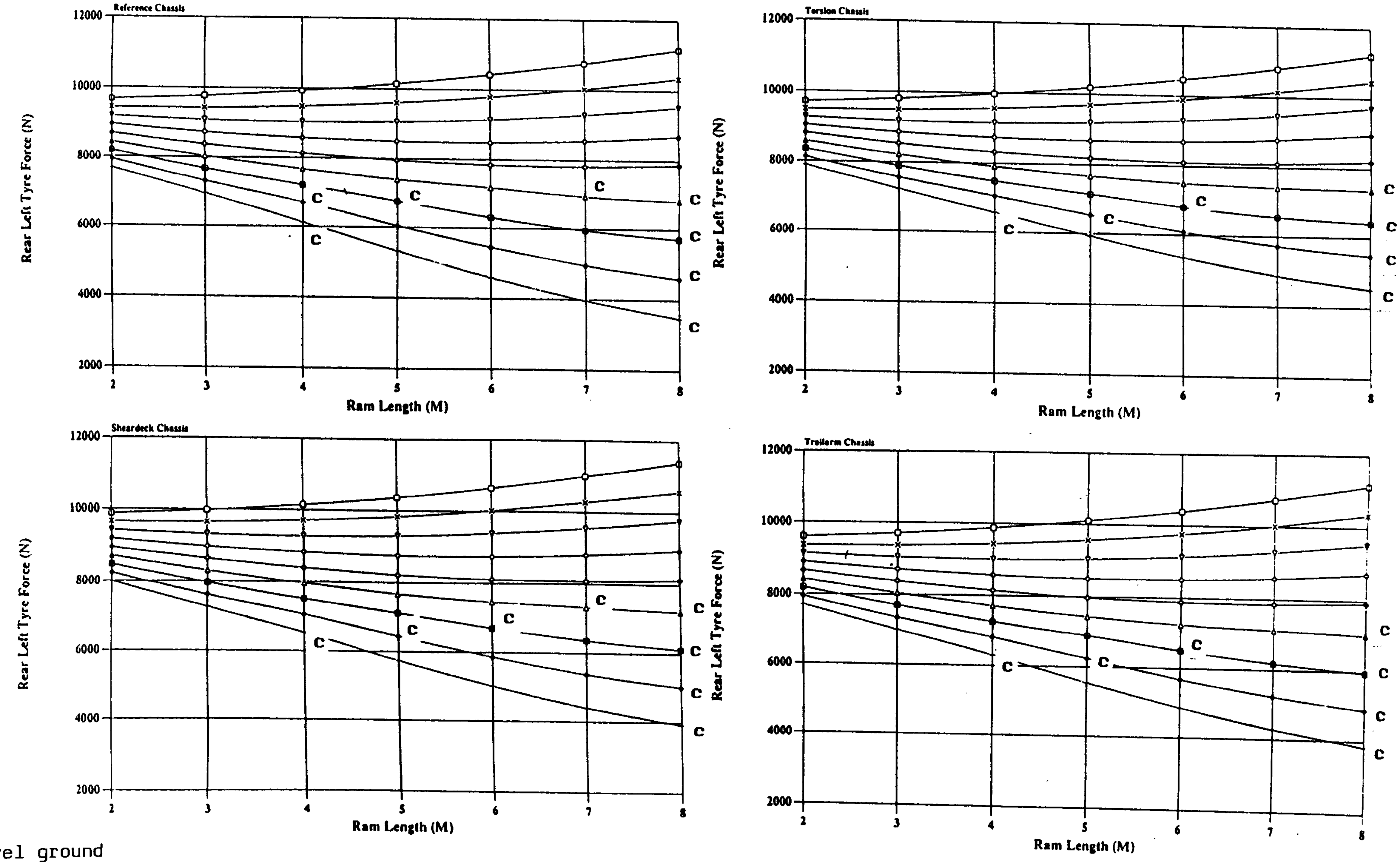

□ = level ground
◁ = 2° ground slope
◇ = 4° ground slope
⊞ = 6° ground slope
– = 8° ground slope

Fig. 5.1c Rear left tyre force versus Ram length and ground slope combinations for a 2500 Kg payload in body position 3 .

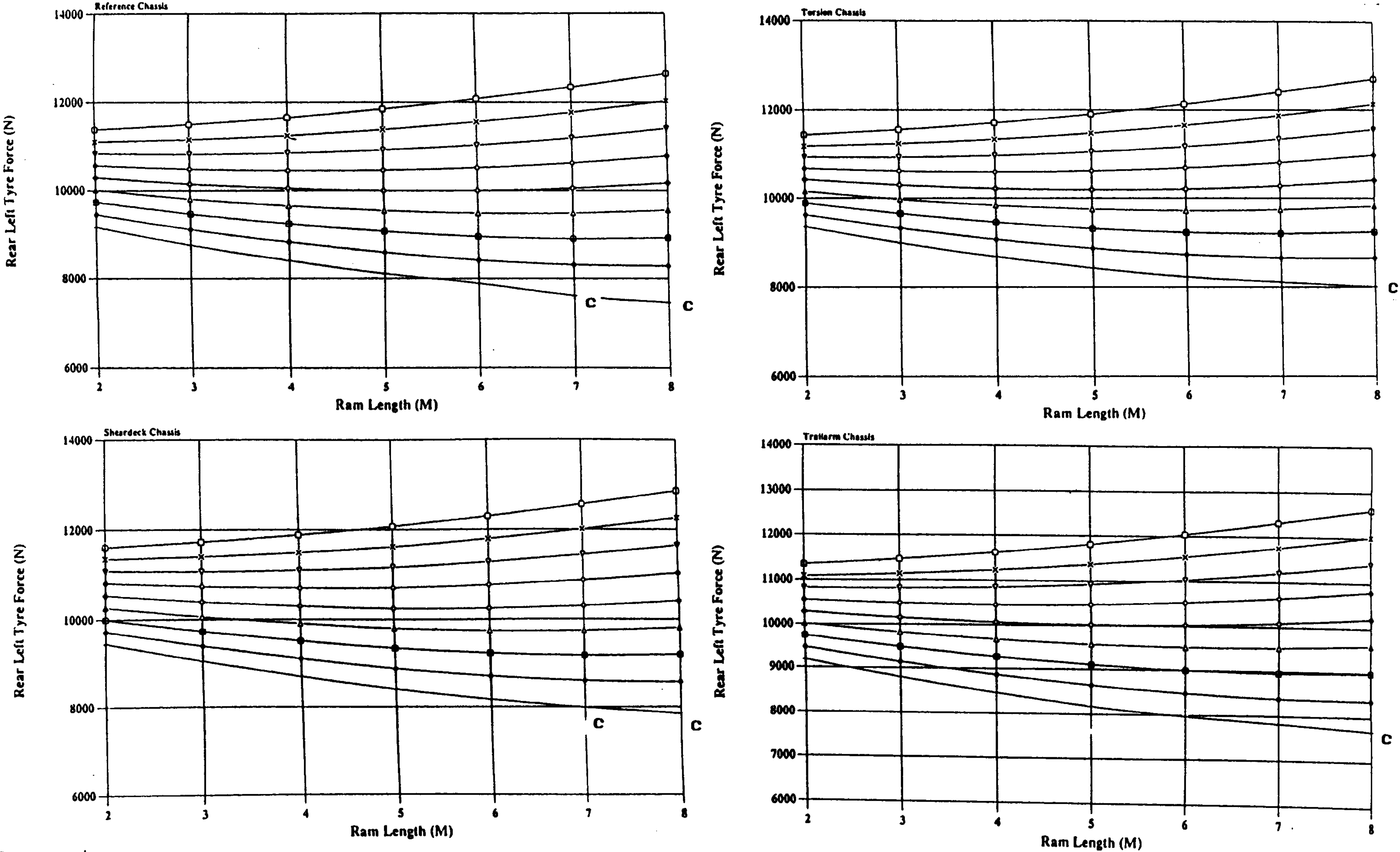

□ = level ground
∇ = 2° ground slope
◇ = 4° ground slope
⊞ = 6° ground slope
⊥ = 8° ground slope

Fig. 5.1d Rear left tyre force versus Ram length and ground slope combinations for a 2500 Kg payload in body position 4 .

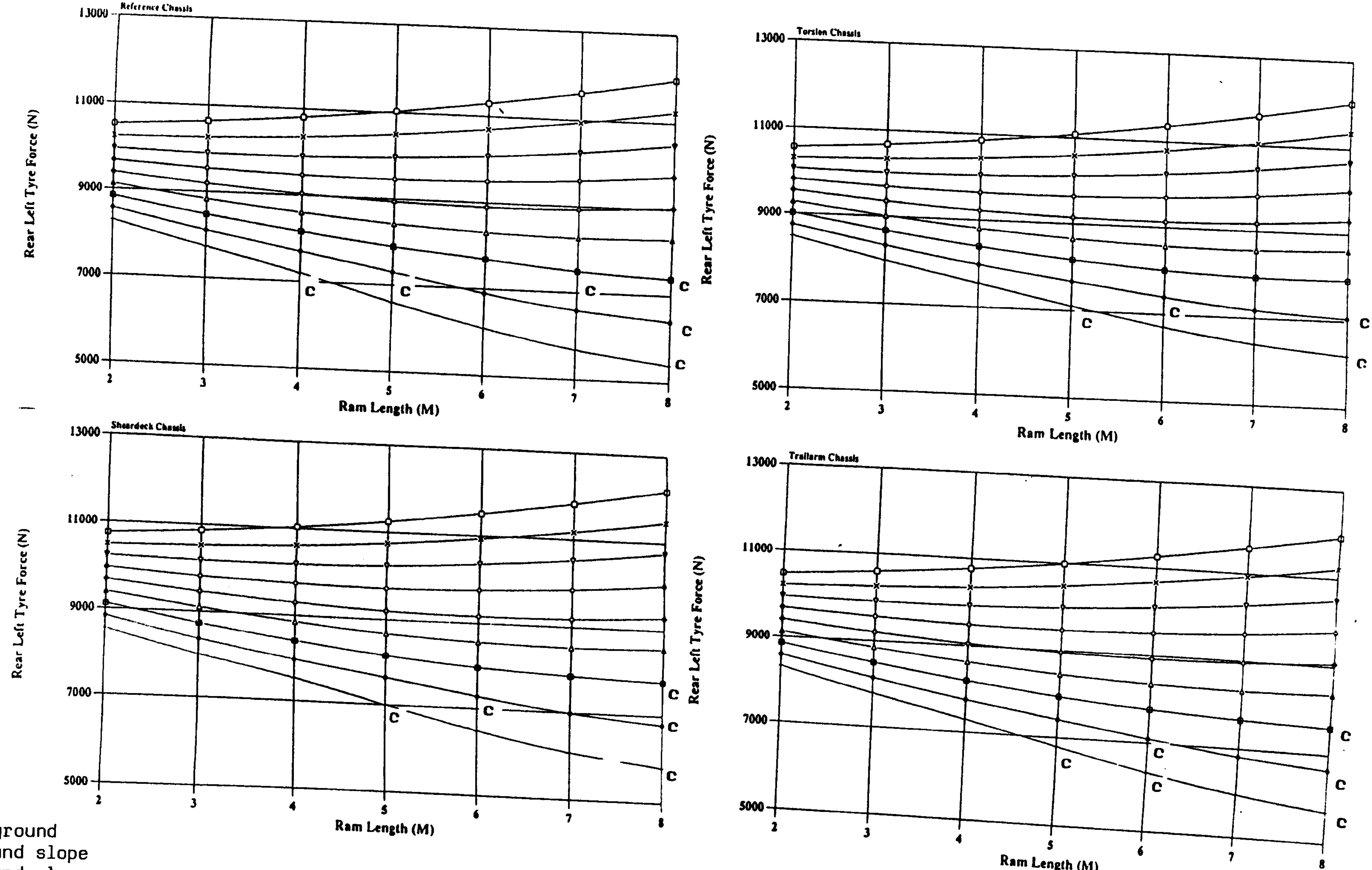

□ = level ground
◁ = 2° ground slope
◇ = 4° ground slope
⊞ = 6° ground slope
— = 8° ground slope

Fig. 5.1e Rear left tyre force versus Ram length and ground slope combinations for a 2500 Kg payload in body position 5 .

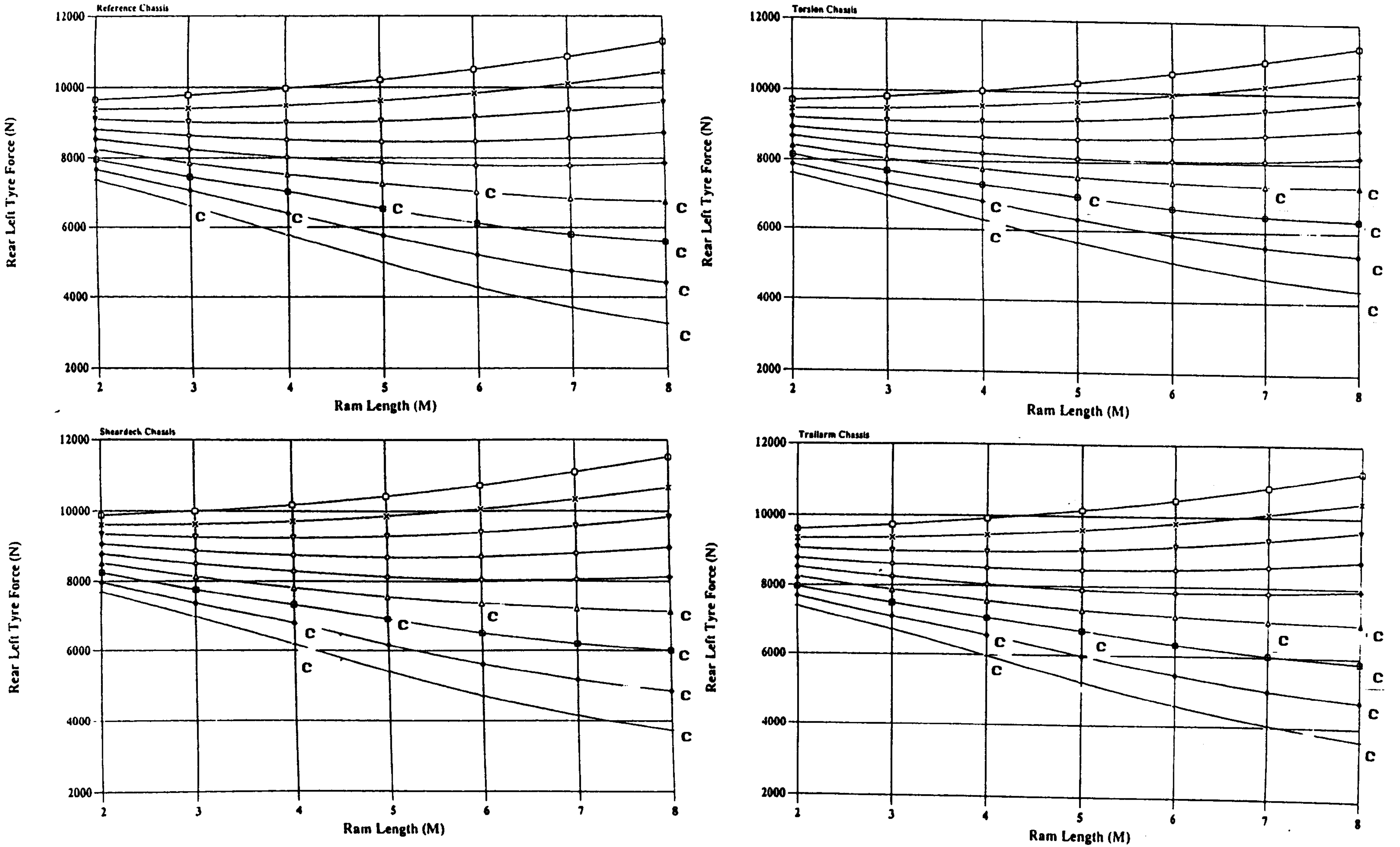

□ = level ground
▽ = 2° ground slope
◇ = 4° ground slope
⊞ = 6° ground slope
– = 8° ground slope

Fig. 5.1f Rear left tyre force versus Ram length and ground slope combinations for a 2500 Kg payload in body position 6 .

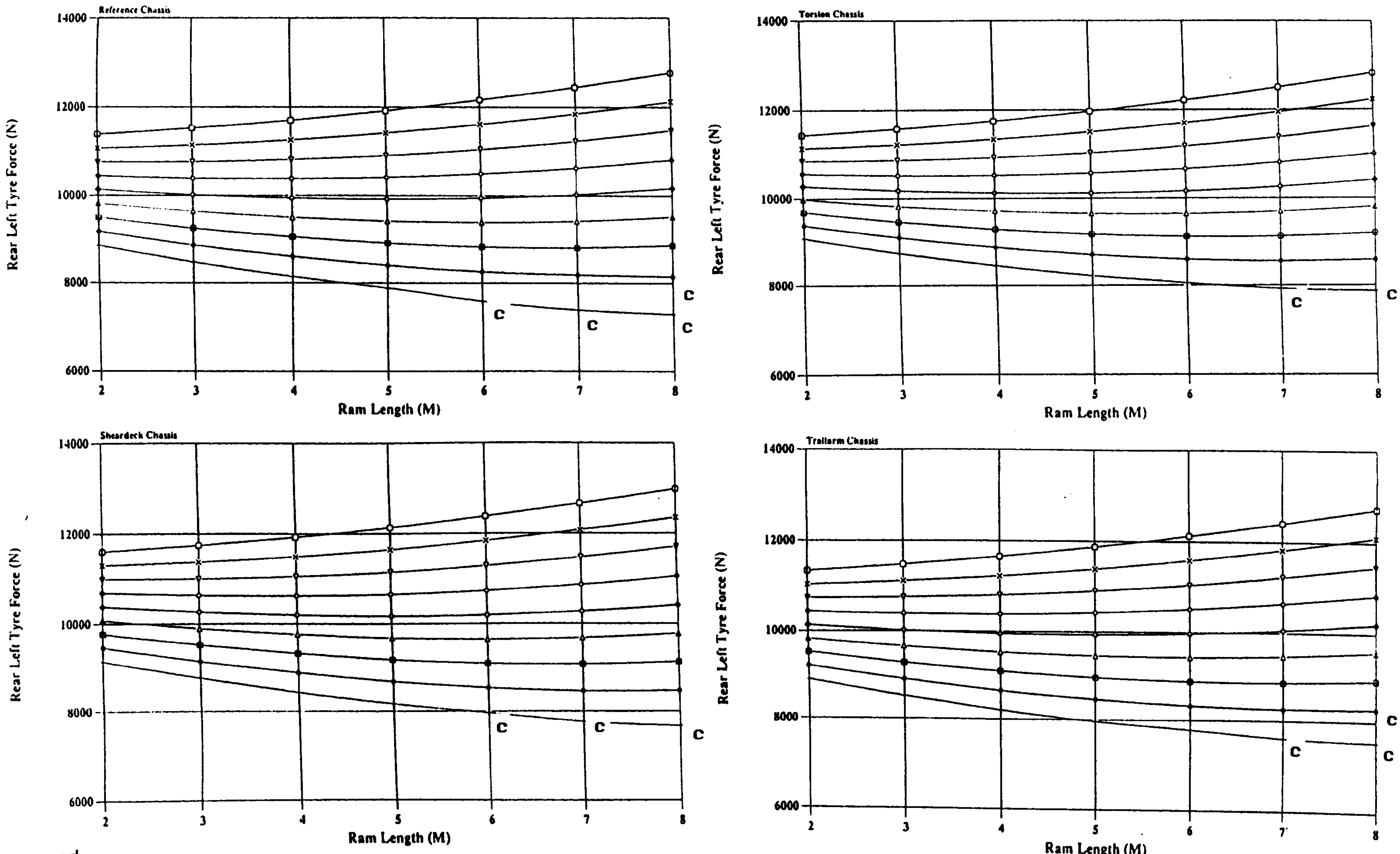

□ = level ground
◁ = 2° ground slope
◇ = 4° ground slope
⊞ = 6° ground slope
- = 8° ground slope

Fig. 5.1g Rear left tyre force versus Ram length and ground slope combinations for a 2500 Kg payload in body position 7 .

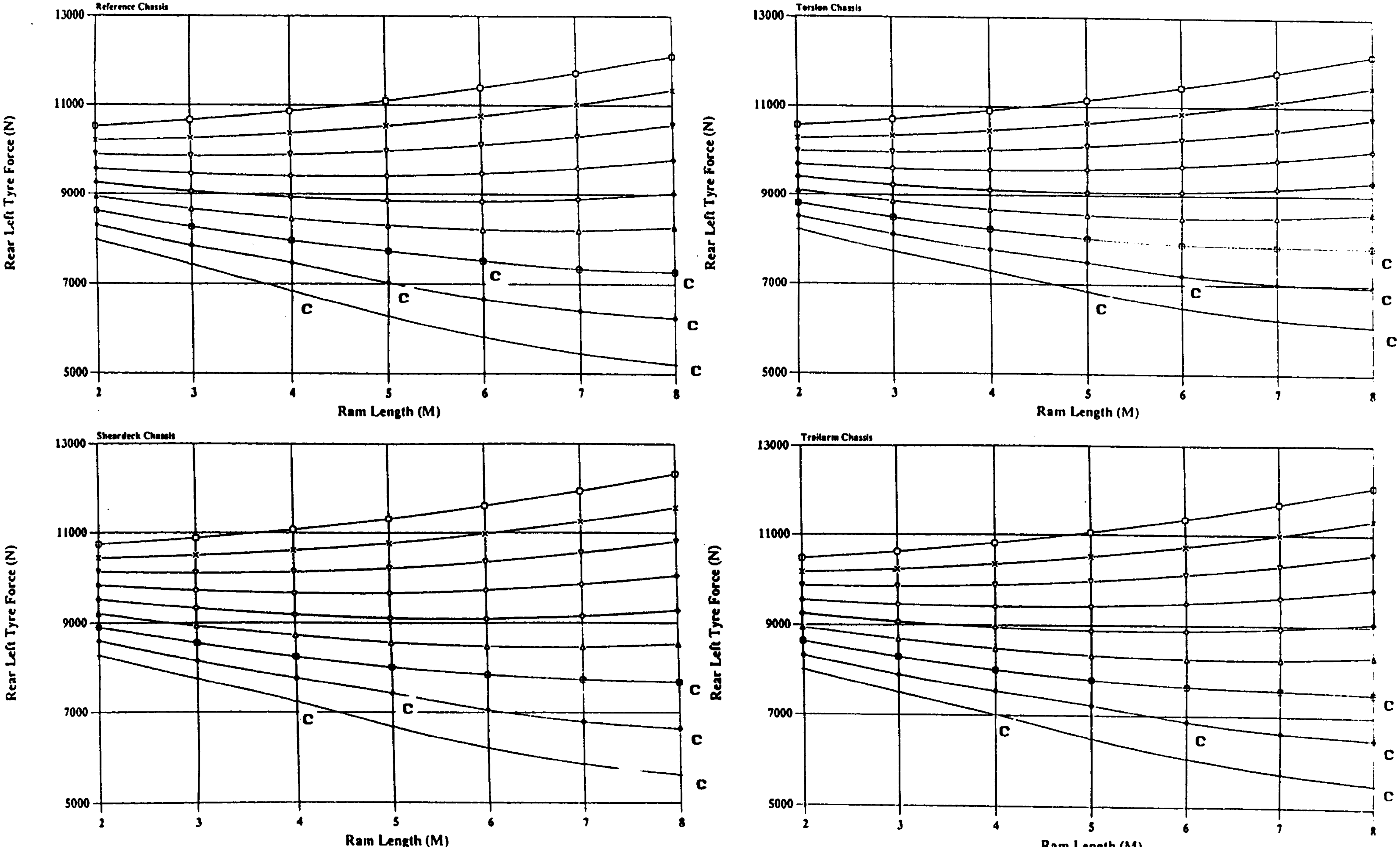

□ = level ground
∇ = 2° ground slope
⊞ = 4° ground slope
⊕ = 6° ground slope
\ = 8° ground slope

Fig. 5.1h Rear left tyre force versus Ram length and ground slope combinations for a 2500 Kg payload in body position 8 .

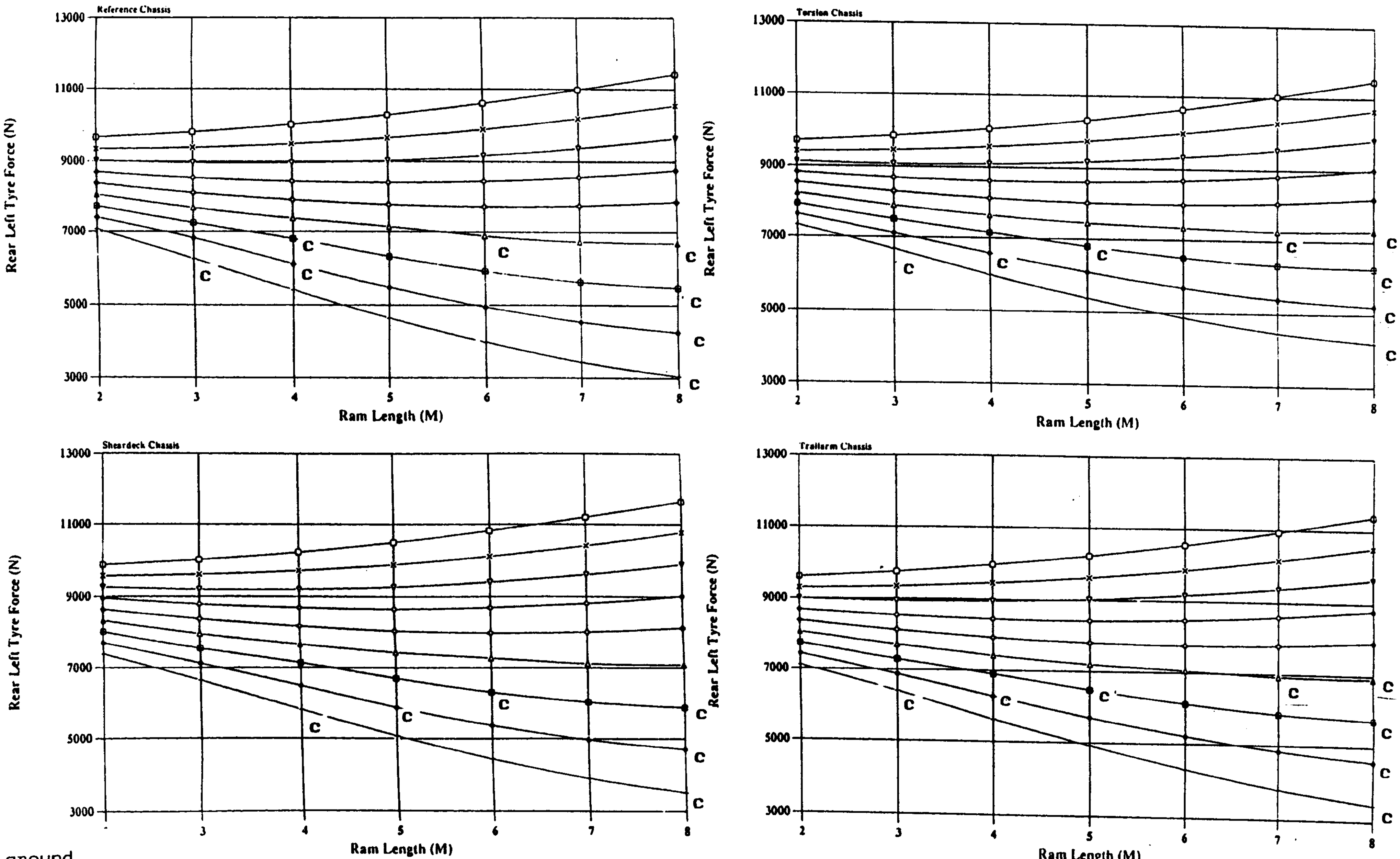

□ = level ground
▽ = 2° ground slope
◇ = 4° ground slope
⊞ = 6° ground slope
– = 8° ground slope

Fig. 5.1i Rear left tyre force versus Ram length and ground slope combinations for a 2500 Kg payload in body position 9 .

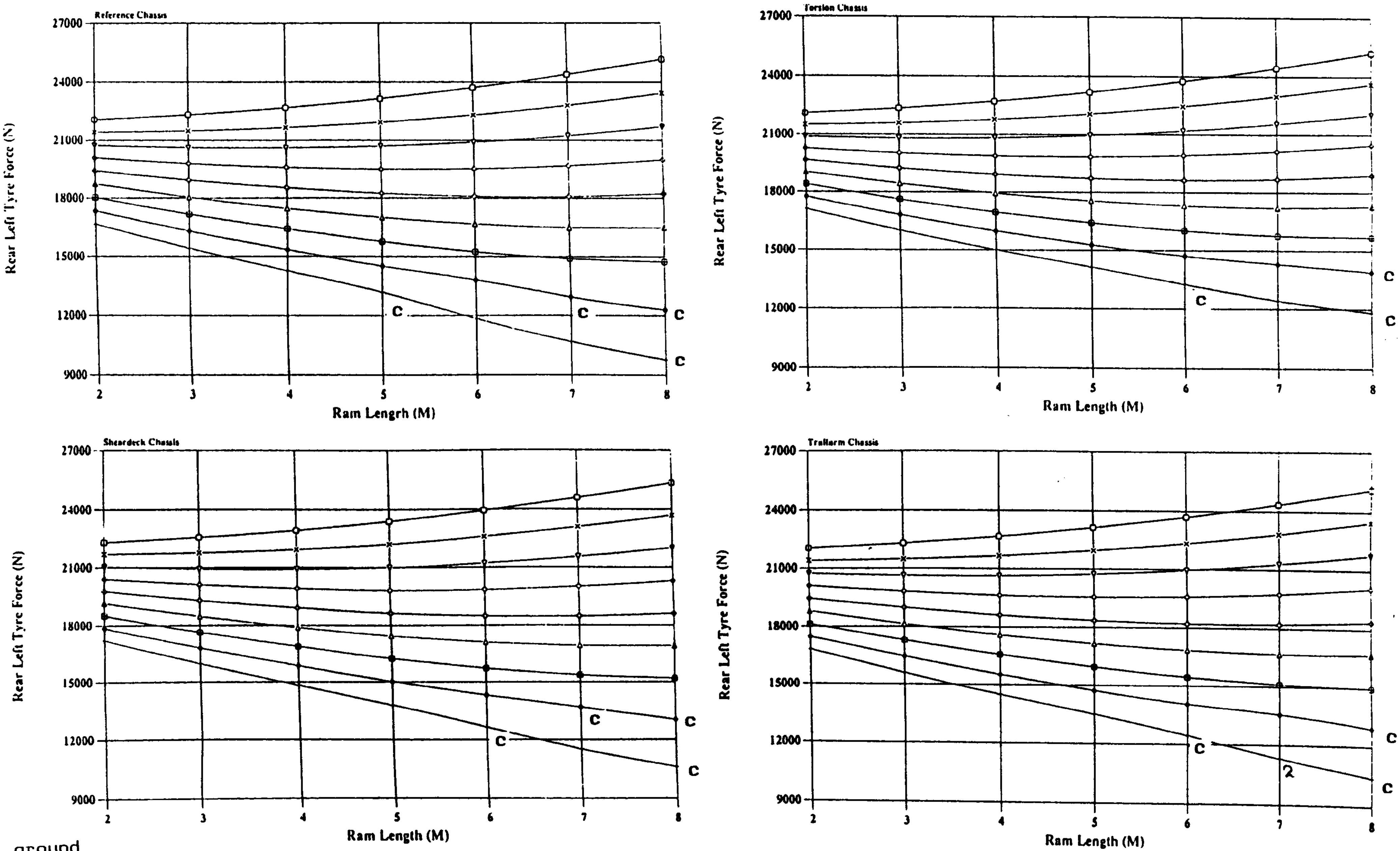

□= level ground
▽= 2° ground slope
◇= 4° ground slope
⊞= 6° ground slope
–= *8° ground slope*

Fig. 5.2a Rear left tyre force versus Ram length and ground slope combinations for a 10000 Kg payload in body position 1 .

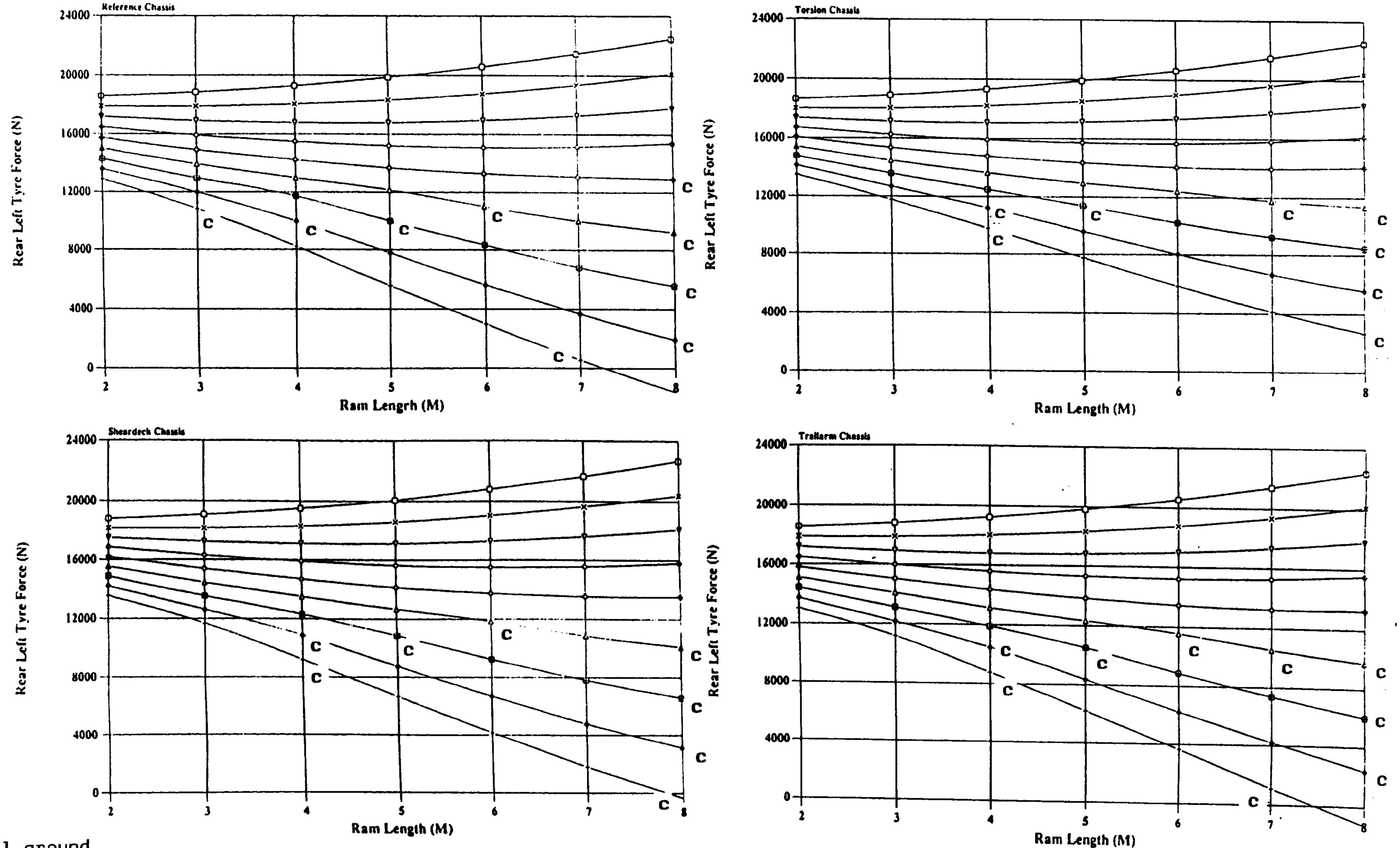

□ = level ground
◁ = 2° ground slope
◇ = 4° ground slope
⊞ = 6° ground slope
− = 8° ground slope

Fig. 5.2b Rear left tyre force versus Ram length and ground slope combinations for a 10000 Kg payload in body position 2 .

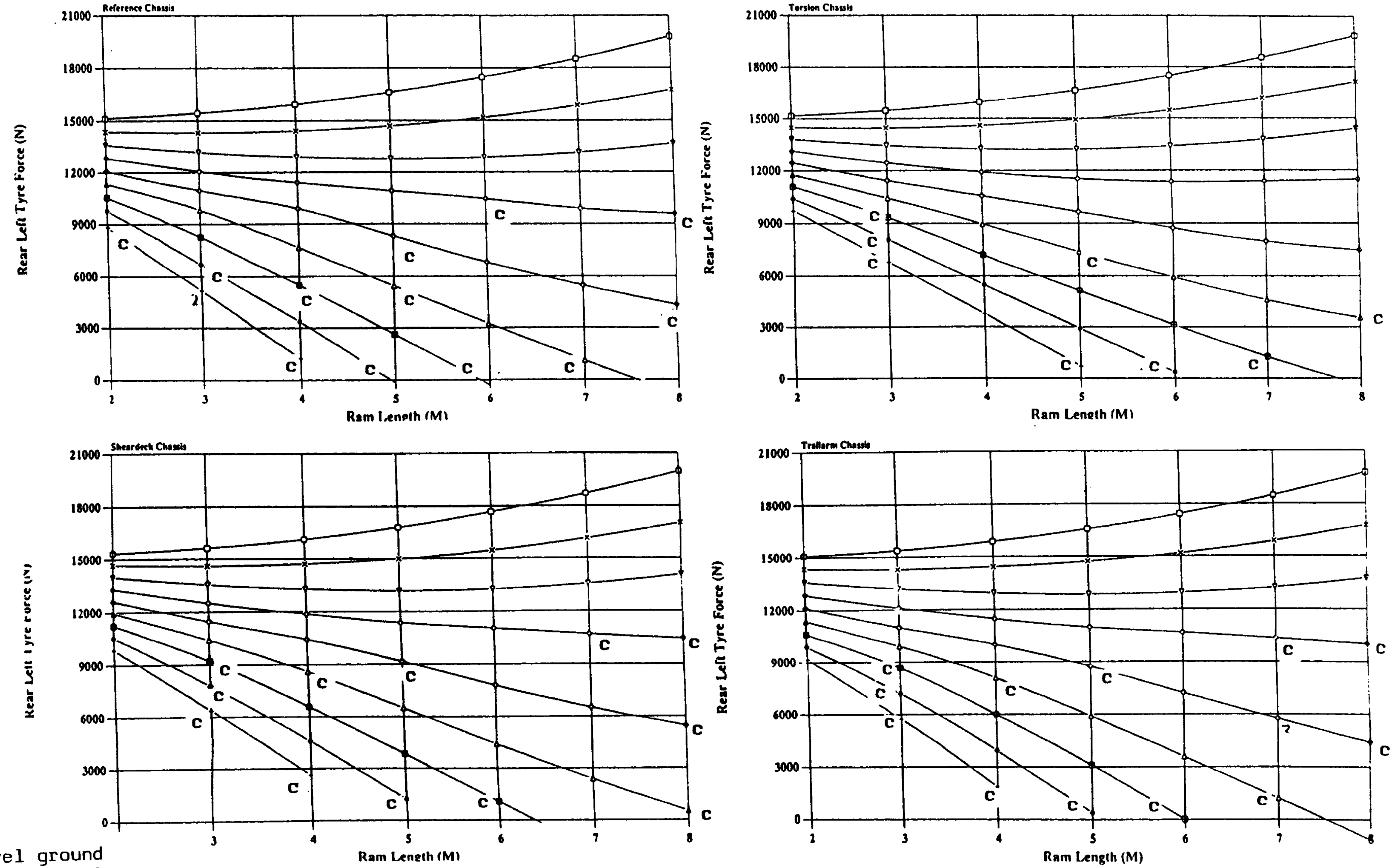

□ = level ground
▽ = 2° ground slope
◇ = 4° ground slope
⊞ = 6° ground slope
– = 8° ground slope

Fig. 5.2c Rear left tyre force versus Ram length and ground slope combinations for a 10000 Kg payload in body position 3 .

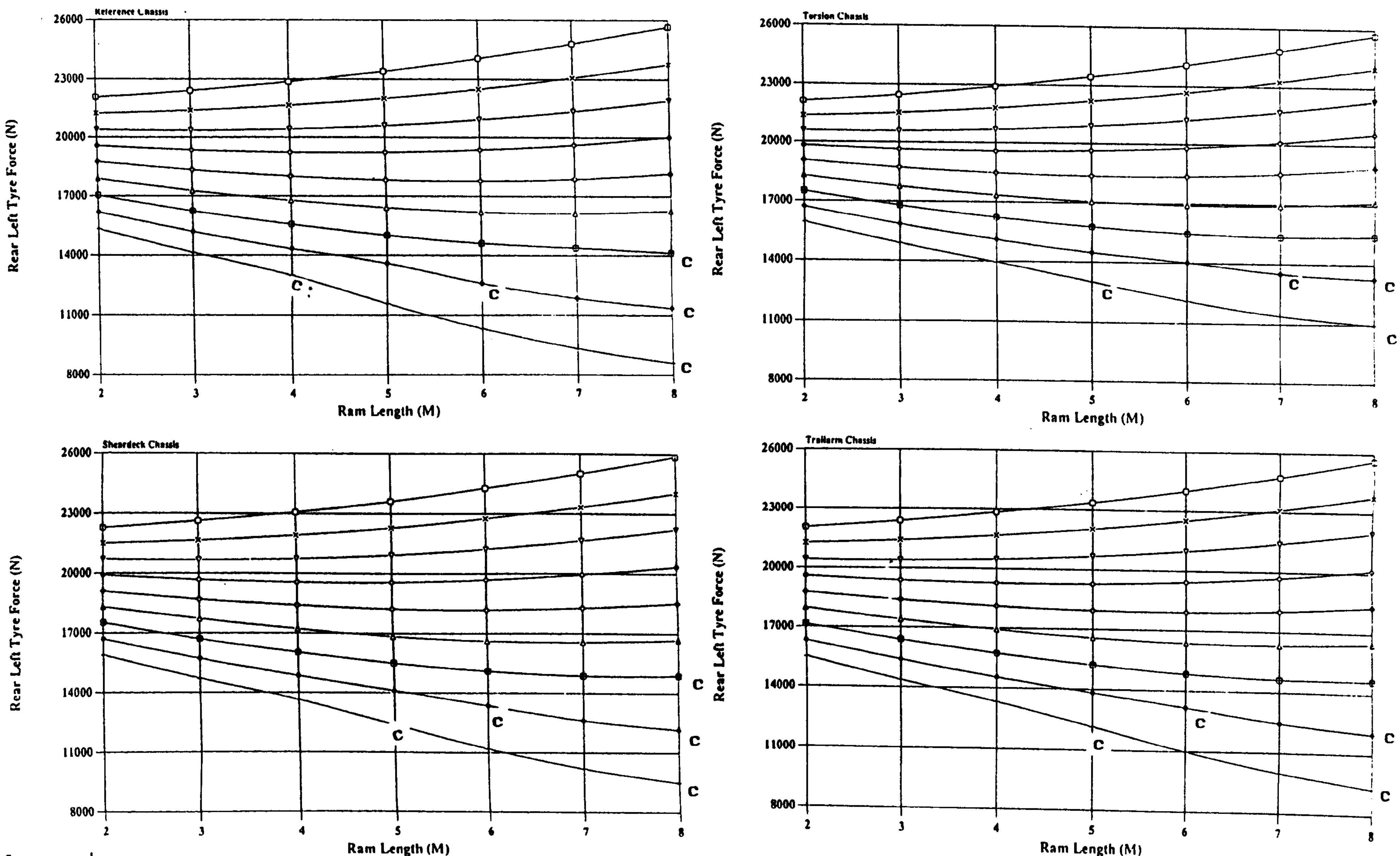

□= level ground
▽= 2° ground slope
◇= 4° ground slope
⊞= 6° ground slope
-= 8° ground slope

Fig. 5.2d Rear left tyre force versus Ram length and ground slope combinations for a 10000 Kg payload in body position 4 .

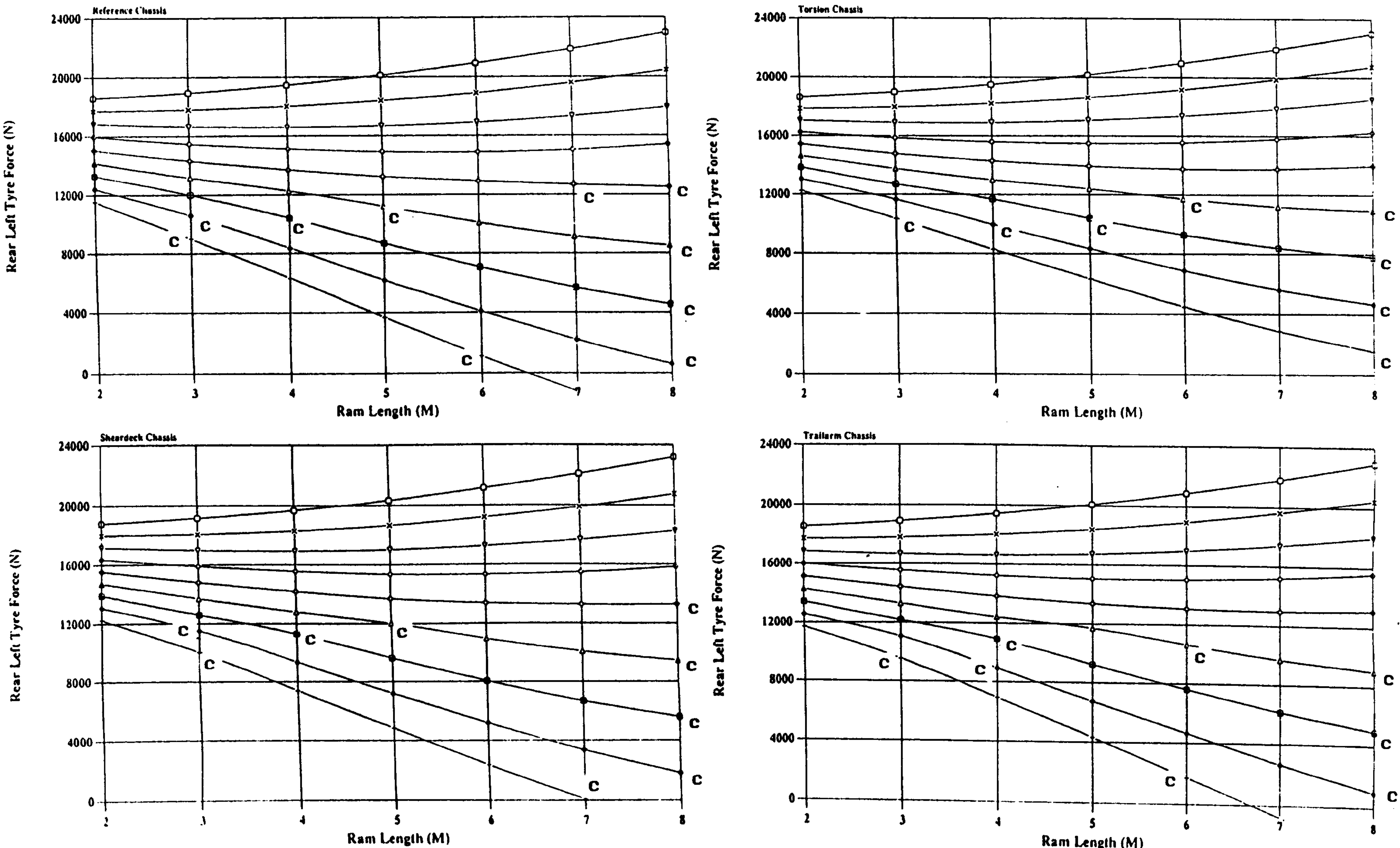

□ = level ground
∇ = 2° ground slope
◇ = 4° ground slope
⊞ = 6° ground slope
- = 8° ground slope

Fig. 5.2e Rear left tyre force versus Ram length and ground slope combinations for a 10000 Kg payload in body position 5 .

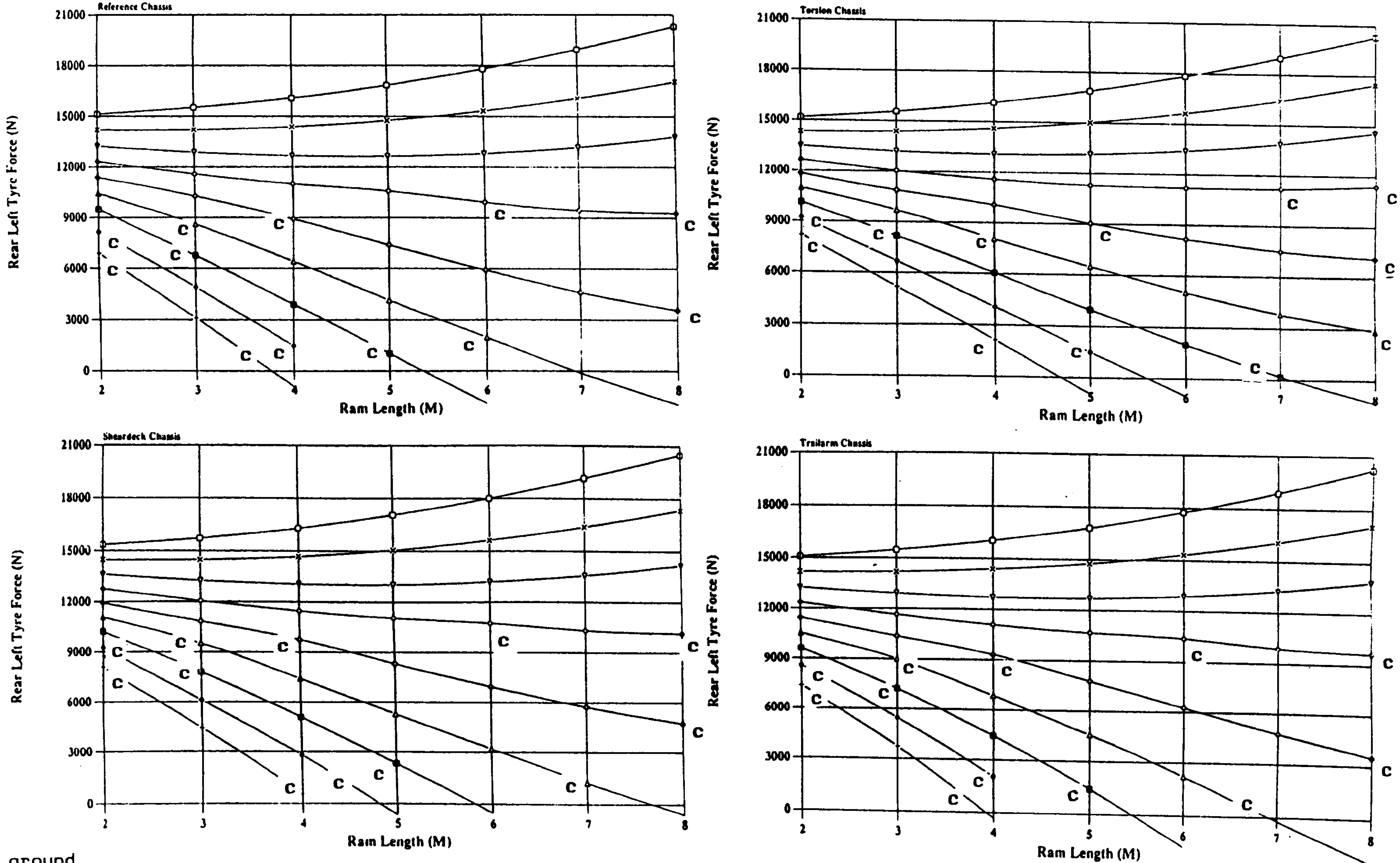

□ = level ground
▽ = 2° ground slope
◇ = 4° ground slope
⊞ = 6° ground slope
– = 8° ground slope

Fig. 5.2f Rear left tyre force versus Ram length and ground slope combinations for a 10000 Kg payload in body position 6 .

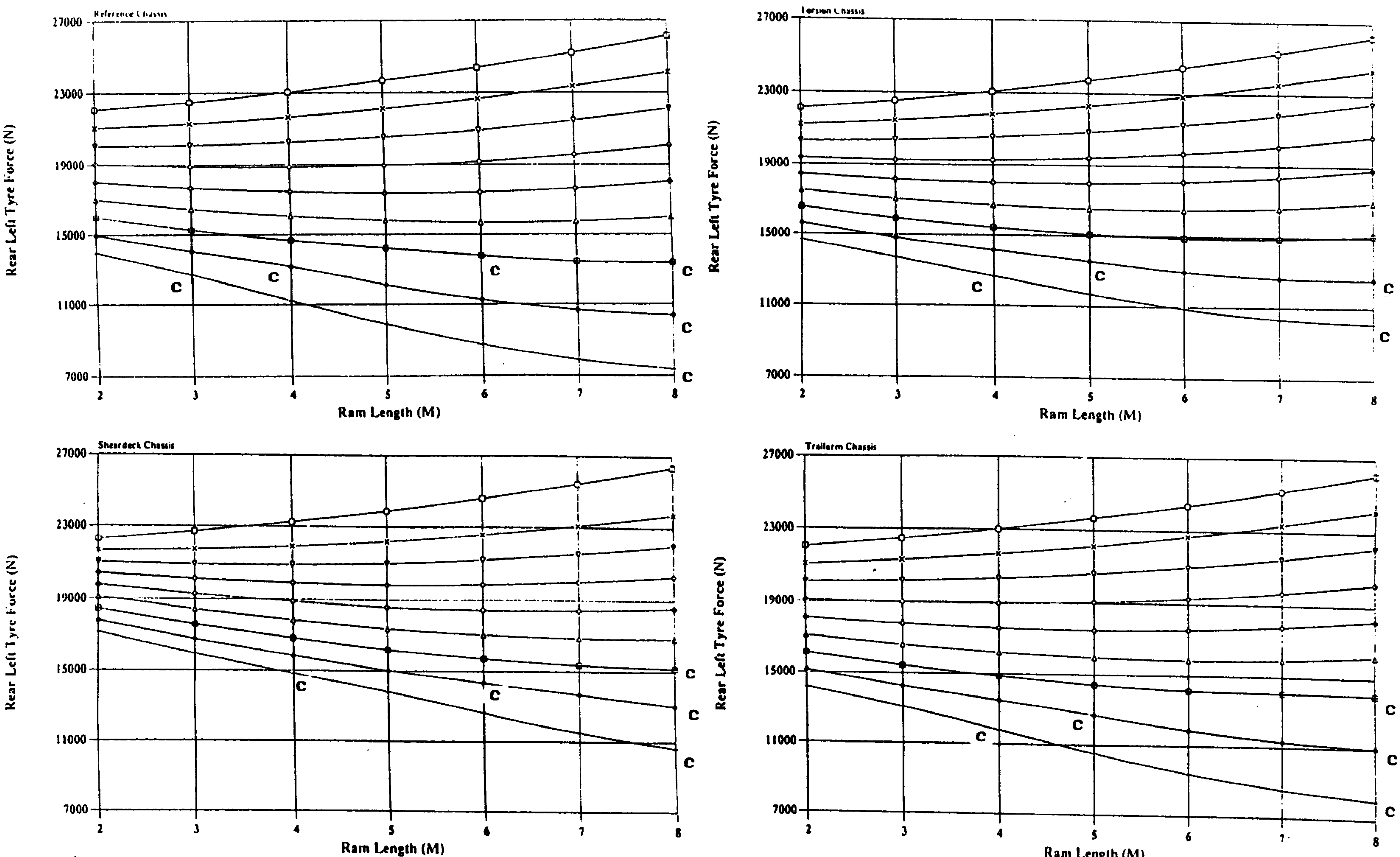

□ = level ground
▽ = 2° ground slope
◇ = 4° ground slope
⊞ = 6° ground slope
⌐ = 8° ground slope

Fig. 5.2g Rear left tyre force versus Ram length and ground slope combinations for a 10000 Kg payload in body position 7 .

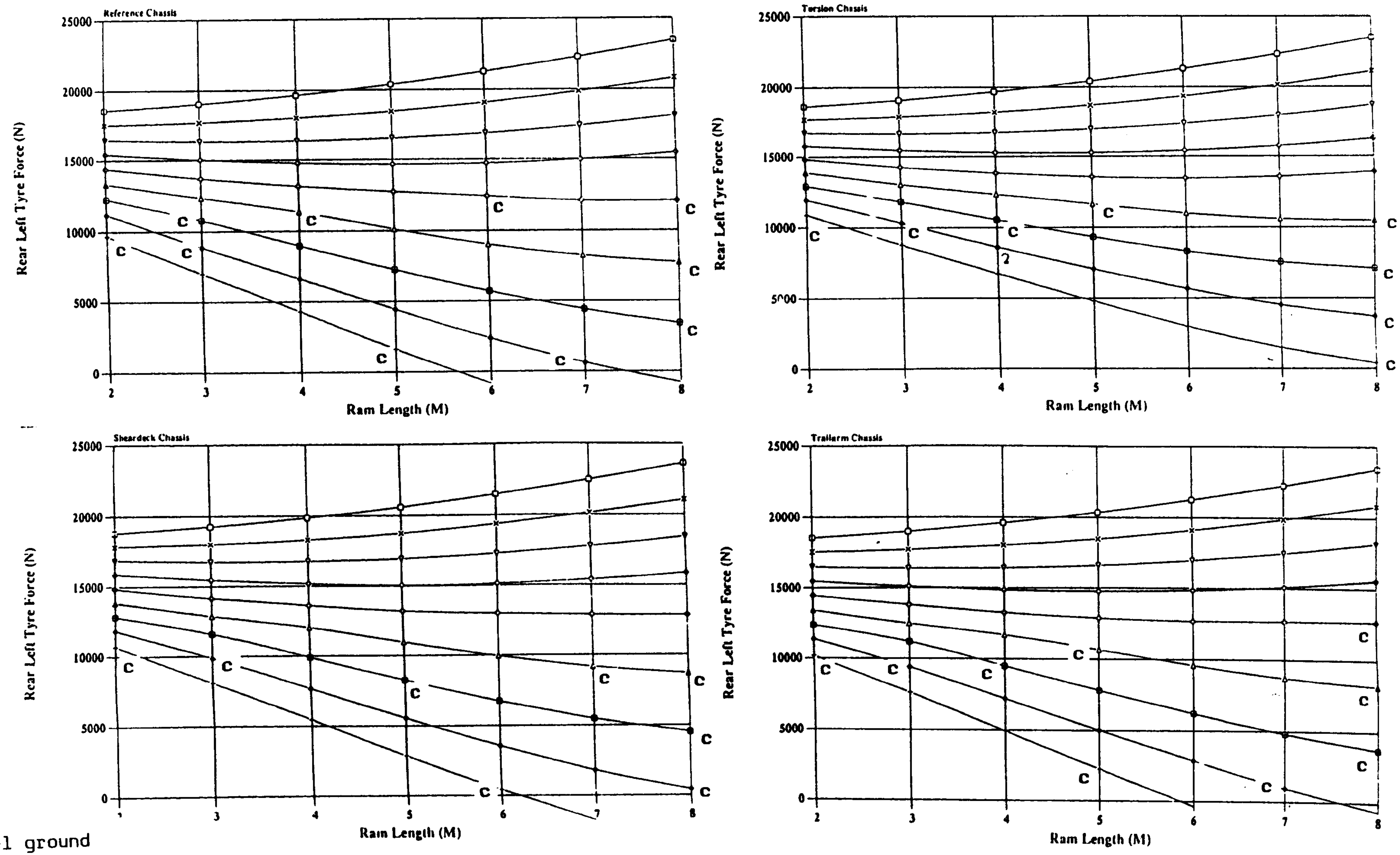

□ = level ground
▽ = 2° ground slope
◇ = 4° ground slope
⊞ = 6° ground slope
– = 8° ground slope

Fig. 5.2h Rear left tyre force versus Ram length and ground slope combinations for a 10000 Kg payload in body position 8 .

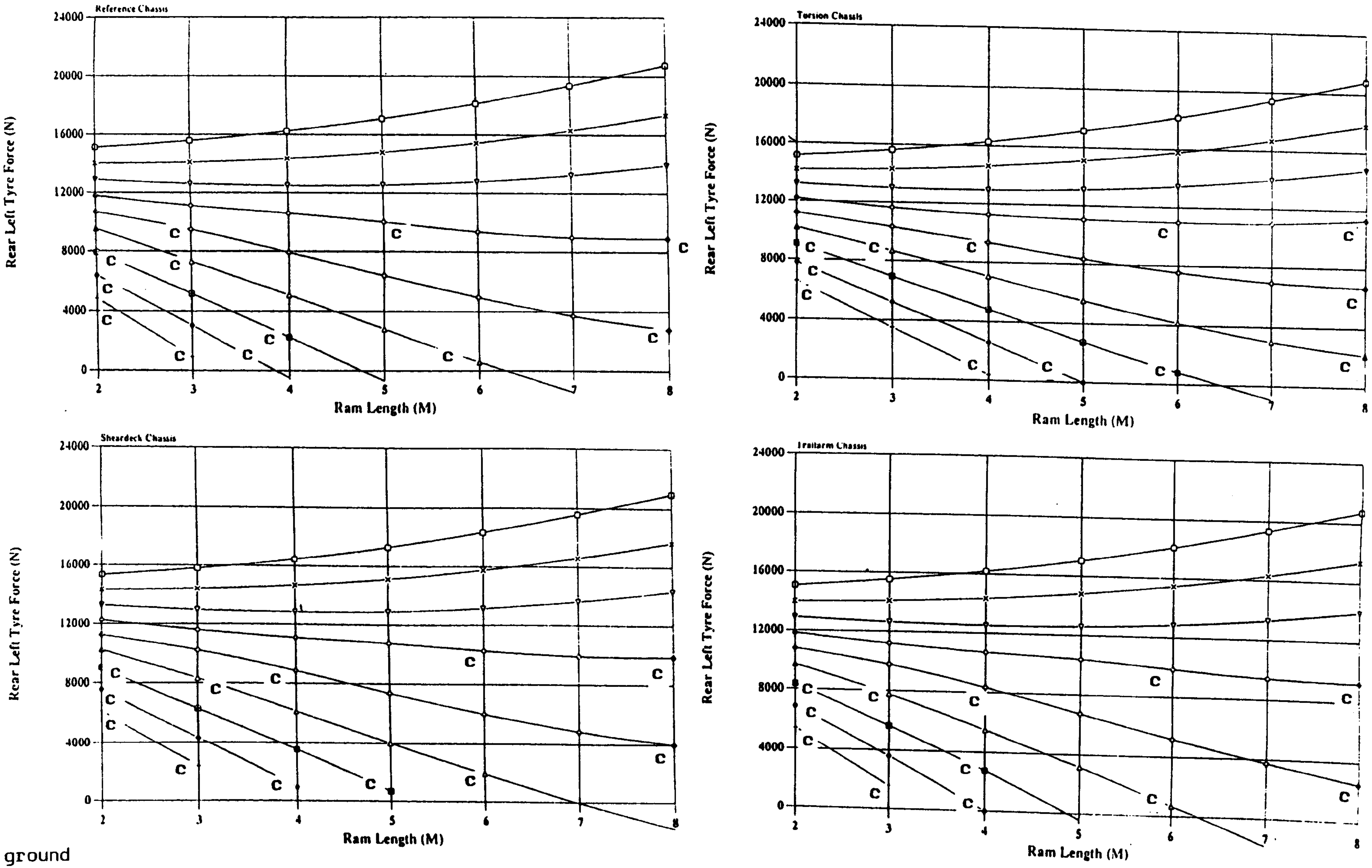

□ = level ground
▽ = 2° ground slope
◇i= 4° ground slope
⊞ = 6° ground slope
_ = 8° ground slope

Fig. 5.2i Rear left tyre force versus Ram length and ground slope combinations for a 10000 Kg payload in body position 9 .

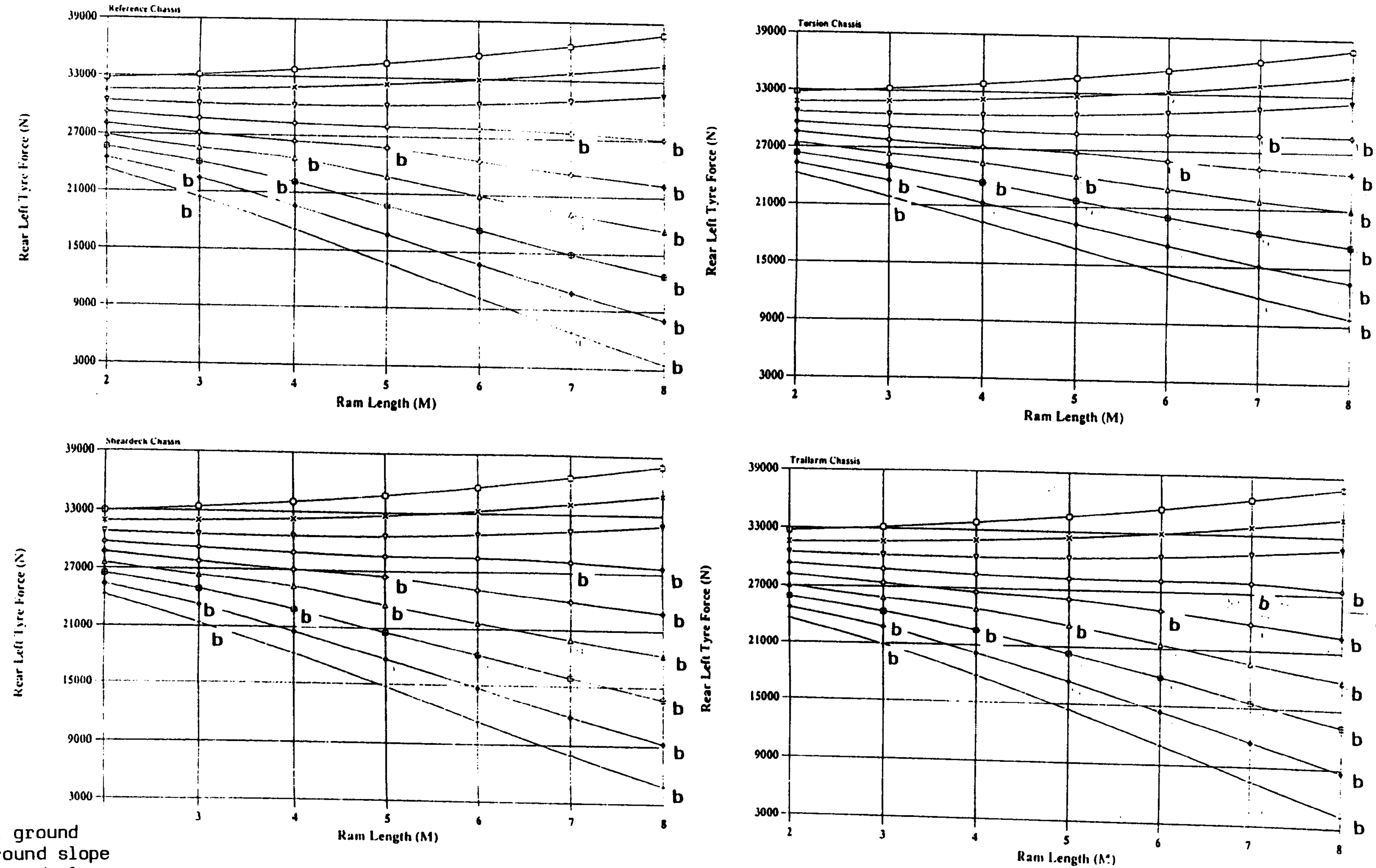

□ = level ground
▽ = 2° ground slope
◇ = 4° ground slope
⊞ = 6° ground slope
– = 8° ground slope

Fig. 5.3a Rear left tyre force versus Ram length and ground slope combinations for a 17500 Kg payload in body position 1 .

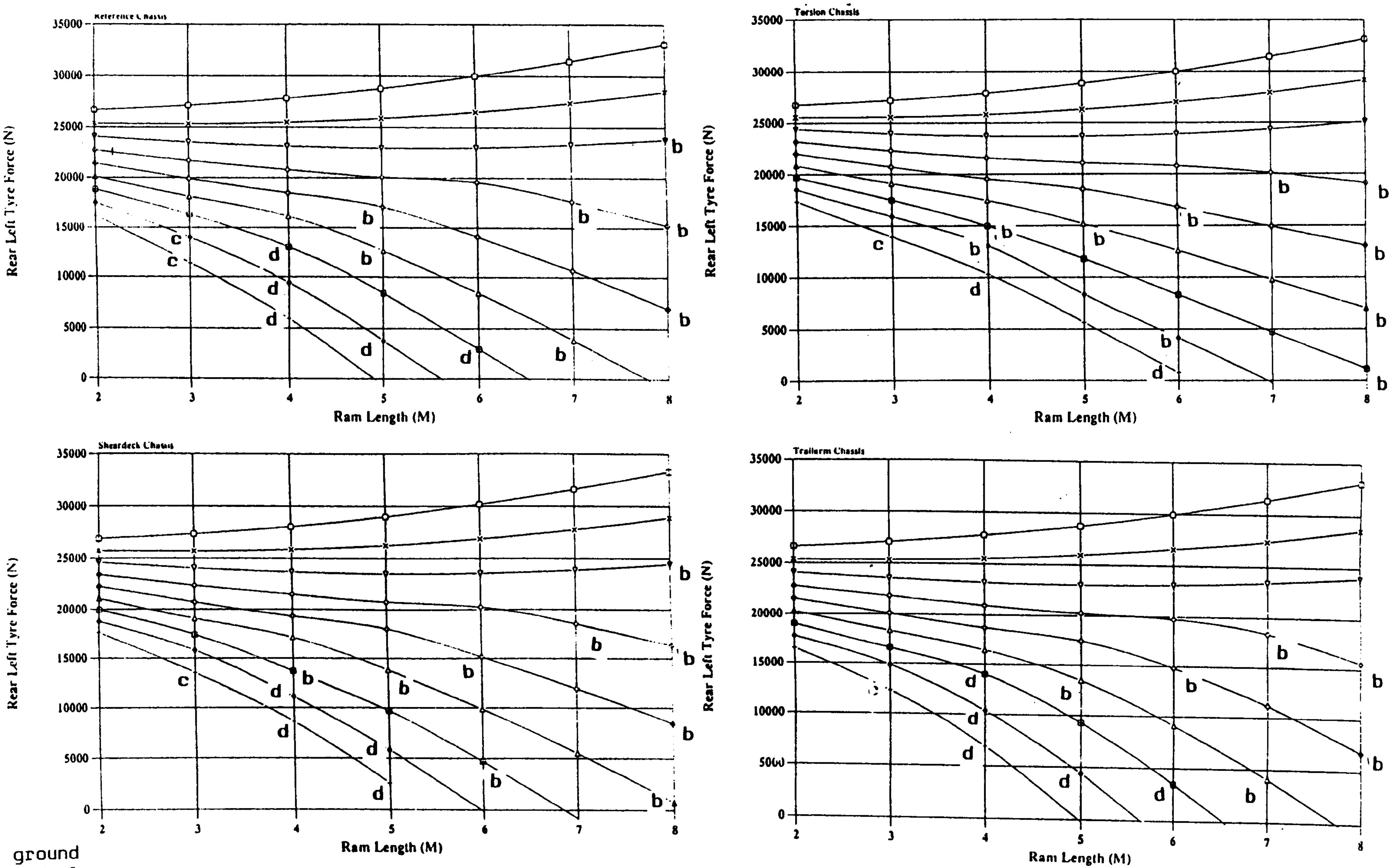

□ = level ground
▽ = 2° ground slope
◇ = 4° ground slope
⊞ = 6° ground slope
– = 8° ground slope

Fig. 5.3b Rear left tyre force versus Ram length and ground slope combinations for a 17500 Kg payload in body position 2 .

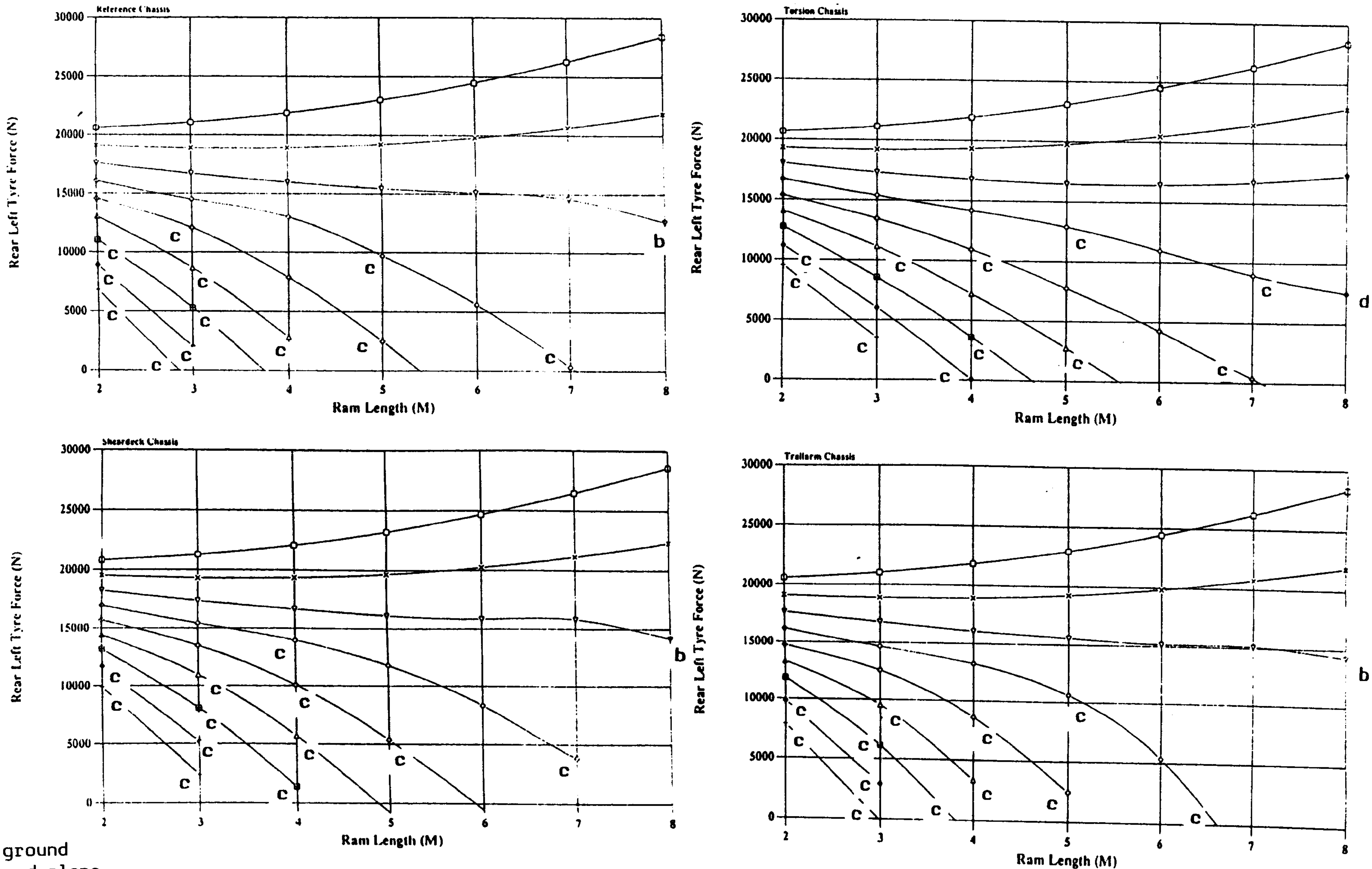

□ = level ground
▽ = 2° ground slope
◇ = 4° ground slope
⊞ = 6° ground slope
– = 8° ground slope

Fig. 5.3c Rear left tyre force versus Ram length and ground slope combinations for a 17500 Kg payload in body position 3 .

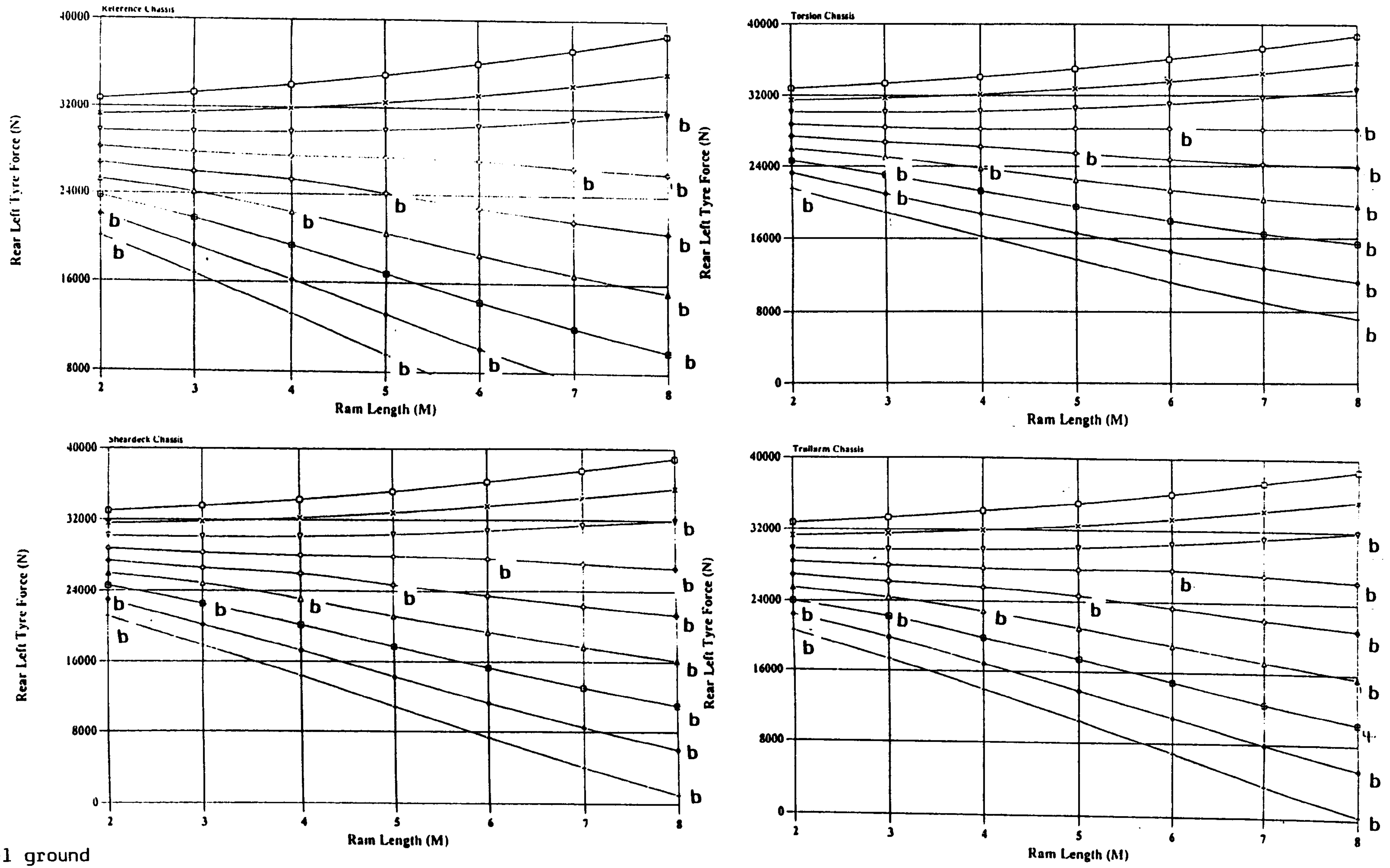

□ = level ground
▽ = 2° ground slope
◇ = 4° ground slope
⊞ = 6° ground slope
- = 8° ground slope

Fig. 5.3d Rear left tyre force versus Ram length and ground slope combinations for a 17500 Kg payload in body position 4 .

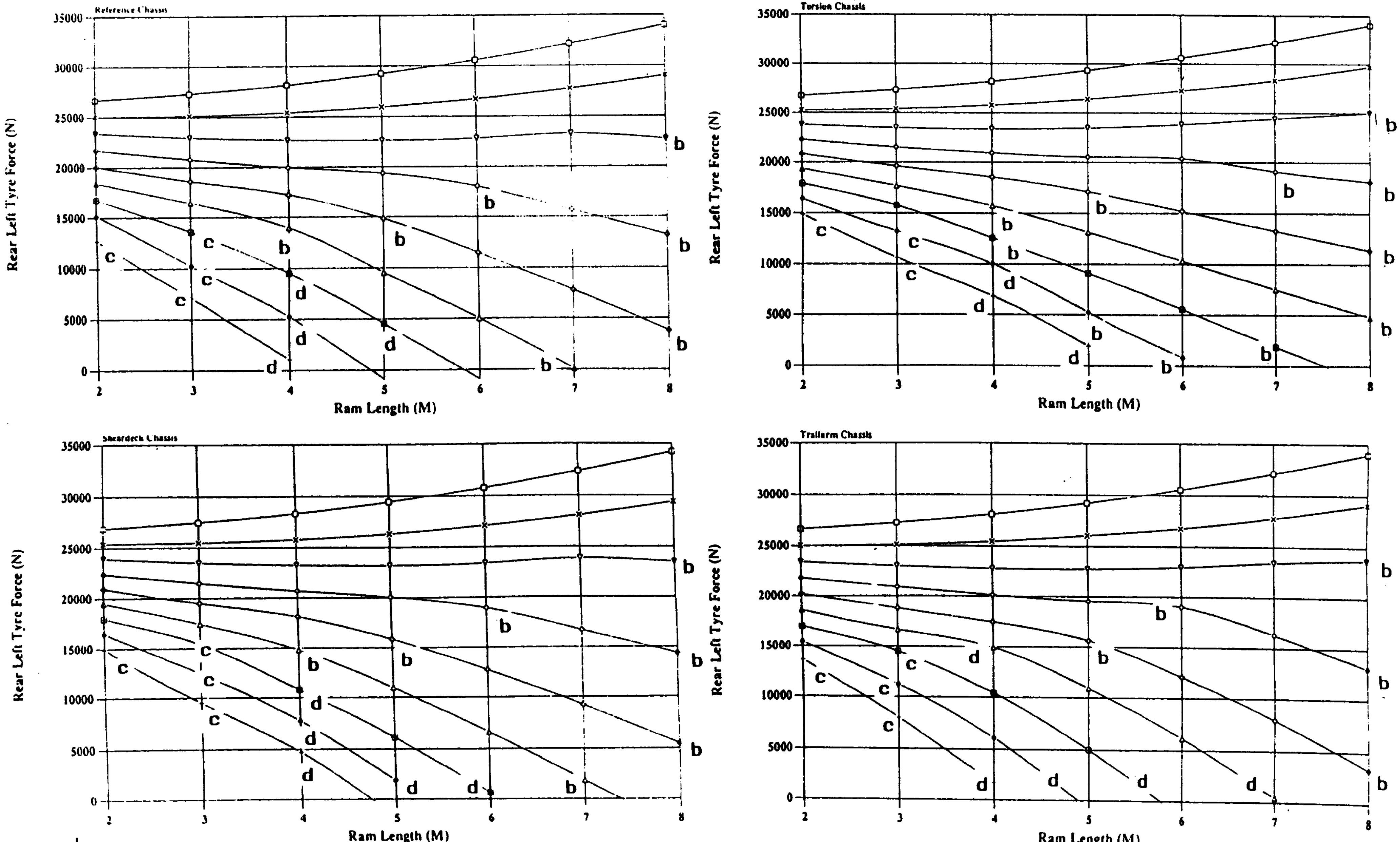

□ = level ground
▽ = 2° ground slope
◇ = 4° ground slope
⊞ = 6° ground slope
− = 8° ground slope

Fig. 5.3e Rear left tyre force versus Ram length and ground slope combinations for a 17500 Kg payload in body position 5 .

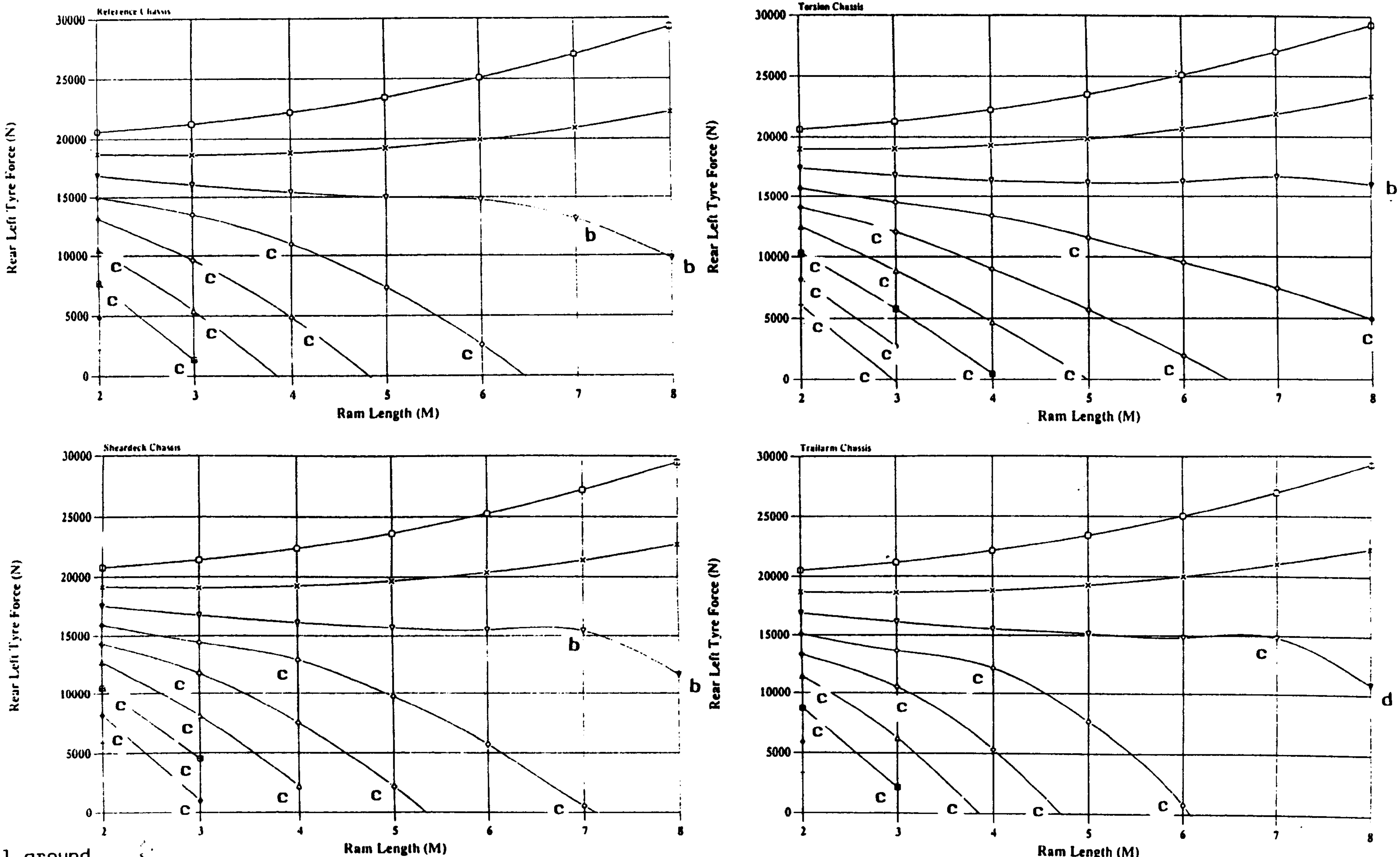

□ = level ground
▽ = 2° ground slope
◇ = 4° ground slope
⊞ = 6° ground slope
– = 8° ground slope

Fig. 5.3f Rear left tyre force versus Ram length and ground slope combinations for a 17500 Kg payload in body position 6 .

PAGE
NUMBERING
AS
ORIGINAL

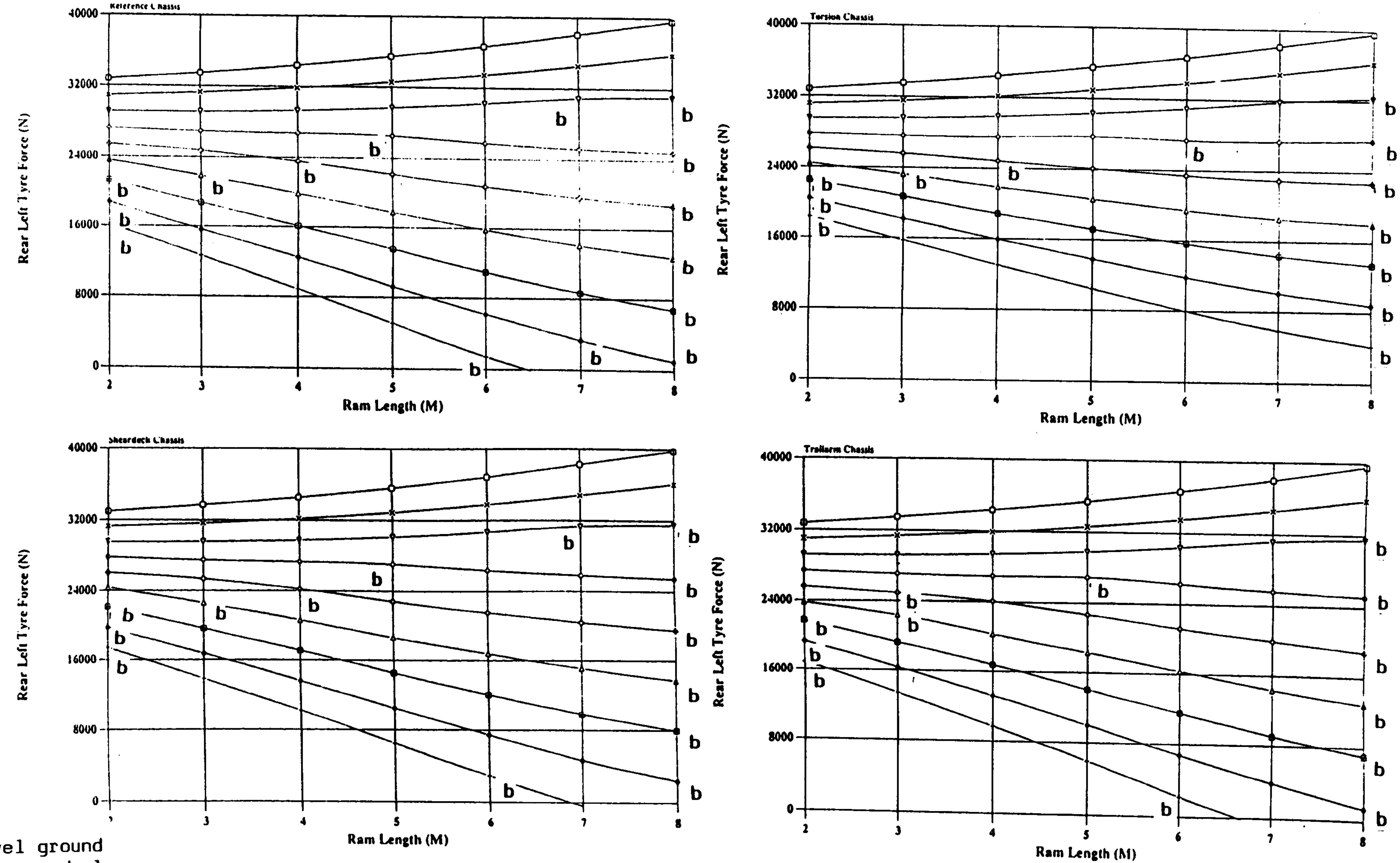

□= level ground
▽= 2° ground slope
◇= 4° ground slope
⊞= 6° ground slope
-= 8° ground slope

Fig. 5.3g Rear left tyre force versus Ram length and ground slope combinations for a 17500 Kg payload in body position 7 .

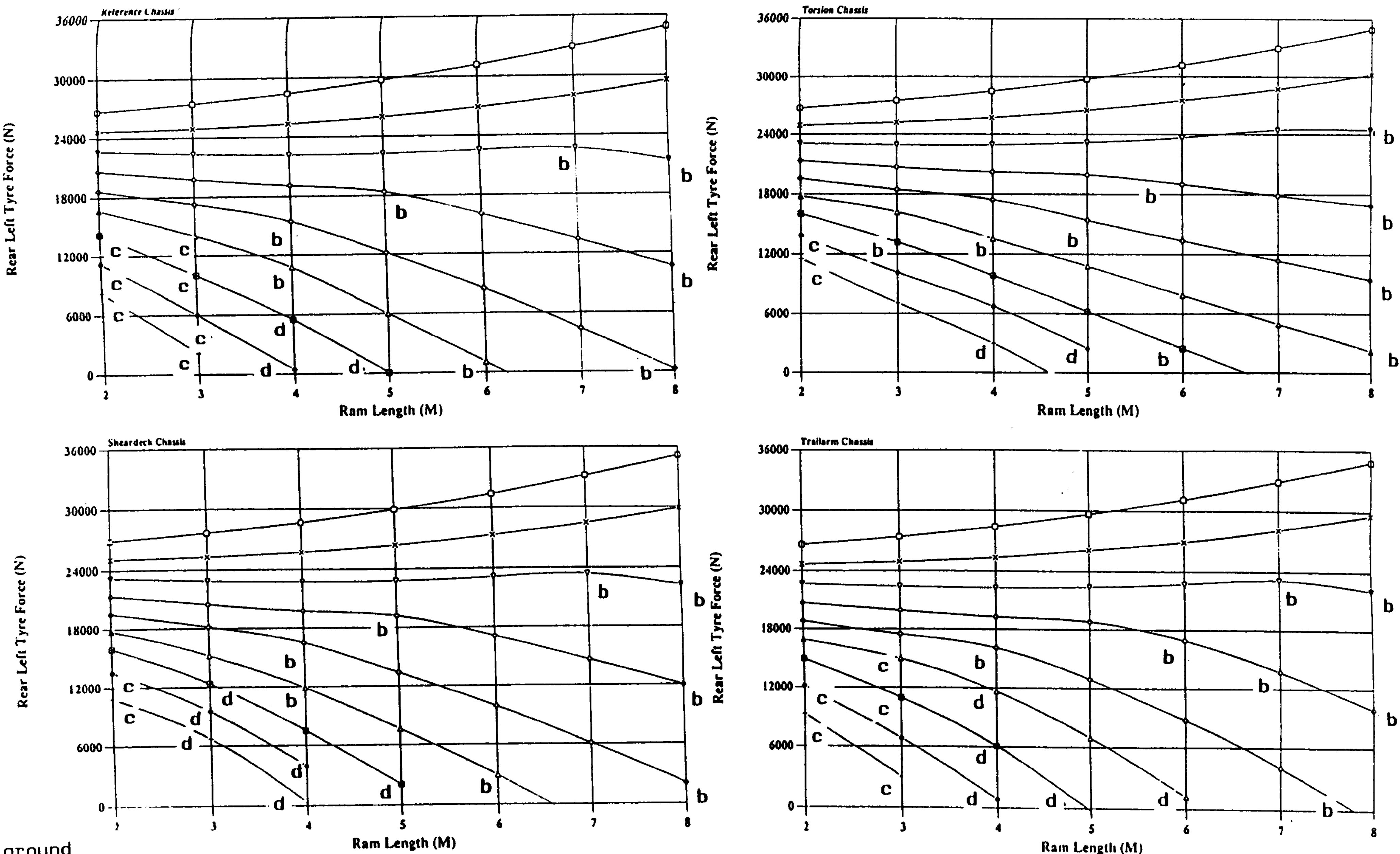

□ = level ground
∇ = 2° ground slope
⊞ = 4° ground slope
⊞ = 6° ground slope
– = 8° ground slope

Fig. 5.3h Rear left tyre force versus Ram length and ground slope combinations for a 17500 Kg payload in body position 8 .

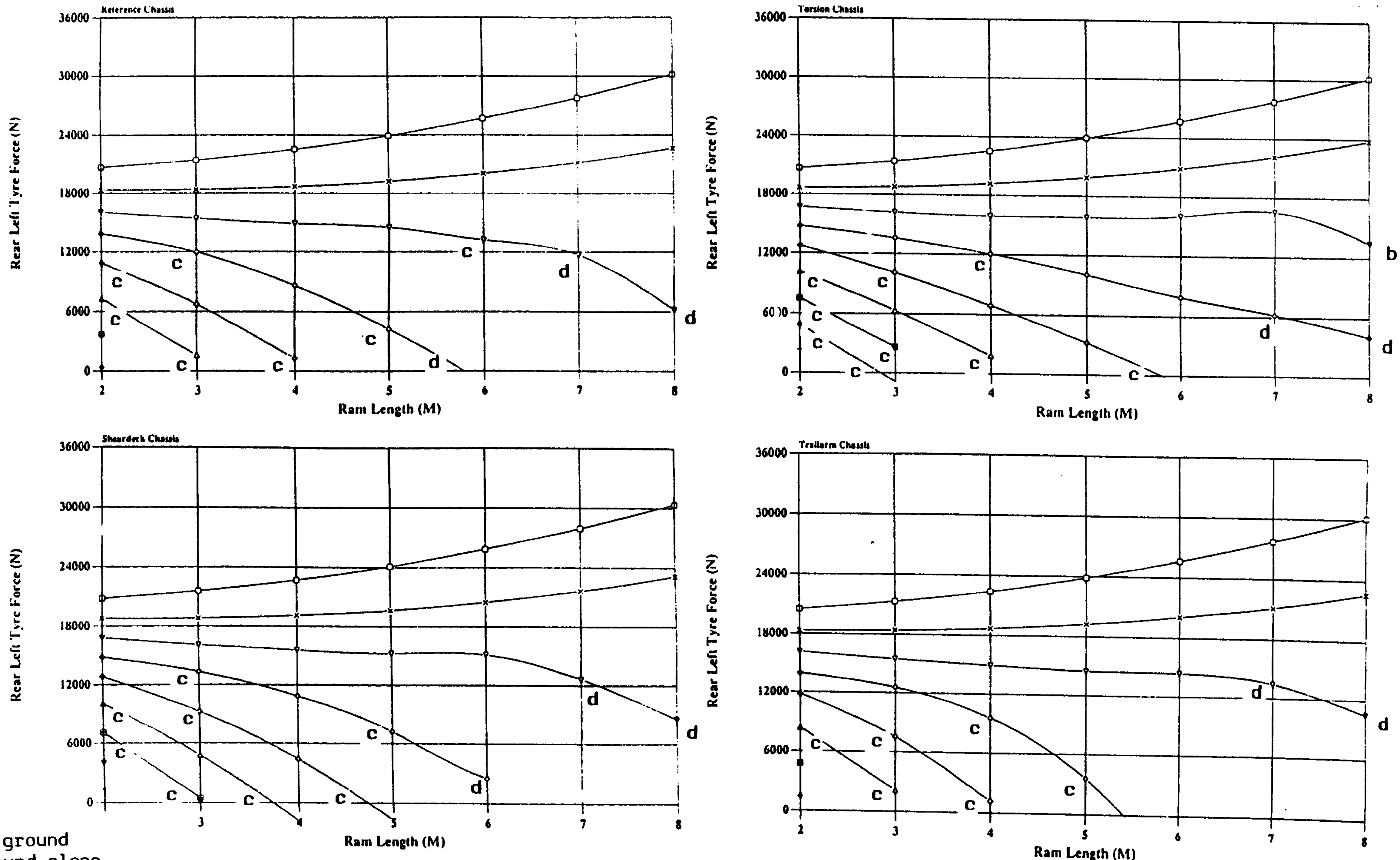

□ = level ground
▽ = 2° ground slope
◇ = 4° ground slope
⊞ = 6° ground slope
_ = 8° *ground slope*

Fig. 5.3i Rear left tyre force versus Ram length and ground slope combinations for a 17500 Kg payload in body position 9 .

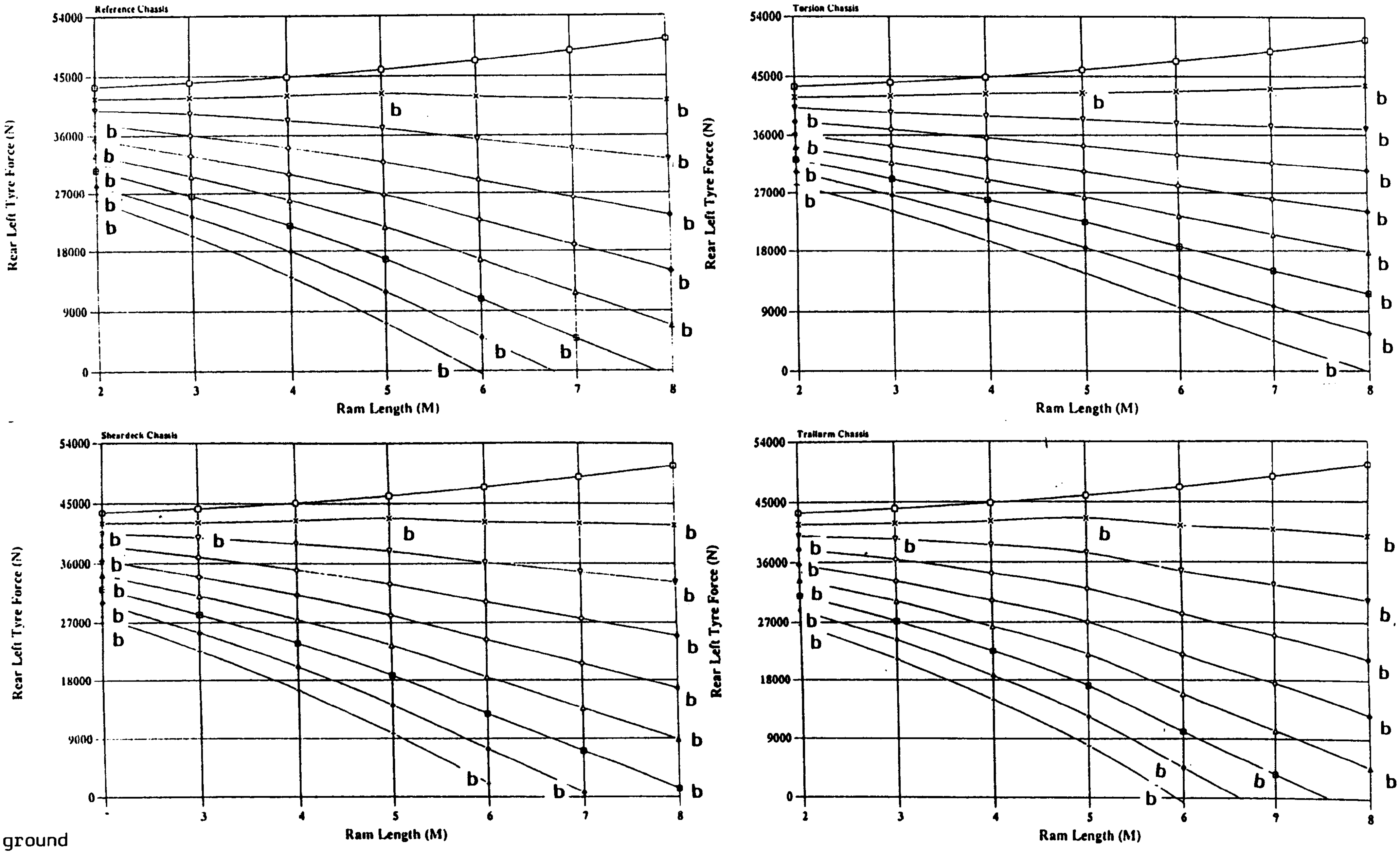

□ = level ground
▽ = 2° ground slope
◇ = 4° ground slope
⊞ = 6° ground slope
— = 8° ground slope

Fig. 5.4a Rear left tyre force versus Ram length and ground slope combinations for a 25000 Kg payload in body position 1 .

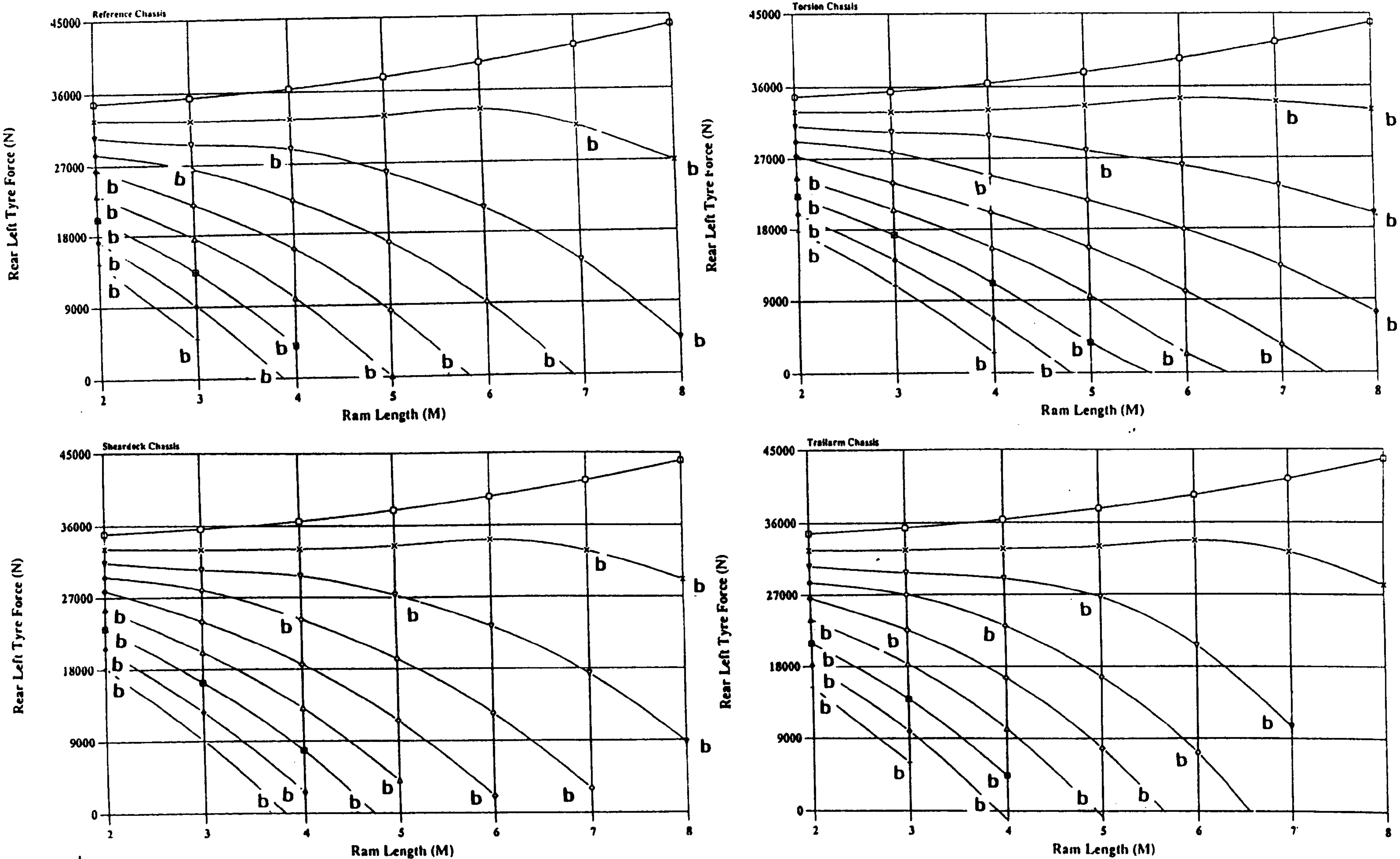

□ = level ground
▽ = 2° ground slope
◇ = 4° ground slope
⊞ = 6° ground slope
– = 8° ground slope

Fig. 5.4b Rear left tyre force versus Ram length and ground slope combinations for a 25000 Kg payload in body position 2 .

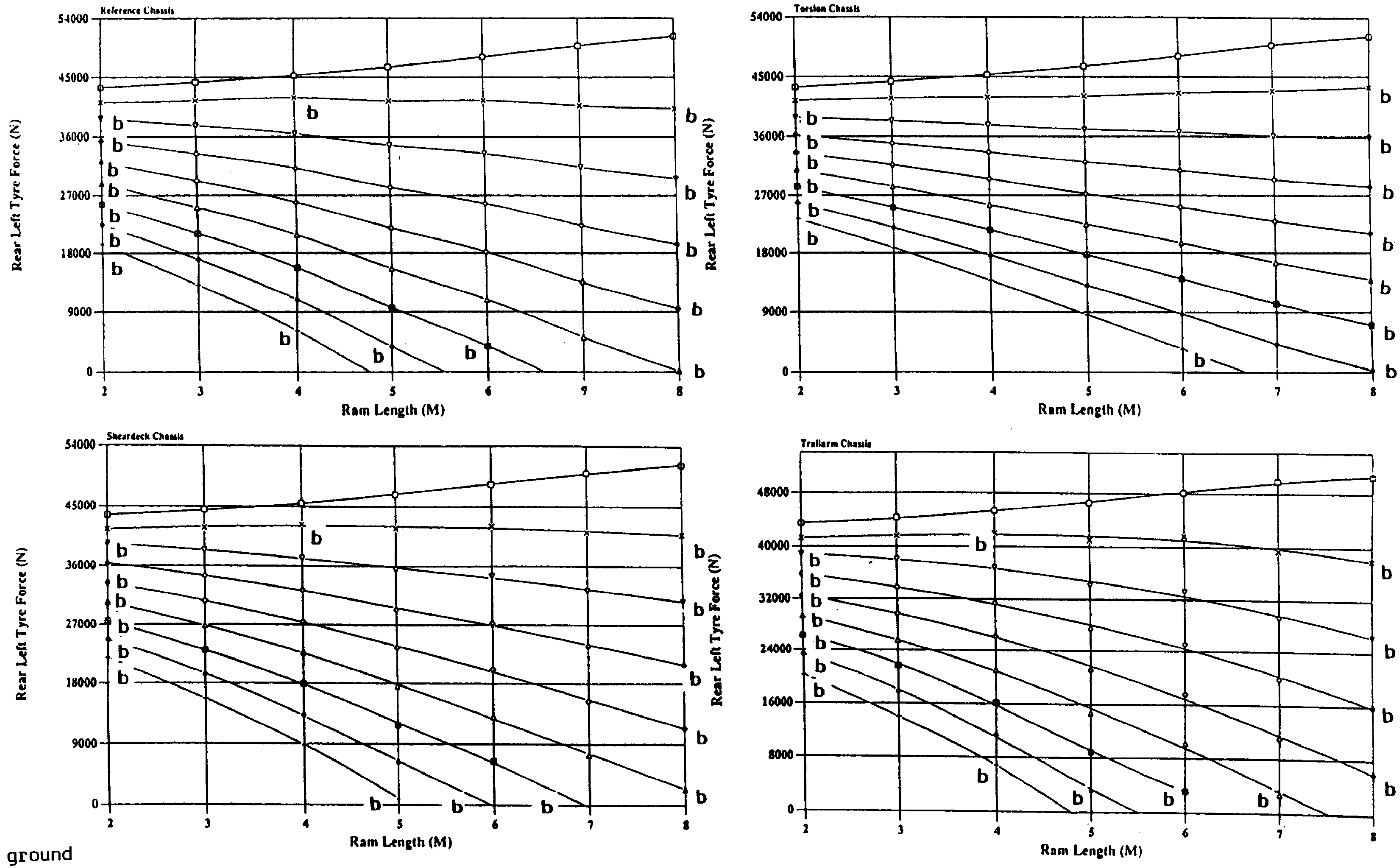

□ = level ground
▽ = 2° ground slope
◇ = 4° ground slope
⊞ = 6° ground slope
– = 8° ground slope

Fig. 5.4c Rear left tyre force versus Ram length and ground slope combinations for a 25000 Kg payload in body position 4 .

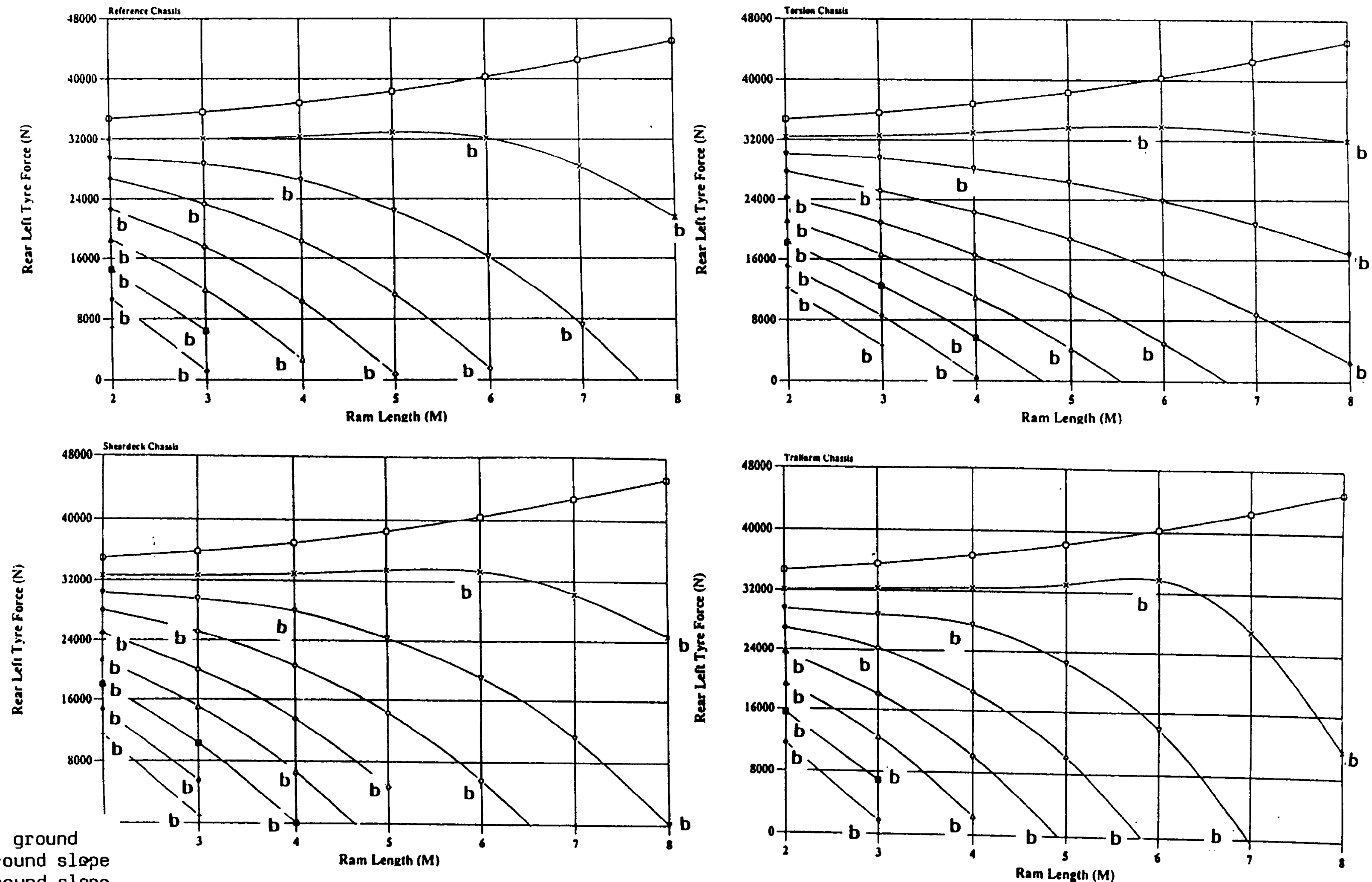

□ = level ground
▽ = 2° ground slope
◇ = 4° ground slope
⊞ = 6° ground slope
⌣ = 8° ground slope

Fig. 5.4d Rear left tyre force versus Ram length and ground slope combinations for a 25000 Kg payload in body position 5 .

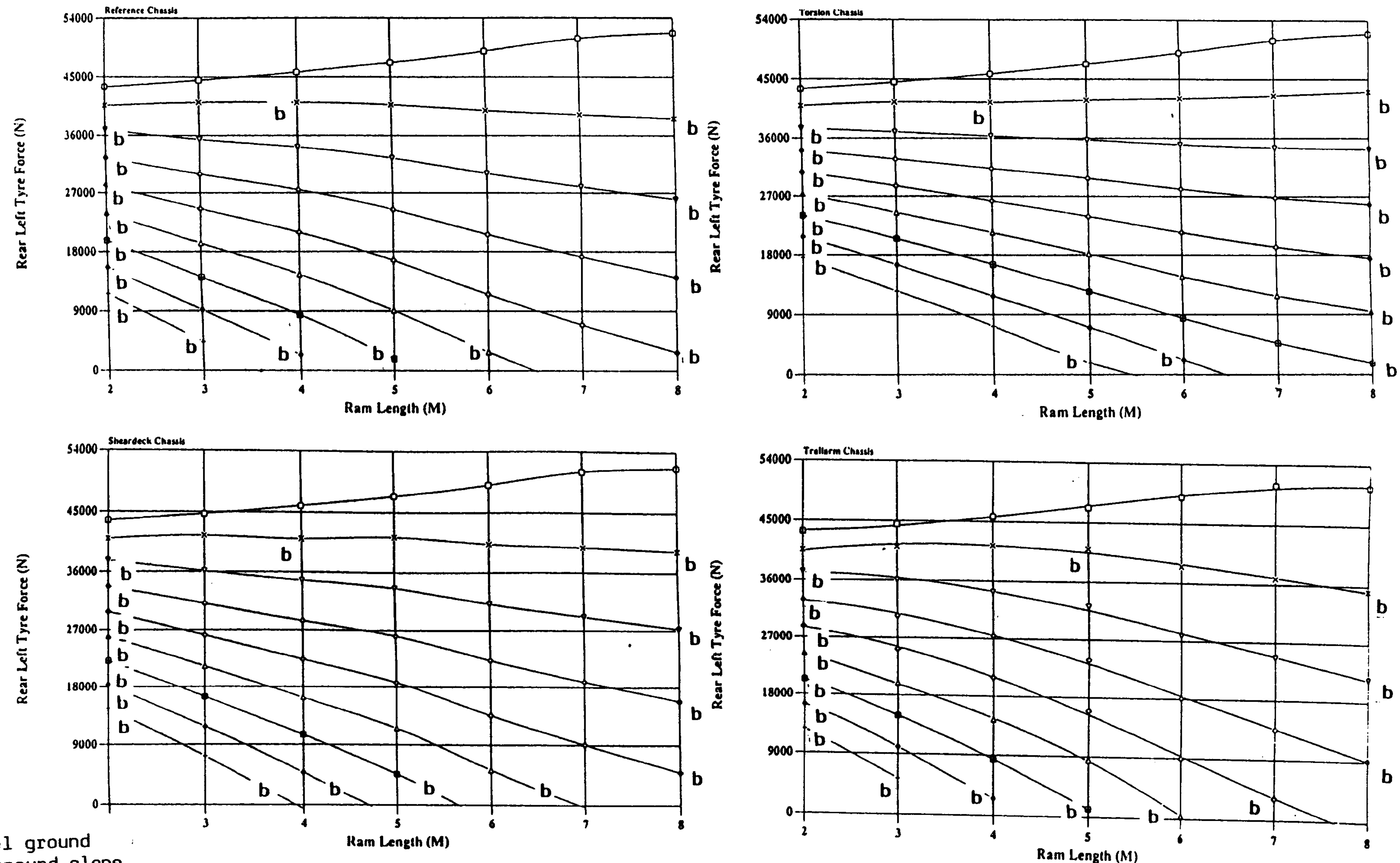

□ = level ground
▽ = 2° ground slope
◇ = 4° ground slope
⊞ = 6° ground slope
— = 8° ground slope

Fig. 5.4e Rear left tyre force versus Ram length and ground slope combinations for a 25000 Kg payload in body position 7 .

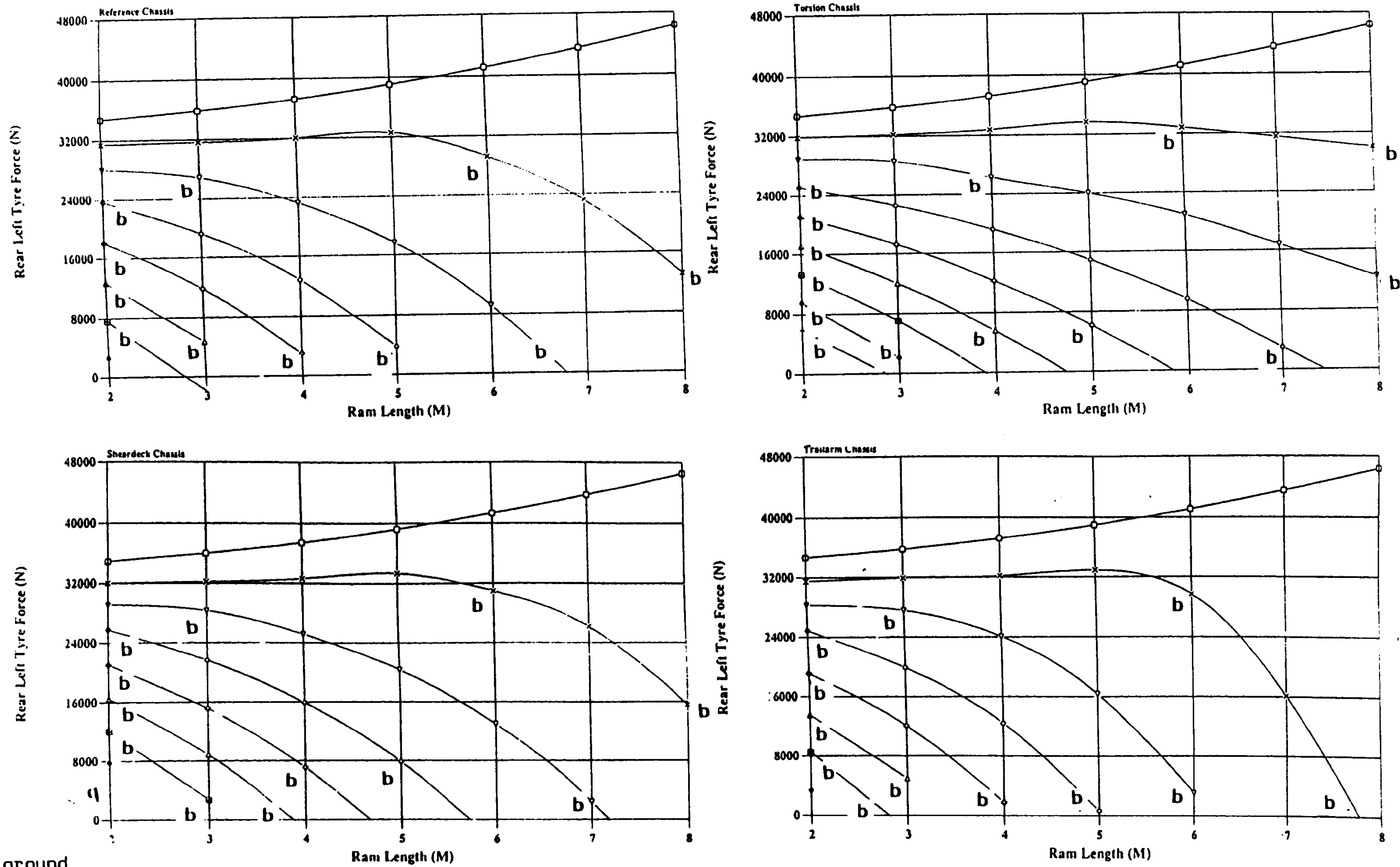

□ = level ground
▽ = 2° ground slope
◇ = 4° ground slope
⊞ = 6° ground slope
– = 8° ground slope

Fig. 5.4f Rear left tyre force versus Ram length and ground slope combinations for a 25000 Kg payload in body position 8 .

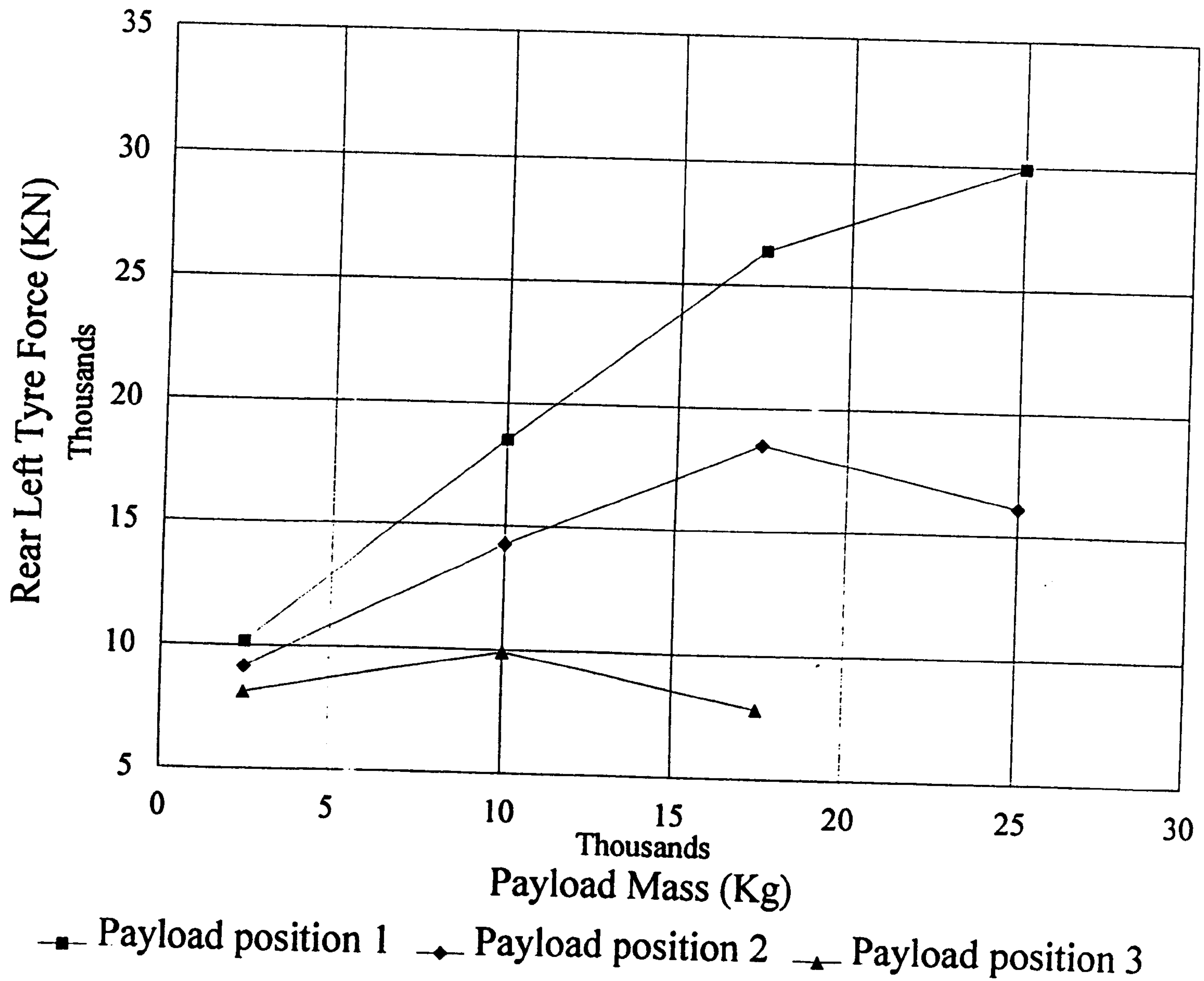

Fig 5.5 Rear left Tyre force versus payload magnitude in fore/aft payload positions 1,2 and 3.

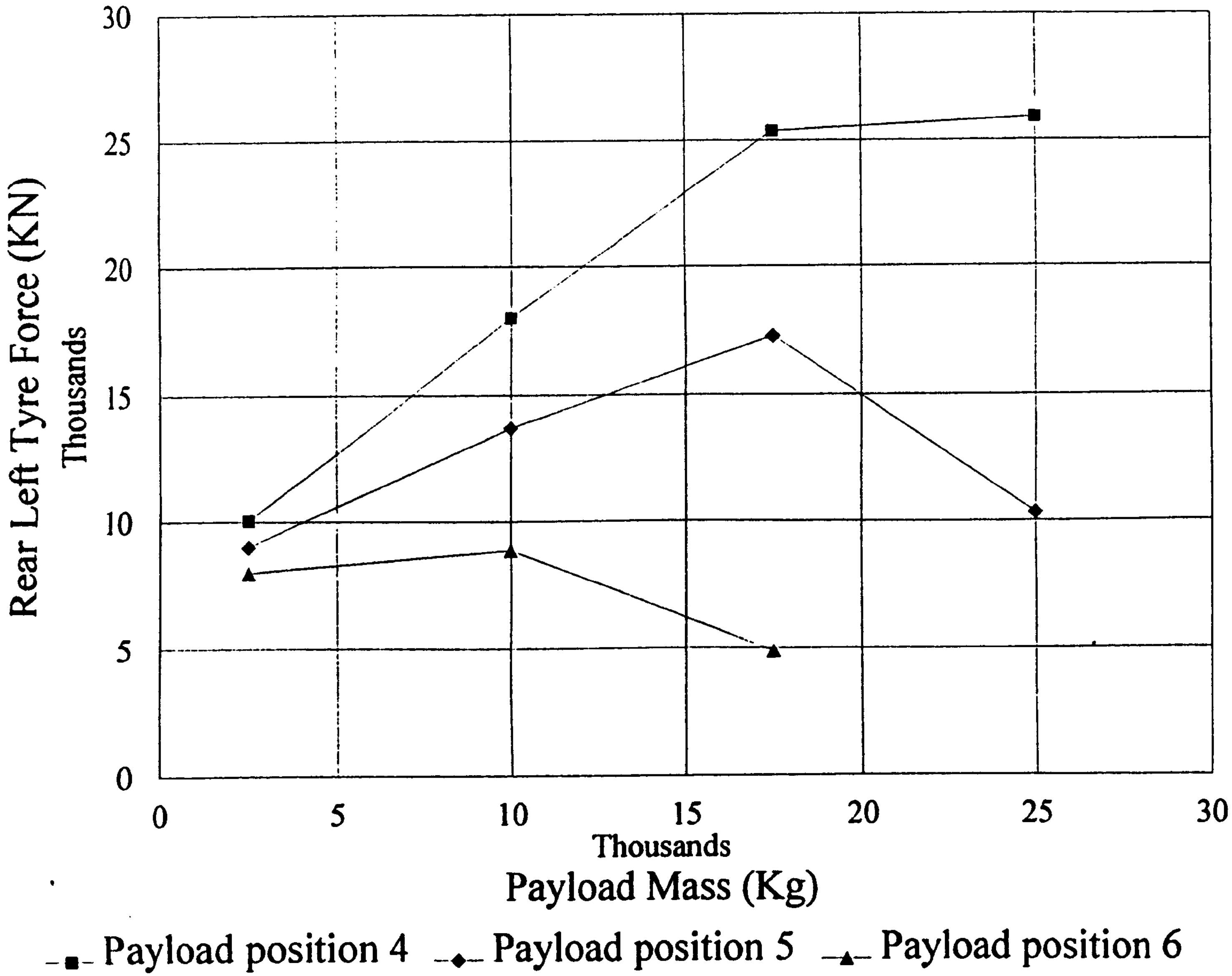

Fig 5.6 Rear left Tyre force versus payload magnitude in fore/aft payload positions 4,5 and 6.

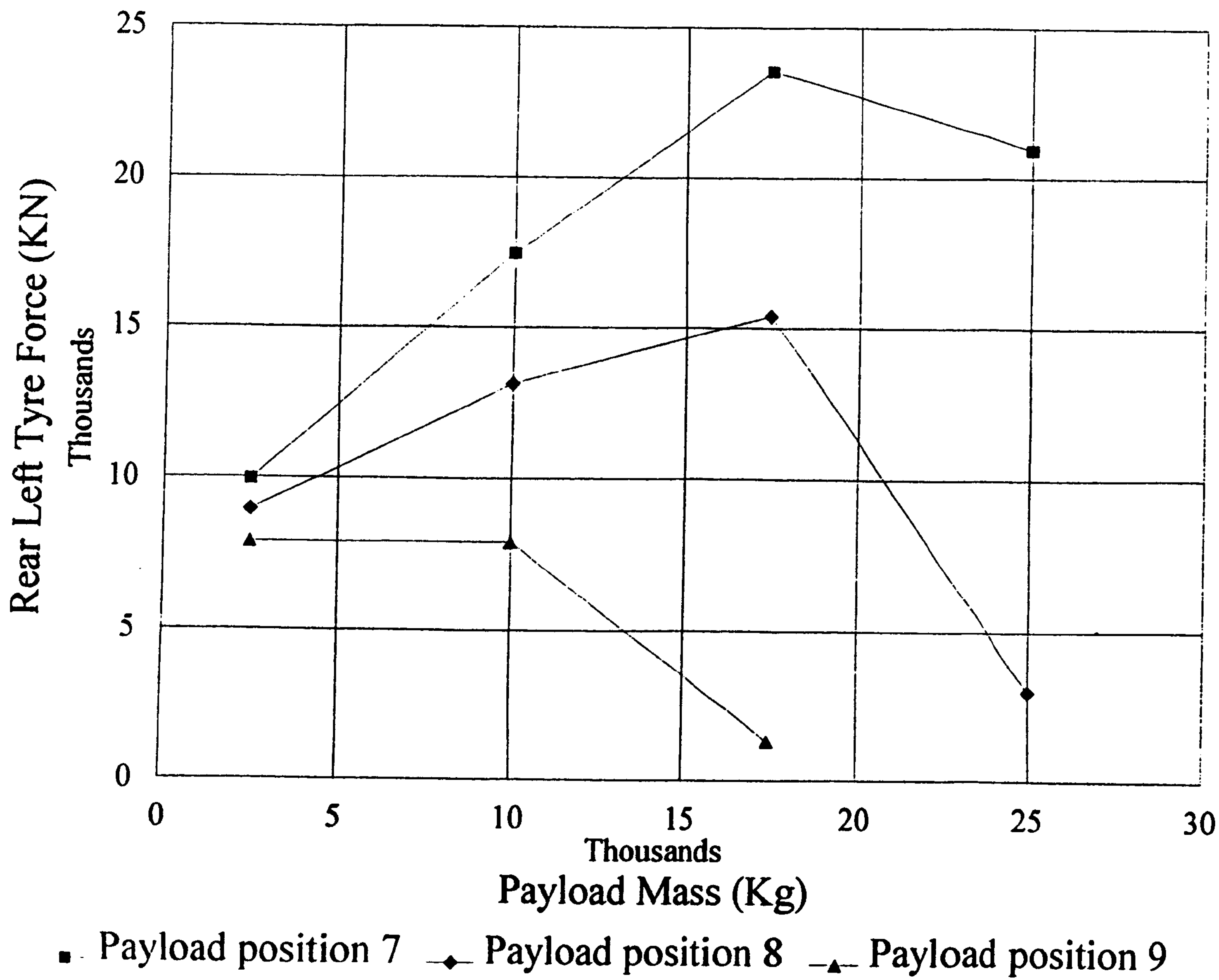

Fig 5.7 Rear left Tyre force versus payload magnitude in fore/aft payload positions 7,8 and 9.

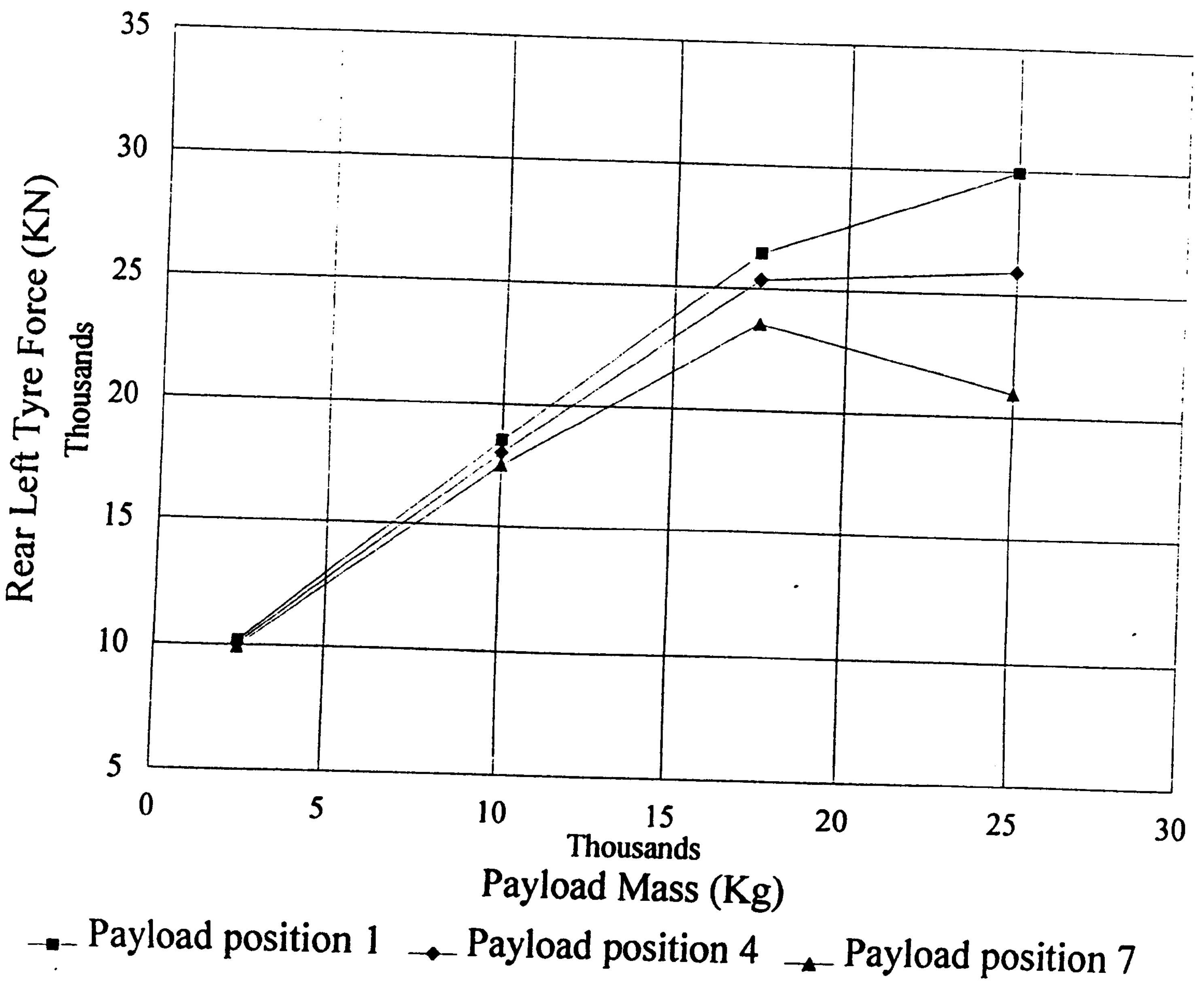

Fig 5.8 Rear left Tyre force versus payload magnitude in vertical payload positions 1,4 and 7.

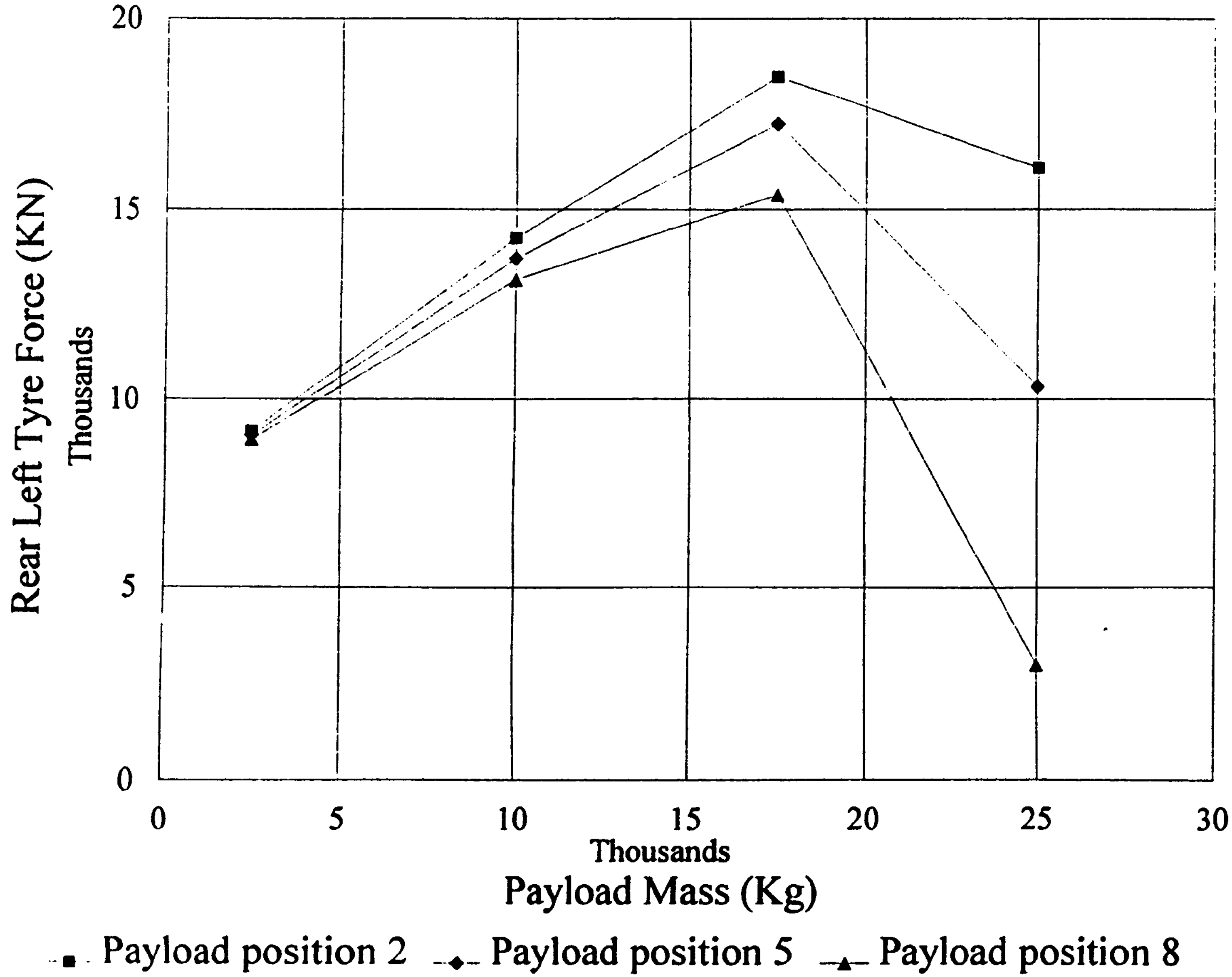

Fig 5.9 Rear left Tyre force versus payload magnitude in vertical payload positions 2,5 and 8.

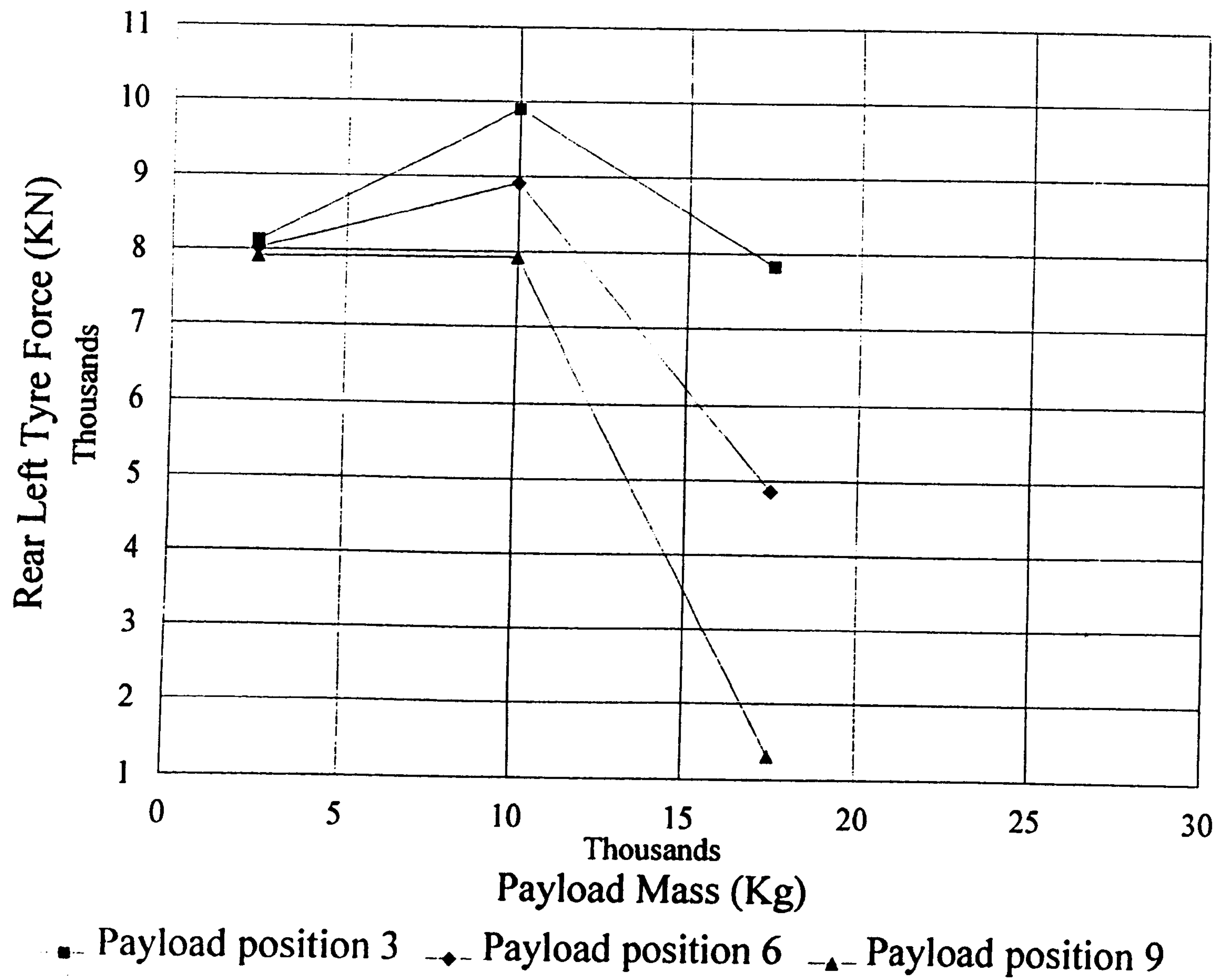

Fig 5.10 Rear left Tyre force versus payload magnitude in vertical payload positions 3,6 and 9.

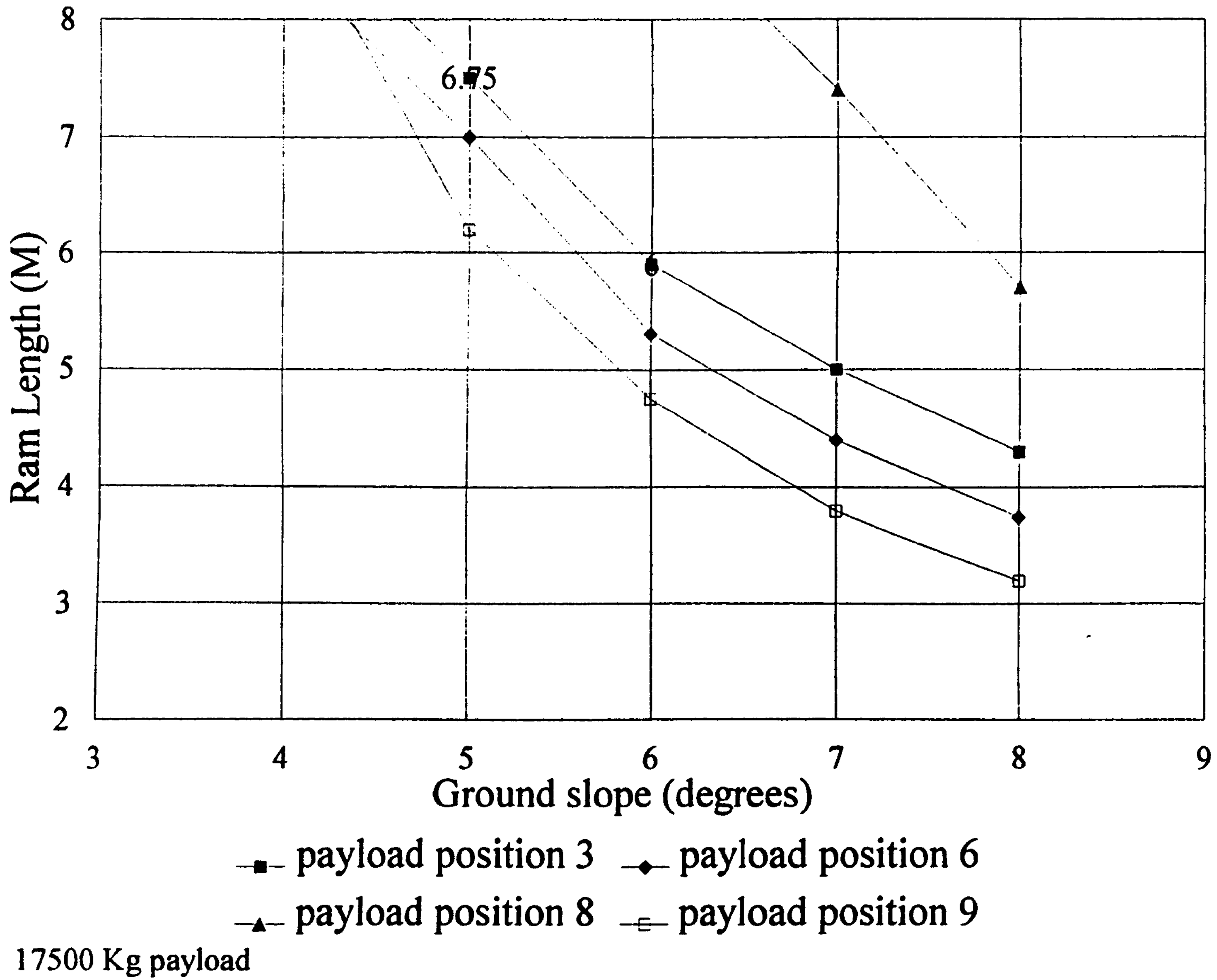

Fig 5.11 Stability envelopes for a 10000 Kg payload in payload positions 3,6,8, and 9.(based on maximum ram length/zero rear left tyre forces)

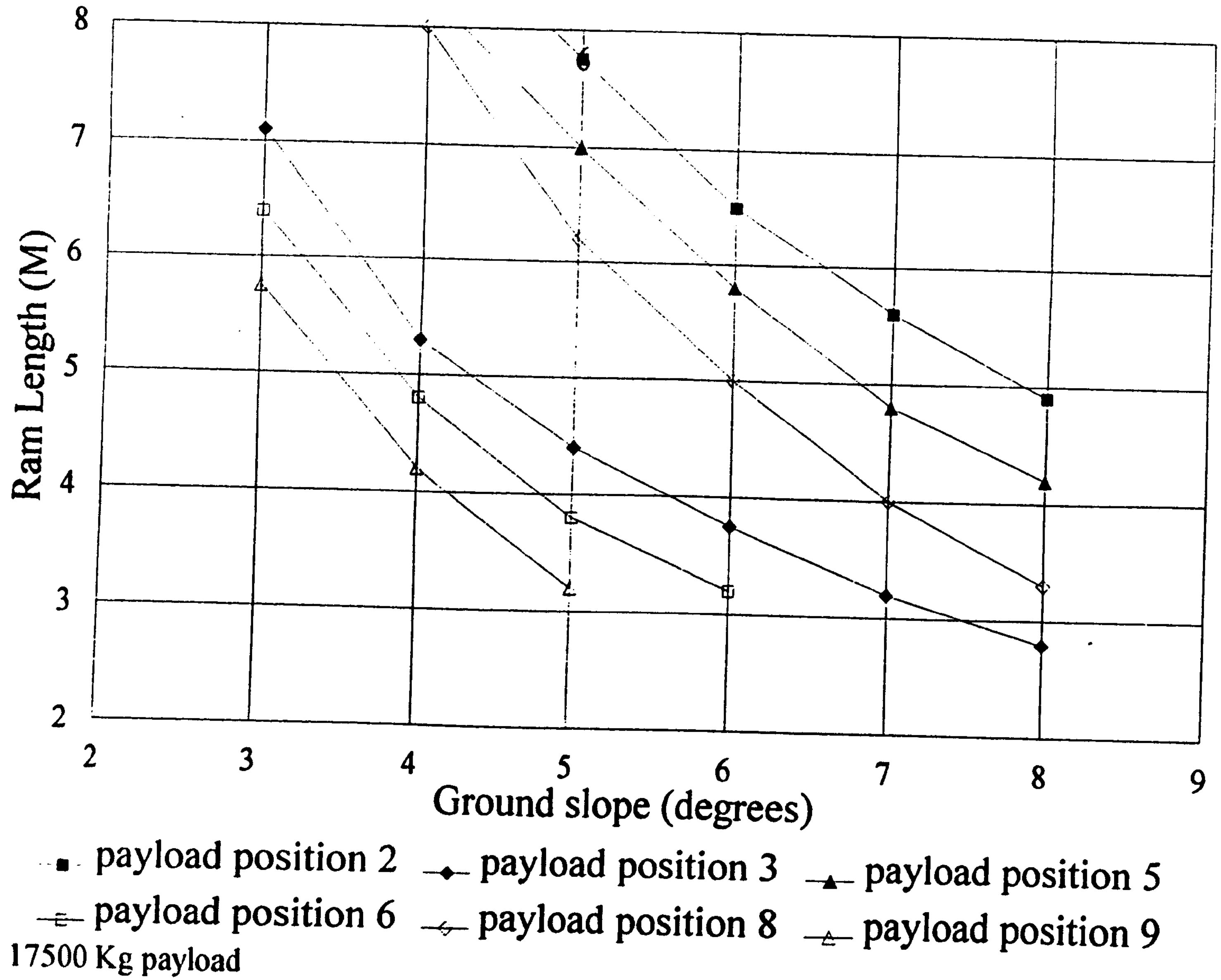

Fig 5.12 Stability envelopes for a 17500 Kg payload in payload positions 2,3,5 6,8 and 9.(based on maximum ram length/zero rear left tyre forces)

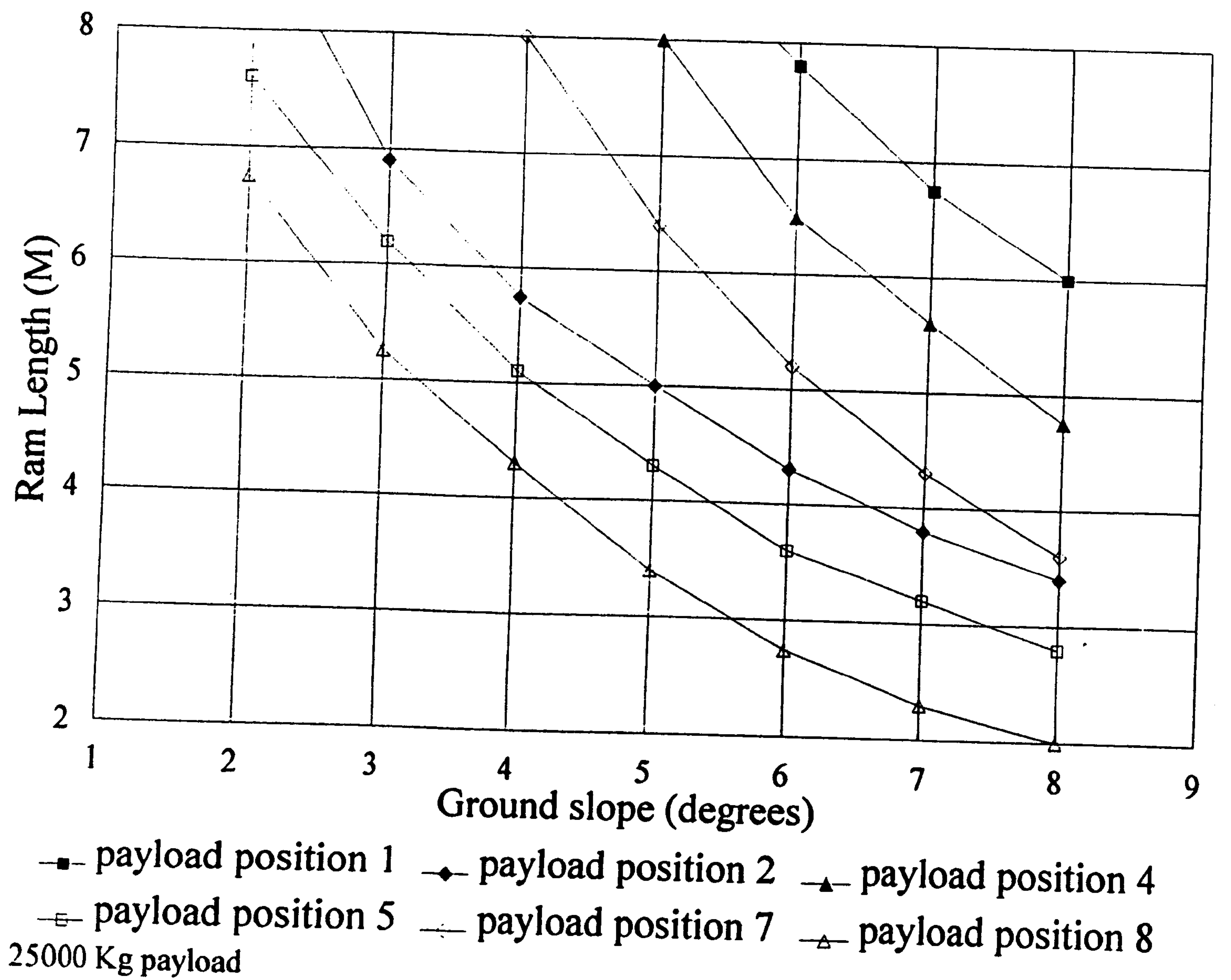

Fig 5.13 Stability envelopes for a 25000 Kg payload in payload positions 1,2,4 5,7 and 8.(based on maximum ram length/zero rear left tyre forces)

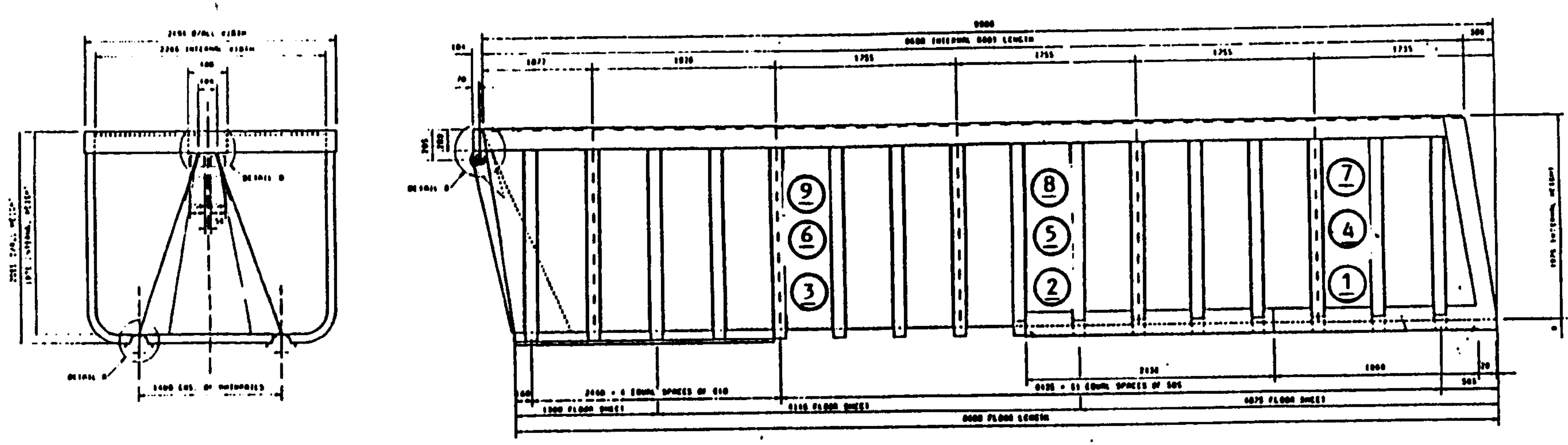

Payload position	Payload coordinates (mm)		
	X	Y	Z
1	2992	676	0
2	4488	676	0
3	5984	676	0
4	2992	1014	0
5	4488	1014	0
6	5984	1014	0
7	2992	1350	0
8	4488	1350	0
9	5984	1350	0

Fig. 5.14 Body payload positional coordinates

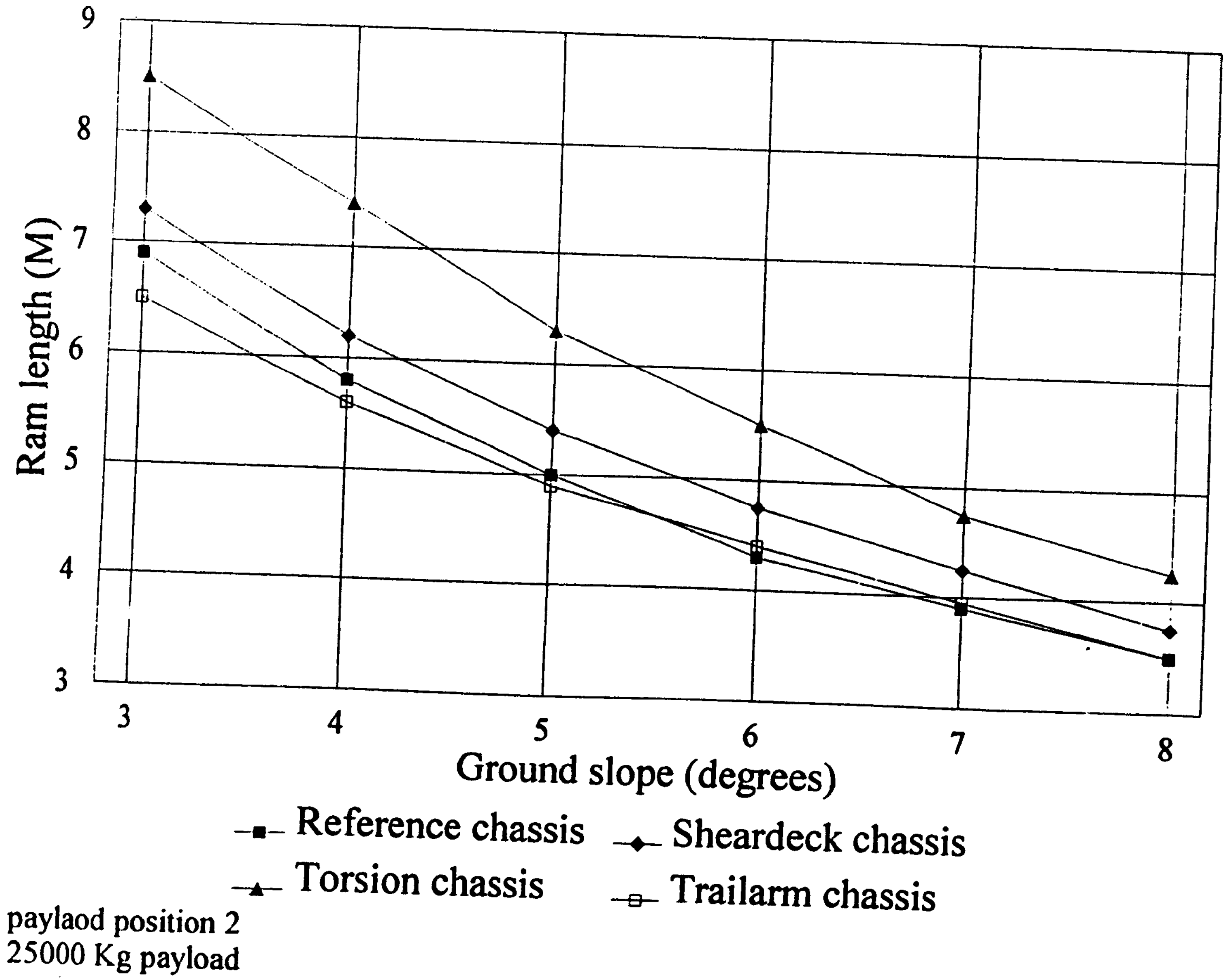

Fig 5.15 Stability envelopes for a 25000 Kg payload in payload position 2 for the four different chassis configurations.(based on maximum ram length/zero rear left tyre forces)

CHAPTER SIX

GENERAL DISCUSSION AND CONCLUSION

6.1 Technique

Theoretical models for predicting the stability behaviour of non-tipping trailers negotiating corners have been established by a number of people. However, no specific work has been found, in published material, relating to tipping trailer stability. The fundamental ideas associated with the dynamic non-tipping trailer models can be used in the static tipping trailer situation. The main criticism of the past models are that they require full scale experimental tests to determine important flexibilities (eg. chassis torsional stiffness and that the contribution of important flexibilities towards lorry stability cannot be assessed very easily. Also, air suspensions have not been considered. At the start of this project in January 1989, it was decided that the model developed for assessing the tipping stability of a trailer, should not require experimental tests to determine important flexibilities, and that design investigations should be relatively easy and cheap to establish the effect of component flexibilities on stability.

6.2 Theoretical model

It was decided that the finite element method, described in Section 1, would be used to model the important flexibilities of the lorry. This enabled the important flexibilities of the lorry to be determined, without the requirement of full scale tilt tests. It also enables design investigations to be undertaken relatively easily and quickly. However, not all flexibilities can be determined theoretically. Experimental investigations, described in Appendix A and B had to be undertaken in order to determine the flexibilities of the airbags and tyres.

6.2.1 Finite element model

Although large movements of the body and payload occur during tipping, these result from small linear elastic deformations of the body to chassis connection points, tyres and suspensions. The finite element model therefore uses beam plate and spring elements which are capable of dealing with small linear elastic deformations. Only the basic beam elements were used to model the chassis structure. However, brick elements could be used instead of the beam elements, which may result in a more accurate model but would significantly complicate the model, and subsequently increasing the cost of running the finite element model design investigations.

The tyres were modelled accurately using linear springs, with the flexibilities obtained from manufacturers information. It was thought at first that they might be incorrect. The vertical flexibility was confirmed to be correct through experimental work described in Appendix B, due to difficulties in the experiment the transverse and fore/aft flexibilities were not confirmed.

The relatively recent developments in suspension systems has seen the proliferation of air bag suspensions, mainly due to the airbag providing a flexible support irrespective of the loading carried, as described in Appendix B. These supports are comprised of a rubber airbag inflated by air, with a mechanical high control device. The ability for the air suspension to increase or decrease the pressure in the airbag, depending on the load carried, results in a non linear system, described in Section 3.4.2. Experimental investigations into the load/deflection characteristics of an airbag, described in Appendix B, enabled a relationship to be determined of the form

$$FL^n = Const$$

Whereas leaf springs could be modelled using a simple linear spring, the operation of airbags and the non linear characteristics prevented this, and a novel approach had to be developed. The novel method of applying non linear loadings to a linear elastic structure, modelled by the finite element method, was successfully achieved and is described in Chapter 3.

Although the accuracy of the finite element model may be improved by the use of beam element with local flexibilities or by the use of brick elements, the method of solution is still good. The method of solution can still be used to highlight areas in the tipping trailer units that influence the stability characteristics, even if the flexibility matrices could be modelled more accurately. Also, the computer program written to execute the many matrix multiplications and iteration procedures has been shown to produce converged solutions with continuity as the suspension changes between the different operating conditions a, b, c, and d, as described in Section 4.6.

6.2.2 Solution procedure

The idea of using the results from finite element model to predict the flexibility of the tractor and trailer unit chassis and the realisation that the finite element package on its own could not be readily used to analyse the non linear loading and combination of payload magnitudes and positions, led to the development of general matrices for the calculation of forces and displacements. This required large unit load flexibility and influence matrices or unit displacement matrices described in Section 4.5 to be generated from the finite element results. This optimised the number of finite element runs required so that the stability characteristics of a lorry could be determined for any combination of payload magnitude and position and ground slope without further finite element runs.

Extensive processing of the finite element results, due to the non linearity of the problem is required by the PC program to determine the required trailer tyre forces. The continuity of the stability graphs, discussed in Chapter 5, shows that the flexibility matrices are accurate, relative to each other.

6.2.3 Configuration of flexibility data

The general force and displacement matrices derived from the finite element results are incorporated into a PC based program. The data for each matrix is inputted by hand. This is a laborious task and would benefit from a more sophisticated data handling system, between the finite element package and the PC program. Any obvious mis-readings were later corrected, by editing the stored data files. Errors can be identified using a number of methods. Firstly there is a degree of symmetry within each matrix and this can be used to cross-check data values. Secondly the program can be run with a symmetrical payload load (ie. Z = 0) and a zero ground slope, resulting in symmetrical vertical and horizontal displacement of the left and right hinges and zero transverse hinge displacement. The vertical tyre forces should be the same for corresponding left and right tyres and the transverse and fore/aft tyre forces should be zero. Thirdly the continuity of forces and displacements can be cross-checked before and after the suspension operating condition changes.

6.3 Implications

The design changes have been investigated in order to assess the influence of the respective components on roll stability, and to demonstrate how design changes can be analysed.

The design changes investigated in Section 5.3, highlight that there is scope for improving the roll stability of articulated tipping vehicles.

The effect of the changes on roll stability compared to the reference chassis can be seen in Fig. 5.15. The graph gives details for a payload magnitude of 2500 kg and payload position of x = 4465, y = 1533, 20, stability envelope for each chassis configuration. The vehicle is in a stable position below the line and in an unstable position above the line, for each respective chassis configuration. The reference chassis enables a maximum ram length of 5.4 m to be reached, for $\theta p = 3^{\circ}$, before the onset of instability. The trailing arm chassis enables a ram length of 5.0 m. The sheardeck chassis enabled a ram length of 5.7 m, and the torsion chassis which made the greatest improvement, enabling a ram length of 7.4 m to be reached, for the same body attitude before the onset of instability was reached.

Also, that the traditional chassis configuration comprising of two I-beams connected by cross members, may not be the optimum design and further design investigations could lead to alternative chassis designs.

6.4 Requirements for further investigations

The current model allows dimensions and flexibilities of lorry components to be changed in order to assess their influence on roll stability. The solution procedure of the theoretical model is correct, however the flexibilities derived from the current finite element model have not been verified. In order to have complete confidence in the flexibilities coefficients, the results from a full scale test should be compared against the F.E. results. While the current flexibility matrices may contain inaccuracies, they can still be used to assess design changes.

There are a number of areas in which the model accuracy could be improved. Firstly the tapered I beams have been modelled as uniform I beams, using average beam properties based on the two ends of the beam due to limitations of the finite element program.

Secondly inter-connections between cross members and the main I beams have been treated as rigid joints. Incorporating local flexibilities would enable simple beam plate elements to model the chassis more accurately. as shown by Beermann [18] and Meyson [19]

Otherwise brick elements could be used instead of the plate and beam elements to model the chassis enabling tapered sections and local flexibilities to be modelled. The accuracy achieved through the use of brick elements in the finite element model has to be considered against the increased complication producing the F.E. model, the increase in computing time to run the finite element program and the increase in difficulty in making design changes.

Currently, fifth wheel separation has not been taken into account and that the rotation of the tractor and trailer at the fifth wheel are the same. It has been shown in the dynamic roll-over situation by Sweatman [3] that fifth wheel separation reduces roll stability. Introducing fifth wheel separation capability would further increase the model accuracy.

A useful inclusion in the computer program would be the facility to calculate stresses within the beam elements. Unit load or unit displacement stress matrices could be generated in the same manner as the flexibility matrices. This would enable the design engineers to identify those areas that are over or understressed, and that would benefit from design investigations.

REFERENCES

1. Keen, R. C. et. al., "Investigation into the Safe use of Tipper Lorries", Bristol Polytechnic, 1984.

2. Henshell, R. D., "PAFEC 75, Data Preparation", PAFEC Ltd, 1978.

3. Sweatman, P. and Tso, Y., "The Influence of Suspension Characteristics on the Roll Over Stability of Articulated Vehicles", Australian Road Research Board, 1988.

4. Kemp, R. et. al. "Articulated Vehicle Roll Stability: Methods of Assessment and Effect of Vehicle Characteristics", Transport Road Research Laboratory (UK) Report 788.

5. Miller, D. and Barter, N., "Roll over of Articulated Vehicles", IMechE Conference on Vehicle Safety Legislation, Paper C203/73, Cranfield 1973.

6. Isermann, H., "Overturning Limit of Articulated Vehicles with Solid and Liquid Loads", Dt. Kraftforsch and Strass verk. Tech, 1970, Motor Industry Research Association Translation, No. 58/70.

7. Hollis, E., "Winds Give Away Lorry Instability", Professional Engineer, April 1989.

8. Holmes, K., "Articulated Vehicle Roll: Effect of Inverting the Coupling", Transport Road Research Laboratory (UK) Report 464, 1972.

9. Sweatman, P. and Tso, Y., "The Dynamic Stability Testing of Articulated Vehicles", Australian Road Research Board, 1989.

10. Laird, L., "Measurement of Heavy Vehicle Suspension Roll Stability Properties, and a Method to Evaluate Overall Stability Performance", PACCAR Technical Centre, Society of Automotive Engineers (USA), Paper 881869.

11. Ervin, R. D., "The Dependency of Truck Roll Stability on Size and Weight Variables", International Journal of Vehicle Design, pp. 192-208, 1986.

12. Sweatman, P. and Mai, L., "Articulated Vehicle Stability - The Role of Vehicle Design", Australian Road Research Board, 1984.

13. Miki, S., "Method of Evaluating Stability and Handling of a Truck Considering Body Torsional Rigidity", Hio Motors Ltd, Japan, Society of Automotive Engineers (USA), Paper 881870.

14. Dickson-Simpson, J., "Leaf in the Air Suspension Book", Transport Engineer, April 1989.

15. Hillebrand, R. D., "Neway Height Control Value for Air Suspension", Lear Siegler Truck Products Corporation", Society of Automotive Engineers (USA) Paper 881881.

16. Nakamura,N . "The measurement of Load Ocurring in a Fifth Wheel Coupling of an articulated Vehicle", MIRA paper, 1985

17. Brock, B., "Body Building, Tapered Safety", Commercial Motor, October 1988.

18 Beerman, H.J., "Joint Deformations and Stresses of Commercial Vehicle Frames under Torsion", International Conference on Vehicle Structures, Cranfield Institute of Technology 16-18 July 1984, Paper C178/84.

19 Megson, T.H.G., "Analysis of Semi-trailer Chassis Subjected to Torsion", International Conference on Vehicle Structures, Cranfield Institute of Technology 16-18 July 1984, Paper C176/84.

APPENDIX A

AIRBAG STIFFNESS

The aim of this experimental work was to determine the force/deflection characteristics of an airbag for given initial air pressures while operating at the normal ride height of 381 mm.

The actual loading and support conditions were found to be difficult to apply with existing equipment. Therefore, simpler, reasonably representative loading and support conditions were imposed. Although these loading and support conditions were incorrect, it was considered that the results obtained could be used as an approximate check on the manufacturers data.

A1 Introduction

An airbag is a rubber/fabric bellow which contains a column of compressed air. The rubber below itself does not significantly contribute to load support, this is mainly due to the column of compressed air. The air spring can only support axial loads with the existence of a suitable mechanism to eliminate sideways movement. When considering axial loads for an airbag, an initial ride height and pressure must be selected before loading can take place.

A2 Theoretical prediction of airbag force/height relationship

A typical curve of force versus height is shown in Fig. A1(a). It was assumed that the force displacement graph can be represented by an equation of the form

$$FL^n = C \qquad \textbf{(A1)}$$

The constant n and C are determined from the intercept and slopes of log-log graphs of F and L and are equivalent to those of an adiabatic compression of a gas.

A3 Experimental procedure

Because the airbags have a normal operating height of 381 mm, the first set of tests were set up using this height, and varying the initial pressure only. Five different initial pressures of 25, 40, 70 and 80 psi were used to obtain the results shown by Fig. A1(a)-A1(e). The airbag was placed in an Instron universal testing machine and allowed to expand to a height of 381 mm. Following pressurisation to 25, 40, 55 70 or 80 psi the air supply was closed. It was then unloaded to a 500 mm height and then compressed to a 250 mm height or up to a 100 psi pressure, whichever came first, and then unloaded back to 381 mm height.

A second set of tests were setup using a constant airbag height and varying the air supply pressure only. Four different airbag heights of 300, 325, 375, 400 and 425 mm were used to obtain the results in Fig. A2. The airbag was placed in an Instron universal testing machine and allowed to expand to one of the predetermined height previously mentioned. It was then pressurised to 90 psi in steps of 10 psi and the corresponding axial force was recorded.

Results

From the experimental work three important results were obtained which enabled the airbag to be accurately modelled. Firstly it was found that when the airbag was compressed with a constant mass of air, equation A1 could predict the force/deflection curve accurately, using suitable values for the constants. The theoretical and experimental force/deflection curves are shown in Fig. A1(a)-A1(e). The constants γ and C, for equation A1, are shown in Table A1, for the five different initial pressures considered.

Secondly, it was found that the airbag axial force was not influenced by its height and was directly related to air pressure only, where the mass of air within the airbag is not constant. The experimental results showing the airbag force/pressure relationship for four different fixed heights are shown in Fig. A2.

Thirdly, it can be seen from Fig. A2 that the maximum airbag force of 30 kN can be used to indicate when the airbag air supply reaches its maximum pressure of 80 psi. Thus preventing the airbags from maintaining height control and allowing the airbags to compress according to equation A1.

From these results the airbags on one side have the same axial force as they are always at the same pressure due to being interconnected. When the suspensions are operating below their maximum working pressure of 80 psi (ie. the mass of air within the airbags is not constant), the airbag force is proportional to airbag pressure. When the suspensions are operating above their maximum working pressure (ie. the mass of air within the airbags is constant), the airbag force is determined from equation A1.

The value of $n = 1.57$ is constant for all airbag operating condition as they change from height control to compression of a fixed mass of gas always occurs when the air pressure reaches 80 psi. It is assumed that the force/deflection characteristics of three airbags side by side, as in the case of the actual trailer air bags, can be represented by a modified form of equation A1. Where F is the airbag force, l is the combined length of the three displaced airbags and C the constant in equation A1. C is unknown as no experimental data exists for the compression of three airbags. Instead, C is calculated using the previous height controlled airbag forces and lengths substituted into equation A1.

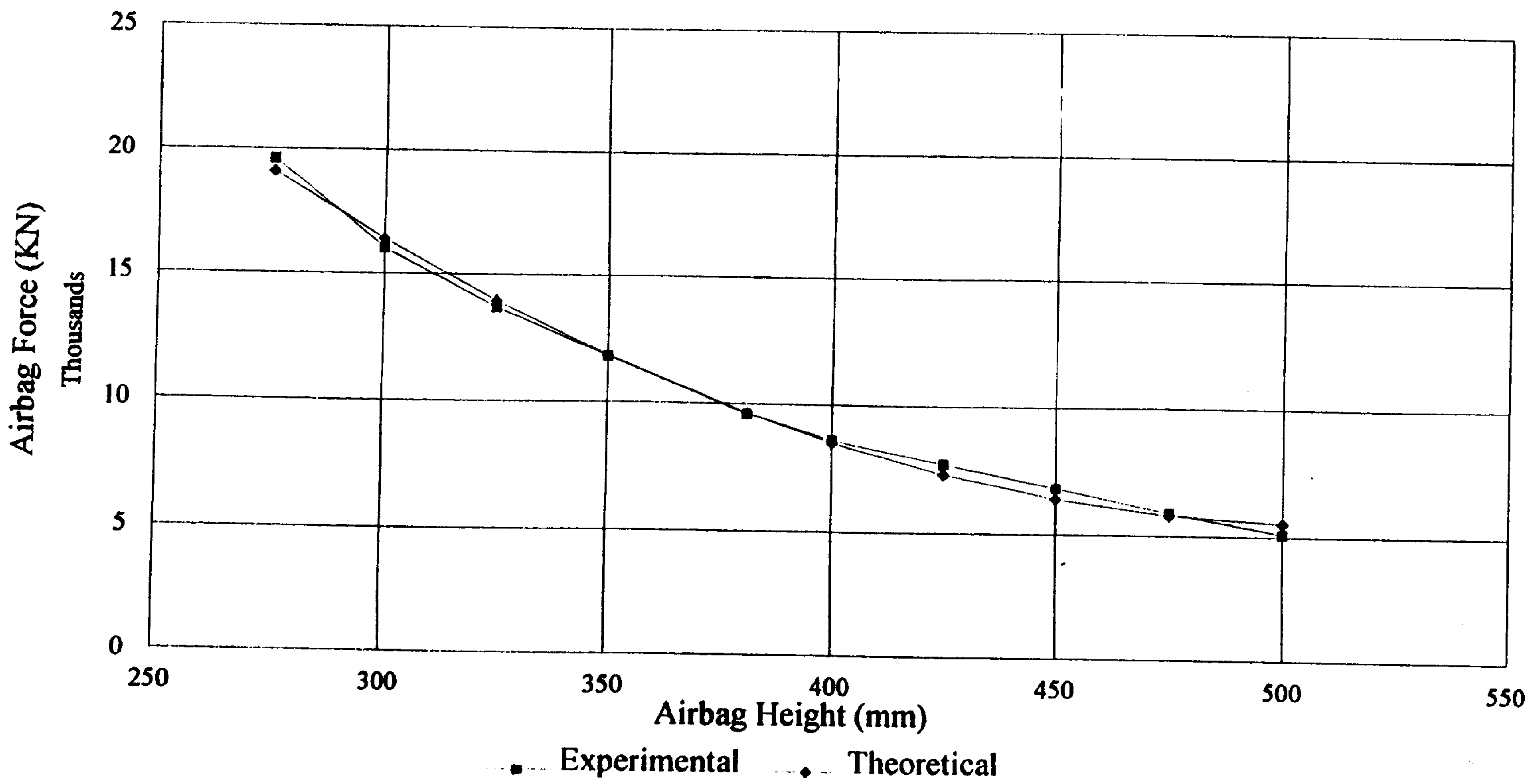

Fig. A1 Variation of airbag force with airbag height for an initial air pressure of 25 psi at an airbag height of 381 mm.

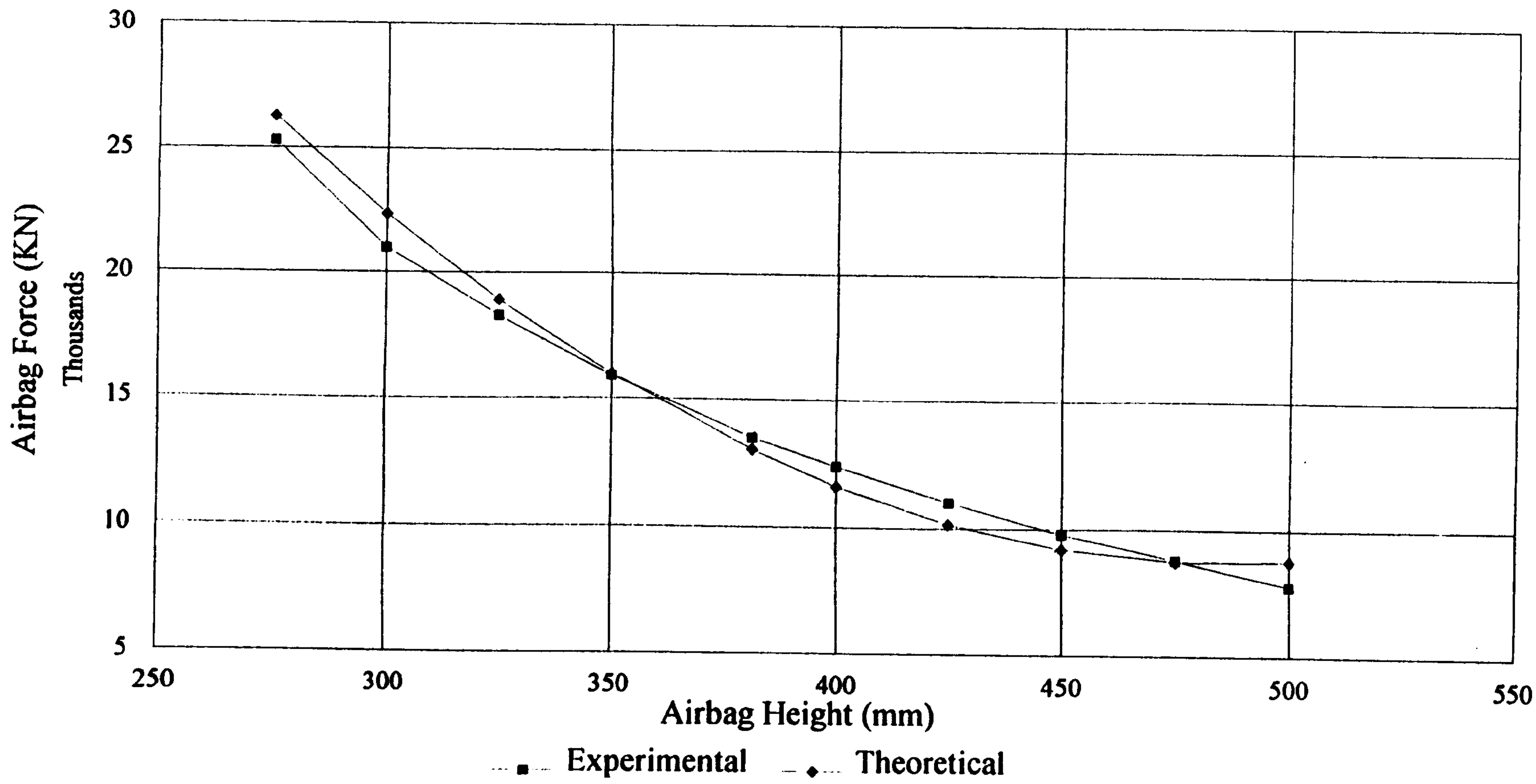

Fig. A2 Variation of airbag force with airbag height for an initial air pressure of 40 psi at an airbag height of 381 mm.

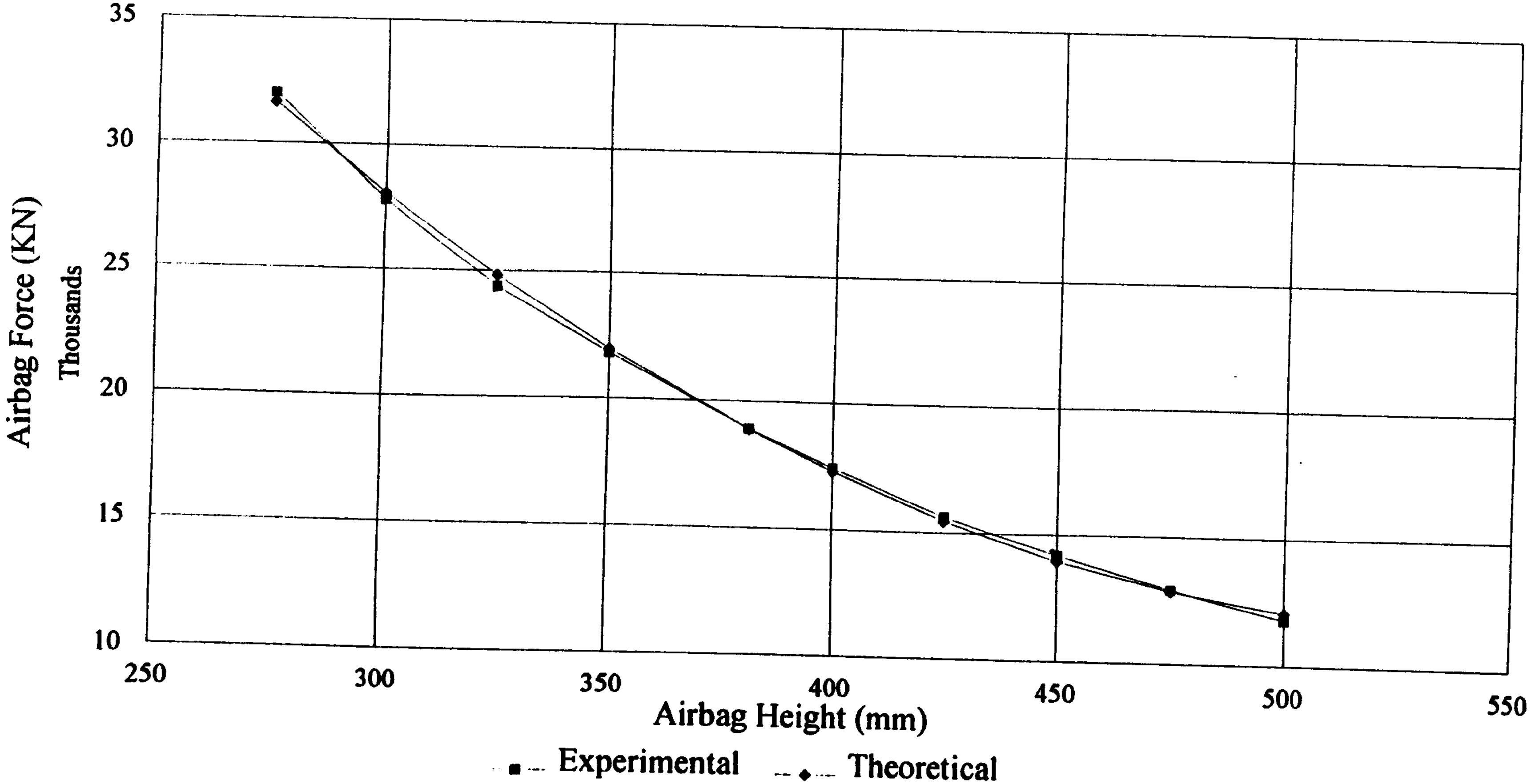

Fig A3 Variation of airbag force with airbag height for an initial air pressure of 55 psi at an airbag height of 381 mm.

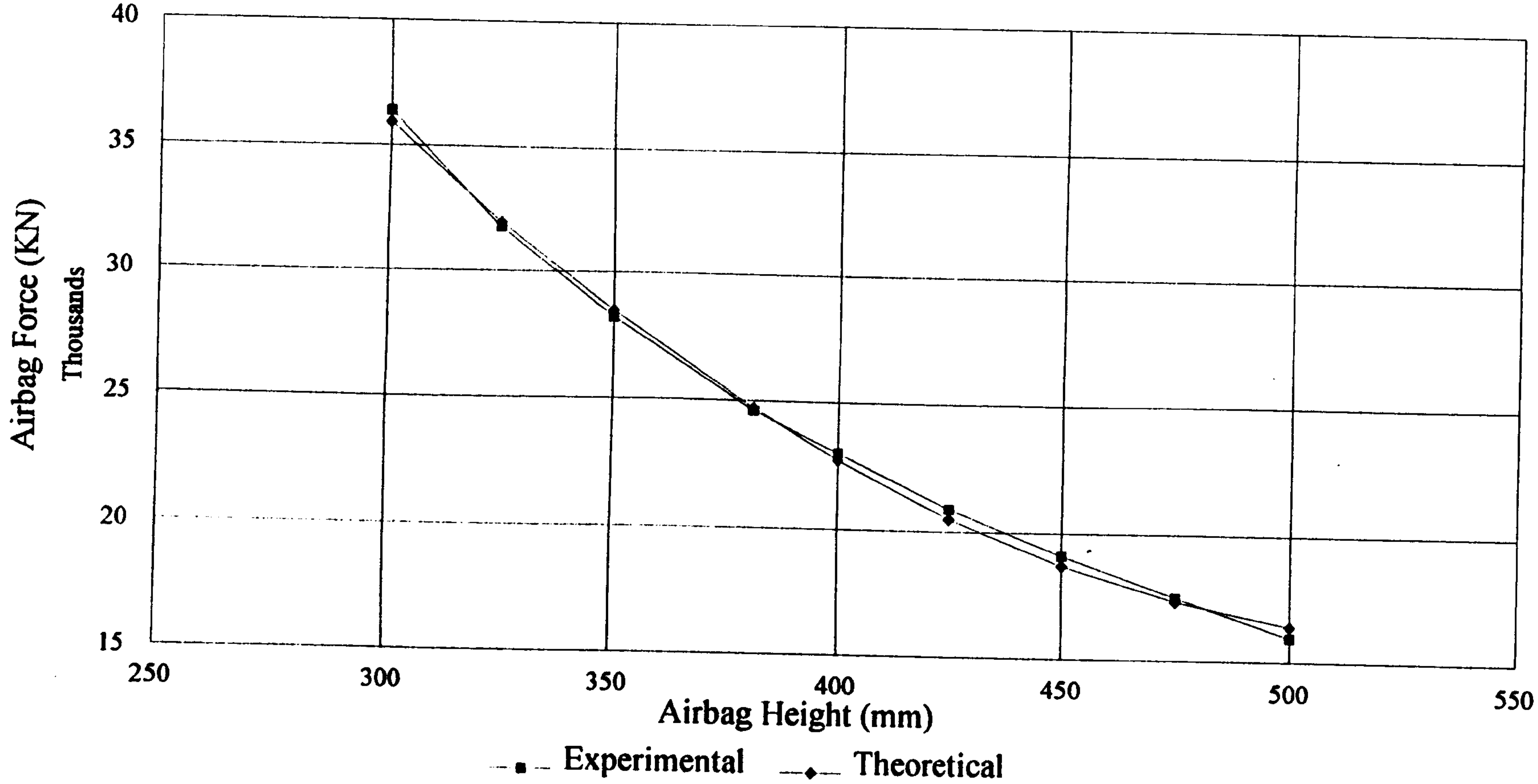

Fig. A4 Variation of airbag force with airbag height for an initial air pressure of 70 psi at an airbag height of 381 mm.

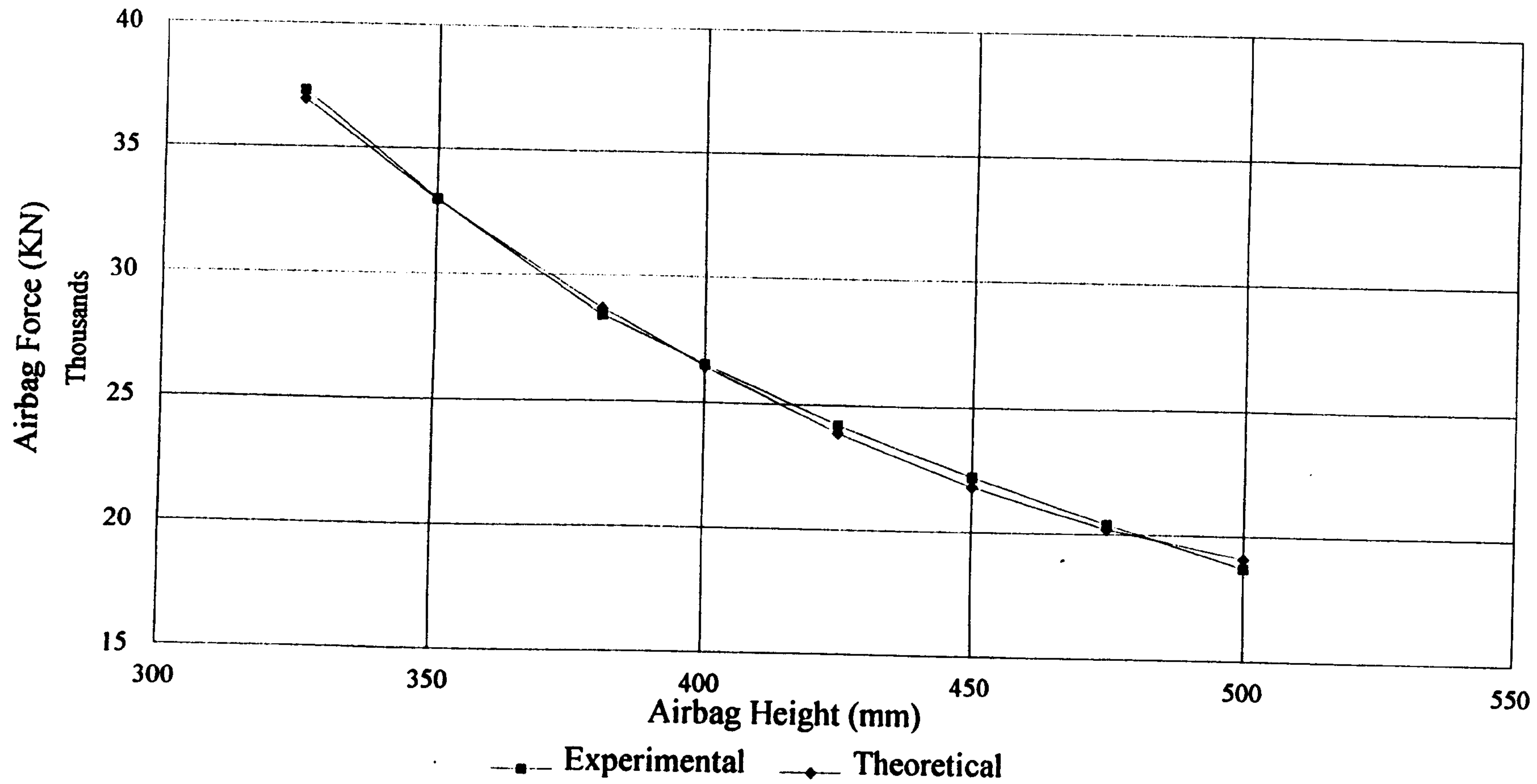

Fig. A5 Variation of airbag force with airbag height for an initial air pressure of 80 psi at an airbag height of 381 mm.

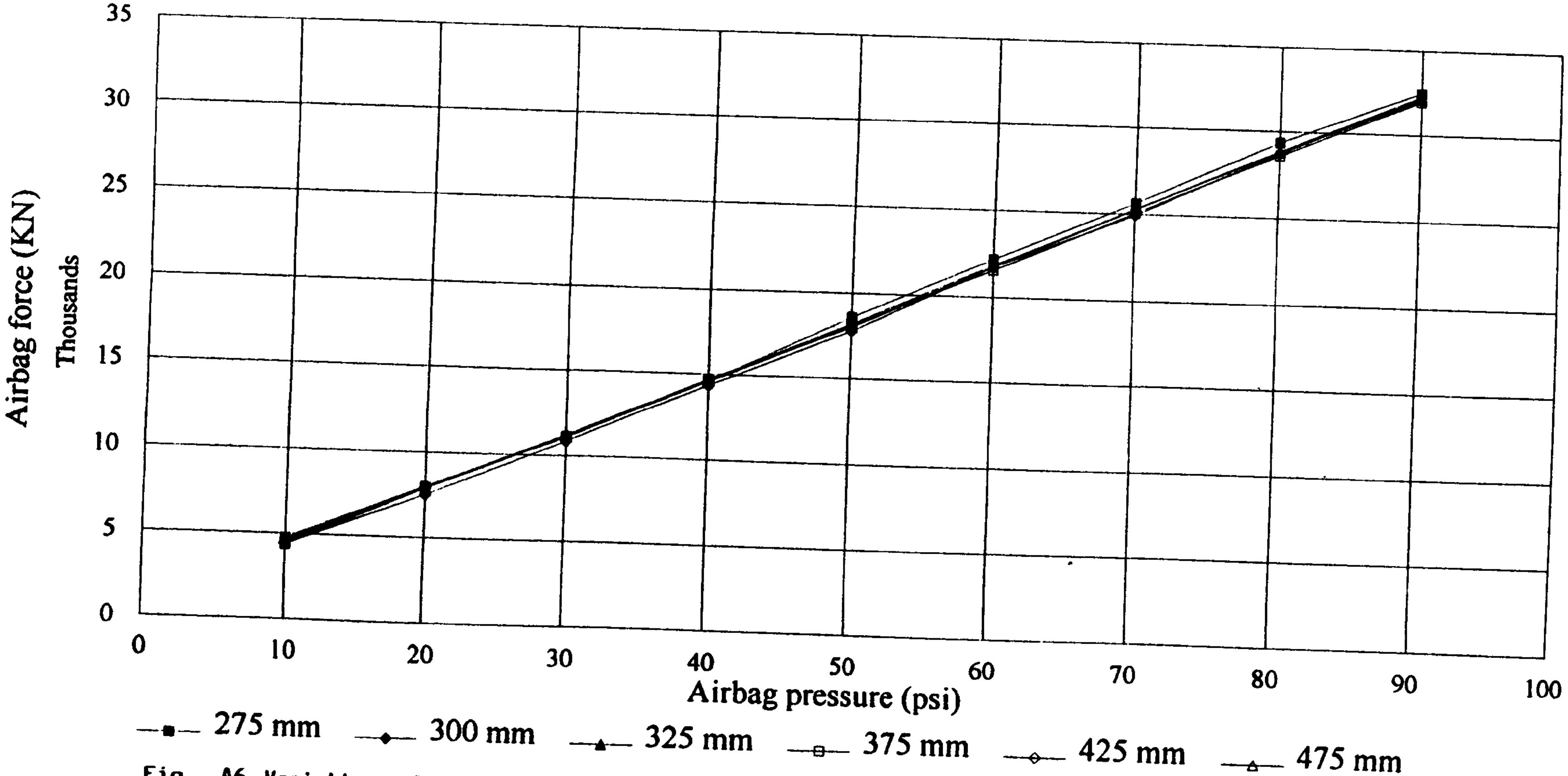

Fig. A6 Variation of airbag force with airbag pressure for six different airbag heights.

APPENDIX B

TYRE STIFFNESS

The aim of this experimental work is to determine the flexibility of a stationary, loaded "super single" lorry wheel in the direction of motion, lateral direction and vertical direction.

B1 Theory

B1.1 In-plane horizontal forces

When considering the deformation of the wheel in the direction of motion during roll over, shown in Fig. B1, the axle is prevented from rotating by the action of the brake. Hence, a movement M_i, applied at the axle results in a pair of reaction forces, F_i, at the axle and the tyre/ground contact. When determining the stiffness $K_x = F_i/\delta_i$ of a tyre when not connected to a trailer, it is more convenient to restrain the top and bottom of the tyre to determine K_x, shown in Fig. B2. The stiffness of the tyre when connected to the trailer will be the same as the stiffness K_x determined experimentally.

The gradient obtained from the graph of δ_i versus F_i shown schematically in Fig. B3, is used to determine the flexibility h_i.

$$\text{Tyre deflection} = hi * Fi.$$

Therefore, the in-plane horizontal stiffness of the tyre K_x is given by

$$K_x = 1/h_i \qquad \textbf{(B1)}$$

B1.2 <u>Out-of-plane horizontal forces</u>

When considering the deformation of the wheel when loaded in the lateral, horizontal direction to motion during roll over, shown in Fig. B4, the axle is prevented from rotating by the axle to which it is connected. Hence, a horizontal force, F_o applied at the axle results in a reaction F_o, at the tyre/ground contact and a moment M_o when determining the stiffness, $K_z = F_o/\delta_o$, of a tyre when not connected to a trailer, it is more convenient to restrain the top and bottom of the tyre to determine K_z, shown in Fig. B5. The actual stiffness of the tyre, when connected to the trailer, will be the same as the stiffness K_z, determined experimentally.

The gradient obtained from the graph of δ_o versus F_o, shown in Fig. B6, is used to determine the flexibility ,h_o

$$\text{Tyre deflection} = h_o * F_o$$

Therefore, the out-of-plane horizontal stiffness of the tyre K_z is given by

$$K_z = 1/h_o \qquad (B2)$$

B1.3 Vertical forces

The vertical load, F_v is applied to the wheel through its axle, as shown in Fig. B7. However, it is experimentally more convenient to apply a diameter load to the whole wheel, as shown in Fig. B8. The gradient of a graph of δ_v versus F_v, shown in Fig. B9, is the same for axle loading as for diametral loading, due to the measuring of displacement at the axle during diametral loading. The gradient, h_v of the graph of δ_v is the flexibility of the wheel in the vertical direction.

The stiffness of the tyre, K_y in the vertical direction is given by

$$K_y = 1/h_v \qquad \text{(B3)}$$

B2 Experimental equipment and procedures

The tyre and rig used to apply a vertical compressive load are shown in Fig. B10. In the position shown an in-plane horizontal force can be applied to the hub of the tyre. In order to apply an out-of-plane horizontal force the tyre is rotated 90° about the vertical axis. To avoid the possibility of slip (due to limiting friction) at the contact between the tyre and the flow or load cell, two Araldite moulds of the vertically loaded tyre tread, under a load of 40 kN, were made. The tyre was placed in the grooves in the Araldite mould during testing. The Araldite moulds at the top and bottom of the tyre were held in the X and Z directions to prevent movement under loading. The effect of the depth of penetration of the Araldite moulds into the tyre was investigated by carrying out full tread penetration and half tread penetration (ie. 6 mm and 12 mm penetrations).

Equations B1, B2, B3, can be used together with experimental measurements to calculate the tyre flexibilities K_x, K_y, and K_z. In particular the gradients of the graphs of δ_i versus F_i, δ_o versus F_o and δ_v versus F_v are required.

B2.1 In-plane horizontal tyre loading (to obtain K_x)

The tyre was placed in a framework securely bolted to the floor and loaded vertically by a hydraulic ram to 40 kN, which is the approximate load on each tyre under operating conditions. The horizontal load was applied using dead weights, with a wire attached to the hub of the tyre and a pulley attached to the framework to convert the vertical load into the required horizontal load. The horizontal displacement was measured using two dial gauges, at a distance of 330 mm above and below the tyre centre, with the average of these displacements taken for the horizontal displacement of the tyre.

B2.2 Out-of-plane horizontal tyre loading (to obtain K_y)

The out-of-plane horizontal tyre stiffness was obtained in the same manner as the in-plane horizontal tyre stiffness, except that the tyre was placed in the framework when rotated 90° about the vertical. The tyre was loaded in the vertical and horizontal direction in the same manner as for the in-plane tyre test. The horizontal displacement was also measured and used in the same manner as previously described in relation to the in-plane loading.

B2.3 Vertical tyre loading (to obtain K_y)

The tyre was placed in the framework and loaded in increments of 5 kN from 0 to 45 kN. The vertical displacement was measured using two dial guages, at a distance of 330 mm either side of the tyre centre, with the average of these displacements taken for the vertical displacement of the tyre hub.

B3 Results

The experimental results, for a 6 mm tyre tread depth in the Araldite mould, are shown in Figs. B11, B12, and B13, with only the final result for the 12 mm tread given. The gradients for these graphs were obtained using a linear regression analysis. The gradients and corresponding tyre stiffnesses for the in-plane, out-of-plane and vertical loadings are given in Tables B1 , B 2, and B 3, respectively. The tyre stiffnesses are compared with the manufacturers' stiffnesses in Table B. 4.

The different tread depths used in the Araldite mould did not make any significant difference to the stiffnesses obtained. The K_x and K_z stiffnesses obtained are greater than the manufacturers' supplied stiffness. The K_y stiffness agreed well with the manufacturers' stiffness.

The present results were found to be within 67%, 8% and 32% of the manufacturers' results for the k_x, k_y and k_z stiffnesses, respectively. The level of agreement, bearing in mind that the loading and support conditions were not correct, was considered to be good enough to allow the manufacturers' data to be confidently used.

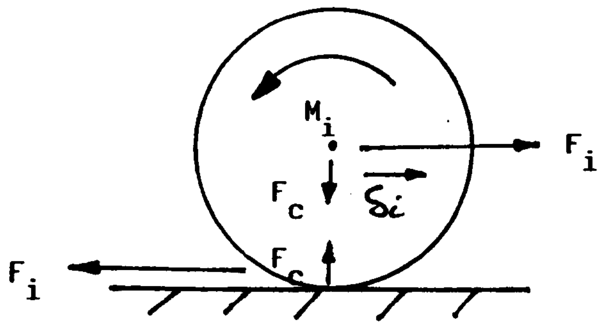

Fig. B1 Free body diagram for in-plane horizontal loading of the wheel

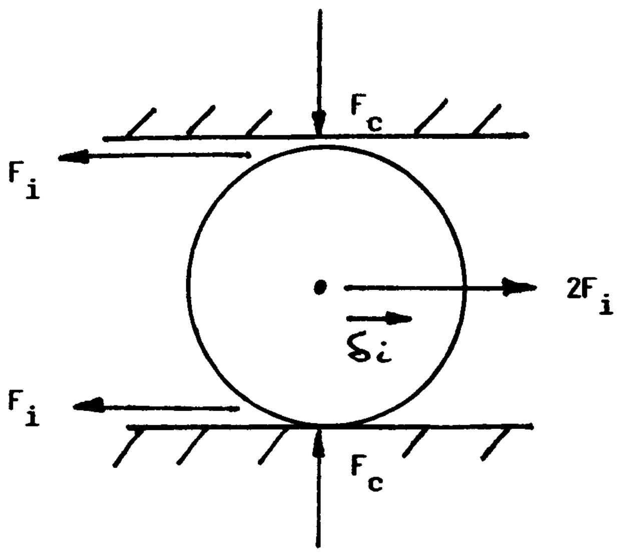

Fig. B2 Free body diagram for applying an inplane horizontal force ,$2F_i$,to the wheel

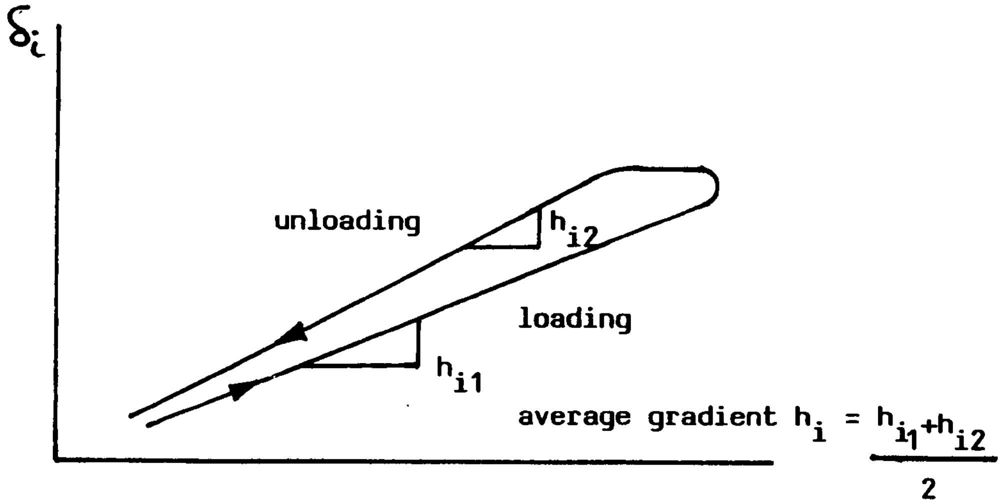

Fig. B3 Schematic diagram of δ_i versus F_i

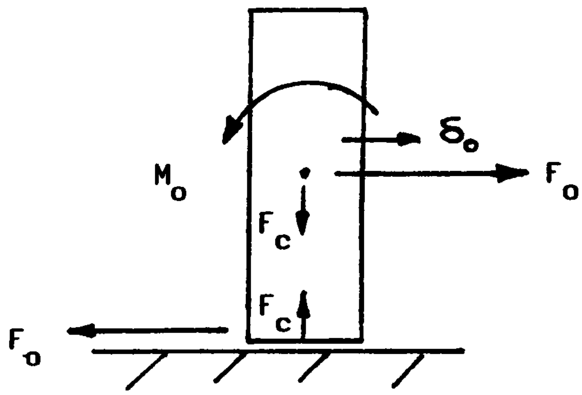

Fig. B4 Free body diagram for out of plane loading of the wheel

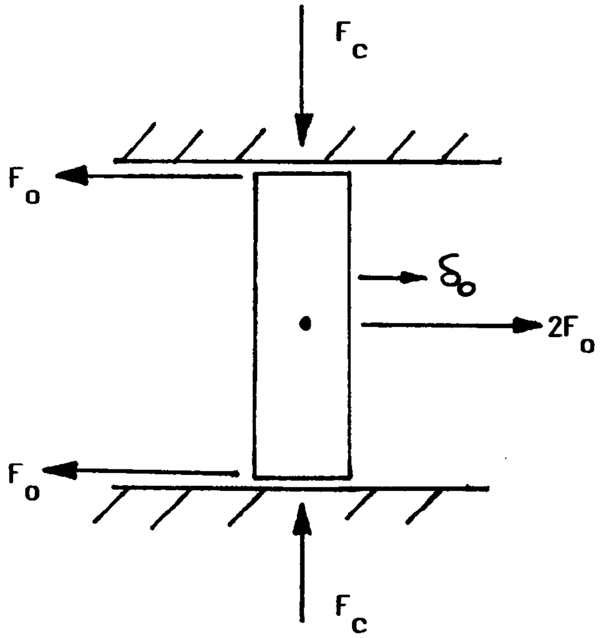

Fig. B5 Free body diagram for applying an out of plane horizontal force, $2F_o$, to the wheel

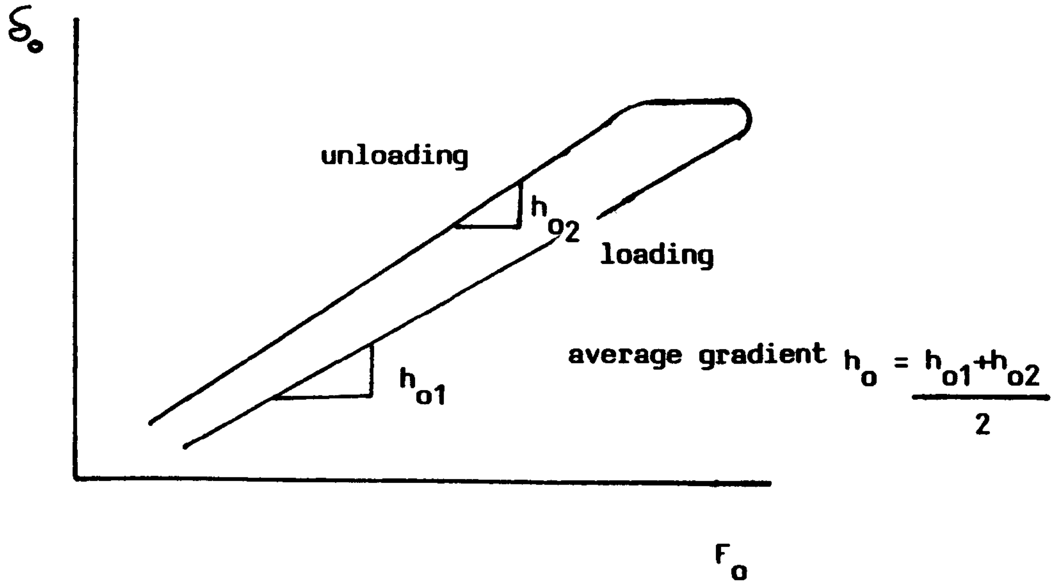

Fig. B6 Schematic diagram of δ_o versus F_o

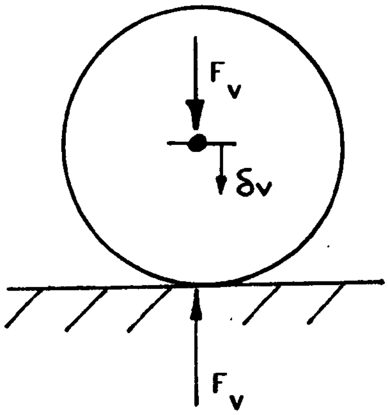

Fig. B7 Free body diagram for vertical wheel loading

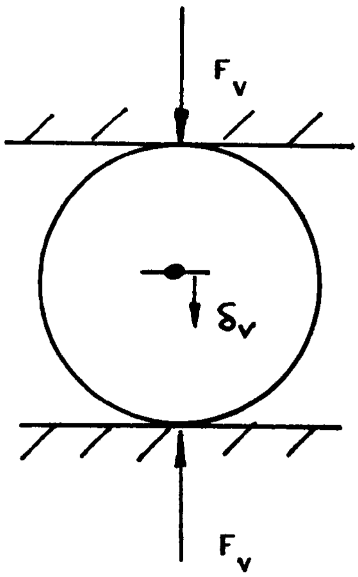

Fig. B8 Free body diagram for applying a vertical Fprce, F_v, to the wheel.

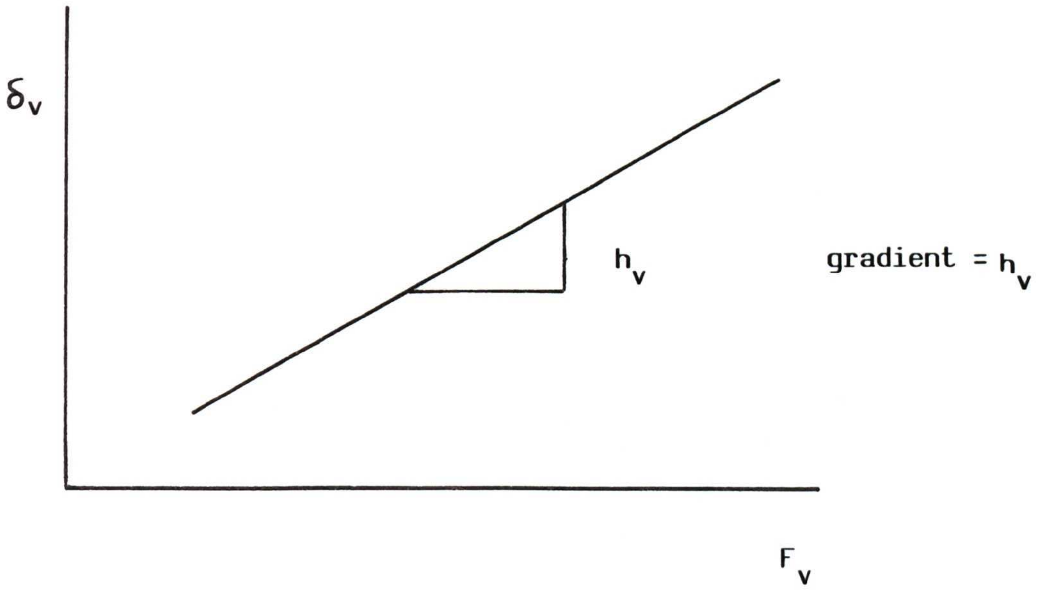

Fig. B9 Schematic diagram of δ_v versus F_v

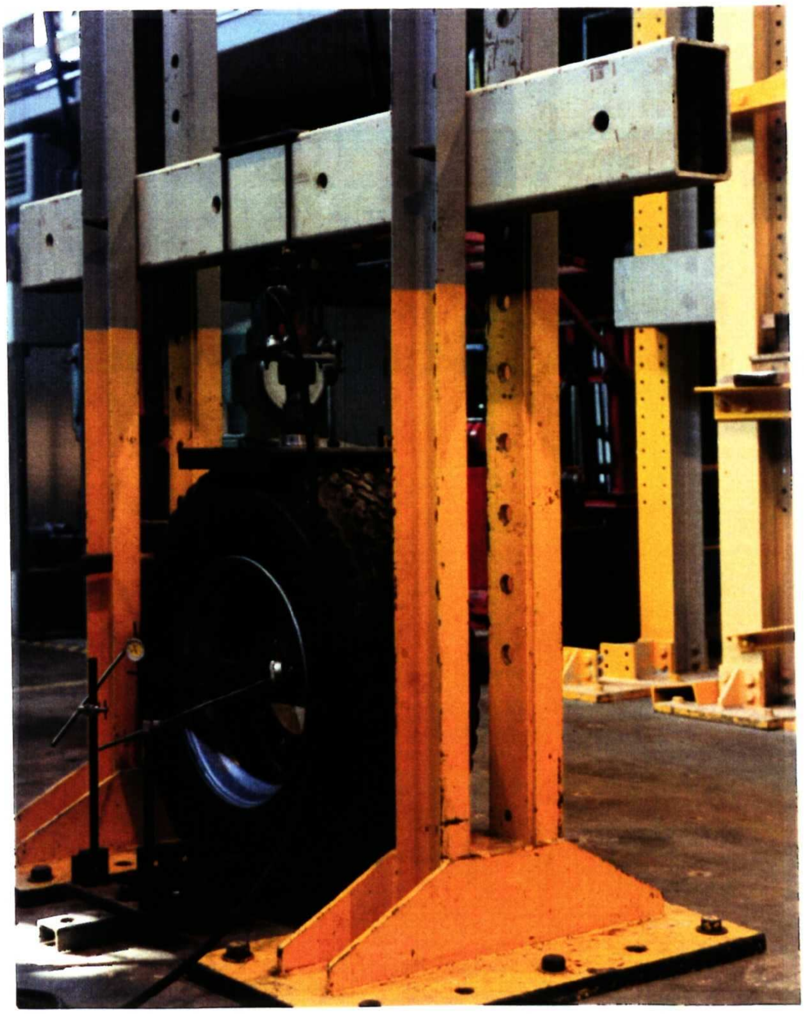

Fig. B10 Loading rig used to apply a vertical force F_v to the tyre

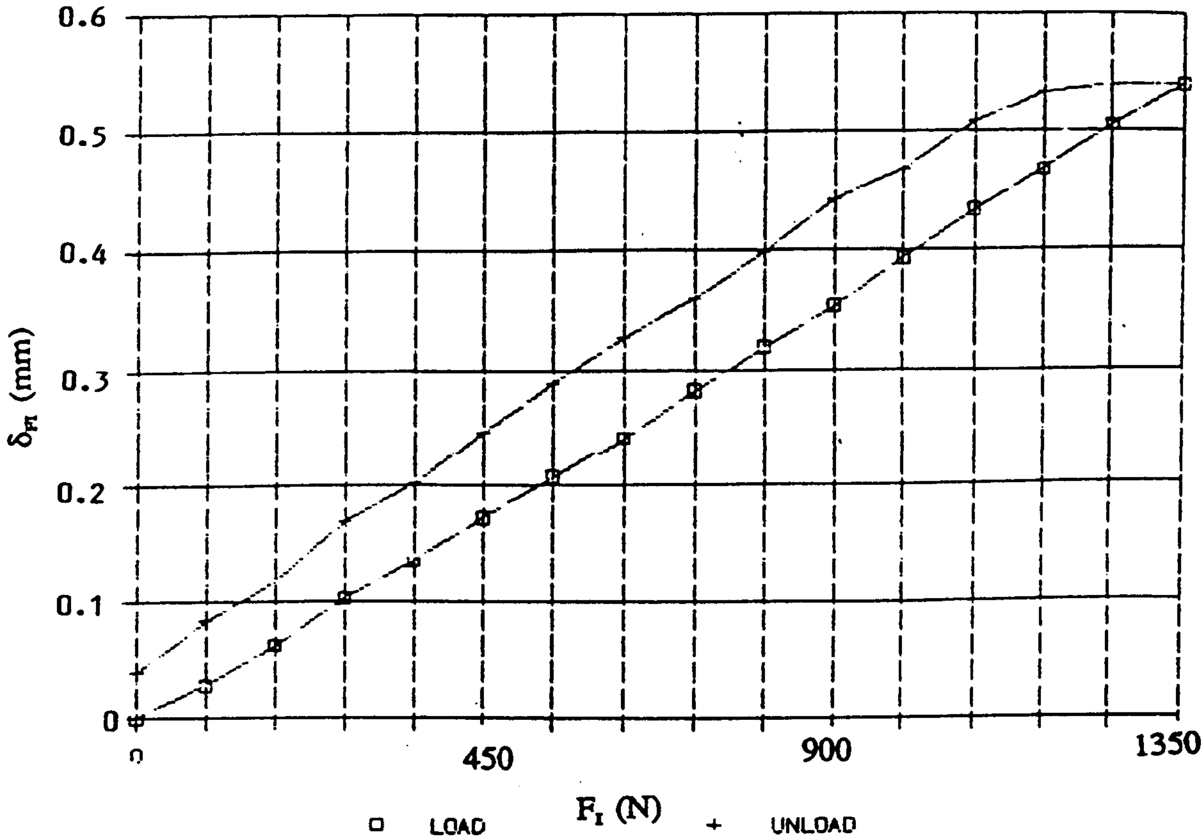

Fig. B11 Variation of δ_{FI} with f_I, for loading and unloading, with a 6 mm tread depth in the Araldite mould.

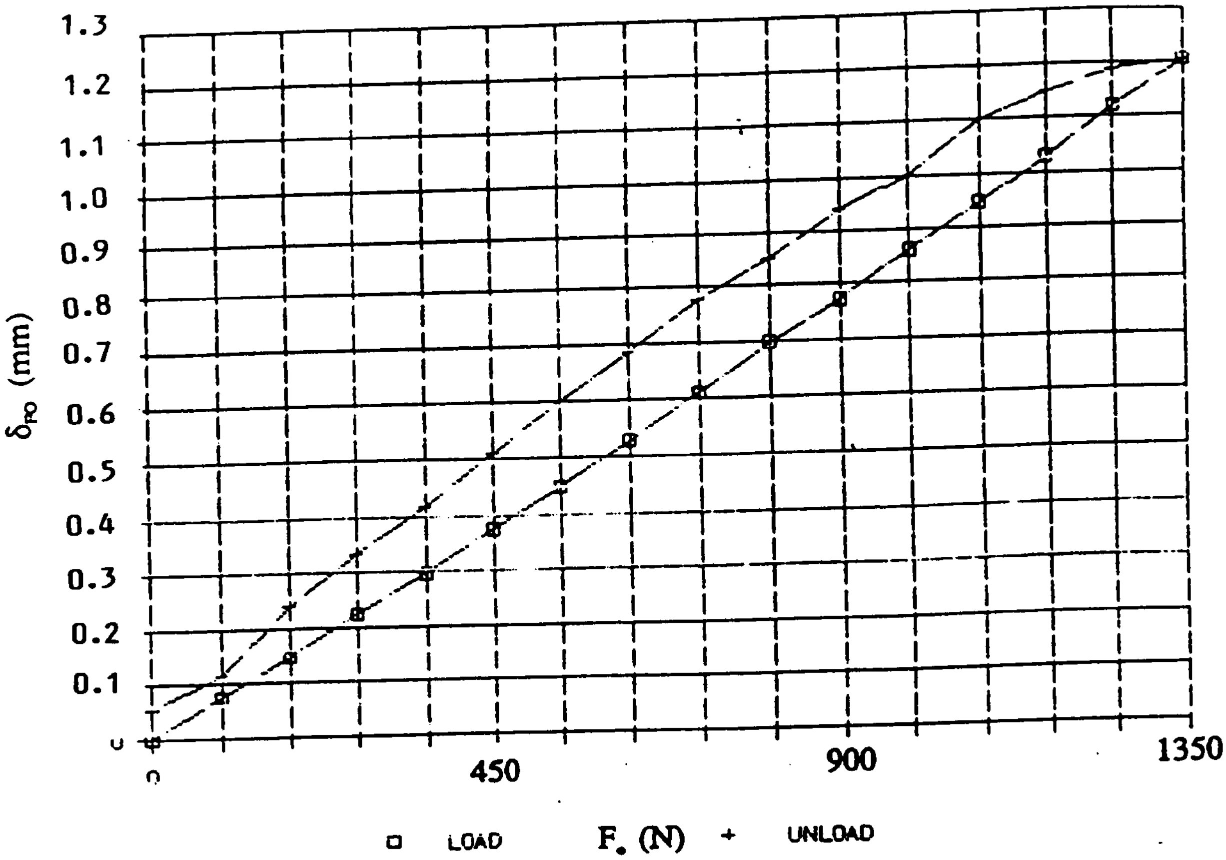

Fig. B12 Variation of δ_{FO} with F_e, for loading and unloading, with a 6 mm tread depth in the Araldite mould.

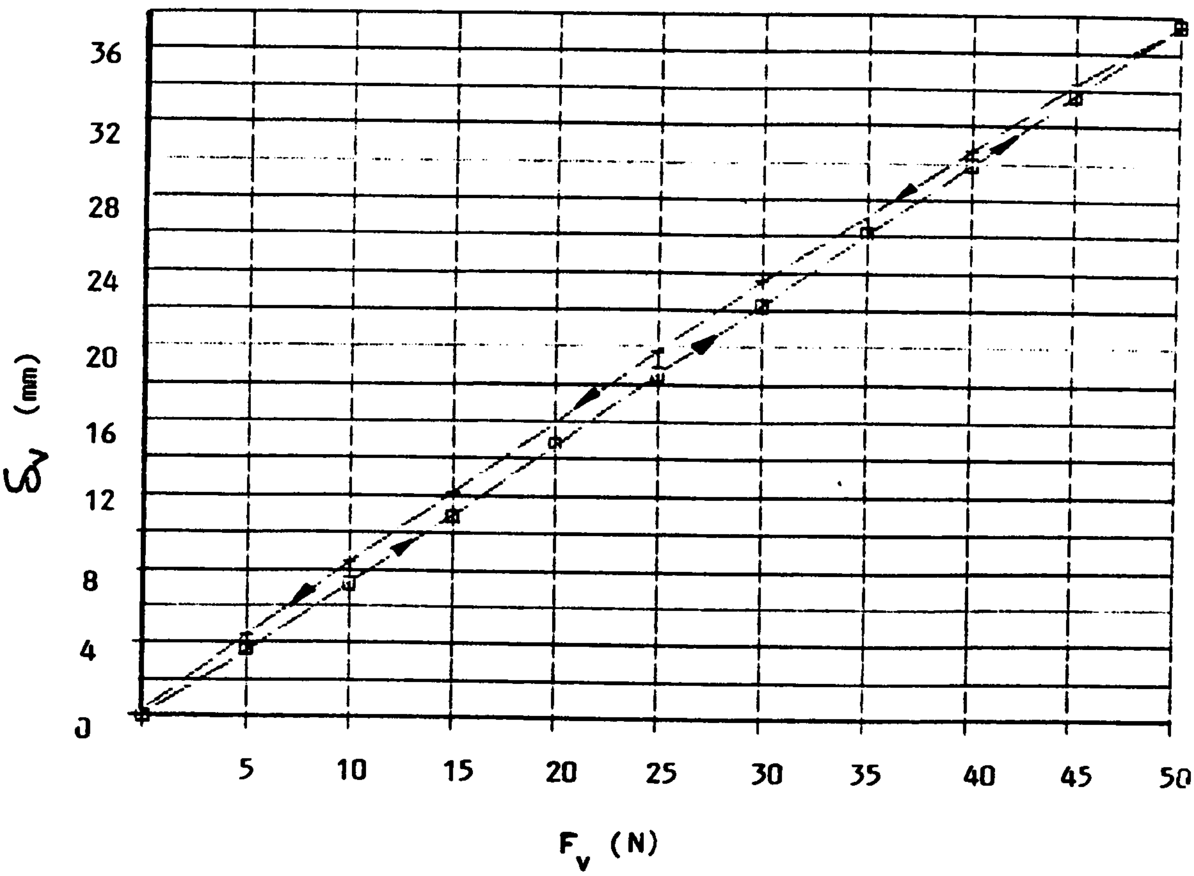

Fig. B13 Variation of with F_v, for loading and unloading, with a 12 mm araldite mould.

Table B1: In-plane, Horizontal Loading Results

Depth of mould tread (mm)	h_{i1} (mm/N)	h_{i2} (mm/N)	h_i (mm/N)	k_x (N/mm)
6	4.068×10^{-4}	4.363×10^{-4}	4.216×10^{-4}	1186
12	4.200×10^{-4}	4.575×10^{-4}	4.388×10^{-4}	1140

Table B2: Out-of-plane, Horizontal Loading Results

Depth of mould tread (mm)	h_{o1} (mm/N)	h_{o2} (mm/N)	h_o (mm/N)	k_z (N/mm)
6	8.968×10^{-4}	9.633×10^{-4}	9.301×10^{-4}	538
12	8.843×10^{-4}	9.599×10^{-4}	9.221×10^{-4}	542

Table B3: Vertical Loading Results

Depth of mould tread, (mm)	h_v (mm/N)	k_y (N/mm)
12	8.666×10^{-4}	1154

Table B4: Comparison of Manufacturers Tyre Stiffnesses with Experimental Results

Depth of mould tread (mm)	k_x (N/mm)	k_y (N/mm)	k_z (N/mm)
6	1186	-	538
12	1140	1154	542
Manufacturers' value	712	1070	412

APPENDIX C

COMPUTER PROGRAM AND FLOW CHART

The program was written on an Akhter 286 PC using Turbo Basic. This language was chosen as a novice programmer would be able to modify the program relatively easily, while the language offered a more sophisticated program construction compared to ordinary Basic. The main advantage is that completely separate subroutines can be developed independently, enabling a large program to be split into manageable sections. The program subroutines are described in conjunction with the program flow chart, shown in Fig. C1(a) to Fig. C1(c) and the corresponding Turbo Basic program(s) shown in Fig. C2 to C28.

C1 Start

The program is controlled by the main program TIPPER.BAS, shown in Fig. C2 which contains the subroutine described next. The subroutines are linked together through the main program, allowing variables to be passed between the subroutines. The subroutines are executed in a sequence described by the routine CONTROL.BAS, shown in Fig. C3.

C2 Input routines

(i) The first input routine contains the undeformed co-ordinates of the hinges, ram/chassis contact, ram/body contact and body centre of gravity, and the beam mass. These variables are fixed for each trailer under consideration with the coding described by the routine INPUTR.BAS. shown in Fig. C4.

(ii) The second input routine contains the undeformed co-ordinates of the payload centre of gravity, the payload mass, the initial ground slope and the ram length, all of which can be determined by the operator. The program is currently set to automatically consider four payload masses in the nine payload positions. The ram length is varied from 2 to 8 in steps of 1 with the ground slope varying from 0° to 10° in steps of 0.1°, for each ram length considered. The coding describing the subroutine is given in VARIAB.BAS, shown in Fig. C5.

C3 Initialise variables routine

The variables used during the program operation are set to zero at the beginning of each new payload magnitude, or payload position, or ground slope, or ram length considered. The coding describing this routine is given in ZERO.BAS, shown in Fig. C6.

C4 Vector positional routine

The co-ordinates of the top of the ram, payload centre of gravity and body mass centre of gravity are determined using the vector analysis described in Section 3.4.1. For the first iteration for each new body or chassis position considered, their co-ordinates are determined for a rigid chassis, with subsequent iterations taking into account chassis deformations. The coding describing this routine is given in VECTOR1.BAS and VECTOR.BAS, shown in Fig. C7 and Fig. C8.

C5 Ram direction routine

The ram direction is described by three cosine resolving functions which independently relate the direction of the ram to the X, Y, or Z axis. These functions are used in the body equilibrium analysis described.in Section 3.4.2 The coding describing this routine is given in RAM.BAS, shown in Fig. C9.

C6 Body equilibrium matrix routine

The body equilibrium matrix, EQM(6,6) is formed using the co-ordinates of the hinges and the ram/body contact, and the ram resolving functions described in Section 3.4.2. The coding describing this routine is given in EQUILB.BAS, shown in Fig. C10.

C7 Body equilibrium matrix inversion routine

The body equilibrium matrix EQM(6,6), described in Section 3.4.2, is inverted to form EQMI(6,6), in order to calculate the body reactions. The coding describing this routine is given in INVERT1.BAS, shown in Fig. C11.

C8 Loading matrix routine

The co-ordinates of the payload and body mass centres of gravity, the payload mass and the body mass, are used to form the force and moment coefficients of the loading matrix LM(6), described in Section 3.4.2. The coding describing this routine is given in BODYF.BAS, shown in Fig. C12.

C9 Body reactions routine

The inverted body equilibrium matrix EQM1(6,6) is multiplied by the loading matrix LM(6) to give the body/chassis contact point reaction forces described in Section 3.4.2. The coding describing this routine is given in BODYF.BAS, shown in Fig. C12.

C10 Suspension routine

This routine chooses the appropriate suspension forces and suspension operating condition, which is compatible with the chassis forces based on one of the four suspension operating conditions described in Section 3.4.3. There are four different matrices corresponding to the four suspension operating conditions, which enable the suspension forces to be calculated. The coding describing this routine is given in SUSP.BAS, CASEa.BAS, CASEb.BAS, CASEc.BAS and CASEd.BAS, show in Fig. C13 to Fig. C17.

C11 Chassis flexibility routine

There are four different matrices for calculating chassis deformations, which correspond to the four suspension operating conditions described in Section 3.4.3. Depending upon the suspension condition, the appropriate matrix is chosen to calculate the chassis deformations, described in Section 3.4.3. The coding describing this routine is given in FLEXI.BAS, FLEXI1.BAS, FLEXI2.BAS, FLEXI3.BAS, FLEXI4.BAS and DISP.BAS, shown in Fig. C18 to Fig. C23.

C12 Tyre force routine

There are four different matrices for calculating tyre forces, which correspond to the four suspension operating conditions described in Section 3.4.3. Depending upon the suspension condition, the appropriate matrix is chosen to calculate the tyre forces, described in Section 3.4.3. The coding describing this routine is given in TYRE.BAS, TYRE1.BAS, TYRE2.BAS, TYRE3.BAS and TYRE4.BAS, shown in Fig. C24 to Fig. C27.

C13 Converge routine

At the end of each iteration except the first, a check is made to see if the procedure has converged or has become unstable. The displacement of the top of the ram is compared with the previous displacement and if the change in this is within the specified tolerance of 1 mm, the solution is deemed to have converged, else a further iteration is undertaken. After convergence the tyre forces are examined and as long as the forces are positive (indicating a downwards force) the trailer is in a stable position. The ram length, tyre force, payload position and payload magnitude are then written to a file. If the trailer is in a stable position, this process is repeated, increasing the ground slope after every converged iteration, so long as the trailer remains stable, up to a maximum ground slope of 10°.

If the tyre force becomes negative (indicating an unstable trailer position) or when the ground slope is equal to 10°, the ram length is increased by 1 m and the ground slope is re-set to zero. The program is then run again for this new body position. When the ram length is 8 m and the ground slope is 10°, the program will have considered the current payload mass and position in 147 body attitudes and ground slopes. At this point, the program can choose a new payload mass and position which is dependent upon the operators supplied data. The program is initiated again until all payload mass and positions have been considered. The program is then terminated. The coding describing this routine is given in CONVERGE.BAS, shown in Fig. C28.

Fig. C1(a) Program flow chart

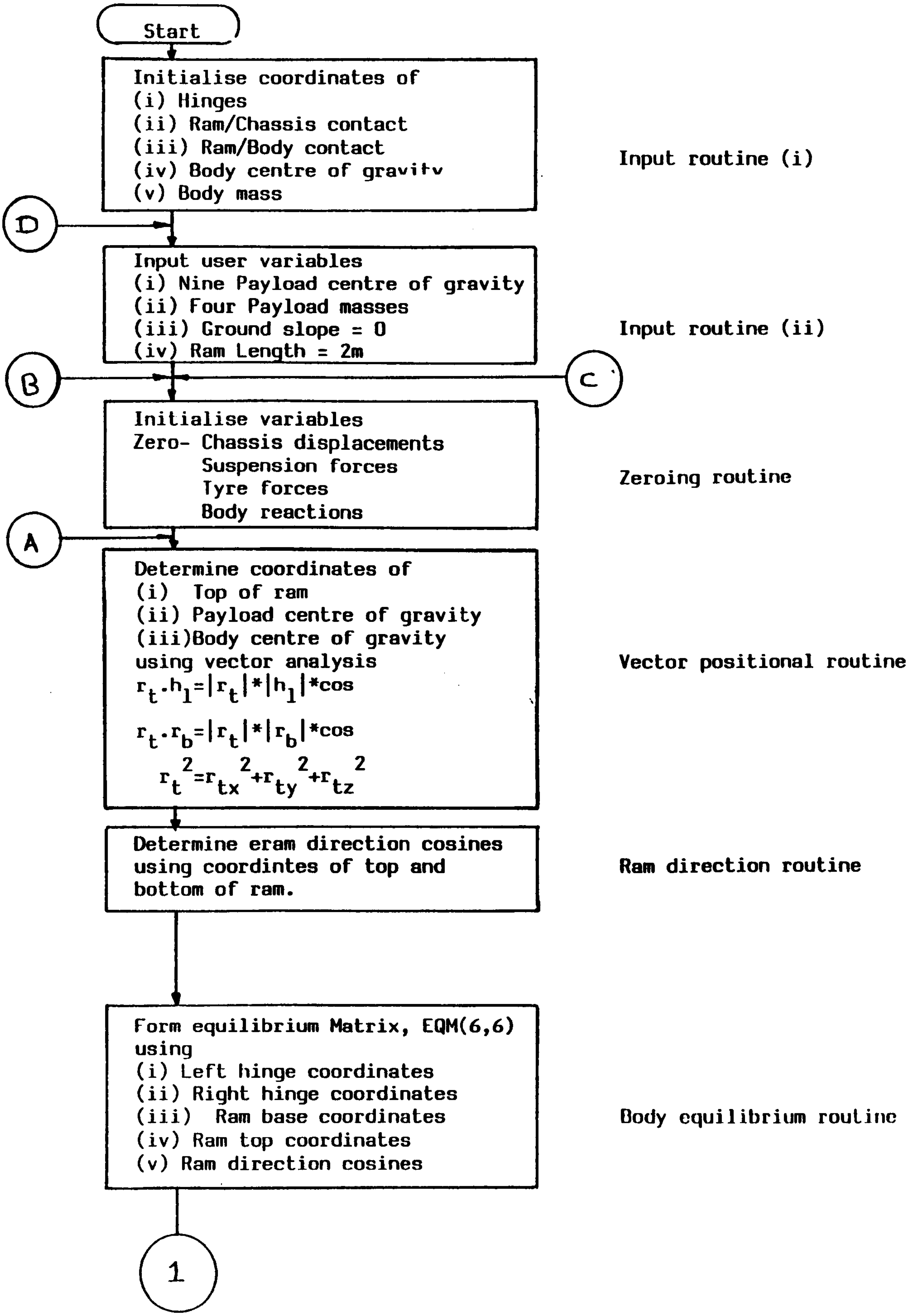

Fig. C1(b) Program flow chart

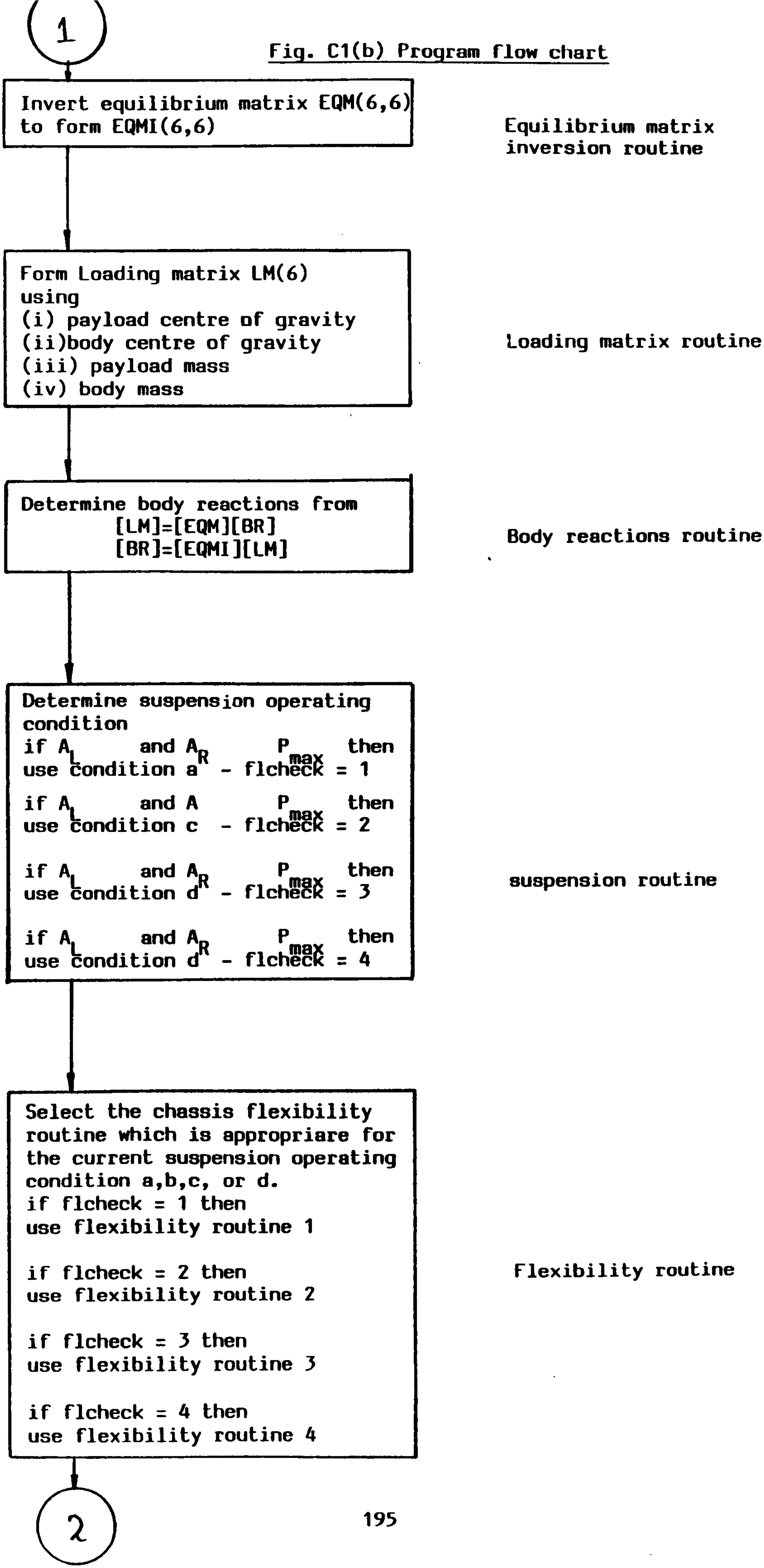

Fig C1(c) Program flow chart

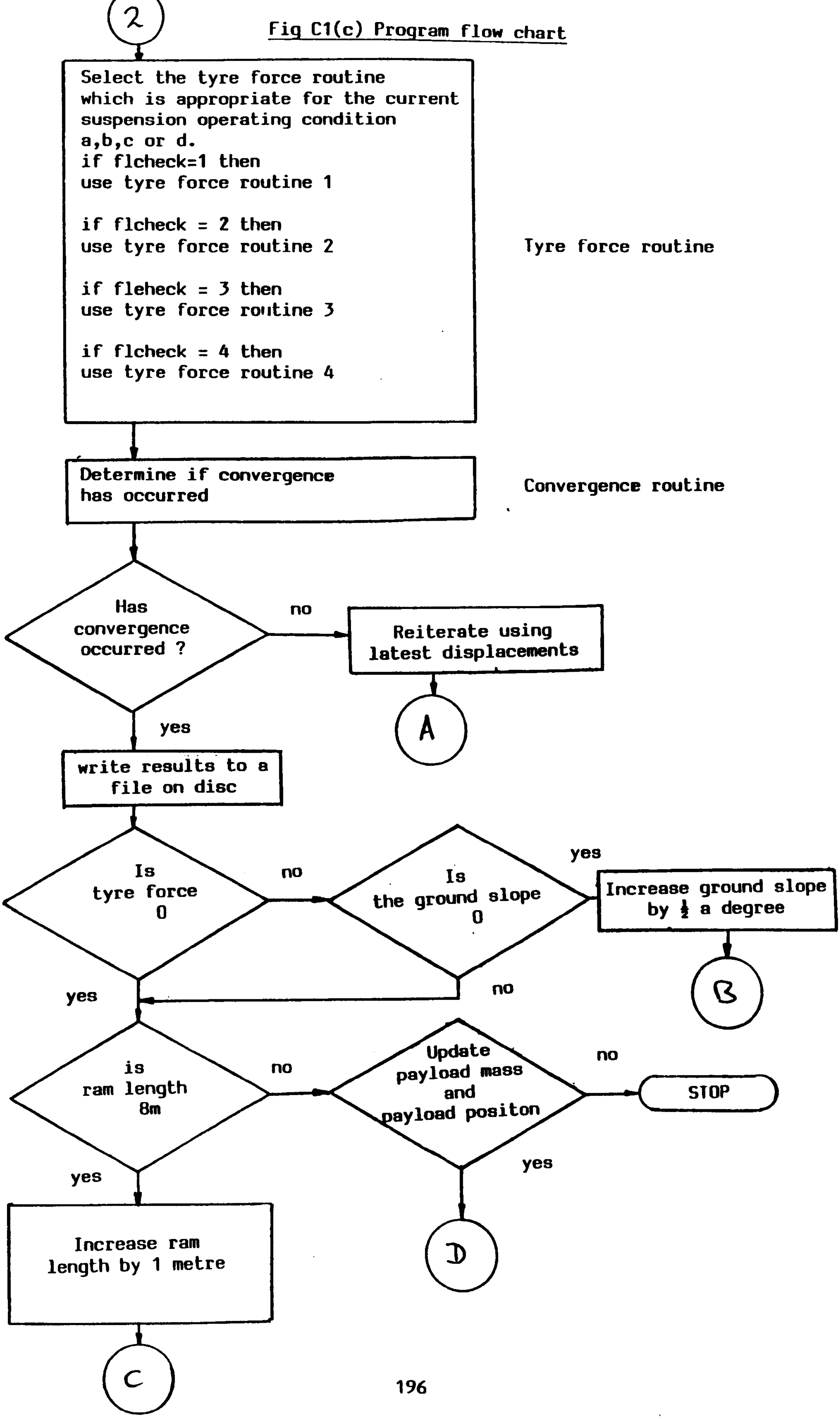

Fig. C2 Tipper.bas

```
' S.G.PICKERING

'*****************************************************************
******
 '
 ' This is the main program described in Appendix C1 which links
the
 ' subroutines together.
 '

'*****************************************************************
******



cls
DIM DYNAMIC lhc#(2,35),rhc#(2,35),rb#(2,35),rt#(2,35),wc#(2,35)
DIM DYNAMIC  bcg#(2,35),pcg#(2,35),BF#(5,35),BR#(7,35)
DIM DYNAMIC  CHL#(15),flex#(8,15),uchassis#(8,35)
DIM DYNAMIC  SUSPR#(35),SUSPL#(35),brconst#(35)
DIM DYNAMIC  eqm#(5,5),eqmi#(5,5)
DIM DYNAMIC k11#(17,17) , k11i#(17,17) , k12#(17,5) , k21#(5,17)
, k22#(5,5)
DIM   DYNAMIC       prescribe#(29,23)    ,    k21k11i#(5,17)   ,
k21k11ik12#(5,5)
DIM DYNAMIC  k22k21k11ik12#(5,5) , k22k21k11ik12i#(5,5)
DIM  DYNAMIC    a#(5)   ,   fab#(5)   ,   fch#(5)   ,   fch1#(5,17)   ,
FCH2#(23),uab#(5,35)
DIM DYNAMIC  TYREF#(5,35),uch#(23,35),FLCHECK(35)
D     I     M               D     Y     N     A     M     I     C
POSI%(4,8),PCGX#(8),PCGY#(8),PCGZ#(8),PM%(4),PM$(4,8)

CALL VARIABS

for y%=1 to 4

 for x%=1 to 8

  if POSI%(y%,x%)=1 then
   PM#=PM%(y%)*9.81
   pcg#(0,0)=PCGX#(x%)
   pcg#(1,0)=PCGY#(x%)
   pcg#(2,0)=PCGZ#(x%)
   B$=STR$(x%)
   FILEN$=PM$(y%,x%)
   A$="PAYLOAD POSITION="+B$


ITER=0
rl#=2000
focount=0
FLAG3=0

 PRINT FILEN$,A$

OPEN "A",#1,FILEN$
WRITE#1,A$
CLOSE#1
```

```
DO UNTIL  rl# > 8000
print "ram length=";rl#;pm#;pcg#(0,0);pcg#(1,0);pcg#(2,0)
OPEN "A",#1,FILEN$
WRITE#1,rl#
CLOSE#1


  concount=0
  FLAGC=0
  thetap#=0
  thetactr=0
  tyre$="go"

 DO UNTIL tyre$="stop" or thetactr>20.1
print "thetap=";thetactr
   CALL CONTROL
   CALL ZERO
   thetactr=thetactr+1/2
   thetap#=thetap#+3.1415927/(180*2)  'increment by 1/2  degree
in rads.
   ITER=1
   n=0
   l=0
   m=0
   pcg#(0,0)=PCGX#(x%)
   pcg#(1,0)=PCGY#(x%)
   pcg#(2,0)=PCGZ#(x%)

 LOOP

 rl#=rl#+1000
 focount=focount+1

LOOP
end if
   A$=""
   B$=""
   C$=""
   FILEN$=""
   D$=""
   E$=""
next x%
next y%
stop

    $INCLUDE "VARIABS.BAS"
    $INCLUDE "ZERO.BAS"
    $INCLUDE "CONTROL.BAS"
    $INCLUDE "INPUTR.BAS"
    $INCLUDE "VECTOR1.BAS"
    $INCLUDE "VECTOR.BAS"
    $INCLUDE "RAM.BAS"
    $INCLUDE "EQUILIB.BAS
    $INCLUDE "BODYF.BAS"

   $SEGMENT

    $INCLUDE "SUSP.BAS"
```

```
   $INCLUDE "CASE1.BAS"
   $INCLUDE "CASE2.BAS"
   $SEGMENT
   $INCLUDE "CASE3.BAS"

   $SEGMENT

   $INCLUDE "CASE4.BAS"
   $INCLUDE "INVERT1.BAS"
   $INCLUDE "FLEXI.BAS"
   $INCLUDE "FLEXI1.BAS"
   $INCLUDE "FLEXI2.BAS"
   $INCLUDE "FLEXI3.BAS"
   $INCLUDE "FLEXI4.BAS"

   $SEGMENT

   $INCLUDE "DISP.BAS"
   $INCLUDE "TYRE.BAS"
   $INCLUDE "TYRE1.BAS"
   $INCLUDE "TYRE2.BAS"
   $INCLUDE "TYRE3.BAS"
   $INCLUDE "TYRE4.BAS"
   $INCLUDE "CONVERGE.BAS"
   $INCLUDE "OUTP.BAS"

end
```

Fig. C3 Control.bas

```
SUB CONTROL
'*****************************************************************
'  This subroutine controls the execution of the subroutines
'  listed below.
'*****************************************************************


SHARED CONVERGED%,n,ITER

IF n = 0 AND ITER =0 THEN
   CALL INPUTR
END IF

   LABEL.LOOPC:
   CALL VECTOR1

   CALL RAM

   CALL EQUILIB

   CALL INVERT1

   CALL BODYF

   CALL SUSP

   CALL FLEXI

   CALL DISP

   CALL TYRE

   CALL CONVERGE
IF CONVERGED%=0 THEN
   n=n+1
   GOTO LABEL.LOOPC

END IF


 END SUB
```

Fig. C4 Inputr.bas

```
SUB INPUTR
SHARED rt#(),rb#(),wc#(),bcg#()
SHARED pcg#(),lhc#(),rhc#(),l,m,n
SHARED rl#,thetap#,BM#,PM#,WX#,WY#,WZ#

'*************************************************************
******
 '    This subroutine contains the undeformed coordinates of
 '     the trailer/body hinges, ram/chassis contact, ram/body
contact,
 '    body c. of g. and the body mass
 '
 '
 '              lhc#(0) - LEFT HINGE X CO-ORD.
   *
 '              lhc#(1) - LEFT HINGE Y CO-ORD.
   *
 '              lhc#(2) - LEFT HINGE Z CO-ORD.
   *
 '
 '             - THE BODY ATTITUDE IS SPECIFIED BY DEFINING THE
   *
 '               THE GROUND SLOPE ANGLE, thetap#, AND THE LENGTH
   *
 '               OF THE RAM , rl#.
   *
 '
 '            - THE APPLIED LOADS TO THE BODY AND THEIR RESPECTIVE
 *
 '               POSITIONS ARE GIVEN .
   *

'*************************************************************
****
l=m=n=0
rt#(0,0)=8977.2 : rt#(1,0)=2029.5 : rt#(2,0)=1E-06
rb#(0,0)=8977.2 : rb#(1,0)=0.0 : rb#(2,0)=1E-06
wc#(0,0)=4488.6 : wc#(1,0)=1014.75 : wc#(2,0)=-1247.0
bcg#(0,0)=4488.6 : bcg#(1,0)=1014.75 : bcg#(2,0)=1E-06
lhc#(0,0)=1E-06 : lhc#(1,0)=1E-06 : lhc#(2,0)=-700
rhc#(0,0)=1E-06 : rhc#(1,0)=1E-06 : rhc#(2,0)=700
BM#=1250*9.81
end sub
```

Fig. C5 Variabs.bas

```
SUB VARIABS
SHARED POSI%(),PCGX£(),PCGY£(),PCGZ£(),PM$()

'************************************************************
*************
'     This routine contains user input variables, which are the
undeformed
'     coordinates of the payload centre of gravity, payload mass
and the
'     initial ground slope and ram length.
'************************************************************
*************

'Line 12
'PAYLOAD CENTRE OF GRAVITY X COORDINATES STORED IN PCGX£(8) IN
mm
'-----------------------------------------------------------
----

PCGX#(0)=2992
PCGX#(1)=4488
PCGX#(2)=5984
PCGX#(3)=2992
PCGX#(4)=4488
PCGX#(5)=5984
PCGX#(6)=2992
PCGX#(7)=4488
PCGX#(8)=5984

'Line 28
'PAYLOAD CENTRE OF GRAVITY Y COORDINATES STORED IN PCGY£(8) IN
mm
'-----------------------------------------------------------
----

PCGY#(0)=676
PCGY#(1)=676
PCGY#(2)=676
PCGY#(3)=1014
PCGY#(4)=1014
PCGY#(5)=1014
PCGY#(6)=1350
PCGY#(7)=1350
PCGY#(8)=1350

'Line 45
'PAYLOAD CENTRE OF GRAVITY Z COORDINATES STORED IN PCGZ£(8) IN
mm
'-----------------------------------------------------------
----
```

```
PCGZ#(0)=1E-06
PCGZ#(1)=1E-06
PCGZ#(2)=1E-06
PCGZ#(3)=1E-06
PCGZ#(4)=1E-06
PCGZ#(5)=1E-06
PCGZ#(6)=1E-06
PCGZ#(7)=1E-06
PCGZ#(8)=1E-06


'Line 60
'PAYLOAD MASSES STORED IN PM£(3) IN kG
'------------------------------------------------------------------
----


PM#(0)=2500
PM#(1)=10000
PM#(2)=17500
PM#(3)=25000


'Line 72
'OUTPUT FILENAMES FOR 2500 kG PAYLOAD (9 FILES)
'------------------------------------------------------------------
----


PM$(0,0)="A:\P2500-1.ROL"
PM$(0,1)="A:\P2500-2.ROL"
PM$(0,2)="A:\P2500-3.ROL"
PM$(0,3)="A:\P2500-4.ROL"
PM$(0,4)="A:\P2500-5.ROL"
PM$(0,5)="A:\P2500-6.ROL"
PM$(0,6)="A:\P2500-7.ROL"
PM$(0,7)="A:\P2500-8.ROL"
PM$(0,8)="A:\P2500-9.ROL"


'Line 90
'OUTPUT FILENAMES FOR 10000 kG PAYLOAD (9 FILES)
'------------------------------------------------------------------
----


PM$(1,0)="A:\P10000-1.ROL"
PM$(1,1)="A:\P10000-2.ROL"
PM$(1,2)="A:\P10000-3.ROL"
PM$(1,3)="A:\P10000-4.ROL"
PM$(1,4)="A:\P10000-5.ROL"
PM$(1,5)="A:\P10000-6.ROL"
PM$(1,6)="A:\P10000-7.ROL"
PM$(1,7)="A:\P10000-8.ROL"
PM$(1,8)="A:\P10000-9.ROL"
```

```
'Line 106
'OUTPUT FILENAMES FOR 17500 kG PAYLOAD (9 FILES)
'-----------------------------------------------------------------
----


PM$(2,0)="A:\P17500-1.ROL"
PM$(2,1)="A:\P17500-2.ROL"
PM$(2,2)="A:\P17500-3.ROL"
PM$(2,3)="A:\P17500-4.ROL"
PM$(2,4)="A:\P17500-5.ROL"
PM$(2,5)="A:\P17500-6.ROL"
PM$(2,6)="A:\P17500-7.ROL"
PM$(2,7)="A:\P17500-8.ROL"
PM$(2,8)="A:\P17500-9.ROL"


PM$(3,0)="A:\P25000-1.ROL"
PM$(3,1)="A:\P25000-2.ROL"
PM$(3,2)="A:\P25000-3.ROL"
PM$(3,3)="A:\P25000-4.ROL"
PM$(3,4)="A:\P25000-5.ROL"
PM$(3,5)="A:\P25000-6.ROL"
PM$(3,6)="A:\P25000-7.ROL"
PM$(3,7)="A:\P25000-8.ROL"
PM$(3,8)="A:\P25000-9.ROL"

END
```

Fig. C6 Zero.bas

```
SUB ZERO
'************************************************************
*******
'  This subroutine sets the program's variables to zero at the
'  beginning of each new payload magnitude or payload mass or
ground
'  slope or ram length considered.
'************************************************************
*******


SHARED lhc#(),rhc#(),rb#(),rt#(),wc#()
SHARED bcg#(),pcg#(),BF#(),BR#()
SHARED CHL#(),flex#(),uchassis#()
SHARED SUSPR#(),SUSPL#(),brconst#()
SHARED a#() , fab#() , fch#() , fchl#() , FCH2#(),uab#()
SHARED TYREF#(),uch#(),FLCHECK()
FOR x=0 TO 2
 FOR y=1 TO 20
  lhc#(x,y)=0
  rhc#(x,y)=0
  rb#(x,y)=0
  rt#(x,y)=0
  wc#(x,y)=0
  bcg#(x,y)=0
  pcg#(x,y)=0
 NEXT y
NEXT x
   ERASE  BF#,BR#
   ERASE  CHL#,flex#,uchassis#
   ERASE  SUSPR#,SUSPL#,brconst#
   ERASE  fch# , FCH2#,uab#
   ERASE  TYREF#,uch#,FLCHECK

DIM DYNAMIC  BF#(5,35),BR#(7,35)
DIM DYNAMIC  CHL#(15),flex#(8,15),uchassis#(8,35)
DIM DYNAMIC  SUSPR#(35),SUSPL#(35),brconst#(35)
DIM DYNAMIC  fch#(5) , FCH2#(23),uab#(5,35)
DIM DYNAMIC  TYREF#(5,35),uch#(23,35),FLCHECK(35)
END SUB
```

Fig. C7 Vector1.bas

```
SUB VECTOR1
'   VECTOR ANALYSIS BY S.G.PICKERING 28/1/91
'*****************************************************************
*******
'This subroutine calls the routine VECTOR.BAS for the payload c.
of g.,
'the body c. of g.  and ram/body contact to determine their
positional
' coordinates using vector analysis
'*****************************************************************
********


  SHARED rt#(),rb#(),wc#(),bcg#()
  SHARED pcg#(),lhc#(),rhc#(),rl#,l,m,n
  CALL VECTOR(rt#(),rb#(),lhc#(),0,l,m,n)
  m=m+1
  CALL VECTOR(bcg#(),rt#(),lhc#(),1,l,m,n)
  CALL VECTOR(pcg#(),rt#(),lhc#(),1,l,m,n)



l=l+1
if n=0 then
  n=n+1
'***************************
' hinge and ram base co-ords are modified by subtracting gravity
load disp-
' lacements as these have been taken into account in the chassis
FE mesh.
'***************************

  lhc#(0,n)=lhc#(0,n-1)+0.2714-0.778
  lhc#(1,n)=lhc#(1,n-1)+10.176-4.946
  lhc#(2,n)=lhc#(2,n-1)
  rhc#(0,n)=rhc#(0,n-1)+0.2714-0.778
  rhc#(1,n)=rhc#(1,n-1)+10.176-4.946
  rhc#(2,n)=rhc#(2,n-1)
  rb#(0,n)=rb#(0,n-1)+0.2542-0.706
  rb#(1,n)=rb#(1,n-1)+1.667+16.809
  rb#(2,n)=rb#(2,n-1)
end if
end sub
```

Fig. C8 Vector.bas

```
231   SUB VECTOR(a#(2),b#(2),c#(2),flag,l,m,n)
'**************************************************************
*******
'This routine contains the coding for multiplying vectors to
determine
'the positional coordinates of the important points on the body
'**************************************************************
********




240   SHARED rl#
250   'N.B  a#(,)-uses l subscript
260   '       b#(,)-uses m subscript
270   '       c#(,)-uses n subscript
280   if ABS(a#(0,l)) <1e-06 then
290   a#(0,l)=1e-06
300   end if
310   if  ABS(a#(1,l)) < 1e-06 then
320   a#(1,l)=1e-06
330   end if
340   if ABS(a#(2,l)) < 1e-06 then
350   a#(2,l)=1e-06
360   end if
370
380 if ABS(b#(0,m)) <1e-06 then
390 b#(0,m)=1e-06
400 end if
410 if ABS(b#(1,m)) < 1e-06 then
420 b#(1,m)=1e-06
430 end if
440 if ABS(b#(2,m)) < 1e-06 then
450 b#(2,m)=1e-06
460 end if
470 if ABS(c#(0,n)) < 1e-06 then
480 c#(0,n)=1e-06
500 end if
510 if ABS(c#(1,n)) < 1e-06 then
520 c#(1,n)=1e-06
530 end if
540 if ABS(c#(2,n)) < 1e-06 then
550 c#(2,n)=1e-06
560 end if
570
580 if flag=0 then
590 'CALC a# VECTOR LENGTH
600 a#=SQR(a#(0,0)^2+a#(1,0)^2+a#(2,0)^2)
610 'CALC b# vector length
620 b#=SQR(b#(0,m)^2+b#(1,m)^2+b#(2,m)^2)
630 'c# vector length
640 c#=700.0
650 ab#=rl#
6                                6                                0
ac#=SQR((a#(0,0)-c#(0,0))^2+(a#(1,0)-c#(1,0))^2+(a#(2,0)-c#(2,
0))^2)
670 end if
680
```

```
690 if flag=1 then
700 'CALC a# VECTOR LENGTH
710 a#=SQR(a#(0,0)^2+a#(1,0)^2+a#(2,0)^2)
720 'CALC b# vector length
730 b#=SQR(b#(0,0)^2+b#(1,0)^2+b#(2,0)^2)
740 'c# vector length
750 c#=700.0
760 'calc ab# vector lngth
7                              7                              0
ab#=SQR((a#(0,0)-b#(0,0))^2+(a#(1,0)-b#(1,0))^2+(a#(2,0)-b#(2,
0))^2)
7                              8                              0
ac#=SQR((a#(0,0)-c#(0,0))^2+(a#(1,0)-c#(1,0))^2+(a#(2,0)-c#(2,
0))^2)
790 end if

810 'calc  cos(gamma) ie angle between vectors a# & b#
820 g#=(a#^2+b#^2-ab#^2)/(2*a#*b#)
830 'calc cos(delta) ie angle between vectors a# & c#
840 d#=(a#^2+c#^2-ac#^2)/(2*a#*c#)
850 'calc ak#=dj#+ej#(aj#) ie ak# in terms of aj#
860 'where dj#=
8                              8                              0
dj#=(a#*c#*d#*b#(0,m)-a#*b#*g#*c#(0,n))/(c#(2,n)*b#(0,m)-b#(2,
m)*c#(0,n))
900 'and
9                              1                              0
ej#=(b#(1,m)*c#(0,n)-c#(1,n)*b#(0,m))/(c#(2,n)*b#(0,m)-b#(2,m)
*c#(0,n))
930 'calc ai#=fi#+gi#(aj#) ie ai# in terms of aj#
940 'where fi
950 fi#=(a#*b#*g#-dj#*b#(2,m))/b#(0,m)
970 'and gi=
980 gi#=(-ej#*b#(2,m)-b#(1,m))/b#(0,m)
' sub ai# & aj# into
1010 'ai#^2+aj#^2+ak#^2=a#^2 to give
1                 0                    2                      0
'ak#^2(gi#^2+ej#^2+1)+ak#(2*fi#*gi#+2*dj#*ej#)+fi#^2+dj#^2-a#^2=0
1030
1040 ae#=gi#^2+ej#^2+1
1050 be#=2*fi#*gi#+2*dj#*ej#
1060 ce#=fi#^2+dj#^2-a#^2
1080 ' CALC ROOTS
1090   disc#=be#*be#-4.0*ae#*ce#
1100   if ABS(disc#/be#) < 1E-04 THEN
1120   disc#=0.0
1130   'print "suspected error in quadratic ??????????????"
1140   end if
1150    if ae#=0 then
1160    xj0#=-ce#/be#
1170    check=1
1180    elseif disc# >= 0 then
1190    xj1#=(-be#+SQR(disc#))/(2*ae#)
1200    xj2#=(-be#-SQR(disc#))/(2*ae#)
1210    check=2
1220    else
1230    print "STOP error in vector quadratic "
1250    end
```

```
1260   end if
1270
1280 if check=1 then
1290  a#(1,(l+1))=xj0#
1300  a#(2,(l+1))=dj#+ej#*xj0#
1310  a#(0,(l+1))=fi#+gi#*xj0#
1320 elseif check=2 then
1330  'calc original cross product of a & b for k term only
1340  acrossb1=a#(0,0)*b#(1,0)-a#(1,0)*b#(0,0)
1350
1360  'calc current cross product of a & b for k term only using
xj1#
1370  xi1#=fi#+gi#*xj1#
1380  xk1#=dj#+ej#*xj1#
1390  acrossb2=xi1#*b#(1,m)-xj1#*b#(0,m)
1410  'calc current cross product of a & b for k term only using
xj2#
1420  xi2#=fi#+gi#*xj2#
1430  xk2#=dj#+ej#*xj2#
1440  acrossb3=xi2#*b#(1,m)-xj2#*b#(0,m)
1455  if acrossb2=0 and acrossb3=0 then
1456  check1=0
1457 goto 1480
1458 end if
1460  check1=acrossb1/acrossb2   'using xj1# co-ord
1470  check2=acrossb1/acrossb3   'using xj2# co-ord
1480   if check1 >=0 then
1490    a#(0,l+1)=xi1#
1500    a#(1,l+1)=xj1#
1510    a#(2,(l+1))=xk1#
1520   elseif check2 >=0 then
1530    a#(0,l+1)=xi2#
1540    a#(1,l+1)=xj2#
1550    a#(2,(l+1))=xk2#
1560   else
1570   print "error in choosing y value on body????????"
1580    stop
1590    end
1600   end if
1610  end if
1930   end sub
```

Fig. C9 Ram.bas

```
SUB RAM
SHARED rt#( ),rb#( ),n
SHARED rl#,nx#,ny#,nz#
'*****************************************************************
*******
'This routine determines the ram resolving cosines functions
nx#,ny#,nz#
'to enable  X,Y,Z components to be calculated.
'*****************************************************************
*******

'bottom of ram co-ords is stored in rb#(2,20)
'top of ram co-ords stored in rt#(2,20)
'ram direction co-sines stored in nx,ny,nz

nx#=(rt#(0,n)-rb#(0,n))/(rl#)
ny#=(rt#(1,n)-rb#(1,n))/(rl#)
nz#=(rt#(2,n)-rb#(2,n))/(rl#)
end sub
```

Fig. C10 Equilib.bas

```
SUB EQUILIB
shared eqm#( ),thetap#,nx#,ny#,nz#,WX#,WY#,WZ#,BM#,PM#,alpha#
shared rt#( ),rb#( ),wc#( ),bcg#( ),pcg#( ),lhc#( ),rhc#( ),BF#( ),n

'*****************************************************************
****
'  EQUILIB.MAT - VALUES ARE ASSIGNED TO THE EQUILIBRIUM MATRIX
 *
'                      eqm( ) AND THE LOADING MATRIX BF( ) .
 *
'*****************************************************************
****
'alpha=1 ASSUMES LEFT HINGE TAKES ALL LATERAL LOADING
alpha#=1
for r=0 to 5
for c=0 to 5
eqm#(r,c)=0.0
next c,r
eqm#(0,0)=1.0
eqm#(0,1)=1.0
eqm#(0,2)=0.0
eqm#(0,3)=0.0
eqm#(0,4)=0.0
eqm#(0,5)=nx#
eqm#(1,0)=-lhc#(2,n)
eqm#(1,1)=-rhc#(2,n)
eqm#(1,2)=0.0
eqm#(1,3)=0.0
eqm#(1,4)=alpha#*lhc#(0,n)+(1-alpha#)*rhc#(0,n)
eqm#(1,5)=-nx#*rt#(2,n)+nz#*rt#(0,n)
eqm#(2,0)=0.0
eqm#(2,1)=0.0
eqm#(2,2)=-lhc#(2,n)
eqm#(2,3)=-rhc#(2,n)
eqm#(2,4)=alpha#*lhc#(1,n)+(1-alpha#)*rhc#(1,n)
eqm#(2,5)=-ny#*rt#(2,n)+nz#*rt#(1,n)
eqm#(3,0)=0.0
eqm#(3,1)=0.0
eqm#(3,2)=1.0
eqm#(3,3)=1.0
eqm#(3,4)=0.0
eqm#(3,5)=ny#
eqm#(4,0)=0.0
eqm#(4,1)=0.0
eqm#(4,2)=0.0
eqm#(4,3)=0.0
eqm#(4,4)=1.0
eqm#(4,5)=nz#
eqm#(5,0)=-lhc#(1,n)
eqm#(5,1)=-rhc#(1,n)
eqm#(5,2)=lhc#(0,n)
eqm#(5,3)=rhc#(0,n)
eqm#(5,4)=0.0
eqm#(5,5)=-nx#*rt#(1,n)+ny#*rt#(0,n)


END SUB
```

Fig. C11 Invert1.bas

```
SUB INVERT1
shared eqm#( ),eqmi#( )

'*************************************************************
******
'  INVERT - THE EQUILIBRIUM MATRIX IS STORED IM EQM( ) . TO SOLVE
 *
'                 FOR BODY REACTIONSN THE EQUILIBRIUM HAS TO BE
INVERTED.*
'              THIS ROUTINE INVERTS EQM( ) AND STORES THE INVERTED
   *
'              MATRIX IN EQMI( ).
   *
'*************************************************************
******
for r=0 to 5
 for c=0 to 5
  eqmi#(r,c)=0
  test#(r,c)=eqm#(r,c)
next c,r

for x=0 to 5
 eqmi#(x,x)=1
next x

for x=0 to 5

 for y=x to 5

  d#=eqm#(x,y) : if d#=0 or d#=1 goto LABEL.ONE
   for k=x to 5
    eqm#(k,y)=eqm#(k,y)/d#
   next k
   for k=0 to 5
    eqmi#(k,y)=eqmi#(k,y)/d#
   next k
LABEL.ONE:

 next y

 if x=5 goto LABEL.TWO

 for y=x+1 to 5

 if eqm#(x,y)=0 goto LABEL.THREE

  for k=x to 5
   eqm#(k,y)=eqm#(k,y)-eqm#(k,x)
  next k
  for k=0 to 5
   eqmi#(k,y)=eqmi#(k,y)-eqmi#(k,x)
  next k
LABEL.THREE:

 next y

next x
```

```
LABEL.TWO:

for x=0 to 5

if eqm#(x,x)=1 then next x
if x<>6 then print "*****NOT INV*******equilib matrix": end

 for x=5 to 1 step -1

  for y=x-1 to 0 step -1

   d#=eqm#(x,y)

    for k=x to 5
     eqm#(k,y)=eqm#(k,y)-eqm#(k,x)*d#
    next k
    for k=0 to 5
     eqmi#(k,y)=eqmi#(k,y)-eqmi#(k,x)*d#
    next k

  next y

 next x


end sub
```

Fig. C12 Bodyf.bas

```
SUB BODYF
s          h          a          r          e          d
eqm#(),thetap#,psi#,ja#,nx#,ny#,nz#,WX#,WY#,WZ#,BM#,PM#,alpha#
s          h          a          r          e          d
eqmi#(),rt#(),rb#(),wc#(),bcg#(),pcg#(),lhc#(),rhc#(),BR#(),n
shared brconst#(),BF#()

'*****************************************************************
********
'  VALUES ARE ASSIGNED TO THE BODY LOADING MATRIX BF#(5)
'*****************************************************************
*********

BF#(0,n)=-WX#

BF1a#=-WZ#*wc#(0,n)+WX#*wc#(2,n)-BM#*SIN(thetap#)*bcg#(0,n)
BF1b#=-PM#*SIN(thetap#)*pcg#(0,n)
BF#(1,n)=BF1a#+BF1b#

BF2a#=-BM#*(SIN(thetap#)*bcg#(1,n)+COS(thetap#)*bcg#(2,n))
BF2b#=-PM#*(SIN(thetap#)*pcg#(1,n)+COS(thetap#)*pcg#(2,n))
BF2c#=-WZ#*wc#(1,n)+WY#*wc#(2,n)
BF#(2,n)=BF2a#+BF2b#+BF2c#

BF#(3,n)=COS(thetap#)*(PM#+BM#)-WY#

BF#(4,n)=-SIN(thetap#)*(PM#+BM#)-WZ#

BF#(5,n)=COS(thetap#)*(BM#*bcg#(0,n)+PM#*pcg#(0,n))-WY#*wc#(0,
n)+WX#*wc#(1,n)


'*****************************************************************
******
'      OBTAIN BODY REACTIONS BY MULTIPLYING INVERTED EQUILIBRIUM
*
'        MATRIX ,eqmi#(), BY APPLIED BODY LOADS MATRIX BF#().
   *
'*****************************************************************
******

for x=0 to 5
BR#(x,n)=0
 for y=0 to 5
  BR#(x,n)=BR#(x,n)+eqmi#(x,y)*BF#(y,n)
 next y
next x

'**** change sign of body reactions so they can be applied
'**** directly to chassis
for x=0 to 5
 BR#(x,n)=-BR#(x,n)
next x
brconst#(n)=BR#(5,n)
BR#(5,n)=brconst#(n)*nx#
BR#(6,n)=brconst#(n)*ny#
BR#(7,n)=brconst#(n)*nz#
```

Fig. C13 Susp.bas

```
SUB SUSP
SHARED SUSPL#( ),SUSPR#( ),n,FLCHECK( ),thetactr

'*************************************************************
*******
' This routine determines the appropriate suspension operating
' condition and calls the appropriate suspension force matrix
'*************************************************************
*******


PMAX=30000
FLCHECK(n)=0

IF thetactr > 0 THEN

IF FLCHECK(n-1)=3 THEN
  CALL CASE3
  FLCHECK(n)=3

ELSE

 IF FLCHECK(n-1)=4 THEN
   CALL CASE4
   FLCHECK(n)=4
  IF SUSPL#(n) < 0 THEN
   CALL CASE3
   FLCHECK(n)=3
  END IF
 END IF
END IF
END IF

IF FLCHECK(n) = 0 THEN
CALL CASE1
FLCHECK(n)=1

 IF SUSPL#(n) < 0 THEN     '(1)

     IF SUSPR#(n) > PMAX THEN    '(2)

        CALL CASE4
        FLCHECK(n)=4

          if SUSPL#(n) < 0 then   '(3)

            SUSPL#(n)=0
            SUSPR#(n)=0
            CALL CASE2
            FLCHECK(n)=2

              if SUSPR#(n) > PMAX THEN  '(4)

               SUSPL#(n)=0
               SUSPR#(n)=0
               CALL CASE3
               FLCHECK(n)=3
              end if     '(4)
```

```
        end if      '(3)

     ELSE         '(2)

    SUSPL#(n)=0
    SUSPR#(n)=0
    CALL CASE2
    FLCHECK(n)=2
    END IF       '(2)


 ELSE  '(1)

    IF SUSPR#(n) >= PMAX THEN
     CALL CASE4
     FLCHECK(n)=4
    END IF

  END IF

END IF
END SUB
```

Fig. C14 Case1.bas

```
SUB CASE1
SHARED BR#( ),n,thetap#,CHL#( ),SUSPR#( ),SUSPL#( )
SHARED uchassis#( )

dim suspml#(1,13)
'*****************************************************************
**********
'  This  routine  contains  the  suspension  force  matrix  for
suspension
' operating condition condition a.
' Suspension  flexibility  matrix is  formed  (suspm#( )).The  two
equations *
' are solved to give right and left suspension forces, using
      *
' the condition of zero relative displacement between the middle
axle  *
' and chassis. This is determined by placing two tie bars between
the  *
' middle axle and chassis and deriving a  flexibility matrix
      *
' which relates tie bar forces to body reactions,chassis and
tractor
' self weight and suspension forces. Setting the tie bar forces
to zero
' simulates the desired condition enabling suspension forces to
be obtained.
'*****************************************************************
**********
suspml#(0,0)=-0.28627e-01
suspml#(0,1)=-0.18198e-01
suspml#(0,2)=-1.0168
suspml#(0,3)=-0.27087
suspml#(0,4)=-0.21127
suspml#(0,5)=-0.21508e-01
suspml#(0,6)=-0.10598e-01
suspml#(0,7)=-0.13069e-01
suspml#(0,8)=-0.22033e-02
suspml#(0,9)=-0.52137e-02
suspml#(0,10)=-0.16194
suspml#(0,11)=-0.01963
suspml#(0,12)=-3.1736
suspml#(0,13)=-1.5410

suspml#(1,0)=-0.18186e-01
suspml#(1,1)=-0.28627e-01
suspml#(1,2)=-0.2708
suspml#(1,3)=-1.0168
suspml#(1,4)=0.21124
suspml#(1,5)=-0.21502e-01
suspml#(1,6)=-0.10605e-01
suspml#(1,7)=0.13083e-01
suspml#(1,8)=-0.22123e-02
suspml#(1,9)=0.52242e-02
suspml#(1,10)=-0.16192
suspml#(1,11)=0.01963
suspml#(1,12)=-1.5413
suspml#(1,13)=-3.1733
```

PAGE NUMBERING AS ORIGINAL

```
'****** body reactions,tractor weight, chassis weight and suspension
'****** forces (not known yet) are stored in chl(14).

CHL#(0)=BR#(0,n)
CHL#(1)=BR#(1,n)
CHL#(2)=BR#(2,n)
CHL#(3)=BR#(3,n)
CHL#(4)=BR#(4,n)
CHL#(5)=BR#(5,n)
CHL#(6)=BR#(6,n)
CHL#(7)=BR#(7,n)
CHL#(8)=-63666.9*cos(thetap#)
CHL#(9)=63666.9*sin(thetap#)
CHL#(10)=-47088*cos(thetap#)
CHL#(11)=47088*sin(thetap#)
' CHL#(12)-unknown yet (SUSPL)
' CHL#(13)-unknown yet (SUSPR)
A#=0
B#=0
C#=0
D#=0
'PRINT A#,B#,C#,D#
for x=0 to 11
 A#=A#-suspml#(1,x)*CHL#(x)/suspml#(1,13)
next x

 B#=-suspml#(1,12)/suspml#(1,13)

for x=0 to 11
 C#=C#-suspml#(0,x)*CHL#(x)/suspml#(0,12)
next x

 D#=-suspml#(0,13)/suspml#(0,12)

SUSPR#(n)=(A#+B#*C#)/(1-B#*D#)
SUSPL#(n)=C#+D#*SUSPR#(n)

CHL#(12)=SUSPL#(n)
CHL#(13)=SUSPR#(n)

END SUB
```

Fig. C15 Case2.bas

```
SUB CASE2
SHARED BR#(),n,thetap#,CHL#(),SUSPR#(),SUSPL#()
shared uchassis#()

DIM  suspm2#(12)
'*****************************************************************
**********
'  This  routine  contains  the  suspension  force  matrix  for
suspension
' operating condition b.
'  Suspension  flexibility  matrix is  formed  (suspm#()).The
equation   *
' is  solved to give the right hand suspension force only, using
      *
' the condition of zero relative displacement between the middle
axle   *
' and chassis. This is determined by placing a  tie bar  between
the   *
' middle axle and chassis and deriving a  flexibility matrix
        *
' which relates tie bar force  to body reactions,chassis and
tractor
' self weight and suspension forces. Setting the tie bar force
to zero
' simulates the desired condition enabling suspension force to
be determined
' for the RIGHT SUSPENSION ONLY. LEFT SUSPENSION FORCE=0
'*****************************************************************
**********
suspm2#(0)=-0.04669
suspm2#(1)=-0.046757
suspm2#(2)=-1.2827
suspm2#(3)=-1.2864
suspm2#(4)=0.0010223
suspm2#(5)=-0.042903
suspm2#(6)=-0.021143
suspm2#(7)=-0.8287e-04
suspm2#(8)=-0.0043983
suspm2#(9)=0.42915e-04
suspm2#(10)=-0.3215
suspm2#(11)=9.65717e-05
suspm2#(12)=-4.7075

'******  body  reactions,tractor  weight,  chassis  weight  and
suspension
'****** forces (not known yet) are stored in chl(14).
for x=0 to 15
 CHL#(x)=0
next x
CHL#(0)=BR#(0,n)
CHL#(1)=BR#(1,n)
CHL#(2)=BR#(2,n)
CHL#(3)=BR#(3,n)
CHL#(4)=BR#(4,n)
CHL#(5)=BR#(5,n)
CHL#(6)=BR#(6,n)
CHL#(7)=BR#(7,n)
CHL#(8)=-63666.9*cos(thetap#)
```

```
CHL#(9)=63666.9*sin(thetap#)
CHL#(10)=-47088*cos(thetap#)
CHL#(11)=47088*sin(thetap#)
' CHL#(12)-unknown yet (SUSPR)

a#=0
for x=0 to 11
 a#=a#+CHL#(x)*suspm2#(x)
next x


SUSPR#(n)=a#/-suspm2#(12)

CHL#(12)=SUSPR#(n)
a#=0
for x=0 to 12
 a#=a#+CHL#(x)*suspm2#(x)
next x


end sub
```

Fig. C16 Case3.bas

```
SUB CASE3
SHARED k11#() , k11i#() , k12#() , k21#() , k22#()
SHARED prescribe#() , k21k11i#() , k21k11ik12#()
SHARED k22k21k11ik12#() , k22k21k11ik12i#()
SHARED fab#() , fch#() , fch1#() , FCH2#()
SHARED BR#() , CHL#() , n ,thetap#,SUSPR#(),uab#()
SHARED FLAGC,FLAG3
SHARED const#
'***************************************************************
*******
'  this  routine  contains  the  suspension  force  matrix  for
suspension
' operating condition d
'***************************************************************
*******


'****************************************************
' FORCES IN FCH2 ARE DETERMINED FROM CHASSIS FORCES
' STORED IN CHL#(15)  AND UNSPRUNG AXLE FORCES.
'
'****************************************************

FCH2#(0)=BR#(0,n)
FCH2#(1)=BR#(2,n)
FCH2#(2)=BR#(4,n)
FCH2#(3)=BR#(1,n)
FCH2#(4)=BR#(3,n)
FCH2#(5)=BR#(5,n)
FCH2#(6)=BR#(6,n)
FCH2#(7)=BR#(7,n)
FCH2#(8)=-2350*9.81*cos(thetap#)
FCH2#(9)=2350*9.81*sin(thetap#)
FCH2#(10)=-800*9.81*cos(thetap#)
FCH2#(11)=800*9.81*sin(thetap#)
FCH2#(12)=-800*9.81*cos(thetap#)
FCH2#(13)=800*9.81*sin(thetap#)
FCH2#(14)=-800*9.81*cos(thetap#)
FCH2#(15)=800*9.81*sin(thetap#)
FCH2#(16)=-6490*9.81*cos(thetap#)
FCH2#(17)=6490*9.81*sin(thetap#)


IF FLAG3 =1 THEN
GOTO LABEL.MISS
END IF
FLAG3=1
a#(0)=1
a#(1)=-1
a#(2)=1
a#(3)=-1
a#(4)=1
a#(5)=-1

prescribe#(0,0)=49187
prescribe#(0,1)=-2946.7
prescribe#(0,2)=2785.0
```

```
prescribe#(0,3)=10570.0
prescribe#(0,4)=-2948.0
prescribe#(0,5)=-57919.0
prescribe#(0,6)=-1715.2
prescribe#(0,7)=-839.1
prescribe#(0,8)=4599.1
prescribe#(0,9)=-6916.7
prescribe#(0,10)=960.4
prescribe#(0,11)=2204.4
prescribe#(0,12)=1155.7
prescribe#(0,13)=1160.9
prescribe#(0,14)=929.1
prescribe#(0,15)=1743.3
prescribe#(0,16)=231.6
prescribe#(0,17)=-52.2
prescribe#(0,18)=-5088.2
prescribe#(0,19)=-617.0
prescribe#(0,20)=4362.9
prescribe#(0,21)=-738.5
prescribe#(0,22)=2244.7
prescribe#(0,23)=-593.7

prescribe#(1,0)=-2946.7
prescribe#(1,1)=1654.0
prescribe#(1,2)=-721.0
prescribe#(1,3)=62.8
prescribe#(1,4)=-212.9
prescribe#(1,5)=2574.7
prescribe#(1,6)=519.3
prescribe#(1,7)=37.0
prescribe#(1,8)=-865.1
prescribe#(1,9)=454.1
prescribe#(1,10)=-151.2
prescribe#(1,11)=-279.9
prescribe#(1,12)=-720.5
prescribe#(1,13)=-9.6
prescribe#(1,14)=-1489.3
prescribe#(1,15)=492.8
prescribe#(1,16)=-41.0
prescribe#(1,17)=18.5
prescribe#(1,18)=738.8
prescribe#(1,19)=97.3
prescribe#(1,20)=-778.5
prescribe#(1,21)=460.7
prescribe#(1,22)=-113.3
prescribe#(1,23)=952.4

prescribe#(2,0)=2785.0
prescribe#(2,1)=-721.0
prescribe#(2,2)=2744.9
prescribe#(2,3)=-2550.0
prescribe#(2,4)=836.0
prescribe#(2,5)=-221.0
prescribe#(2,6)=-6.3
prescribe#(2,7)=7.5
prescribe#(2,8)=-329.2
prescribe#(2,9)=-339.4
prescribe#(2,10)=-66.5
```

```
prescribe#(2,11)=47.6
prescribe#(2,12)=-70.9
prescribe#(2,13)=-469.4
prescribe#(2,14)=-38.8
prescribe#(2,15)=-1991.9
prescribe#(2,16)=2.3
prescribe#(2,17)=-0.1
prescribe#(2,18)=327.4
prescribe#(2,19)=42.7
prescribe#(2,20)=414.0
prescribe#(2,21)=45.4
prescribe#(2,22)=-459.1
prescribe#(2,23)=24.8

prescribe#(3,0)=10569
prescribe#(3,1)=62.9
prescribe#(3,2)=-2550.0
prescribe#(3,3)=53220.0
prescribe#(3,4)=-16054.0
prescribe#(3,5)=-61830
prescribe#(3,6)=-1891.1
prescribe#(3,7)=914.
prescribe#(3,8)=-768
prescribe#(3,9)=8538.5
prescribe#(3,10)=-113.4
prescribe#(3,11)=-3120.4
prescribe#(3,12)=81.5
prescribe#(3,13)=-1602.8
prescribe#(3,14)=155.2
prescribe#(3,15)=-2317.4
prescribe#(3,16)=275.3
prescribe#(3,17)=59.0
prescribe#(3,18)=3176.1
prescribe#(3,19)=73.7
prescribe#(3,20)=1436.1
prescribe#(3,21)=-51.5
prescribe#(3,22)=13563.0
prescribe#(3,23)=-98.5

prescribe#(4,0)=-2948.1
prescribe#(4,1)=-212.9
prescribe#(4,2)=836.0
prescribe#(4,3)=-16051
prescribe#(4,4)=0.25822e06
prescribe#(4,5)=18491
prescribe#(4,6)=950.8
prescribe#(4,7)=-273.2
prescribe#(4,8)=1271.0
prescribe#(4,9)=-3129.1
prescribe#(4,10)=-82.8
prescribe#(4,11)=1505.7
prescribe#(4,12)=-70.8
prescribe#(4,13)=617.0
prescribe#(4,14)=-31.7
prescribe#(4,15)=493.8
prescribe#(4,16)=-115.8
prescribe#(4,17)=-38.0
prescribe#(4,18)=-28689.0
```

```
prescribe#(4,19)=51.8
prescribe#(4,20)=0.13944e06
prescribe#(4,21)=45.1
prescribe#(4,22)=-0.37073e06
prescribe#(4,23)=20.2

prescribe#(5,0)=-57917.0
prescribe#(5,1)=2575.2
prescribe#(5,2)=-228.0
prescribe#(5,3)=-61829
prescribe#(5,4)=18491
prescribe#(5,5)=0.12472e06
prescribe#(5,6)=3672.5
prescribe#(5,7)=-78.0
prescribe#(5,8)=-3472.2
prescribe#(5,9)=-1554.2
prescribe#(5,10)=-786.9
prescribe#(5,11)=868.8
prescribe#(5,12)=-1194.0
prescribe#(5,13)=422.5
prescribe#(5,14)=-1057.5
prescribe#(5,15)=565.1
prescribe#(5,16)=-508.2
prescribe#(5,17)=-6.0
prescribe#(5,18)=2146.5
prescribe#(5,19)=506.2
prescribe#(5,20)=-5941.3
prescribe#(5,21)=764.0
prescribe#(5,22)=-15556.0
prescribe#(5,23)=676.6

prescribe#(6,0)=-1705.3
prescribe#(6,1)=515.9
prescribe#(6,2)=-6.3
prescribe#(6,3)=-1891.4
prescribe#(6,4)=942.9
prescribe#(6,5)=3674.3
prescribe#(6,6)=9520.0
prescribe#(6,7)=-8.7
prescribe#(6,8)=-1736.2
prescribe#(6,9)=-198.5
prescribe#(6,10)=-234.1
prescribe#(6,11)=171.7
prescribe#(6,12)=-54.2
prescribe#(6,13)=55.8
prescribe#(6,14)=3.1
prescribe#(6,15)=-20.2
prescribe#(6,16)=-5626.1
prescribe#(6,17)=-4.8
prescribe#(6,18)=-1674.5
prescribe#(6,19)=151.5
prescribe#(6,20)=2309.3
prescribe#(6,21)=36.6
prescribe#(6,22)=-1367.1
prescribe#(6,23)=-2.0

prescribe#(7,0)=-841.5
prescribe#(7,1)=37.7
```

```
prescribe#(7,2)=7.5
prescribe#(7,3)=917.9
prescribe#(7,4)=-278.9
prescribe#(7,5)=-71.1
prescribe#(7,6)=1.2
prescribe#(7,7)=2535.0
prescribe#(7,8)=-74.1
prescribe#(7,9)=-514.3
prescribe#(7,10)=-14.8
prescribe#(7,11)=49.0
prescribe#(7,12)=-18.9
prescribe#(7,13)=66.2
prescribe#(7,14)=-16.0
prescribe#(7,15)=35.9
prescribe#(7,16)=0.6
prescribe#(7,17)=-1004.8
prescribe#(7,18)=67.1
prescribe#(7,19)=9.5
prescribe#(7,20)=10.0
prescribe#(7,21)=12.1
prescribe#(7,22)=255.7
prescribe#(7,23)=10.2

prescribe#(8,0)=4598.4
prescribe#(8,1)=-865.0
prescribe#(8,2)=-329.2
prescribe#(8,3)=-768.0
prescribe#(8,4)=1271.1
prescribe#(8,5)=-3471.0
prescribe#(8,6)=-1702.9
prescribe#(8,7)=-72.4
prescribe#(8,8)=11796.0
prescribe#(8,9)=-3193.1
prescribe#(8,10)=-2623.5
prescribe#(8,11)=2286.4
prescribe#(8,12)=-1891.7
prescribe#(8,13)=957.6
prescribe#(8,14)=-990.3
prescribe#(8,15)=367.5
prescribe#(8,16)=194.7
prescribe#(8,17)=-39.2
prescribe#(8,18)=-11540
prescribe#(8,19)=1669.6
prescribe#(8,20)=4994.3
prescribe#(8,21)=1210.0
prescribe#(8,22)=-2218.1
prescribe#(8,23)=633.5

prescribe#(9,0)=-6916.9
prescribe#(9,1)=454.2
prescribe#(9,2)=-339.4
prescribe#(9,3)=8538.6
prescribe#(9,4)=-3129.1
prescribe#(9,5)=-1554.6
prescribe#(9,6)=-167.4
prescribe#(9,7)=-512.8
prescribe#(9,8)=-3192.7
prescribe#(9,9)=13055
```

```
prescribe#(9,10)=-631.7
prescribe#(9,11)=-8454.7
prescribe#(9,12)=-529.5
prescribe#(9,13)=-2947.4
prescribe#(9,14)=-319.7
prescribe#(9,15)=-770.8
prescribe#(9,16)=29.2
prescribe#(9,17)=-33.1
prescribe#(9,18)=6643.7
prescribe#(9,19)=406.3
prescribe#(9,20)=-3772.9
prescribe#(9,21)=338.6
prescribe#(9,22)=3670.0
prescribe#(9,23)=204.5

prescribe#(10,0)=960.2
prescribe#(10,1)=-151.2
prescribe#(10,2)=-66.5
prescribe#(10,3)=-113.4
prescribe#(10,4)=-82.7
prescribe#(10,5)=-786.7
prescribe#(10,6)=-236.3
prescribe#(10,7)=-14.6
prescribe#(10,8)=-2623.5
prescribe#(10,9)=-631.6
prescribe#(10,10)=8260.1
prescribe#(10,11)=439.8
prescribe#(10,12)=-375.9
prescribe#(10,13)=174.1
prescribe#(10,14)=-194.3
prescribe#(10,15)=68.8
prescribe#(10,16)=30.1
prescribe#(10,17)=-12.8
prescribe#(10,18)=1655.2
prescribe#(10,19)=-3934.8
prescribe#(10,20)=-1006.9
prescribe#(10,21)=240.5
prescribe#(10,22)=327.9
prescribe#(10,23)=124.3

prescribe#(11,0)=2204.7
prescribe#(11,1)=-280.0
prescribe#(11,2)=47.6
prescribe#(11,3)=-3120.5
prescribe#(11,4)=1505.5
prescribe#(11,5)=868.6
prescribe#(11,6)=142.9
prescribe#(11,7)=47.7
prescribe#(11,8)=2286.3
prescribe#(11,9)=-8454.7
prescribe#(11,10)=441.7
prescribe#(11,11)=9424.0
prescribe#(11,12)=362.5
prescribe#(11,13)=-145.9
prescribe#(11,14)=183.6
prescribe#(11,15)=-83.1
prescribe#(11,16)=-22.9
prescribe#(11,17)=28.3
```

```
prescribe#(11,18)=-5413.6
prescribe#(11,19)=-285.0
prescribe#(11,20)=3671.9
prescribe#(11,21)=-231.9
prescribe#(11,22)=-2245.5
prescribe#(11,23)=-117.4

prescribe#(12,0)=1155.4
prescribe#(12,1)=-720.5
prescribe#(12,2)=-70.9
prescribe#(12,3)=81.5
prescribe#(12,4)=-70.8
prescribe#(12,5)=-1193.6
prescribe#(12,6)=-53.3
prescribe#(12,7)=-18.6
prescribe#(12,8)=-1891.3
prescribe#(12,9)=-529.4
prescribe#(12,10)=-376.0
prescribe#(12,11)=362.4
prescribe#(12,12)=8378.1
prescribe#(12,13)=87.5
prescribe#(12,14)=-260.9
prescribe#(12,15)=133.6
prescribe#(12,16)=14.4
prescribe#(12,17)=-4.5
prescribe#(12,18)=1114.6
prescribe#(12,19)=241.8
prescribe#(12,20)=-741.3
prescribe#(12,21)=-4009.4
prescribe#(12,22)=251.8
prescribe#(12,23)=166.8

prescribe#(13,0)=1161.2
prescribe#(13,1)=-9.5
prescribe#(13,2)=-469.3
prescribe#(13,3)=-1602.9
prescribe#(13,4)=616.9
prescribe#(13,5)=421.7
prescribe#(13,6)=53.8
prescribe#(13,7)=65.9
prescribe#(13,8)=957.2
prescribe#(13,9)=-2947.2
prescribe#(13,10)=174.3
prescribe#(13,11)=-146.0
prescribe#(13,12)=91.7
prescribe#(13,13)=5968.0
prescribe#(13,14)=105.8
prescribe#(13,15)=-1645.0
prescribe#(13,16)=-8.9
prescribe#(13,17)=4.6
prescribe#(13,18)=-2065.7
prescribe#(13,19)=-112.1
prescribe#(13,20)=1239.7
prescribe#(13,21)=-60.0
prescribe#(13,22)=-918.7
prescribe#(13,23)=-67.6

prescribe#(14,0)=928.9
```

```
prescribe#(14,1)=-1489.3
prescribe#(14,2)=-38.8
prescribe#(14,3)=155.3
prescribe#(14,4)=-31.6
prescribe#(14,5)=-1057.3
prescribe#(14,6)=3.2
prescribe#(14,7)=-15.8
prescribe#(14,8)=-990.3
prescribe#(14,9)=-319.7
prescribe#(14,10)=-194.3
prescribe#(14,11)=183.6
prescribe#(14,12)=-260.8
prescribe#(14,13)=105.8
prescribe#(14,14)=8545.0
prescribe#(14,15)=48.4
prescribe#(14,16)=6.1
prescribe#(14,17)=-1.1
prescribe#(14,18)=565.4
prescribe#(14,19)=125.0
prescribe#(14,20)=-412.5
prescribe#(14,21)=166.8
prescribe#(14,22)=125.5
prescribe#(14,23)=-4118.9

prescribe#(15,0)=1743.3
prescribe#(15,1)=492.5
prescribe#(15,2)=-1991.9
prescribe#(15,3)=-2317.6
prescribe#(15,4)=493.7
prescribe#(15,5)=564.7
prescribe#(15,6)=-20.1
prescribe#(15,7)=35.6
prescribe#(15,8)=367.5
prescribe#(15,9)=-770.7
prescribe#(15,10)=68.8
prescribe#(15,11)=-83.1
prescribe#(15,12)=133.7
prescribe#(15,13)=-1645.0
prescribe#(15,14)=51.2
prescribe#(15,15)=5312.0
prescribe#(15,16)=-1.2
prescribe#(15,17)=1.0
prescribe#(15,18)=397.2
prescribe#(15,19)=-44.2
prescribe#(15,20)=-1471.5
prescribe#(15,21)=-85.4
prescribe#(15,22)=-352.7
prescribe#(15,23)=-33.4

prescribe#(16,0)=231.7
prescribe#(16,1)=-40.9
prescribe#(16,2)=2.3
prescribe#(16,3)=275.2
prescribe#(16,4)=-115.5
prescribe#(16,5)=-508.3
prescribe#(16,6)=-5625.6
prescribe#(16,7)=0.7
prescribe#(16,8)=194.1
```

```
prescribe#(16,9)=27.9
prescribe#(16,10)=29.9
prescribe#(16,11)=-22.0
prescribe#(16,12)=14.3
prescribe#(16,13)=-8.8
prescribe#(16,14)=6.1
prescribe#(16,15)=-1.2
prescribe#(16,16)=5910.0
prescribe#(16,17)=0.2
prescribe#(16,18)=172.1
prescribe#(16,19)=-19.3
prescribe#(16,20)=-186.4
prescribe#(16,21)=-9.2
prescribe#(16,22)=148.7
prescribe#(16,23)=-3.9

prescribe#(17,0)=-52.2
prescribe#(17,1)=18.6
prescribe#(17,2)=-0.1
prescribe#(17,3)=58.9
prescribe#(17,4)=-38.0
prescribe#(17,5)=-6.0
prescribe#(17,6)=-3.4
prescribe#(17,7)=-1004.6
prescribe#(17,8)=-39.0
prescribe#(17,9)=-32.8
prescribe#(17,10)=-12.9
prescribe#(17,11)=28.3
prescribe#(17,12)=-4.5
prescribe#(17,13)=4.6
prescribe#(17,14)=-1.1
prescribe#(17,15)=1.0
prescribe#(17,16)=-0.2
prescribe#(17,17)=1547.0
prescribe#(17,18)=128.4
prescribe#(17,19)=8.3
prescribe#(17,20)=-124.2
prescribe#(17,21)=2.9
prescribe#(17,22)=63.4
prescribe#(17,23)=0.7

prescribe#(18,0)=-5088.2
prescribe#(18,1)=738.8
prescribe#(18,2)=327.4
prescribe#(18,3)=3175.1
prescribe#(18,4)=-28689
prescribe#(18,5)=2145.0
prescribe#(18,6)=-1689.7
prescribe#(18,7)=65.5
prescribe#(18,8)=-11540
prescribe#(18,9)=6644.3
prescribe#(18,10)=1656.1
prescribe#(18,11)=-5412.1
prescribe#(18,12)=1114.1
prescribe#(18,13)=-2062.2
prescribe#(18,14)=565.4
prescribe#(18,15)=397.2
prescribe#(18,16)=171.0
```

```
prescribe#(18,17)=127.9
prescribe#(18,18)=53949
prescribe#(18,19)=-1050.8
prescribe#(18,20)=-80065
prescribe#(18,21)=-712.4
prescribe#(18,22)=65800
prescribe#(18,23)=-361.7

prescribe#(19,0)=-616.9
prescribe#(19,1)=97.2
prescribe#(19,2)=42.7
prescribe#(19,3)=73.7
prescribe#(19,4)=51.8
prescribe#(19,5)=506.0
prescribe#(19,6)=152.4
prescribe#(19,7)=9.4
prescribe#(19,8)=1669.6
prescribe#(19,9)=406.3
prescribe#(19,10)=-3934.2
prescribe#(19,11)=-283.4
prescribe#(19,12)=241.8
prescribe#(19,13)=-112.1
prescribe#(19,14)=125.0
prescribe#(19,15)=-44.3
prescribe#(19,16)=-19.4
prescribe#(19,17)=8.2
prescribe#(19,18)=-1050.8
prescribe#(19,19)=2515.0
prescribe#(19,20)=640.6
prescribe#(19,21)=-154.7
prescribe#(19,22)=-208.0
prescribe#(19,23)=-80.0

prescribe#(20,0)=4362.8
prescribe#(20,1)=-778.4
prescribe#(20,2)=414.0
prescribe#(20,3)=1437.2
prescribe#(20,4)=0.13944e06
prescribe#(20,5)=-5939.7
prescribe#(20,6)=2332.1
prescribe#(20,7)=11.2
prescribe#(20,8)=4994.2
prescribe#(20,9)=-3773.4
prescribe#(20,10)=-1007.6
prescribe#(20,11)=3669.8
prescribe#(20,12)=-740.9
prescribe#(20,13)=1239.3
prescribe#(20,14)=-412.0
prescribe#(20,15)=-1469.8
prescribe#(20,16)=-184.5
prescribe#(20,17)=-123.3
prescribe#(20,18)=-80065
prescribe#(20,19)=640.6
prescribe#(20,20)=0.18397e06
prescribe#(20,21)=473.6
prescribe#(20,22)=-0.2488e06
prescribe#(20,23)=263.9
```

```
prescribe#(21,0)=-738.5
prescribe#(21,1)=460.7
prescribe#(21,2)=45.4
prescribe#(21,3)=-51.5
prescribe#(21,4)=45.1
prescribe#(21,5)=763.9
prescribe#(21,6)=34.1
prescribe#(21,7)=11.9
prescribe#(21,8)=1210.0
prescribe#(21,9)=338.6
prescribe#(21,10)=240.5
prescribe#(21,11)=-231.8
prescribe#(21,12)=-4009.8
prescribe#(21,13)=-56.4
prescribe#(21,14)=166.8
prescribe#(21,15)=-85.5
prescribe#(21,16)=-9.2
prescribe#(21,17)=2.9
prescribe#(21,18)=-712.4
prescribe#(21,19)=-154.7
prescribe#(21,20)=473.6
prescribe#(21,21)=2564.6
prescribe#(21,22)=-160.8
prescribe#(21,23)=-106.7

prescribe#(22,0)=2244.8
prescribe#(22,1)=-113.4
prescribe#(22,2)=-459.1
prescribe#(22,3)=13560
prescribe#(22,4)=-0.37074e06
prescribe#(22,5)=-15556
prescribe#(22,6)=-1403.1
prescribe#(22,7)=249.8
prescribe#(22,8)=-2217.9
prescribe#(22,9)=3670.1
prescribe#(22,10)=328.0
prescribe#(22,11)=-2245.7
prescribe#(22,12)=251.8
prescribe#(22,13)=-918.9
prescribe#(22,14)=125.6
prescribe#(22,15)=-352.9
prescribe#(22,16)=147.7
prescribe#(22,17)=63.7
prescribe#(22,18)=65800
prescribe#(22,19)=-208.0
prescribe#(22,20)=-0.2488e06
prescribe#(22,21)=-160.8
prescribe#(22,22)=0.55698e06
prescribe#(22,23)=-80.7

prescribe#(23,0)=-593.6
prescribe#(23,1)=952.4
prescribe#(23,2)=24.8
prescribe#(23,3)=-98.5
prescribe#(23,4)=20.2
prescribe#(23,5)=676.5
prescribe#(23,6)=-2.0
prescribe#(23,7)=10.1
```

```
prescribe#(23,8)=633.5
prescribe#(23,9)=204.5
prescribe#(23,10)=124.3
prescribe#(23,11)=-117.4
prescribe#(23,12)=166.9
prescribe#(23,13)=-67.6
prescribe#(23,14)=-4118.2
prescribe#(23,15)=-31.4
prescribe#(23,16)=-3.9
prescribe#(23,17)=0.7
prescribe#(23,18)=-361.7
prescribe#(23,19)=-80.0
prescribe#(23,20)=263.9
prescribe#(23,21)=-106.7
prescribe#(23,22)=-80.7
prescribe#(23,23)=2633.9

prescribe#(24,0)=92.9
prescribe#(24,1)=-12.7
prescribe#(24,2)=-6.1
prescribe#(24,3)=-0.04
prescribe#(24,4)=-62.2
prescribe#(24,5)=-89.7
prescribe#(24,6)=-3.9
prescribe#(24,7)=-1.4
prescribe#(24,8)=-155.1
prescribe#(24,9)=-50.5
prescribe#(24,10)=-1739.6
prescribe#(24,11)=31.9
prescribe#(24,12)=-33.3
prescribe#(24,13)=12.9
prescribe#(24,14)=-17.1
prescribe#(24,15)=5.7
prescribe#(24,16)=1.0
prescribe#(24,17)=-1.9
prescribe#(24,18)=760.8
prescribe#(24,19)=439.6
prescribe#(24,20)=-410.2
prescribe#(24,21)=21.3
prescribe#(24,22)=153.3
prescribe#(24,23)=10.9


prescribe#(25,0)=77.0
prescribe#(25,1)=-52.0
prescribe#(25,2)=-4.3
prescribe#(25,3)=11.0
prescribe#(25,4)=18.9
prescribe#(25,5)=-85.0
prescribe#(25,6)=-5.9
prescribe#(25,7)=-1.1
prescribe#(25,8)=-143.4
prescribe#(25,9)=-28.9
prescribe#(25,10)=-26.9
prescribe#(25,11)=23.7
prescribe#(25,12)=-1721.8
prescribe#(25,13)=-9.6
prescribe#(25,14)=-18.9
```

```
prescribe#(25,15)=12.2
prescribe#(25,16)=1.2
prescribe#(25,17)=-0.2
prescribe#(25,18)=372.4
prescribe#(25,19)=17.3
prescribe#(25,20)=113.7
prescribe#(25,21)=428.2
prescribe#(25,22)=-40.3
prescribe#(25,23)=12.1

prescribe#(26,0)=63.4
prescribe#(26,1)=-109.0
prescribe#(26,2)=0.6
prescribe#(26,3)=16.0
prescribe#(26,4)=-81.6
prescribe#(26,5)=-77.8
prescribe#(26,6)=0.8
prescribe#(26,7)=-1.3
prescribe#(26,8)=-71.3
prescribe#(26,9)=-22.3
prescribe#(26,10)=-14.4
prescribe#(26,11)=14.3
prescribe#(26,12)=-19.3
prescribe#(26.13)=11.6
prescribe#(26,14)=-1710.1
prescribe#(26,15)=-11.3
prescribe#(26,16)=0.4
prescribe#(26,17)=-0.1
prescribe#(26,18)=3.4
prescribe#(26,19)=9.3
prescribe#(26,20)=311.0
prescribe#(26,21)=12.4
prescribe#(26,22)=202.5
prescribe#(26,23)=420.5

prescribe#(27,0)=-77.5
prescribe#(27,1)=10.2
prescribe#(27,2)=5.0
prescribe#(27,3)=-2.0
prescribe#(27,4)=62.7
prescribe#(27,5)=77.5
prescribe#(27,6)=-0.2
prescribe#(27,7)=1.2
prescribe#(27,8)=140.7
prescribe#(27,9)=40.2
prescribe#(27,10)=-303.3
prescribe#(27,11)=-24.7
prescribe#(27,12)=27.2
prescribe#(27,13)=-10.0
prescribe#(27,14)=13.9
prescribe#(27,15)=-4.6
prescribe#(27,16)=-0.5
prescribe#(27,17)=1.7
prescribe#(27,18)=-756.4
prescribe#(27,19)=-479.3
prescribe#(27,20)=405.2
prescribe#(27,21)=-17.4
prescribe#(27,22)=-152.4
```

```
prescribe#(27,23)=-8.9

prescribe#(28,0)=-64.8
prescribe#(28,1)=44.4
prescribe#(28,2)=3.6
prescribe#(28,3)=-10.2
prescribe#(28,4)=-19.7
prescribe#(28,5)=72.4
prescribe#(28,6)=5.4
prescribe#(28,7)=1.3
prescribe#(28,8)=123.3
prescribe#(28,9)=23.3
prescribe#(28,10)=22.9
prescribe#(28,11)=-19.8
prescribe#(28,12)=-317.1
prescribe#(28,13)=10.6
prescribe#(28,14)=16.2
prescribe#(28,15)=-10.8
prescribe#(28,16)=-1.1
prescribe#(28,17)=0.2
prescribe#(28,18)=-360.6
prescribe#(28,19)=-14.7
prescribe#(28,20)=-121.5
prescribe#(28,21)=-470.6
prescribe#(28,22)=43.0
prescribe#(28,23)=-10.3

prescribe#(29,0)=-53.5
prescribe#(29,1)=93.2
prescribe#(29,2)=-1.0
prescribe#(29,3)=-14.3
prescribe#(29,4)=81.2
prescribe#(29,5)=66.6
prescribe#(29,6)=-0.8
prescribe#(29,7)=1.1
prescribe#(29,8)=60.9
prescribe#(29,9)=18.9
prescribe#(29,10)=12.4
prescribe#(29,11)=-12.4
prescribe#(29,12)=16.5
prescribe#(29,13)=-10.5
prescribe#(29,14)=-327.0
prescribe#(29,15)=11.8
prescribe#(29,16)=-0.3
prescribe#(29,17)=0.1
prescribe#(29,18)=2.6
prescribe#(29,19)=-7.9
prescribe#(29,20)=-315.4
prescribe#(29,21)=-10.6
prescribe#(29,22)=-201.2
prescribe#(29,23)=-464.1

'*****************************************************
' FORCES IN FCH2 ARE DETERMINED FROM CHASSIS FORCES
' STORED IN CHL#(15)  AND UNSPRUNG AXLE FORCES.
'
'*****************************************************
```

```
'*********************************
' determine k11#(17,17) inverted and
' store in k11i#(17,17)
'*********************************
'

for x=0 to 17
 for y=0 to 17

  k11#(x,y)=prescribe#(x,y)

 next y
next x

' call invert2
for x=0 to 17
 for y=0 to 17
  k11i#(x,y)=0
 next y
next x

for x=0 to 17
 k11i#(x,x)=1
next x

for x=0 to 17

 for y=x to 17

  d#=k11#(x,y) : if d#=0 or d#=1 goto LABEL.ONE2
   for k=x to 17
    k11#(k,y)=k11#(k,y)/d#
   next k
   for k=0 to 17
    k11i#(k,y)=k11i#(k,y)/d#
   next k
LABEL.ONE2:

 next y

 if x=17 goto LABEL.TWO2

 for y=x+1 to 17

 if k11#(x,y)=0 goto LABEL.THREE2

  for k=x to 17
   k11#(k,y)=k11#(k,y)-k11#(k,x)
  next k
  for k=0 to 17
   k11i#(k,y)=k11i#(k,y)-k11i#(k,x)
next k

LABEL.THREE2:

 next y

next x
```

```
LABEL.TWO2:

for x=0 to 17

if k11#(x,x)=1 then next x
if x<>17+1 then print "*****NOT INV*******invert2": end

 for x=17 to 1 step -1

  for y=x-1 to 0 step -1

   d#=k11#(x,y)

    for k=x to 17
     k11#(k,y)=k11#(k,y)-k11#(k,x)*d#
    next k
    for k=0 to 17
     k11i#(k,y)=k11i#(k,y)-k11i#(k,x)*d#
    next k

  next y

 next x


'**********************************
' determine k21#(5,17)  and multiply
' by k11i#(17,17) and
' store in k21k11i#(5,17)
'**********************************

for x=18 to 23
 for y=0 to 17
k21#((x-18),y)=prescribe#(x,y)

 next y
next x


for x=0 to 5
 for y=0 to 17
   k21k11i#=0.0
    for z=0 to 17

    k21k11i#=k21k11i#+k21#(x,z)*k11i#(z,y)

   next z
  k21k11i#(x,y)=k21k11i#
 next y
next x

'**********************************
'determine k12(17,5) and multiply
'k21k11i#(5,17) by k12#(5,17) and
'store in k21k11ik12#(5,5).
'**********************************
'
for x=0 to 17
```

```
 for y=18 to 23

  k12#(x,(y-18))=prescribe#(x,y)

 next y
next x

for x=0 to 5
 for y=0 to 5
   k21k11ik12#=0.0
    for z=0 to 17

    k21k11ik12#=k21k11ik12#+k21k11i#(x,z)*k12#(z,y)

   next z
  k21k11ik12#(x,y)=k21k11ik12#
 next y
next x


'********************************
'determine  k22(5,5)and subtract
'k21k11ik12#(5,5) from it and
'store in k22k21k11ik12#(5,5).
'********************************

for x=18 to 23
 for y=18 to 23
  k22#((x-18),(y-18))=prescribe#(x,y)
 next y
next x

for x=0 to 5
 for y=0 to 5
  k22k21k11ik12#(x,y)=k22#(x,y)-k21k11ik12#(x,y)
 next y
next x


'  CALL INVERT3

for x=0 to 5
 for y=0 to 5
  k22k21k11ik12i#(x,y)=0
 next y
next x
for x=0 to 5
 k22k21k11ik12i#(x,x)=1
next x

for x=0 to 5

 for y=x to 5

  d#=k22k21k11ik12#(x,y) : if d#=0 or d#=1 goto LABEL.ONE3
   for k=x to 5
    k22k21k11ik12#(k,y)=k22k21k11ik12#(k,y)/d#
   next k
```

```
   for k=0 to 5
    k22k21k11ik12i#(k,y)=k22k21k11ik12i#(k,y)/d#
   next k
LABEL.ONE3:

 next y

 if x=5  goto LABEL.TWO3

 for y=x+1 to 5

 if k22k21k11ik12#(x,y)=0 goto LABEL.THREE3

  for k=x to 5
   k22k21k11ik12#(k,y)=k22k21k11ik12#(k,y)-k22k21k11ik12#(k,x)
  next k
  for k=0 to 5
   k22k21k11ik12i#(k,y)=k22k21k11ik12i#(k,y)-k22k21k11ik12i#(k,x)
next k

LABEL.THREE3:

 next y

next x

LABEL.TWO3:

for x=0 to 5

if k22k21k11ik12#(x,x)=1 then next x
if x<>5+1 then print "*****NOT INV*******invert3": end

 for x=5  to 1 step -1

  for y=x-1 to 0 step -1

   d#=k22k21k11ik12#(x,y)

    for k=x to 5

k22k21k11ik12#(k,y)=k22k21k11ik12#(k,y)-k22k21k11ik12#(k,x)*d#
    next k
    for k=0 to 5

k22k21k11ik12i#(k,y)=k22k21k11ik12i#(k,y)-k22k21k11ik12i#(k,x)*d#
    next k

  next y

 next x

'*********************************
'determine  k22k21k11ik12i#(5,5) multiplied
'by airbag force unity matrix a#(5) and
'store in fab#(5).
'*********************************
```

```
for x=0 to 5
fab#(x)=0
 for y=0 to 5
 fab#(x)=fab#(x)+k22k21k11ik12i#(x,y)*a#(y)
next y
' PRINT "Fab(";x;")=";fab#(x)
next x

'PRINT
'**********************************
'determine  k22k21k11ik12i#(5,5) multiplied
'by k21k11i#(5,5) and
'store in fch#(5,5)
'**********************************

for x=0 to 5
 for y=0 to 17
   fch3#=0.0
    for z=0 to 5

    fch3#=fch3#+k22k21k11ik12i#(x,z)*k21k11i#(z,y)

   next z
  fch1#(x,y)=fch3#
 next y
next x

LABEL.MISS:
'**********************************
'determine  fch1#(5,17) multiplied
'by chassis force unity matrix FCH2#(17) and
'store in fch#(17).
'**********************************

for x=0 to 5
fch#(x)=0
 for y=0 to 17

 fch#(x)=fch#(x)+fch1#(x,y)*FCH2#(y)

 next y
next x

IF FLAGC = 0 THEN
const1#=uab#(0,n-1)-uab#(1,n-1)+uab#(2,n-1)-uab#(3,n-1)+uab#(4
,n-1)-uab#(5,n-1)
const#=30000*(3*381+const1#)^1.57
END IF
FLAGC=1
print "constant=",const#,"**********************case3"
count1#=20000
count2#=200000
step1#=(count2#-count1#)/10
eqn#=1

do until eqn# > -0.000001 and eqn# < 0.000001

f#=count1#
```

```
uab#(0,n)=fab#(0)*f#-fch#(0)
uab#(1,n)=fab#(1)*f#-fch#(1)
uab#(2,n)=fab#(2)*f#-fch#(2)
uab#(3,n)=fab#(3)*f#-fch#(3)
uab#(4,n)=fab#(4)*f#-fch#(4)
uab#(5,n)=fab#(5)*f#-fch#(5)

eqn1#=(3*381+uab#(0,n)-uab#(1,n)+uab#(2,n)-uab#(3,n)+uab#(4,n)
-uab#(5,n))

eqn#=(f#^(1/1.57))*eqn1#-(const#)^(1/1.57)

if eqn# <-0.000001 then
 count1#=count1#+step1#
end if

if eqn# >0.000001 then
 count2# =count1#
 count1# =count1#-step1#
 step1#=(count2#-count1#)/10
 end if

 loop

f1#=const#/((3*381+uab#(0,n)-uab#(1,n)+uab#(2,n)-uab#(3,n)+uab
#(4,n)-uab#(5,n))^1.57)
SUSPR#(n)=f#
'print
'print uab#(0,n),"case3",fch#(0),f#,fab#(0)
'print uab#(1,n)
'print uab#(2,n)
'print uab#(3,n)
'print uab#(4,n)
'print uab#(5,n)
'input azt
'stop
END SUB
```

Fig. C17 Case4.bas

```
SUB CASE4
S H A R E D
BR#( ),n,thetap#,CHL#( ),SUSPR#( ),SUSPL#( ),uab#( ),uchassis#( )

DIM suspm4#(13),flex4a#(5,13)
SHARED FLAGC
SHARED const#
'*****************************************************************
**********
'This routine contains the suspension force matrix and chassis
flexibility
' matrix for suspension operating condition c.
'
' Suspension flexibility matrix is formed (suspm#()).The
equation *
' is solved to give the right hand suspension force only, using
  *
' the condition of zero relative displacement between the middle
axle *
' and chassis. This is determined by placing a tie bar between
the *
' middle axle and chassis and deriving a flexibility matrix
  *
' which relates tie bar force to body reactions,chassis and
tractor
' self weight and suspension forces. Setting the tie bar force
to zero
' simulates the desired condition enabling suspension force to
be determined
' for the left SUSPENSION
'*****************************************************************
**********

IF FLAGC = 0 THEN
const1#=uab#(0,n-1)-uab#(1,n-1)+uab#(2,n-1)-uab#(3,n-1)+uab#(4
,n-1)-uab#(5,n-1)
const#=30000*(3*381+const1#)^1.57
END IF
FLAGC=1
'PRINT "CONST=";const#
f1#=const#/((3*381+uab#(0,n-1)-uab#(1,n-1)+uab#(2,n-1)-uab#(3,
n-1)+uab#(4,n-1)-uab#(5,n-1))^1.57)
f#=f1#

suspm4#(0)=-0.046744
suspm4#(1)=-0.04670
suspm4#(2)=-1.2866
suspm4#(3)=-1.2832
suspm4#(4)=-0.0011292
suspm4#(5)=-0.042928
suspm4#(6)=-0.021167
suspm4#(7)=-0.5722e-04
suspm4#(8)=-0.0044022
suspm4#(9)=-0.17166e-04
suspm4#(10)=-0.3231
suspm4#(11)=-1.0596e-04
suspm4#(13)=-4.7075
suspm4#(12)=-4.6992
```

```
'****** body reactions,tractor weight, chassis weight and
suspension
'****** forces (not known yet) are stored in chl(14).

for x=0 to 15
 CHL#(x)=0
next x

f2#=1
do until f2# < 1 and f2# > -1

CHL#(0)=BR#(0,n)
CHL#(1)=BR#(1,n)
CHL#(2)=BR#(2,n)
CHL#(3)=BR#(3,n)
CHL#(4)=BR#(4,n)
CHL#(5)=BR#(5,n)
CHL#(6)=BR#(6,n)
CHL#(7)=BR#(7,n)
CHL#(8)=-63666.9*cos(thetap#)
CHL#(9)=63666.9*sin(thetap#)
CHL#(10)=-46597.5*cos(thetap#)
CHL#(11)=46597.5*sin(thetap#)
CHL#(12)=f#
' CHL#(13)-unknown yet (SUSPL)

a#=0
for x=0 to 12
 a#=a#+CHL#(x)*suspm4#(x)
next x

SUSPL#(n)=a#/-suspm4#(13)

CHL#(13)=SUSPL#(n)

flex4a#(0,0)=0.02146
flex4a#(0,1)=0.00823
flex4a#(0,2)=0.45320
flex4a#(0,3)=0.91450
flex4a#(0,4)=-0.1873
flex4a#(0,5)=0.01804
flex4a#(0,6)=0.05501
flex4a#(0,7)=-0.01135
flex4a#(0,8)=0.03941
flex4a#(0,9)=-0.00941
flex4a#(0,10)=0.27982
flex4a#(0,11)=-0.02487
flex4a#(0,13)=1.7487
flex4a#(0,12)=2.5165

flex4a#(1,0)=0.084921
flex4a#(1,1)=-0.00626
flex4a#(1,2)=-0.2320
flex4a#(1,3)=-0.23140
flex4a#(1,4)=-0.04533
flex4a#(1,5)=-0.00266
flex4a#(1,6)=-0.05354
flex4a#(1,7)=-0.00316
```

```
flex4a#(1,8)=-0.04315
flex4a#(1,9)=-0.00597
flex4a#(1,10)=-0.01099
flex4a#(1,11)=-0.01120
flex4a#(1,13)=-1.8879
flex4a#(1,12)=-2.3635

flex4a#(2,0)=0.03724
flex4a#(2,1)=0.04131
flex4a#(2,2)=0.62180
flex4a#(2,3)=1.32040
flex4a#(2,4)=-0.2182
flex4a#(2,5)=0.03396
flex4a#(2,6)=0.00032
flex4a#(2,7)=-0.01333
flex4a#(2,8)=-0.00987
flex4a#(2,9)=-0.00675
flex4a#(2,10)=0.30916
flex4a#(2,11)=-0.02576
flex4a#(2,13)=2.13540
flex4a#(2,12)=3.19510

flex4a#(3,0)=0.02481
flex4a#(3,1)=0.01596
flex4a#(3,2)=0.4270
flex4a#(3,3)=0.4961
flex4a#(3,4)=-0.05050
flex4a#(3,5)=0.01699
flex4a#(3,6)=-0.008
flex4a#(3,7)=-0.00289
flex4a#(3,8)=-0.01161
flex4a#(3,9)=-0.00337
flex4a#(3,10)=0.1822
flex4a#(3,11)=-0.01077
flex4a#(3,13)=0.8695
flex4a#(3,12)=0.4434

flex4a#(4,0)=0.05506
flex4a#(4,1)=0.08421
flex4a#(4,2)=0.8047
flex4a#(4,3)=1.7908
flex4a#(4,4)=-0.2501
flex4a#(4,5)=0.05111
flex4a#(4,6)=-0.05432
flex4a#(4,7)=-0.0158
flex4a#(4,8)=-0.05903
flex4a#(4,9)=-0.004908
flex4a#(4,10)=0.33796
flex4a#(4,11)=-0.02616
flex4a#(4,13)=2.5326
flex4a#(4,12)=3.9072

flex4a#(5,0)=-0.02343
flex4a#(5,1)=-0.02233
flex4a#(5,2)=-0.5692
flex4a#(5,3)=-0.3987
flex4a#(5,4)=-0.0579
flex4a#(5,5)=-0.01829
```

```
flex4a#(5,6)=0.01101
flex4a#(5,7)=-0.00289
flex4a#(5,8)=-0.014302
flex4a#(5,9)=-0.01369
flex4a#(5,10)=-0.02866
flex4a#(5,11)=-0.01002
flex4a#(5,13)=-2.3064
flex4a#(5,12)=-2.6568


for x=0 to 5
uab#(x,n)=0
 for y=0 to 13
  uab#(x,n)=uab#(x,n)+flex4a#(x,y)*CHL#(y)/1000.0
 next y
'print uab#(x,n)
next x

f#=const#/((3*381+uab#(0,n)-uab#(1,n)+uab#(2,n)-uab#(3,n)+uab#
(4,n)-uab#(5,n))^1.57)
SUSPR#(n)=f#
f2#=f#-f1#
f1#=f#
loop

end sub
```

Fig. C18 Flexi.bas

```
SUB FLEXI
SHARED FLCHECK( ),uchassis#( ),n

'*************************************************************
***&***
'  This routine calls the appropriate chassis flexibility matrix
'  for the current suspension operating condition
'*************************************************************
*******

IF FLCHECK(n)=1 THEN
 CALL FLEXI1
'PRINT "CALLING CASE1"
ELSEIF FLCHECK(n)=2 THEN
 CALL FLEXI2
'PRINT "CALLING CASE2"
ELSEIF FLCHECK(n)=3 THEN
'PRINT "CALLING CASE3"
 CALL FLEXI3
ELSEIF FLCHECK(n)=4 THEN
 CALL FLEXI4
'PRINT "CALLING CASE4"
END IF

end sub
```

Fig. C19 Flexi1.bas

```
SUB FLEXI1
SHARED BR#(),n,thetap#,CHL#(),SUSPR#(),SUSPL#()
SHARED uchassis#(),uab#()
DIM  flex1#(8,13),flex1a#(5,13)
'*************************************************************
**********
'This routine contains the chassis flexibility matrix for
determining
'displacements for suspension operating condition a.
'*************************************************************
**********


CHL#(0)=BR#(0,n)
CHL#(1)=BR#(1,n)
CHL#(2)=BR#(2,n)
CHL#(3)=BR#(3,n)
CHL#(4)=BR#(4,n)
CHL#(5)=BR#(5,n)
CHL#(6)=BR#(6,n)
CHL#(7)=BR#(7,n)
CHL#(8)=-63666.9*cos(thetap#)
CHL#(9)=63666.9*sin(thetap#)
CHL#(10)=-47088*cos(thetap#)
CHL#(11)=47088*sin(thetap#)
CHL#(12)=SUSPL#(n)
CHL#(13)=SUSPR#(n)

flex1#(0,0)=0.15622
flex1#(0,1)=0.091892
flex1#(0,2)=0.0839
flex1#(0,3)=0.0505
flex1#(0,4)=-0.1082
flex1#(0,5)=0.11628
flex1#(0,6)=-0.013469
flex1#(0,7)=0.040835
flex1#(0,8)=-0.012217
flex1#(0,9)=0.028565
flex1#(0,10)=0.002803
flex1#(0,11)=-0.004309
flex1#(0,12)=0.0926
flex1#(0,13)=0.0693

flex1#(1,0)=0.083911
flex1#(1,1)=0.050547
flex1#(1,2)=1.3528
flex1#(1,3)=0.7072
flex1#(1,4)=0.1345
flex1#(1,5)=0.044217
flex1#(1,6)=-0.079945
flex1#(1,7)=0.008794
flex1#(1,8)=-0.077668
flex1#(1,9)=0.001147
flex1#(1,10)=0.25059
flex1#(1,11)=0.01449
flex1#(1,12)=2.2495
flex1#(1,13)=1.7450
```

```
flex1#(2,0)=-0.10824
flex1#(2,1)=0.10823
flex1#(2,2)=0.1345
flex1#(2,3)=-0.1345
flex1#(2,4)=1.2801
flex1#(2,5)=0
flex1#(2,6)=0
flex1#(2,7)=-0.083615
flex1#(2,8)=0
flex1#(2,9)=-0.063022
flex1#(2,10)=0
flex1#(2,11)=0.361328
flex1#(2,12)=0.1051
flex1#(2,13)=-0.1051

flex1#(3,0)=0.091889
flex1#(3,1)=0.15622
flex1#(3,2)=0.0505
flex1#(3,3)=0.0839
flex1#(3,4)=0.1082
flex1#(3,5)=0.11628
flex1#(3,6)=-0.013469
flex1#(3,7)=-0.040825
flex1#(3,8)=-0.012217
flex1#(3,9)=-0.028555
flex1#(3,10)=0
flex1#(3,11)=0.004309
flex1#(3,12)=0.0693
flex1#(3,13)=0.0926

flex1#(4,0)=0.05054
flex1#(4,1)=0.083924
flex1#(4,2)=0.7072
flex1#(4,3)=1.3528
flex1#(4,4)=-0.1345
flex1#(4,5)=0.044217
flex1#(4,6)=-0.079947
flex1#(4,7)=-0.008803
flex1#(4,8)=-0.077671
flex1#(4,9)=-0.001155
flex1#(4,10)=0.25059
flex1#(4,11)=-0.01448
flex1#(4,12)=1.7450
flex1#(4,13)=2.2495

flex1#(5,0)=-0.10824
flex1#(5,1)=0.10823
flex1#(5,2)=0.1345
flex1#(5,3)=-0.1345
flex1#(5,4)=1.2785
flex1#(5,5)=0
flex1#(5,6)=0
flex1#(5,7)=-0.083615
flex1#(5,8)=0
flex1#(5,9)=-0.063022
flex1#(5,10)=0
flex1#(5,11)=0.3613498
flex1#(5,12)=0.1051
```

```
flex1#(5,13)=-0.1050

flex1#(6,0)=0.11628
flex1#(6,1)=0.11628
flex1#(6,2)=0.0442
flex1#(6,3)=0.0442
flex1#(6,4)=0
flex1#(6,5)=0.11845
flex1#(6,6)=-0.012583
flex1#(6,7)=0.014970
flex1#(6,8)=-0.01119
flex1#(6,9)=0
flex1#(6,10)=0.0042985
flex1#(6,11)=0
flex1#(6,12)=0.0667
flex1#(6,13)=0.0667

flex1#(7,0)=-0.01347
flex1#(7,1)=-0.01347
flex1#(7,2)=-0.0800
flex1#(7,3)=-0.0800
flex1#(7,4)=0
flex1#(7,5)=-0.012583
flex1#(7,6)=0.28262
flex1#(7,7)=0.000408
flex1#(7,8)=0.26394
flex1#(7,9)=0
flex1#(7,10)=0.05793
flex1#(7,11)=0
flex1#(7,12)=0.0316
flex1#(7,13)=0.0316

flex1#(8,0)=0.040836
flex1#(8,1)=-0.040836
flex1#(8,2)=0.0088
flex1#(8,3)=-0.0088
flex1#(8,4)=-0.0836
flex1#(8,5)=0
flex1#(8,6)=0
flex1#(8,7)=0.32029
flex1#(8,8)=0
flex1#(8,9)=0.40854
flex1#(8,10)=0
flex1#(8,11)=0.121884
flex1#(8,12)=0.0069
flex1#(8,13)=-0.0070

for x=0 to 8
 uchassis#(x,n)=0
 for y=0 to 13

 uchassis#(x,n)=uchassis#(x,n)+flex1#(x,y)*CHL#(y)/1000.0

 next y

next x
```

```
flexla#(0,0)=0.01475
flexla#(0,1)=-0.00232
flexla#(0,2)=0.35340
flexla#(0,3)=0.53990
flexla#(0,4)=-0.10940
flexla#(0,5)=0.01012
flexla#(0,6)=0.05110
flexla#(0,7)=-0.00654
flexla#(0,8)=0.03859
flexla#(0,9)=-0.00749
flexla#(0,10)=0.22016
flexla#(0,11)=-0.01764
flexla#(0,12)=1.1810
flexla#(0,13)=1.3474

flexla#(1,0)=0.01032
flexla#(1,1)=-0.00408
flexla#(1,2)=-0.21130
flexla#(1,3)=-0.15390
flexla#(1,4)=-0.06140
flexla#(1,5)=-0.00102
flexla#(1,6)=-0.05277
flexla#(1,7)=-0.00415
flexla#(1,8)=-0.04298
flexla#(1,9)=-0.00636
flexla#(1,10)=1.3456e-03
flexla#(1,11)=-0.01269
flexla#(1,12)=-1.7704
flexla#(1,13)=-2.1217

flexla#(2,0)=0.02867
flexla#(2,1)=0.02783
flexla#(2,2)=0.49410
flexla#(2,3)=0.84130
flexla#(2,4)=-0.11860
flexla#(2,5)=0.02383
flexla#(2,6)=-0.00468
flexla#(2,7)=-0.00717
flexla#(2,8)=-0.01091
flexla#(2,9)=-0.00429
flexla#(2,10)=0.23287
flexla#(2,11)=-0.01651
flexla#(2,12)=1.4093
flexla#(2,13)=1.6999

flexla#(3,0)=0.03043
flexla#(3,1)=0.02480
flexla#(3,2)=0.51080
flexla#(3,3)=0.81040
flexla#(3,4)=-0.11580
flexla#(3,5)=0.02364
flexla#(3,6)=-0.00472
flexla#(3,7)=-0.00694
flexla#(3,8)=-0.01093
flexla#(3,9)=-0.00499
flexla#(3,10)=0.23224
flexla#(3,11)=-0.01684
flexla#(3,12)=1.3457
```

```
flexla#(3,13)=1.4240

flexla#(4,0)=0.04472
flexla#(4,1)=0.06794
flexla#(4,2)=0.6508
flexla#(4,3)=1.2129
flexla#(4,4)=-0.13010
flexla#(4,5)=0.03888
flexla#(4,6)=-0.06035
flexla#(4,7)=-0.00837
flexla#(4,8)=-0.06029
flexla#(4,9)=-0.00194
flexla#(4,10)=0.24591
flexla#(4,11)=-0.01501
flexla#(4,12)=1.6568
flexla#(4,13)=2.1038

flexla#(5,0)=-0.02188
flexla#(5,1)=-0.01988
flexla#(5,2)=-0.54610
flexla#(5,3)=-0.31180
flexla#(5,4)=-0.07600
flexla#(5,5)=-0.01645
flexla#(5,6)=0.01192
flexla#(5,7)=-0.00401
flexla#(5,8)=0.01449
flexla#(5,9)=-0.00182
flexla#(5,10)=-0.01482
flexla#(5,11)=-0.01171
flexla#(5,12)=-2.1747
flexla#(5,13)=-2.3856


for x=0 to 5
 uab#(x,n)=0
 for y=0 to 13
  uab#(x,n)=uab#(x,n)+flexla#(x,y)*CHL#(y)/1000.0
 next y
next x

end sub
```

Fig. C20 Flexi2.bas

```
SUB FLEXI2
SHARED BR#(),n,thetap#,CHL#(),SUSPR#(),SUSPL#(),uab#()
shared uchassis#()
DIM flex2#(8,12),flex2a#(5,12)
'*************************************************************
**********
' This routine contains the chassis flexibility matrix for
determining
' displacements for suspension operating condition b.
'*************************************************************
**********
CHL#(0)=BR#(0,n)
CHL#(1)=BR#(1,n)
CHL#(2)=BR#(2,n)
CHL#(3)=BR#(3,n)
CHL#(4)=BR#(4,n)
CHL#(5)=BR#(5,n)
CHL#(6)=BR#(6,n)
CHL#(7)=BR#(7,n)
CHL#(8)=-63666.9*cos(thetap#)
CHL#(9)=63666.9*sin(thetap#)
CHL#(10)=-47088*cos(thetap#)
CHL#(11)=47088*sin(thetap#)
CHL#(12)=SUSPR#(n)

flex2#(0,0)=0.15671
flex2#(0,1)=0.092201
flex2#(0,2)=0.1011
flex2#(0,3)=0.0551
flex2#(0,4)=-0.1046
flex2#(0,5)=0.11664
flex2#(0,6)=-0.01329
flex2#(0,7)=0.041056
flex2#(0,8)=-0.01218
flex2#(0,9)=0.028653
flex2#(0,10)=0.00555
flex2#(0,11)=-0.00398
flex2#(0,12)=0.0954

flex2#(1,0)=0.10114
flex2#(1,1)=0.061504
flex2#(1,2)=1.9650
flex2#(1,3)=0.8703
flex2#(1,4)=0.2617
flex2#(1,5)=0.057164
flex2#(1,6)=-0.073557
flex2#(1,7)=0.01666
flex2#(1,8)=-0.076338
flex2#(1,9)=0.004285
flex2#(1,10)=0.34809
flex2#(1,11)=0.02631
flex2#(1,12)=2.6727

flex2#(2,0)=-0.10466
flex2#(2,1)=0.11050
flex2#(2,2)=0.2617
flex2#(2,3)=-0.1006
flex2#(2,4)=1.3065
```

```
flex2#(2,5)=0.002684
flex2#(2,6)=0.001328
flex2#(2,7)=-0.081978
flex2#(2,8)=0.000278
flex2#(2,9)=-0.062368
flex2#(2,10)=0.02025
flex2#(2,11)=0.3638
flex2#(2,12)=0.0877

flex2#(3,0)=0.092198
flex2#(3,1)=0.15642
flex2#(3,2)=0.0615
flex2#(3,3)=0.0868
flex2#(3,4)=0.1105
flex2#(3,5)=0.11651
flex2#(3,6)=-0.013355
flex2#(3,7)=-0.040683
flex2#(3,8)=-0.012193
flex2#(3,9)=-0.028498
flex2#(3,10)=0.00455
flex2#(3,11)=0.00452
flex2#(3,12)=0.1092

flex2#(4,0)=0.055131
flex2#(4,1)=0.086843
flex2#(4,2)=0.8703
flex2#(4,3)=1.3963
flex2#(4,4)=-0.1006
flex2#(4,5)=0.047666
flex2#(4,6)=-0.078245
flex2#(4,7)=-0.006707
flex2#(4,8)=-0.077317
flex2#(4,9)=-0.000319
flex2#(4,10)=0.27656
flex2#(4,11)=-0.011333
flex2#(4,12)=2.4966

flex2#(5,0)=-0.10466
flex2#(5,1)=0.11050
flex2#(5,2)=0.2617
flex2#(5,3)=-0.1006
flex2#(5,4)=1.3049
flex2#(5,5)=0.002684
flex2#(5,6)=0.001328
flex2#(5,7)=-0.081978
flex2#(5,8)=0.000278
flex2#(5,9)=-0.062368
flex2#(5,10)=0.02026
flex2#(5,11)=0.363796
flex2#(5,12)=0.0877

flex2#(6,0)=0.11665
flex2#(6,1)=0.11651
flex2#(6,2)=0.0572
flex2#(6,3)=0.0477
flex2#(6,4)=0.0027
flex2#(6,5)=0.11872
flex2#(6,6)=-0.012448
```

```
flex2#(6,7)=0.000168
flex2#(6,8)=-0.011162
flex2#(6,9)=0.000068
flex2#(6,10)=0.00636
flex2#(6,11)=2.51086e-05
flex2#(6,12)=0.0863

flex2#(7,0)=-0.01329
flex2#(7,1)=-0.013356
flex2#(7,2)=-0.0736
flex2#(7,3)=-0.0783
flex2#(7,4)=0.0013
flex2#(7,5)=-0.012448
flex2#(7,6)=0.28269
flex2#(7,7)=0.000083
flex2#(7,8)=0.26395
flex2#(7,9)=0.000033
flex2#(7,10)=0.05894
flex2#(7,11)=1.22324e-04
flex2#(7,12)=0.0413

flex2#(8,0)=0.041058
flex2#(8,1)=-0.040695
flex2#(8,2)=0.0167
flex2#(8,3)=-0.0067
flex2#(8,4)=-0.0820
flex2#(8,5)=0.000167
flex2#(8,6)=0.000081
flex2#(8,7)=0.62117
flex2#(8,8)=0.000015
flex2#(8,9)=0.40858
flex2#(8,10)=0.001253
flex2#(8,11)=0.122037
flex2#(8,12)=0.0050

for x=0 to 8
  uchassis#(x,n)=0
next x

for x=0 to 8
 for y=0 to 12
  uchassis#(x,n)=uchassis#(x,n)+flex2#(x,y)*CHL#(y)/1000.0
 next y
next x


' flexibility matrix for right suspension disps.

flex2a#(0,0)=0.018728
flex2a#(0,1)=0.000204
flex2a#(0,2)=0.4946
flex2a#(0,3)=0.5775
flex2a#(0,4)=-0.0801
flex2a#(0,5)=0.013101
flex2a#(0,6)=0.052578
flex2a#(0,7)=-0.004723
flex2a#(0,8)=0.0389
flex2a#(0,9)=-0.006763
```

```
flex2a#(0,10)=0.2426
flex2a#(0,11)=-0.01492
flex2a#(0,12)=1.5613

flex2a#(1,0)=0.00537
flex2a#(1,1)=-0.007224
flex2a#(1,2)=-0.3871
flex2a#(1,3)=-0.2008
flex2a#(1,4)=-0.0979
flex2a#(1,5)=-0.004738
flex2a#(1,6)=-0.054578
flex2a#(1,7)=-0.00641
flex2a#(1,8)=-0.043866
flex2a#(1,9)=-0.007265
flex2a#(1,10)=-0.02664
flex2a#(1,11)=-0.01608
flex2a#(1,12)=-2.3880

flex2a#(2,0)=0.032808
flex2a#(2,1)=0.030458
flex2a#(2,2)=0.6413
flex2a#(2,3)=0.8805
flex2a#(2,4)=-0.0881
flex2a#(2,5)=0.026942
flex2a#(2,6)=-0.003141
flex2a#(2,7)=-0.005281
flex2a#(2,8)=-0.01059
flex2a#(2,9)=-0.003536
flex2a#(2,10)=0.2563
flex2a#(2,11)=-0.01367
flex2a#(2,12)=1.9229

flex2a#(3,0)=0.030137
flex2a#(3,1)=0.024613
flex2a#(3,2)=0.5002
flex2a#(3,3)=0.8076
flex2a#(3,4)=-0.1180
flex2a#(3,5)=0.023416
flex2a#(3,6)=-0.00483
flex2a#(3,7)=-0.007074
flex2a#(3,8)=-0.01095
flex2a#(3,9)=-0.005042
flex2a#(3,10)=0.2306
flex2a#(3,11)=-0.01704
flex2a#(3,12)=1.4081

flex2a#(4,0)=0.049183
flex2a#(4,1)=0.070781
flex2a#(4,2)=0.8093
flex2a#(4,3)=1.2552
flex2a#(4,4)=-0.0971
flex2a#(4,5)=0.042237
flex2a#(4,6)=-0.058694
flex2a#(4,7)=-0.006332
flex2a#(4,8)=-0.059944
flex2a#(4,9)=-0.001126
flex2a#(4,10)=0.2712
flex2a#(4,11)=-0.01195
```

```
flex2a#(4,12)=2.3441

flex2a#(5,0)=-0.030173
flex2a#(5,1)=-0.025156
flex2a#(5,2)=-0.8407
flex2a#(5,3)=-0.3903
flex2a#(5,4)=-0.1372
flex2a#(5,5)=-0.022681
flex2a#(5,6)=0.008841
flex2a#(5,7)=-0.007793
flex2a#(5,8)=0.01385
flex2a#(5,9)=-0.003325
flex2a#(5,10)=-0.06174
flex2a#(5,11)=-0.01739
flex2a#(5,12)=-2.8321


for x=0 to 5
  uab#(x,n)=0
 for y=0 to 12
  uab#(x,n)=uab#(x,n)+flex2a#(x,y)*CHL#(y)/1000.0
 next y
next x

end sub
```

Fig. C21 Flexi3.bas

```
SUB FLEXI3
S                H                A                R                E                D
FCH2#(),SUSPR#(),k11i#(),k12#(),n,uchassis#(),uab#(),uch#()
DIM k12uabfch2#(17),k12uab#(17)

'*************************************************************
*******
'  This  routine  calculates  the  chassis  displacements  for
suspension
' operating condition d
'*************************************************************
*******


'*************************************************************
**********
' Suspension STIFFNESS matrix is formed PRESCRIBE#().The FIRST
FIVE
' ROWS ARE MULTIPLIED BY FCH2#() ,WHICH IS WHERE ALL THE APPLIED
LOADS ARE
' STORED , TO GIVE LEFT AND RIGHT HINGE DisplacementS
      *
'*************************************************************
**********

FCH2#(18)=SUSPR#(n)
FCH2#(19)=SUSPR#(n)
FCH2#(20)=SUSPR#(n)
FCH2#(21)=SUSPR#(n)
FCH2#(22)=SUSPR#(n)
FCH2#(23)=SUSPR#(n)


for x=0 to 17
   k12uab#=0.0
  for y=0 to 5
    k12uab#=k12uab#+k12#(x,y)*uab#(y,n)
  next y
  k12uab#(x)=k12uab#
next x

for x=0 to 17
 k12uabfch2#(x)=FCH2#(x)-k12uab#(x)
next x

for x=0 to 17
   uch#=0.0
  for y=0 to 17
    uch#=uch#+k11i#(x,y)*k12uabfch2#(y)
  next y
 uch#(x,n)=uch#
next x

uchassis#(0,n)=uch#(0,n)
uchassis#(1,n)=uch#(1,n)
uchassis#(2,n)=uch#(2,n)
uchassis#(3,n)=uch#(3,n)
uchassis#(4,n)=uch#(4,n)
```

```
'assuming uchassis#(5,n)=uchassis#(2,n)
uchassis#(5,n)=uch#(2,n)
uchassis#(6,n)=uch#(5,n)
uchassis#(7,n)=uch#(6,n)
uchassis#(8,n)=uch#(7,n)


uch#(18,n)=uab#(0,n)
uch#(19,n)=uab#(1,n)
uch#(20,n)=uab#(2,n)
uch#(21,n)=uab#(3,n)
uch#(22,n)=uab#(4,n)
uch#(23,n)=uab#(5,n)

end sub
```

Fig. C22 Flexi4.bas

```
SUB FLEXI4
SHARED BR#(),n,thetap#,CHL#(),SUSPR#(),SUSPL#(),uchassis#()
DIM flex4#(8,13)
'***************************************************************
**********
'This routine contains the chassis flexibility matrix for
determining
' displacements for suspension operating condition c
'***************************************************************
**********


CHL#(0)=BR#(0,n)
CHL#(1)=BR#(1,n)
CHL#(2)=BR#(2,n)
CHL#(3)=BR#(3,n)
CHL#(4)=BR#(4,n)
CHL#(5)=BR#(5,n)
CHL#(6)=BR#(6,n)
CHL#(7)=BR#(7,n)
CHL#(8)=-63666.9*cos(thetap#)
CHL#(9)=63666.9*sin(thetap#)
CHL#(10)=-47088*cos(thetap#)
CHL#(11)=47088*sin(thetap#)
CHL#(12)=SUSPL#(n)
CHL#(13)=SUSPR#(n)

flex4#(0,0)=0.15642
flex4#(0,1)=0.092201
flex4#(0,2)=0.0868
flex4#(0,3)=0.0615
flex4#(0,4)=-0.1105
flex4#(0,5)=0.11651
flex4#(0,6)=-0.013355
flex4#(0,7)=0.040693
flex4#(0,8)=-0.012194
flex4#(0,9)=0.028507
flex4#(0,10)=0.004545
flex4#(0,11)=-0.0045217
flex4#(0,12)=0.1092
flex4#(0,13)=0.1035

flex4#(1,0)=0.086829
flex4#(1,1)=0.055139
flex4#(1,2)=1.3963
flex4#(1,3)=0.8703
flex4#(1,4)=0.1007
flex4#(1,5)=0.047666
flex4#(1,6)=-0.078242
flex4#(1,7)=0.006697
flex4#(1,8)=-0.077314
flex4#(1,9)=0.000309
flex4#(1,10)=0.27656
flex4#(1,11)=0.011344
flex4#(1,12)=2.4966
flex4#(1,13)=2.2539

flex4#(2,0)=-0.11051
```

```
flex4#(2,1)=0.10465
flex4#(2,2)=0.1007
flex4#(2,3)=-0.2617
flex4#(2,4)=1.3065
flex4#(2,5)=-0.002694
flex4#(2,6)=-0.001324
flex4#(2,7)=-0.081975
flex4#(2,8)=-0.000274
flex4#(2,9)=-0.062363
flex4#(2,10)=-0.02025
flex4#(2,11)=0.363796
flex4#(2,12)=-0.0876
flex4#(2,13)=-0.5017

flex4#(3,0)=0.092198
flex4#(3,1)=0.15671
flex4#(3,2)=0.0551
flex4#(3,3)=0.1012
flex4#(3,4)=0.1046
flex4#(3,5)=0.11664
flex4#(3,6)=-0.013289
flex4#(3,7)=-0.041046
flex4#(3,8)=-0.012179
flex4#(3,9)=-0.028642
flex4#(3,10)=0.005475
flex4#(3,11)=0.0039788
flex4#(3,12)=0.0954
flex4#(3,13)=0.1464

flex4#(4,0)=0.061492
flex4#(4,1)=0.10116
flex4#(4,2)=0.8703
flex4#(4,3)=1.9650
flex4#(4,4)=-0.2616
flex4#(4,5)=0.057163
flex4#(4,6)=-0.073561
flex4#(4,7)=-0.016678
flex4#(4,8)=-0.076342
flex4#(4,9)=-0.0043
flex4#(4,10)=0.34807
flex4#(4,11)=-0.026295
flex4#(4,12)=2.6727
flex4#(4,13)=4.1598

flex4#(5,0)=-0.11051
flex4#(5,1)=0.10465
flex4#(5,2)=0.1007
flex4#(5,3)=-0.2617
flex4#(5,4)=1.3049
flex4#(5,5)=-0.002694
flex4#(5,6)=-0.001324
flex4#(5,7)=-0.081975
flex4#(5,8)=-0.000274
flex4#(5,9)=-0.062363
flex4#(5,10)=-0.02024
flex4#(5,11)=0.363796
flex4#(5,12)=-0.0876
flex4#(5,13)=-0.5018
```

```
flex4#(6,0)=0.11651
flex4#(6,1)=0.11665
flex4#(6,2)=0.0477
flex4#(6,3)=0.0572
flex4#(6,4)=-0.0027
flex4#(6,5)=0.11872
flex4#(6,6)=-0.012448
flex4#(6,7)=-0.000165
flex4#(6,8)=-0.011162
flex4#(6,9)=-0.000065
flex4#(6,10)=0.0063609
flex4#(6,11)=-0.0002489
flex4#(6,12)=0.0863
flex4#(6,13)=0.1071

flex4#(7,0)=-0.013355
flex4#(7,1)=-0.013291
flex4#(7,2)=-0.0783
flex4#(7,3)=-0.0736
flex4#(7,4)=-0.0013
flex4#(7,5)=-0.012448
flex4#(7,6)=0.28268
flex4#(7,7)=-0.000082
flex4#(7,8)=0.26395
flex4#(7,9)=-0.000033
flex4#(7,10)=0.058947
flex4#(7,11)=-0.0001245
flex4#(7,12)=0.0413
flex4#(7,13)=0.0515

flex4#(8,0)=0.040696
flex4#(8,1)=-0.041058
flex4#(8,2)=0.0067
flex4#(8,3)=-0.0167
flex4#(8,4)=-0.0820
flex4#(8,5)=-0.000166
flex4#(8,6)=-0.000083
flex4#(8,7)=0.62117
flex4#(8,8)=-0.000019
flex4#(8,9)=0.40858
flex4#(8,10)=-0.001255
flex4#(8,11)=0.12204
flex4#(8,12)=-0.0050
flex4#(8,13)=-0.0315

for x=0 to 8
uchassis#(x,n)=0.0
 for y=0 to 13

uchassis#(x,n)=uchassis#(x,n)+flex4#(x,y)*CHL#(y)/1000.0
 next y
next x

end sub
```

Fig. C23 Disp.bas

```
SUB DISP
shared lhc#(),rhc#(),rb#(),uchassis#(),n
'*****************************************************************
*****************
'
'
'      Hinge and ram co-ordinates are updated using chassis
displacements
' taking into consideration the origin movement. Firstly the
origin
' movement is determined from averaging the displacements of the
' two hinges in each of the co-ordinate directions.
'      Then the displacements at the hinges and ram base are
modified to
'  give zero origin movement by subtracting the origin
displacements
' previously determined from their actual displacements.
'
'
'*****************************************************************
*****************

' determine origin movement.

xorigin=(uchassis#(0,n)+uchassis#(3,n))/2
yorigin=(uchassis#(1,n)+uchassis#(4,n))/2
zorigin=(uchassis#(2,n)+uchassis#(5,n))/2
' print xorigin,yorigin,zorigin
' determine modified chassis displacements

lhc#(0,n+1)=lhc#(0,0)+uchassis#(0,n)-xorigin
lhc#(1,n+1)=lhc#(1,0)+uchassis#(1,n)-yorigin
lhc#(2,n+1)=lhc#(2,0)+uchassis#(2,n)-zorigin
rhc#(0,n+1)=rhc#(0,0)+uchassis#(3,n)-xorigin
rhc#(1,n+1)=rhc#(1,0)+uchassis#(4,n)-yorigin
rhc#(2,n+1)=rhc#(2,0)+uchassis#(5,n)-zorigin
rb#(0,n+1)=rb#(0,0)+uchassis#(6,n)-xorigin
rb#(1,n+1)=rb#(1,0)+uchassis#(7,n)-yorigin
rb#(2,n+1)=rb#(2,0)+uchassis#(8,n)-zorigin

end sub
```

Fig. C24 Tyre.bas

```
SUB TYRE
SHARED FLCHECK( ),TYREF#( ),n,tyre$

'**************************************************************
*******
' This routine calls the appropriate tyre force matrix for the
' current suspension operating condition
'**************************************************************
*******



IF FLCHECK(n)=1 THEN
 CALL TYRE1
' PRINT "CALLING TYRE1"
ELSEIF FLCHECK(n)=2 THEN
 CALL TYRE2
' PRINT "CALLING TYRE2"
ELSEIF FLCHECK(n)=3 THEN
' PRINT "CALLING TYRE3"
 CALL TYRE3
ELSEIF FLCHECK(n)=4 THEN
 CALL TYRE4
'  PRINT "CALLING TYRE4"
END IF

FOR X=0 TO 5
IF TYREF#(X,n) < 0 THEN
tyre$="stop"
END IF
NEXT X

end sub
```

Fig. C25 Tyre1.bas

```
SUB TYRE1
SHARED BR#(),n,thetap#,CHL#(),SUSPR#(),SUSPL#(),TYREF#()
DIM tyre1#(5,13)
'*****************************************************************
**********
' This routine contains the chassis tyre force matrix for
suspension
' operating condition a
'*****************************************************************
**********

tyre1#(0,0)=0.0105
tyre1#(0,1)=-0.0102
tyre1#(0,2)=-0.0413
tyre1#(0,3)=0.0412
tyre1#(0,4)=-0.088
tyre1#(0,5)=0.000138
tyre1#(0,6)=0.0000209
tyre1#(0,7)=-0.00593
tyre1#(0,8)=0.00184
tyre1#(0,9)=-0.00912
tyre1#(0,10)=-0.0826
tyre1#(0,11)=-0.0181
tyre1#(0,12)=0.911
tyre1#(0,13)=0.669

tyre1#(1,0)=-0.0192
tyre1#(1,1)=-0.0274
tyre1#(1,2)=-0.854
tyre1#(1,3)=-0.434
tyre1#(1,4)=-0.163
tyre1#(1,5)=-0.0214
tyre1#(1,6)=-0.0106
tyre1#(1,7)=-0.00978
tyre1#(1,8)=-0.00219
tyre1#(1,9)=-0.00709
tyre1#(1,10)=-0.2446
tyre1#(1,11)=-0.0238
tyre1#(1,12)=-1.74
tyre1#(1,13)=-1.39

tyre1#(2,0)=-0.00137
tyre1#(2,1)=0.00166
tyre1#(2,2)=-0.168
tyre1#(2,3)=0.168
tyre1#(2,4)=-0.109
tyre1#(2,5)=0.000139
tyre1#(2,6)=0.0000153
tyre1#(2,7)=-0.00583
tyre1#(2,8)=0.0000131
tyre1#(2,9)=-0.00266
tyre1#(2,10)=-0.0826
tyre1#(2,11)=-0.0167
tyre1#(2,12)=0.810
tyre1#(2,13)=0.770

tyre1#(3,0)=-0.0102
tyre1#(3,1)=0.0105
```

```
tyrel#(3,2)=0.0412
tyrel#(3,3)=-0.0413
tyrel#(3,4)=0.088
tyrel#(3,5)=0.000138
tyrel#(3,6)=0.0000138
tyrel#(3,7)=0.00592
tyrel#(3,8)=0.0000122
tyrel#(3,9)=0.00912
tyrel#(3,10)=-0.0826
tyrel#(3,11)=0.0181
tyrel#(3,12)=0.669
tyrel#(3,13)=0.911

tyrel#(4,0)=-0.0274
tyrel#(4,1)=-0.0192
tyrel#(4,2)=-0.434
tyrel#(4,3)=-0.854
tyrel#(4,4)=0.163
tyrel#(4,5)=-0.0214
tyrel#(4,6)=-0.0106
tyrel#(4,7)=0.0098
tyrel#(4,8)=-0.00219
tyrel#(4,9)=0.0071
tyrel#(4,10)=-0.2446
tyrel#(4,11)=0.0238
tyrel#(4,12)=-1.39
tyrel#(4,13)=-1.74

tyrel#(5,0)=0.00165
tyrel#(5,1)=-0.00137
tyrel#(5,2)=0.168
tyrel#(5,3)=-0.168
tyrel#(5,4)=0.109
tyrel#(5,5)=0.000141
tyrel#(5,6)=0.0000147
tyrel#(5,7)=0.00582
tyrel#(5,8)=0.0000128
tyrel#(5,9)=0.00266
tyrel#(5,10)=-0.0826
tyrel#(5,11)=0.0167
tyrel#(5,12)=0.770
tyrel#(5,13)=0.810

CHL#(0)=BR#(0,n)
CHL#(1)=BR#(1,n)
CHL#(2)=BR#(2,n)
CHL#(3)=BR#(3,n)
CHL#(4)=BR#(4,n)
CHL#(5)=BR#(5,n)
CHL#(6)=BR#(6,n)
CHL#(7)=BR#(7,n)
CHL#(8)=-63666.9*cos(thetap#)
CHL#(9)=63666.9*sin(thetap#)
CHL#(10)=-47088*cos(thetap#)
CHL#(11)=47088*sin(thetap#)
CHL#(12)=SUSPL#(n)
CHL#(13)=SUSPR#(n)
```

Fig. C26 Tyre2.bas

```
SUB TYRE2
SHARED BR#(),n,thetap#,CHL#(),SUSPR#(),SUSPL#(),TYREF#()
DIM tyre2#(5,12)
'*****************************************************************
**********
' This routine contains the chassis tyre force matrix for the
suspension
' operating condition b
'*****************************************************************
**********

tyre2#(0,0)=0.0085
tyre2#(0,1)=-0.0115
tyre2#(0,2)=-0.112
tyre2#(0,3)=0.0224
tyre2#(0,4)=-0.103
tyre2#(0,5)=-0.00136
tyre2#(0,6)=-0.00071
tyre2#(0,7)=-0.00683
tyre2#(0,8)=-0.00013
tyre2#(0,9)=-0.00949
tyre2#(0,10)=-0.09378
tyre2#(0,11)=-0.01944
tyre2#(0,12)=0.5620

tyre2#(1,0)=-0.0134
tyre2#(1,1)=-0.0237
tyre2#(1,2)=-0.647
tyre2#(1,3)=-0.379
tyre2#(1,4)=-0.120
tyre2#(1,5)=-0.0170
tyre2#(1,6)=-0.00843
tyre2#(1,7)=-0.00712
tyre2#(1,8)=-0.00174
tyre2#(1,9)=-0.00603
tyre2#(1,10)=-0.2116
tyre2#(1,11)=-0.01979
tyre2#(1,12)=-1.0800

tyre2#(2,0)=-0.00558
tyre2#(2,1)=-0.00102
tyre2#(2,2)=-0.318
tyre2#(2,3)=0.129
tyre2#(2,4)=-0.140
tyre2#(2,5)=-0.00302
tyre2#(2,6)=-0.00154
tyre2#(2,7)=-0.00775
tyre2#(2,8)=-0.00031
tyre2#(2,9)=-0.00343
tyre2#(2,10)=-0.10623
tyre2#(2,11)=-0.01953
tyre2#(2,12)=0.544

tyre2#(3,0)=-0.00822
tyre2#(3,1)=0.0118
tyre2#(3,2)=0.112
tyre2#(3,3)=-0.0225
tyre2#(3,4)=0.103
```

```
tyre2#(3,5)=0.00163
tyre2#(3,6)=0.00075
tyre2#(3,7)=0.00683
tyre2#(3,8)=0.00016
tyre2#(3,9)=0.00949
tyre2#(3,10)=-0.07125
tyre2#(3,11)=0.01944
tyre2#(3,12)=1.02

tyre2#(4,0)=-0.0331
tyre2#(4,1)=-0.0228
tyre2#(4,2)=-0.636
tyre2#(4,3)=-0.908
tyre2#(4,4)=0.121
tyre2#(4,5)=-0.0256
tyre2#(4,6)=-0.0127
tyre2#(4,7)=0.0072
tyre2#(4,8)=-0.0026
tyre2#(4,9)=0.00607
tyre2#(4,10)=-0.27684
tyre2#(4,11)=0.01987
tyre2#(4,12)=-2.05

tyre2#(5,0)=0.00586
tyre2#(5,1)=0.0013
tyre2#(5,2)=0.318
tyre2#(5,3)=-0.129
tyre2#(5,4)=0.140
tyre2#(5,5)=0.0033
tyre2#(5,6)=0.00157
tyre2#(5,7)=0.00774
tyre2#(5,8)=0.00034
tyre2#(5,9)=0.00342
tyre2#(5,10)=-0.0588
tyre2#(5,11)=0.01953
tyre2#(5,12)=1.04

CHL#(0)=BR#(0,n)
CHL#(1)=BR#(1,n)
CHL#(2)=BR#(2,n)
CHL#(3)=BR#(3,n)
CHL#(4)=BR#(4,n)
CHL#(5)=BR#(5,n)
CHL#(6)=BR#(6,n)
CHL#(7)=BR#(7,n)
CHL#(8)=-63666.9*cos(thetap#)
CHL#(9)=63666.9*sin(thetap#)
CHL#(10)=-47088*cos(thetap#)
CHL#(11)=47088*sin(thetap#)
CHL#(12)=SUSPR#(n)


for x=0 to 5
 TYREF#(x,n)=0
 for y=0 to 12

 TYREF#(x,n)=TYREF#(x,n)+tyre2#(x,y)*CHL#(y)

  next y

 next x
```



```
 end sub
```

Fig. C28 Tyre4.bas

```
SUB TYRE4
SHARED BR#(),n,thetap#,CHL#(),SUSPR#(),SUSPL#(),TYREF#()
DIM tyre4#(5,13)
'*****************************************************************
**********
' This routine contains the chassis tyre force matrix for the
suspension
' operating condition c
'*****************************************************************
**********

tyre4#(0,0)=0.0117
tyre4#(0,1)=-0.00822
tyre4#(0,2)=-0.0225
tyre4#(0,3)=0.112
tyre4#(0,4)=-0.103
tyre4#(0,5)=0.00163
tyre4#(0,6)=0.000757
tyre4#(0,7)=-0.00683
tyre4#(0,8)=0.000172
tyre4#(0,9)=-0.00949
tyre4#(0,10)=-0.07125
tyre4#(0,11)=-0.01944
tyre4#(0,12)=1.02
tyre4#(0,13)=0.890

tyre4#(1,0)=-0.0228
tyre4#(1,1)=-0.0331
tyre4#(1,2)=-0.908
tyre4#(1,3)=-0.636
tyre4#(1,4)=-0.121
tyre4#(1,5)=-0.0256
tyre4#(1,6)=-0.0127
tyre4#(1,7)=-0.00718
tyre4#(1,8)=-0.00263
tyre4#(1,9)=-0.00605
tyre4#(1,10)=-0.2768
tyre4#(1,11)=-0.01987
tyre4#(1,12)=-2.05
tyre4#(1,13)=-2.02

tyre4#(2,0)=0.0013
tyre4#(2,1)=0.00586
tyre4#(2,2)=-0.129
tyre4#(2,3)=0.318
tyre4#(2,4)=-0.140
tyre4#(2,5)=0.0033
tyre4#(2,6)=0.00157
tyre4#(2,7)=-0.00775
tyre4#(2,8)=0.000337
tyre4#(2,9)=-0.00343
tyre4#(2,10)=-0.0588
tyre4#(2,11)=-0.01953
tyre4#(2,12)=1.04
tyre4#(2,13)=1.24

tyre4#(3,0)=-0.0115
tyre4#(3,1)=0.0085
```

```
tyre4#(3,2)=0.0224
tyre4#(3,3)=-0.112
tyre4#(3,4)=0.103
tyre4#(3,5)=-0.00136
tyre4#(3,6)=-0.000723
tyre4#(3,7)=0.00683
tyre4#(3,8)=-0.000141
tyre4#(3,9)=0.00949
tyre4#(3,10)=-0.09378
tyre4#(3,11)=0.01944
tyre4#(3,12)=0.562
tyre4#(3,13)=0.690

tyre4#(4,0)=-0.0237
tyre4#(4,1)=-0.0134
tyre4#(4,2)=-0.379
tyre4#(4,3)=-0.647
tyre4#(4,4)=0.120
tyre4#(4,5)=-0.0170
tyre4#(4,6)=-0.000843
tyre4#(4,7)=0.00713
tyre4#(4,8)=-0.00175
tyre4#(4,9)=0.00604
tyre4#(4,10)=-0.21160
tyre4#(4,11)=0.01977
tyre4#(4,12)=-1.08
tyre4#(4,13)=-1.10

tyre4#(5,0)=-0.00102
tyre4#(5,1)=-0.00557
tyre4#(5,2)=0.129
tyre4#(5,3)=-0.318
tyre4#(5,4)=0.140
tyre4#(5,5)=-0.00302
tyre4#(5,6)=-0.00154
tyre4#(5,7)=0.00775
tyre4#(5,8)=-0.000311
tyre4#(5,9)=0.00343
tyre4#(5,10)=-0.10622
tyre4#(5,11)=0.01953
tyre4#(5,12)=0.544
tyre4#(5,13)=0.344

CHL#(0)=BR#(0,n)
CHL#(1)=BR#(1,n)
CHL#(2)=BR#(2,n)
CHL#(3)=BR#(3,n)
CHL#(4)=BR#(4,n)
CHL#(5)=BR#(5,n)
CHL#(6)=BR#(6,n)
CHL#(7)=BR#(7,n)
CHL#(8)=-63666.9*cos(thetap#)
CHL#(9)=63666.9*sin(thetap#)
CHL#(10)=-47088*cos(thetap#)
CHL#(11)=47088*sin(thetap#)
CHL#(12)=SUSPL#(n)
CHL#(13)=SUSPR#(n)
```

```
for x=0 to 5
 TYREF#(x,n)=0
 for y=0 to 13

 TYREF#(x,n)=TYREF#(x,n)+tyrel#(x,y)*CHL#(y)

 next y

next x

'for x=0 to 5

'PRINT "TYREF1=";TYREF#(x,n)

'next x
end sub
```

Fig. C29 Converge.bas

```
SUB CONVERGE
s            h            a            r            e            d
rt#(),n,SUSPL#(),SUSPR#(),CONVERGED%,rl#,thetap#,TYREF#()
,focount
SHARED tyrel#(),concount,const#,FLCHECK(),FILEN$,thetactr
CONVERGED%=0
'***********************************************************
************
'  This routine determines if the procedure has converged
by comparing
'   the current and previous displacements of the top of
the ram. A
'  displacement of < 1 mm is deemed to be convergence.
'***********************************************************
***************



if n > 1 then

if rt#(0,n)-rt#(0,n-1) < 1 and rt#(0,n)-rt#(0,n-1)  > -1
then
if rt#(1,n)-rt#(1,n-1) < 1 and rt#(1,n)-rt#(1,n-1)  > -1
then
if rt#(2,n)-rt#(2,n-1) < 1 and rt#(2,n)-rt#(2,n-1)  > -1
then
' convergence has occured, iteration is terminated
'print  "stop  ,convergence  has  occured,  iteration  is
terminated"

if thetactr=0 or thetactr=1 or thetactr=2 or thetactr=3 or
thetactr=4  or  thetactr=5  or  thetactr=6  or  thetactr=7  or
thetactr=8 or thetactr=9 or thetactr=10 then
OPEN "A", #1 ,FILEN$

WRITE#1,TYREF#(2,n)
WRITE#1,FLCHECK(n)

close #1
end if
concount=concount+1
CONVERGED%=1

'CALL OUTP

end if
end if
end if
end if

END SUB
```

APPENDIX D

PROGRAM USER GUIDE

The program user guide is aimed at giving the information necessary to enable the user to run the program, use the results, change the nine payload centre of gravity co-ordinates and the four payload masses and input new flexibility, stiffness and influence matrices when a new finite element model is to be considered.

D1 Program Execution

The program can be executed in two different ways. Firstly, when the user is using the Turbo Basic package, the program can be executed by the run command in the menu. The program is complied to memory only and then run, after which the program will have to be re-complied if further runs are required. The advantage of compiling to memory is that it is quick to swap between running and modifying a program compared to an executable program, which is then run as a stand alone program without the aid of the Turbo Basic package. Although the program can be run immediately, the executable program cannot be modified in any way. This guide will only concern itself with the former method of program execution as this is the most useful.

The disc in Fig. D1 contains the Turbo Basic program subroutines and is found attached to the inside of the rear cover. To run the program, the user must have a copy of the Turbo Basic package. To invoke the Turbo Basic package, the user must insert this disc into an IBM compatible PC and type TB when in drive A. This command will invoke the Turbo Basic menu which the user will use to edit the subroutines and to run the program. To run the program and interpret the results, the user must follow instructions (i) to (v) below, having invoked the Turbo Basic package.

(i) Place the cursor over the FILE menu (using the arrow keys) and press return to reveal its submenu.

(ii) Place the cursor over the LOAD option and press return twice to give the list of files on drive A:

(iii) Place the cursor over the filename TIPPER.BAS and press return, which loads this file into the screen editor and returns the cursor to the main menu.

(iv) Place the cursor of the RUN menu and press return, which will compile TIPPER.BAS to memory and then run it. The compile time is approximately 1 minute and the run time for 9 payload positions and four payload masses is approximately 24 hours.

(v) The program's rules are written to C: drive (as writing the data to the hard disk instead of the floppy disc reduces the running time). The results for each payload position and mass are stored in separate files, with 36 files required for the current program. For each ram length considered the rear left tyre force is recorded for ground slopes of 0° to 10° in steps of 1°. The trailer type, payload mass and position and ram length are recorded with each set of tyre fore results. The results can be used in conjunction with a graphs package to obtain the stability graphs shown in Figs. 5.1(a) to 5.4(f).

D2 Changing program variables

The program variables which the user can change for a given trailer design, are the 9 payload centre of gravity co-ordinates, 4 payload masses and the 36 output filenames and their destination (ie. A:, B: or C: drive). These variables are all stored in the Turbo Basic program VARIABS.BAS.

The payload centre of gravity, X, Y and Z co-ordinates are stored in the variable matrices PCGX#(8), PCGY#(8) and PCGZ#(8), respectively. The 9 X-co-ordinates are located under line 12 and can have any value in the range 0 to 8976 mm. The 9 Y-co-ordinates are located under line 28 and can have any value in the range 0 to 2028 mm. The 9 Z-co-ordinates are located under line 45 and can have any value in the -1014 to 1014 mm.

The payload masses are stored in the variable matrix PM#(3). The 4 masses are located under line 60 and can have any value in the range 0 to 25,000 Kg.

The output filenames are stored in the variable matrix PM$(3,8) and can have up to a seven letter prefix and a three letter suffix. The output filenames for the first, second, third and fourth payload masses are located under line 72, 90, 106 and 122, respectively.

To change any of the above variables, the user must repeat steps (i) to (iii) described in Section D1 loading VARIABS.BAS, instead of TIPPER.BAS. To modify this file the cursor must select the EDIT menu, allowing modifications to be made. When the desired modifications have been made, the user must press the ESC key to return to the main menu, where the modified file is saved. To save the file, the user must place the cursor over the FILE menu and press return, which will reveal the save command.

D3 Changing flexibility, stiffness and influence matrices

To determine chassis displacements, suspension displacements, suspension forces and trailer tyre forces 13 unit load flexibility, stiffness and influence matrices are required. The matrices are generated using the lorry finite element models for suspension conditions one to four, described in Section 3.4.3.

D3.1 Flexibility matrices

The unit load flexibility matrices allow the hinges, ram/chassis contact and airbag displacements to be determined, for any loading arrangement for suspension operating conditions one, two and four. The hinge and ram/chassis contact displacement flexibility matrix variable names and their subroutine locations are shown in Table D1. The airbag displacement flexibility matrix variable names and their subroutine locations are shown in Table D2.

D3.2 Influence matrices

The unit load influence matrices allow the suspension and tyre forces to be determined for any loading arrangement for suspension operating conditions one, two and four. The suspension for influence matrix variable names and their subroutine locations are shown in Table D3. The tyre force influence matrix variable names and their subroutine locations are shown in Table D4.

D3.3 Stiffness matrix

The stiffness matrix allows hinge ram/chassis contact and airbag displacements and the suspension and tyre forces to be determined for any loading arrangement, for suspension operating condition d. The stiffness matrix variable name is PRESCRIBE#(29, 23) and its subroutine name is CASE3.BAS.

Table D1

CHASSIS DISPLACEMENT FLEXIBILITY MATRICES LOCATION				
SUSPENSION CONDITION	ONE	TWO	THREE	FOUR
SUBROUTINE NAME	FLEX1.BAS	FLEX2.BAS	CASE3.BAS	FLEX4.BAS
VARIABLE NAME	FLEXI# (8, 13)	FLEX2# (8, 13)	PRESCRIBE# (29, 33) C	FLEX4# (8, 13)

Table D2

AIRBAG DISPLACEMENT FLEXIBILITY MATRICES LOCATION				
SUSPENSION CONDITION	ONE	TWO	THREE	FOUR
SUBROUTINE NAME	FLEX1.BAS	FLEX2.BAS	CSE3.BAS	CASE4.BAS
VARIABLE NAME	FLEX1A# (5, 13)	FLEX2A# (5, 13)	PRESCRIBE# (29, 33)	FLEX4A# (5, 13)

Table D3

SUSPENSION FORGE INFLUENCE MATRICES LOCATION				
SUSPENSION CONDITION	ONE	TWO	THREE	FOUR
SUBROUTINE NAME	CASE1.BAS	CASE2.BAS	CASE3.BAS	CA54.BAS
VARIABLE NAME	SUSPM# (1, 13)	SUSPM2# (1, 13)	PRESCRIBE# (29, 33)	SUSPM4# (1, 13)

Table D4

TYRE FORCE INFLUENCE MATRICES LOCATION				
SUSPENSION CONDITION	ONE	TWO	THREE	FOUR
SUBROUTINE NAME	TYRE1.BAS	TYRE2.BAS	CASE3.BAS	TYRE4.BAS
VARIABLE NAME	TYRE1# (5, 13)	TYRE2# (5, 13)	PRESCRIBE# (29, 33)	TYRE4# (5, 13)

APPENDIX E

FINITE ELEMENT ANALYSES AND FLEXIBILITY, INFLUENCE AND STIFFNESS MATRICES

E1 Introduction

To determine chassis displacements, suspension forces and tyre forces, a total of thirteen flexibility, influence and stiffness matrices are required for a given articulated tipper design. The flexibility and influence matrices are used when the suspension is operating under conditions a b or c. The stiffness matrix is used when the suspension is only operating under condition d. This appendix gives details, shown in Tables 4.3 to 4.15, of these matrices for the original chassis, and describes how the different types of matrix are obtained. Also, a typical PAFEC data file is shown in Fig. E1.

E2 Flexibility matrices

The flexibility matrices, shown in Tables 4.3 to 4.8, enable the displacement of the body/chassis contact points and the airbags to be determined for any loading condition. For each matrix the top row gives details, for each column, of the force and its respective direction in which it is applied to the structure and its corresponding node in the PAFEC model. For Tables 4.3 to 4.5 the left column gives details of the chassis displacement to which the row coefficients correspond. For Tables 4.6 to 4.8 the left column gives details of the airbag displacement to which the row coefficients correspond.

The matrix coefficients are determined a column at a time. A unit force is applied in the direction of the force which corresponds to that column. The LOADS module in the PAFEC data program, shown in Fig. E1, is used to apply the unit force to the finite element mesh. The displacement at the nodes corresponding to the body/chassis contact points and the end of the airbags, resulting from the unit force form the column matrix coefficients.

E2 Influence matrices

The influence matrices, shown in Tables 4.9 to 4.14, enable the suspension and tyre forces to be determined for any loading condition. For each matrix the top row gives details, for each column, of the force and its respective direction in which it is applied to the structure and its corresponding node in the PAFEC model. For Tables 4.9 to 4.11 the left column gives details of the suspension forces to which the row coefficients correspond. For Tables 4.12 to 4.14 the left column gives details of tyre forces to which the row coefficients correspond.

The matrix coefficients are determined a column at a time. A unit force is applied in the direction of the force which corresponds to that column. The LOADS module in the PAFEC data program, shown in Fig. E1, is used to apply the unit force to the finite element mesh. The forces in the tie bars resulting from the unit force form the column matrix coefficients for the suspension force influence matrices shown in Tables 4.9 to 4.11. The forces in the springs representing the trailer tyre resulting from the unit force form the column matrix coefficients for the tyre force influence matrices shown in Tables 4.12 to 4.14.

E3 Stiffness matrix

The stiffness matrix, shown in Table 4.15, enables the chassis displacements, suspension forces and tyre forces, to be determined for any loading condition. The matrix top row gives details, for each column, of the force and its respective direction in which it is applied to the structure and its corresponding node in the PAFEC model. The left column gives details of the chassis displacements (N186-X to N314-X), chassis and tractor sprung and unsprung weight (N315-Y to N313Z), suspension forces (N195-Y to N223-Y) and tyre forces (N231-Y to N236-Y) to which the row coefficients correspond.

The matrix coefficients are determined a column at a time. A unit displacement is applied in the direction of the force which corresponds to that column. The PRESCRIBE.DISPLACEMENTS module in the PAFEC data program, shown in Table E1, is used to apply the unit displacement to the finite element meshes. The reaction forces resulting from the unit displacement form the column matrix coefficients for the stiffness matrix shown in Table 4.15.

Fig. E1 A typical pafec data file

```
STJNLD(TWOTIE.SUSPLJ)
RUNPAFEC(RUN=SUSPL)
----
TITLE CASE1 TWO TIERODS
CONTROL
OPLIB.TWOTIE
FULL.SAVE.OUTPUT
REACTIONS
CONTROL.END
NODES
AXIS=1
NODE.NUMB    X         Y         Z
C 1-79 : PLATE NODES
1           9535.5   -22.0     -700.0
2           9535.5   -22.0     -537.5
3           9535.5   -22.0     -375.0
4           9535.5   -22.0     -253.3
5           9535.5   -22.0     -131.5
6           9535.5   -22.0     0.0
7           9535.5   -22.0     131.5
8           9535.5   -22.0     253.3
9           9535.5   -22.0     375.0
10          9535.5   -22.0     537.5
11          9535.5   -22.0     700.0
12          9406.0   -22.0     -700.0
13          9406.0   -22.0     -375.0
14          9406.0   -22.0     -131.5
15          9406.0   -22.0     131.5
16          9406.0   -22.0     375.0
17          9406.0   -22.0     700.0
18          9276.5   -22.0     -700.0
19          9276.5   -22.0     -537.5
20          9276.5   -22.0     -375.0
21          9276.5   -22.0     -253.0
22          9276.5   -22.0     -131.5
23          9276.5   -22.0     0.0
24          9276.5   -22.0     131.5
25          9276.5   -22.0     253.0
26          9276.5   -22.0     375.0
27          9276.5   -22.0     537.5
28          9276.5   -22.0     700.0
29          9183.1   -22.0     -700.0
30          9183.1   -22.0     -375.0
31          9183.1   -22.0     -131.5
32          9183.1   -22.0     131.5
33          9183.1   -22.0     375.0
34          9183.1   -22.0     700.0
35          9089.7   -22.0     -700.0
36          9089.7   -22.0     -537.5
37          9089.7   -22.0     -375.0
38          9089.7   -22.0     -253.3
39          9089.7   -22.0     -131.5
C  NODE 40 IS KING PIN
40          9089.7   -22.0     0.0
41          9089.7   -22.0     131.5
42          9089.7   -22.0     253.3
43          9089.7   -22.0     375.0
44          9089.7   -22.0     537.5
```

```
45          9089.7  -22.0    700.0
46          8977.2  -22.0    -700.0
47          8977.2  -22.0    -375.0
C NODES 48 & 49 LOCATE RAM PIN
48          8977.2  -22.0    -131.5
49          8977.2  -22.0    131.5
50          8977.2  -22.0    375.0
51          8977.2  -22.0    700.0
52          8864.7  -22.0    -700.0
53          8864.7  -22.0    -537.5
54          8864.7  -22.0    -375.0
55          8864.7  -22.0    -253.3
56          8864.7  -22.0    -131.5
57          8864.7  -22.0    0.0
58          8864.7  -22.0    131.5
59          8864.7  -22.0    253.3
60          8864.7  -22.0    375.0
61          8864.7  -22.0    537.5
62          8864.7  -22.0    700.0
63          8741.3  -22.0    -700.0
64          8741.3  -22.0    -375.0
65          8741.3  -22.0    -131.5
66          8741.3  -22.0    131.5
67          8741.3  -22.0    375.0
68          8741.3  -22.0    700.0
69          8618.0  -22.0    -700.0
70          8618.0  -22.0    -537.5
71          8618.0  -22.0    -375.0
72          8618.0  -22.0    -253.0
73          8618.0  -22.0    -131.5
74          8618.0  -22.0    0.0
75          8618.0  -22.0    131.5
76          8618.0  -22.0    253.3
77          8618.0  -22.0    375.0
78          8618.0  -22.0    537.5
79          8618.0  -22.0    700.0
C  FITH WHEEL BEAM NODES : 80 167
80          9535.5  67.5    -700
81          9535.5  67.5    -537.5
82          9535.5  67.5    -375.0
83          9535.5  67.5    -253.3
84          9535.5  67.5    -131.5
85          9535.5  67.5     0.0
86          9535.5  67.5    131.5
87          9535.5  67.5    253.3
88          9535.5  67.5    375.0
89          9535.5  67.5    537.5
90          9535.5  67.5    700.0
91          9276.5  57.0    -700.0
92          9276.5  57.0    -537.5
93          9276.5  57.0    -375.0
94          9276.5  57.0    -253.3
95          9276.5  57.0    -131.5
96          9276.5  57.0    0.0
97          9276.5  57.0    131.5
98          9276.5  57.0    253.3
99          9276.5  57.0    375.0
100         9276.5  57.0    537.5
```

101	9276.5	57.0	700.0
102	8864.7	15.90	-131.5
103	8864.7	15.90	0.00
104	8864.7	15.90	131.5
105	8618.0	83.0	-700.0
106	8618.0	83.0	-537.5
107	8618.0	83.0	-375.0
108	8618.0	83.0	-253.3
109	8618.0	83.0	-131.5
110	8618.0	83.0	0.0
111	8618.0	83.0	131.5
112	8618.0	83.0	253.3
113	8618.0	83.0	375.0
114	8618.0	83.0	537.5
115	8618.0	83.0	700.0
116	9535.5	57.0	-700.0
117	9406.0	57.0	-700.0
118	9276.5	57.0	-700.0
119	9183.1	57.0	-700.0
120	9089.7	57.0	-700.0
121	8977.2	57.0	-700.0
122	8864.7	57.0	-700.0
123	8741.3	57.0	-700.0
124	8618.0	57.0	-700.0
125	9535.5	15.9	-375
126	9406.0	15.5	-375
127	9276.5	15.9	-375
128	9276.5	45.5	-375
129	9183.1	45.5	-375
130	9089.7	45.5	-375
131	8977.2	45.5	-375
132	8864.7	45.5	-375
133	8741.3	45.5	-375
134	8618.0	45.5	-375
135	9276.5	54.5	-131.5
136	9183.1	54.5	-131.5
137	9089.7	54.5	-131.5
138	8977.2	54.5	-131.5
139	8864.7	54.5	-131.5
140	8741.3	54.5	-131.5
141	8618.0	54.5	-131.5
142	9276.5	54.5	131.5
143	9183.1	54.5	131.5
144	9089.7	54.5	131.5
145	8977.2	54.5	131.5
146	8864.7	54.5	131.5
147	8741.3	54.5	131.5
148	8618.0	54.5	131.5
149	9535.5	15.9	375.0
150	9406.0	15.9	375.0
151	9276.5	15.9	375.0
152	9276.5	45.5	375.0
153	9183.1	45.5	375.0
154	9089.7	45.5	375.0
155	8977.2	45.5	375.0
156	8864.7	45.5	375.0
157	8741.3	45.5	375.0
158	8618.0	45.5	375.0

159	9535.5	57.0	700.0
160	9406.0	57.0	700.0
161	9276.5	57.0	700.0
162	9183.1	57.0	700.0
163	9089.7	57.0	700.0
164	8977.2	57.0	700.0
165	8864.7	57.0	700.0
166	8741.3	57.0	700.0
167	8618.0	57.0	700.0
168	8530.0	57.0	-700.0
169	7210.0	15.5	-700.0
170	6905.0	-53.0	-700.0
171	6680.0	-140.0	-700.0
172	6680.0	2.0	-700.0
173	5332.5	-170.5	-700.0
174	3985.0	-201.0	-700.0
175	3985.0	-292.0	-700.0
176	3093.0	-191.0	-700.0
177	3093.0	-297.0	-700.0
178	2670.0	-186.5	-700.0
179	2670.0	-263.0	-700.0
180	1778.0	-176.5	-700.0
181	1778.0	-268.0	-700.0
182	1355.0	-172.0	-700.0
183	1355.0	-234.0	-700.0
184	463.0	-162.0	-700.0
185	463.0	-240.0	-700.0
C NODE 186 & 205			
186	0.0	0.0	-700.0
187	8530.0	57.0	700.0
188	7210.0	15.5	700.0
189	6905.0	-53.0	700.0
190	6680.0	-140.0	700.0
191	6680.0	2.0	700.0
192	5332.5	-170.5	700.0
193	3985.0	-201.0	700.0
194	3985.0	-292.0	700.0
195	3093.0	-191.0	700.0
196	3093.0	-297.0	700.0
197	2670.0	-186.5	700.0
198	2670.0	-263.0	700.0
199	1778.0	-176.5	700.0
200	1778.0	-268.0	700.0
201	1355.0	-172.0	700.0
202	1355.0	-234.0	700.0
203	463.0	-162.5	700.0
204	463.0	-240.0	700.0
205	0.00	0.0	700.0
206	4032.75	-652.0	-700.0
207	3438.0	-652.0	-700.0
208	3093.0	-652.0	-700.0
209	2717.75	-623.0	-700.0
210	2123.0	-623.0	-700.0
211	1778.0	-623.0	-700.0
212	1402.75	-594.0	-700.0
213	808.0	-594.0	-700.0
214	463.0	-594.0	-700.0
215	4032.75	-652.0	700.0

```
216          3438.0  -652.0     700.0
217          3093.0  -652.0     700.0
218          2717.75 -623.0     700.0
219          2123.0  -623.0     700.0
220          1778.0  -623.0     700.0
221          1402.75 -594.0     700.0
222          808.0   -594.0     700.0
223          463.0   -594.0     700.0
C  OX FREEDOM FOR SUSPENSION NODES
225          4032.75 -653.0     -700.0
226          2717.75 -624.0     -700.0
227          1402.75 -595.0     -700.0
228          4032.75 -653.0     700.0
229          2717.75 -624.0     700.0
230          1402.75 -595.05    700.0
231          3438.0  -1252.0    -925.0
232          2123.0  -1223.0    -925.0
233          808.0   -1194.0    -925.0
234          3438.0  -1252.0    925.0
235          2123.0  -1223.0    925.0
236          808.0   -1194.0    925.0
C 237          9089.7   -1272.0    0.0
238          3438.0  -652.0     -925.0
239          2123.0  -623.0     -925.0
240          808.0   -594.0     -925.0
241          3438.0  -652.0     925.0
242          2123.0  -623.0     925.0
243          808.0   -594.0     925.0
244          808.0   -530.5     -925.0
245          808.0   -530.5     -700.0
246          808.0   -530.5     700.0
247          808.0   -530.5     925.0
248          2123.0  -559.5     -925.0
249          2123.0  -559.5     -700.0
250          2123.0  -559.5     700.0
251          2123.0  -559.5     925.0
252          3438.0  -588.5     -925.0
253          3438.0  -588.5     -700
254          3438.0  -588.5     700
255          3438.0  -588.5     925.0
C TRACTOR NODES
256          7389.7        -376.7   381.5
257          7889.7        -381.3   381.5
258          8289.7      -385     381.5
259          8989.7  -391.4   381.5
260          9089.7     -392.4   381.5
261          9189.7      -393.3   381.5
262          10280.7    -403.4   381.5
263          10959.7   -409.6   381.5
264          11389.7    -413.6   381.5
265          12089.7    -420     431.5
266          12789.7    -426.4   481.5
267          13289.7    -431.1   481.5
268          7390.3      -376.7   -381.5
269          7889.7      -381.3   -381.5
270          8289.7      -385     -381.5
271          8989.7      -391.4   -381.5
272          9089.7      -392.4    -381.5
```

```
273        9189.7      -393.3    -381.5
274       10280.7     -403.4   -381.5
275       10959.7    -409.6    -381.5
276       11389.7     -413.6   -381.5
277       12089.1     -420      -431.5
278       12789.7     -426.4   -481.5
279       13289.7     -431.1   -481.5
280       8289.7       -703.5    1086
281       8289.7       -703.5    753.5
282       12089.7     -703.5    981
283        8289.7      -703.5   -753.5
284        8289.7      -703.5   -1086
285       12089.7  -703.5   -981
286        8289.7      -1240.5   1086
287        8289.7      -1240.5   753.5
288       12089.7     -1240.5        981
289        8289.7      -1240.5   -753.5
290        8289.7      -1240.5   -1086
291       12089.7     -1240.5   -981
292        9089.7      9.5        381.5
293        9089.7      9.5            0
294        9089.7      9.5        -381.5
295        9089.7      -392.4         0
296       10959.7     -340.5          0
C 297        0 0 0
C 298        0 0 0
299        8289.7      -703.5     381.5
300        8289.7      -703.5     -381.5
301       12089.7     -703.5     431.5
302       12089.7     -703.5     -431.5
C ROLL BARS
303      12789.7  -425.4  481.5
304      12789.7  -425.4  -481.5
305      12091.6  -703.5  431.5
306      12091.6  -703.5  -431.5
307      7889.7  -383.0  381.5
308      7889.7  -383.0  -381.5
309      8289.7  -705.0  381.5
310      8289.7  -705.0  -381.5
C MID-SUSPENSION CHASSIS NODES
311      2123 -182.6 -700
312      2123 -182.6  700
313      10959.7 -340.5 0
314      8977.2 -22.0 0
C SPRUNG CHASSIS C.OF.G
315      3985,-292,0
C FRONT AXLE MID POINT
316 3438 -588.5 0
C MIDDLE AXLE MID POINT
317 2123 -559.5 0
C REAR AXLE MID POINT
318 808 -530.5 0
ELEMENTS
NUMB GROUP.NUMB  ELEM.TYPE   PROPS      TOPOLOGY
1    1  44210       28        18 20 1 3 19 12 13 2
2    1  44210       28        20 22 3 5 21 13 14 4
3    1  44210       28        22 24 5 7 23 14 15 6
4    1  44210       28        24 26 7 9 25 15 16 8
```

5	1	44210	28	26 28 9 11 27 16 17 10
6	1	44210	28	35 37 18 20 36 29 30 19
7	1	44210	28	37 39 20 22 38 30 31 21
8	1	44210	28	39 41 22 24 40 31 32 23
9	1	44210	28	41 43 24 26 42 32 33 25
10	1	44210	28	43 45 26 28 44 33 34 27
11	1	44210	28	52 54 35 37 53 46 47 36
12	1	44210	28	54 56 37 39 55 47 48 38
13	1	44210	28	56 58 39 41 57 48 49 40
14	1	44210	28	58 60 41 43 59 49 50 42
15	1	44210	28	60 62 43 45 61 50 51 44
16	1	44210	28	69 71 52 54 70 63 64 53
17	1	44210	28	71 73 54 56 72 64 65 55
18	1	44210	28	73 75 56 58 74 65 66 57
19	1	44210	28	75 77 58 60 76 66 67 59
20	1	44210	28	77 79 60 62 78 67 68 61
21	1	34200	7	1 2 80 81
22	1	34200	7	2 3 81 82
23	1	34200	7	3 4 82 83
24	1	34200	7	4 5 83 84
25	1	34200	7	5 6 84 85
26	1	34200	7	6 7 85 86
27	1	34200	7	7 8 86 87
28	1	34200	7	8 9 87 88
29	1	34200	7	9 10 88 89
30	1	34200	7	10 11 89 90
31	1	34200	2	18 19 91 92
32	1	34200	2	19 20 92 93
33	1	34200	2	20 21 93 94
34	1	34200	2	21 22 94 95
35	1	34200	2	22 23 95 96
36	1	34200	2	23 24 96 97
37	1	34200	2	24 25 97 98
38	1	34200	2	25 26 98 99
39	1	34200	2	26 27 99 100
40	1	34200	2	27 28 100 101
41	1	34200	3	56 57 102 103
42	1	34200	3	57 58 103 104
43	1	34200	6	69 70 105 106
44	1	34200	6	70 71 106 107
45	1	34200	6	71 72 107 108
46	1	34200	6	72 73 108 109
47	1	34200	6	73 74 109 110
48	1	34200	6	74 75 110 111
49	1	34200	6	75 76 111 112
50	1	34200	6	76 77 112 113
51	1	34200	6	77 78 113 114
52	1	34200	6	78 79 114 115
53	1	34200	1	1 12 116 117
54	1	34200	1	12 18 117 118
55	1	34200	1	18 29 118 119
56	1	34200	1	29 35 119 120
57	1	34200	1	35 46 120 121
58	1	34200	1	46 52 121 122
59	1	34200	1	52 63 122 123
60	1	34200	1	63 69 123 124
61	1	34200	3	3 13 125 126
62	1	34200	3	13 20 126 127

63	1	34200	4	20	30	128	129
64	1	34200	4	30	37	129	130
65	1	34200	4	37	47	130	131
66	1	34200	4	47	54	131	132
67	1	34200	4	54	64	132	133
68	1	34200	4	64	71	133	134
69	1	34200	5	22	31	135	136
70	1	34200	5	31	39	136	137
71	1	34200	5	39	48	137	138
72	1	34200	5	48	56	138	139
73	1	34200	5	56	65	139	140
74	1	34200	5	65	73	140	141
75	1	34200	5	24	32	142	143
76	1	34200	5	32	41	143	144
77	1	34200	5	41	49	144	145
78	1	34200	5	49	58	145	146
79	1	34200	5	58	66	146	147
80	1	34200	5	66	75	147	148
81	1	34200	3	9	16	149	150
82	1	34200	3	16	26	150	151
83	1	34200	4	26	33	152	153
84	1	34200	4	33	43	153	154
85	1	34200	4	43	50	154	155
86	1	34200	4	50	60	155	156
87	1	34200	4	60	67	156	157
88	1	34200	4	67	77	157	158
89	1	34200	1	11	17	159	160
90	1	34200	1	17	28	160	161
91	1	34200	1	28	34	161	162
92	1	34200	1	34	45	162	163
93	1	34200	1	45	51	163	164
94	1	34200	1	51	62	164	165
95	1	34200	1	62	68	165	166
96	1	34200	1	68	79	166	167
97	1	34200	1	69	168	124	168
98	1	34200	11	168	169		
99	1	34200	12	169	170		
100	1	34200	13	170	171		
101	1	34200	14	171	173		
102	1	34200	15	173	174		
103	1	34200	16	174	176		
104	1	34200	17	176	178		
105	1	34200	18	178	311		
106	1	34200	19	180	182		
107	1	34200	20	182	184		
108	1	34200	21	184	186		
109	1	34200	1	79	187	167	187
110	1	34200	11	187	188		
111	1	34200	12	188	189		
112	1	34200	13	189	190		
113	1	34200	14	190	192		
114	1	34200	15	192	193		
115	1	34200	16	193	195		
116	1	34200	17	195	197		
117	1	34200	18	197	312		
118	1	34200	19	199	201		
119	1	34200	20	201	203		
120	1	34200	21	203	205		

```
121  1      34200       10     171 190 172 191
C 122  1      34200        8     174 193 175 194
123  1      34200        9     176 195 177 196
124  1      34200        8     178 197 179 198
125  1      34200        9     180 199 181 200
126  1      34200        8     182 201 183 202
127  1      34200        9     184 203 185 204
C SUSPENSION ELEMENTS LEFT 131,136,142
128  1      34200       22     174 206
129  2      34200       24     225 207
130  2      34200       31     207 208
C 131  2      30100       25     176 208
132  2      30100       26     231 238
133  1      34200       22     178 209
134  2      34200       24     226 210
135  2      34200       31     210 211
C  136  2      30100       25     180 211
137  2      30100       26     232 239
138  1      34200       22     182 212
139  2      34200       24     227 213
140  2      34200       31     213 214
C 141  2      30100       25     184 214
142  2      30100       26     233 240
C SUSPENSION ELEMENT RIGHT  146,151,156
143  1      34200       22     193 215
144  2      34200       24     228 216
145  2      34200       31     216 217
C  146  2      30100       25     195 217
147  2      30100       26     234 241
148  1      34200       22     197 218
149  2      34200       24     229 219
150  2      34200       31     219 220
C 151  2      30100       25     199 220
152  2      30100       26     235 242
153  1      34200       22     201 221
154  2      34200       24     230 222
155  2      34200       31     222 223
C 156  2      30100       25     203 223
157  2      30100       26     236 243
C AXLE TUBES
C 159  2      34200       23     207 216 253 254
C 160  2      34200       23     210 219 249 250
C 161  2      34200       23     213 222 245 246
162  2      30100       29     231 0
163  2      30100       29     232 0
164  2      30100       29     233 0
165  2      30100       29     234 0
166  2      30100       29     235 0
167  2      30100       29     236 0
C ADDITIONAL AXLE TUBES
169  2      34200       23     207 238 253 252
170 2       34200       23     210 239 249 248
171 2       34200       23     213 240 245 244
172 2       34200       23     216 241 254 255
173 2       34200       23     219 242 250 251
174 2       34200       23     222 243 246 247
C TRACTOR UNIT CHASSIS
175 3         34200   36        256 257
```

```
176 3   34200      36       257 258
177 3   34200      36       258 259
178 3   34200      36       259 260
179 3   34200      36       260 261
180 3   34200      36       261 262
181 3   34200      36       262 263
182 3   34200      36       263 264
183 3   34200      36       264 265
184 3   34200      36       265 266
185 3   34200      36     266 267
186 3   34200      36       267 279
187 3   34200      36       256 268
188 3   34200      36       268 269
189 3   34200      36       269 270
190 3   34200      36       270 271
191 3   34200      36      271 272
192 3   34200      36       272 273
193 3   34200      36       273 274
194 3   34200      36       274 275
195 3   34200       36      275 276
196 3   34200      36     276 277
197 3   34200      36       277 278
198 3   34200      36       278 279
199 3   34200      36       261 273
200 3   34200    36       264 276
C  TRACTOR SPRINGS
C FRONT TYRES
201 3   30100 35 282 288
202 3   30100 34 288 0
203 3   30100 35 285 291
204 3   30100 34 291 0
C REAR TYRES
205 3   30100 35  280 286
206 3   30100 34  286 0
207 3   30100 35 281 287
208 3   30100 34 287 0
209 3   30100 35 283 289
210 3   30100 34 289 0
211 3   30100 35 284 290
212 3   30100 34 290 0
C FRONT SUSPENSIONS
213 3   30100 33 265 301
214 3   30100 33 277 302
C  REAR SUSPENSIONS
215 3   30100  32 258 299
216 3   30100  32 270 300
C FITH  WHEEL BEAMS
217 3   34200      36       292 293
218 3   34200      36       293 294
C TRACTOR AXLES
C REAR
219 3   34200      37       280 281
220 3   34200      37       281 299
221 3   34200      37       299 300
222 3   34200      37       300 283
223 3   34200      37       283 284
C FRONT
224 3   34200      37       282 301
```

```
225 3   34200       37        301 302
226 3   34200       37        302 285
C ROLL BARS
227 3 34200 39  303 305
228 3 34200 39  305 306
229 3 34200 39  306 304
230 3 34200 38  307 309
231 3 34200 38  309 310
232 3 34200 38  310 308
C ADDITIONAL MAINRAIL BEAMS
233 1 34200 18 311 180
234 1 34200 18 312 199
C MID SUSPENSION SUPPORTS
 235 1 34400 40 311 210
 236 1 34400 40 312 219
C ADDITIONAL CHASSIS MASSES
237 2 30200 41 238
238 2 30200 41 239
239 2 30200 41 240
240 2 30200 41 241
241 2 30200 41 242
242 2 30200 41 243
C TRACTOR C.OF.G BEAMS
243 3 34200 18 263 313
244 3 34200 18 313 275
C HINGE BAR
245 1 34200 42 186 205
C RAM CENTRE 314
246 1 34200 17 48 314
247 1 34200 17 314 49
C FRONT CROSS MEM DIVIDED TO ALLOW SPRUNG CHASSIS LOADING AT
N315.
248 1 34200 8  174 315 175 315
249 1 34200 8  193 315 194 315
C AXLES DIVIDED TO ALLOW UNSPRUNG CHASIS LOADS AT N316 N317 N318
250 2 34200 23 207 316 253 316
251 2 34200 23 216 316 254 316
252 2 34200 23 210 317 249 317
253 2 34200 23 219 317 250 317
254 2 34200 23 213 318 245 318
255 2 34200 23 222 318 246 318
256 1 30200 43 315
REPEATED.FREEDOMS
N1   N2   DIRECTION
206  225  12345
209  226  12345
212  227  12345
215  228  12345
218  229  12345
221  230  12345
231  238  13
232  239  13
233  240  13
234  241  13
235  242  13
236  243  13
C TRACTOR TYRES
282 288 13
```

```
285 291 13
280 286 13
281 287 13
283 289 13
284 290 13
C TRACTOR SUSPENSION
265 301 13
277 302 13
299 258 13
270 300 13
C FIFTH WHEEL
260 292 123456
272 294 123456
C FIFTH WHEEL/PLATE
292 43 2
293 40 13
294 37 2
C ROLL BAR NODES
305 301 123
306 302 123
307 257 123
308 269 123
309 299 123
310 300 123
303 266 123
304 278 123
RESTRAINTS
NODE.NUMB      DIRECTION
C  CHASSIS TYRES
 231             2456
 232             2456
 233             2456
 234             2456
 235             2456
 236             2456
C TRACTOR TYRES
288 2456
291 2456
286 2456
287 2456
289 2456
290 2456
BEAMS
SECTION.NUMB  MATE.NUMB  IYY              IZZ          AXIS.NUMB
TORSIONAL.CONSTANT   AREA
1    1     3.663E06      13.677E06        1            92.5E03
  3250
2    1     1.464E06      9.193E06         1            93.333E03
  2800
3    1     2.46E06       0.393E06         1            60.0E03
  1800
4    1     0.571E06      5.343E06         1            77.666E03
  6570
5    1     0.189E06      6.351E06         1           755.208E03
  3625
6    1     0.813E06      2.686E06         1            10.208E03
  1225
7    1     0.388E06      7.801E06         1            43.520E03
```

```
  2040
8    1       15.224E06     5.124E06          1              11.834E06
  2900
9    1       0.362E06      1.298E06          1               8.125E06
  1000
10   1       2.569E06      2.569E06          1               5.138E06
  1717
11   1       3.664E06     25.025E06          1               94229
  3458
12   1       3.665E06     69.249E06          1               98812
  4008
13   1       3.665E06    105.286E06          1              101875
  4375
14   1       3.664E06    125.099E06          1               95211
  4162
15   1       3.664E06    170.164E06          1               96512
  4406
16   1       3.664E06    186.195E06          1               96950
  4488
17   1       3.664E06    174.025E06          1               96640
  4430
18   1       3.664E06    162.496E06          1               96438
  4372
19   1       3.664E06    151.253E06          1               96128
  4314
20   1       3.664E06    140.986E06          1               95723
  4258
C 21 -HINGE BAR MAIN RAILS
21   1       3.664E06    140.986E06          1               95723
  4258
22   1       8.919E06     17.756E06          1               24063
  2875
23   1       8.055E07     8.055E07          1              16.109E07
 49700
C 24 MOST  STIFF HALF OF TRAILING ARM
24   1       2.084E06     0.7771E06          1               1.926E06
  3908
C 31 LEAST STIFF HALF OF TRAILING ARM
31 1         1.042E06     0.3886E06          1               0.963E06
  1954
C  36 TRACTOR FRAME
36 2         1.585E06     27.551E06          1               30744
  2598
C 37 TRACTOR AXLES
37 2         100E08        100E08            1               100000
    10000
C 38 REAR ROLL BAR
38 2         133901.3   133901.3             1               267802.5
  1297.2
C 39 FRONT ROLL BAR
39 2       397358.0    397358.0              1               794716.0
  2234.6
C MID SUSPENSION SUPPORT
40 2     0              0                     0              0
   900
42 1     1.11313E06   1.11313E06             1                2.22626E06
   1995
MATERIAL
```

```
MATERIAL.NUMB       NU      E           RO
1                   0.3     210E03    7.8E-06
2                   0.3     210E03    0.0
PLATES.AND.SHELLS
PLATE.OR.SHELL.NUMBER        MATERIAL.NUMBER        THICKNESS
          28                            1                   8
SPRINGS
NUMBER.OF.SPRING    AXIS.NUMB    KX       KY        KZ        TXX
      25                 1        0        197.0     0.00       0
      26                 1        0        1070.0    0.00       0
C     27               1        0       1060.0   0.00       2.63477E08
      29                 1        749.0    0.00      412.0      0
C     30                 1        4360.0   0.00      4360.0     0
C     REAR TRACTOR SUSPENSION
      32                 1        0 872
C     FRONT TRACTOR SUSPENSION
      33                 1        0 403
C     TRACTOR TYRES KX & KZ
      34                 1        755 0 350
C     TRACTOR TYRES KY
     35                  1         0 981
MASSES
NUMB.OF.MASS    MASS
41              17.666
43              1220.0
LOADS
NODE.NUMB DIRECTION.OF.LOAD VALUE.OF.LOAD
C RAM FORCES
C LEFT SUSPENSION ?
   176      2                           1
   208      2                          -1
   180      2                           1
   211      2                          -1
   184      2                           1
   214      2                          -1
C  186 1    18051
C  186 2   -12495
C  186 3    1
C  205 1   -28805
C  205 2   -43486
C BODY REACTIONS
C 314 1 10754
C 314 2 -41745
C 314 3 0
C TRACTOR WEIGHT
C 313 2    -63424
C 313 3     5549
STRESS.ELEMENTS
START    FINISH
1    260
C IN.DRAW
C DRAW.NUMB        INFO.NUMB ORIENTATION                  SCALE
C   1              2          0                           0.05
C OUT.DRAW
C DRAW.NUMB    PLOT.TYPE      ORIENTATION    SCALE
C  1           1             0              0.05
END.OF.DATA
++++
```